HISTORICAL RIPARIAN HABITAT CHANGES OF AN ENDANGERED BIRD SPECIES: INTERIOR LEAST TERNS ALONG THE RED RIVER BELOW DENISON DAM

by

Kristen B. Newcomer, B.S.

A thesis submitted to the Graduate Council of
Texas State University in partial fulfillment
of the requirements for the degree of
Master of Science
with a Major in Geography
May 2017

Committee Members:

Jason P. Julian, Chair

Kimberly Meitzen

Clay Green

DEDICATION

To my Son—

I hope you grow to love the beauty and intricacy of God's creation as I have, and learn that studying it can be immensely delightful form of worship.

Love,

Your Mother

ACKNOWLEDGEMENTS

First, I would like to thank my advisor and committee chair, Dr. Jason Julian, for working with me, and especially for being flexible and understanding with my health condition and the life changes that occurred during the course of finishing this project. Your patience gave me room to finish at my own pace without feeling like a burden. Thank you.

In the same vein, I am thankful to my other committee members, Dr. Kimberly Meitzen and Dr. Clay Green, for their patience, flexibility, and understanding as well. Thank you for your help, feedback, and comments on this project. Mostly though, I deeply appreciate your willingness to stick with me until the very end.

I wish to express my sincerest gratitude to Dr. Alberto Giordano, Dr. Ron Hagelman, as Chair and Associate Chair of the Geography Department, and especially to Ms. Allison Glass-Smith for being quick to be concerned about my health as much as my academic performance. When I needed surgery during the second semester of graduate school, these people moved mountains to give me the space to recover without being overburdened by graduate assistantship duties. I am still amazed by the help and support that you gave me during that time. Even more than that, I am deeply grateful for Ms. Allison Glass-Smith's role in being my advocate during that time. I did not even have to ask for help, as soon as I explained my health condition, you jumped right to action in trying to help me. Words cannot express how supported I felt by you, and by extension, the whole department.

Taking time for my recovery from surgery would not have been possible without the help from the Geology teaching assistants and staff. Thank you to Dr. Rene DeHon for your flexibility and support. A special thanks to Ms. Barbara Grahmann, the Geology Lab Coordinator, and to Mr. James Lancaster and Ms. Taylor Christian, my fellow Geology Lab Instructional Assistants, for covering my labs when I needed to step out to recover from surgery. I am profoundly grateful for your willingness to help lift my burden by taking on extra work. I cannot imagine a more supportive team of people to work with.

Briefly, I would also like to thank Dr. Yongmei Lu for graciously granting me an extension in her class during my time of surgery and recovery. The support from all the people mentioned above from the Geography Department at Texas State University reflects the attitude of the entire department─ one that I am deeply grateful to have been a part of. This attitude of support and advocacy for the students is a large part of what makes the Geography Department at Texas State a very special place indeed.

I would express appreciation to the entire staff at TNRIS, especially to Mr. Richard Wade and Mr. Joey Thomas. Thank you for the unique opportunity to work with you, and especially for letting me utilize resources at TNRIS to finish this thesis. I am grateful for your support of my academic endeavors. I will miss working with everyone there.

Lastly, I cannot express the full indebtedness I have to my wonderful husband. Ben, you have sustained me throughout this long journey. Without your encouragement, support, caring, and way of pushing me forward at times, I cannot imagine finishing this project. Thank you for willingness to stay “in the trenches” with me, and for not letting me give up. I love you.

TABLE OF CONTENTS

LIST OF TABLES

LIST OF FIGURES

LIST OF ABBREVIATIONS

Abbreviation	Description
ILT	Interior Least Tern
SNH	Sandbar nesting habitat
MBC	Muddy Boggy Creek
Q_s	Sediment discharge
D_{50}	Median sediment particle size
Q or Q_{w}	Stream discharge (m^3/s)
S	Channel slope
USGS	U. S. Geological Survey
MAF	Mean annual flood ($Q_{2.33}$)
Ω	Gross stream power
γ	Specific weight of water (9800 N/m^3)
SSP	Specific stream power (ω)
W	Channel width
SS	Segment-scale
RS	Reach-scale
GLO	General Land Office

EROS	Earth Resources Observation and Science Center
TNRIS	Texas Natural Resources Information System
UOCSA	University of Oklahoma Center for Spatial Analysis
NAIP	National Agricultural Imagery Program
DEM	Digital elevation model
NED	National Elevation Dataset
USHCN	U. S. Historical Climate Network
SSURGO	Natural Resources Conservation Service's Soil Geographic Database
IHA	Indicators of Hydrologic Analysis
TNC	The Nature Conversancy
EFC	Environmental flow component
SC%	Silt-Clay percentage

ABSTRACT

The Red River along the Texas-Oklahoma border provides ideal Interior Least Tern (*Sterna antillarium athalassos*) habitat because of its wide river channel with large, open sandbars that are sparsely vegetated and close to aquatic food sources. Over the last century, tern sandbar nesting habitat along the Red River has been lost or gained in response to water resource projects, dams, reservoirs, floods, droughts, land cover changes, and invasive vegetation. This projects presents the spatial and temporal changes in tern sandbar habitat on a 170-km reach of the Red River below Denison Dam that have occurred since the 1890s. Specifically, this project investigates how the hydrology, land cover, sediment budget, channel geometry, sandbar area, and suitable tern habitat area has changed from the late 1890s to 2014. Historical surveys and aerial photography were used to map floodplain land cover and calculate channel geometry and sandbar area. Suitable tern sandbar habitat was delineated based on three main criteria: minimum distance of 76-m from tall trees or shrubs, no vegetation on sandbar, and minimum distance of 60-m from channel margins. Streamflow and precipitation data from this time period were used to assess hydrology changes, and sediment yield estimates were gathered from previous studies and compared to suspend-sediment gage information within the study area. Sandbar area was variable over the 118-year timeline, tending to increase when channel width and specific stream power increased. Suitable tern sandbar habitat overall decreased by about 0.7%, largely due to decrease in channel width and

increase in vegetated sandbar area. Lack of high flows after the completion of Denison Dam decreased specific stream power, allowing vegetation to encroach on sandbars, decreasing both channel width and suitable habitat area. These interrelationships between hydrology, land cover, sediment, channel geometry, sandbar area, and suitable tern sandbar habitat area will help inform future management policies for the Red River, as well as other threatened riparian bird species.

I. INTRODUCTION

Natural riparian zones, as interfaces between terrestrial and aquatic systems, are some of the most diverse, dynamic, and complex biophysical habitats on Earth (Naiman and Décamps 1997). The variety of habitats offered by riparian zones and floodplains is the result of the dynamic interaction between water and land that occurs with the variable hydrologic regime of the river. Flow variability, particularly flood pulses, can influence species diversity by its capacity to create heterogeneity within the riparian zone. These flood pulses connect the channel to various lentic, lotic, and semi-lotic water bodies within the floodplain, as well as transport nutrients and sediment across the floodplain (Junk, Bayley, and Sparks 1989; Bayley 1995). Many species have adapted to and benefited from the natural disturbance of the flood pulse (Junk, Bayley, and Sparks 1989; Lytle and Poff 2004). The fluctuation of river stage by this flood pulse creates an ever-changing mosaic of habitat patches, ecotones, and successional stages that is largely responsible for the high biodiversity of these systems (Allan 2004).

The high biodiversity of riparian zones can be seen in the example of the Mississippi River system. The riparian zone of the Mississippi River is home to over 60 different species of mammals, about 190 species of reptiles and amphibians, and about 100 species of birds (Naiman and Décamps 1997). Indeed, riparian zones provide important transitory habitats for migratory bird species. More species of birds are generally found in riparian habitats than in adjacent ones (Naiman and Décamps 1997). These migratory birds use sandbars within the active channel for breeding and nesting. Shallow-water habitats near sandbars provide an ample food source for these birds, and large channel widths offer protection from predators as these birds tend to nest some distance away from riparian trees. These migratory bird species depend on flood pulses within the natural disturbance regime to create suitable sandbar habitats for summer nesting. As flow regulation through impoundments and other water resource projects has been introduced to many of the rivers these migratory birds utilize, habitat loss has endangered many of these unique species. The reduction or alteration of the flood pulses on these rivers has changed the interaction of water, sediment, and vegetation that led to the diversity of habitats, including suitable sandbar habitat for breeding and nesting of migratory birds.

Interior Least Terns (*Stera antillarium athalassos*; ILT) is one of these endangered, migratory bird species that breed and nest along sandbars of large Great Plains rivers and other major tributaries of the Lower Mississippi River, including the Red River along the Texas-Oklahoma border (Lott and Wiley 2012a; Lott et al. 2013). ILTs select large, open sandbars on wide river channels that are sparsely vegetated and a suitable distance from large shrubs and trees. Historically, the rivers of the Great Plains and Lower Mississippi Valley provided ample sandbar nesting habitat (SNH), but decreased numbers in ILT populations in the 1980s led to concern about nesting habitat loss from increased water resource projects such as dams and reservoirs (Lott and Wiley 2012a; Lott et al. 2013). It was hypothesized that the filling in of reservoirs behind large dams and altered flow regimes decreased the amount or quality of SNH. However, it was recently recommended that the species be removed from the federal endangered species list as a result of recovery in population, largely due to resilience in the species (USFWS 2013). Populations have stabilized or expanded as ILTs have demonstrated meta-population dynamics by rapidly adjusting to colonizing anthropogenic habitats such as gravel pits, mines, and industrial sites (Campbell 2003; Lott et al. 2013). Regulation-era floods have remained effective at maintaining suitable SNH despite the severe alteration of channels and flow regimes, although the relationship between high flow events and sandbar characteristics remains uncertain.

Despite increases in populations of ILT, the relationships between sandbar characteristics and hydrology for many Great Plains rivers remain unclear. One of the biggest unknowns in current models for SNH is the lack of detailed understanding of how timing, magnitude, and duration of high flow events affect SNH availability (Lott and Wiley 2012a; Lott et al. 2013). Also missing is the understanding of the full range of past habitat conditions for ILT. Without such knowledge, it is difficult to understand how river management might affect ILT populations and how to best develop management strategies that will be effective in continuing to promote ILT recovery (Lott and Wiley 2012a).

Only recently have specific impacts of dam operations on ILT habitats been explored for many of the Great Plains rivers, and there is an emerging body of research on the controls of complex habitats such as sandbars, which are important for species of turtles, fishes, and other migratory birds as well as the ILT (Tracey-Smith, Galat, and Jacobson 2012; Stucker, Buhl, and Sherfy 2012; Alexander, Schultze, and Zelt 2013). Lott and Wiley (2012b) performed a survey of ILT nesting populations on the Red River below Denison Dam during the 2008 breeding season, which represents the largest below-dam ILT population. While it has been well-established that dams interrupt and alter most of a river's important ecological processes (Ligon, Dietrich, and Trush 1995), Lott and Wiley (2012b) observed more suitable SNH along the Red River below Denison

Dam than previously recorded, and noted that areas within this river segment that had the largest flooding risk to ILT nests were areas downstream of unregulated tributaries. These findings suggest that additional research on the Red River is needed to understand all the factors that are affecting the amount of SNH along these Great Plains rivers.

A majority of studies on the effects of dam operations to river ecosystems use flow as the "master variable" guiding the ecological health and integrity of the system (Poff et al. 1997; Poff and Zimmerman 2010). However, flow is not the only variable affecting the formation and maintenance of sandbars—just as important are changes in sediment supply, flow of nutrients, energy and biota, changes in floodplain land cover/use (Ligon, Dietrich, and Trush 1995; Julian et al. 2012), as well as broader geomorphic responses to dams such as channel widening/narrowing, increased/decreased lateral migration of channels, or change in channel pattern (Meitzen et al. 2013). Regulation-era flows seem to be effective at maintaining suitable SNH, but the exact relationships are still unknown. It appears that the understanding of how these other factors affect sandbar formation will be vitally important in parsing out the patterns and processes that control SNH for ILTs and other species.

It is difficult to understand and untangle patterns and processes in areas with complex and interdependent geomorphic controls (Julian et al. 2016). However, a long period of empirical data reflecting the historical range of variability of a river pre-impact and post-impact is useful in inferring these types of processes and patterns (Julian et al. 2012). This historical range gives the full range of past habitat conditions for the ILT, which aids in understanding the specific impacts of dams and other human modifications for ILT SNH. To document the geomorphic controls affecting ILT SNH, this study investigated the historical range of variability of streamflow, precipitation, sediment supply, changes in floodplain land cover, and channel geometry for a 170-kilometer reach of the Red River below Denison Dam. An upstream/downstream comparison of these factors was also performed to explore the impact that unregulated tributaries, namely Muddy Boggy Creek (MBC), have on ILT SNH.

II. THEORETICAL FRAMEWORK AND RESEARCH QUESTIONS

Theoretical Framework

A river's flow regime is important for sustaining biodiversity and ecological integrity (Poff and Zimmerman 2010), but habitat consists of a combination of physical and biological components that span across the disciplines of geomorphology, hydrology, and ecology (Meitzen et al. 2013; Julian et al. 2016). This study aimed at a more complete view of the physical-biological linkage in stream habitats by incorporating the interactions among hydrology, geomorphology, and ecology (Figure 1). Hydrologic regimes naturally vary across gradients of climate, geology, vegetation, and catchment size, while geomorphic setting varies geographically in response to geology and physiography (Poff, Bledsoe, and Cuhaciyan 2006). However, human-induced variation in the hydrologic and sediment regimes (from land use/cover change, flow regulation, and channel modification) are superimposed on these natural variations (Figure 1). Disentangling natural and human-induced sources of variation can be difficult (Poff, Bledsoe, and Cuhaciyan 2006), especially when feedbacks occur between variables (Julian et al. 2012). By using a long period of empirical data, as this study does, patterns can be assessed to infer channel processes. Since the range and variation of flows on a geomorphic setting over recent historical time sets a template for contemporary ecological processes (Poff and Zimmerman 2010), this approach will be useful in understanding the drivers and impacts of this historical range of variability.

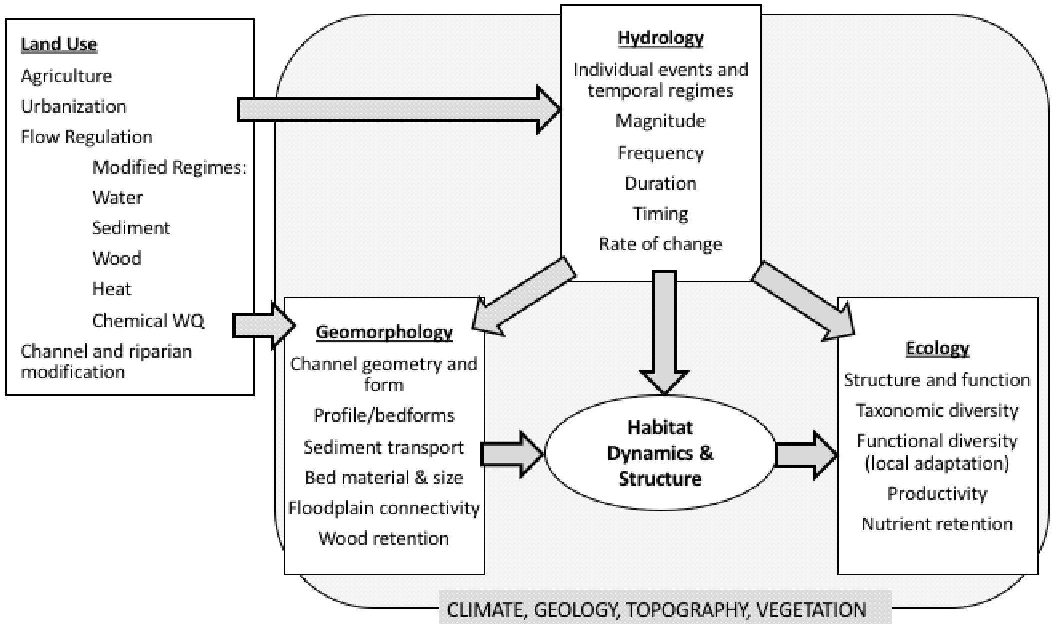

Figure 1. Conceptual illustration of the relationship between hydrology, geomorphology, and ecology of stream and river systems*. Land use and flow regulation modifies the hydrologic and geomorphic processes and, thus, induces ecological responses. Climate, geology, topography, and vegetation act as extrinsic controlling factors to hydrology, geomorphology, and ecology. Adapted from Poff, Bledsoe, and Cuhaciyan 2006.*

Feedbacks between riparian vegetation and channel width can be incorporated into a biogeomorphic response model (Figure 2) that shows the effects of hydrologic regime on vegetation and channel geometry. Knox (1972) developed a biogeomorphic response model to characterize sediment yield at the watershed scale, but with appropriate modification, this model can be used just as effectively to model changes in active channel width at the floodplain scale (Julian et al. 2012). Increased precipitation generally leads to increased vegetation and consequently less geomorphic work (Figure 2A and Figure 2C). Independent of decadal precipitation, large floods are a common phenomenon in Great Plains rivers (Figure 2B). These large floods can destroy mostly non-cohesive boundary materials of large Great Plains rivers, causing widening of the channel through bank erosion (Figure 2D) and removal of large areas of floodplain forest (Figure 2C).

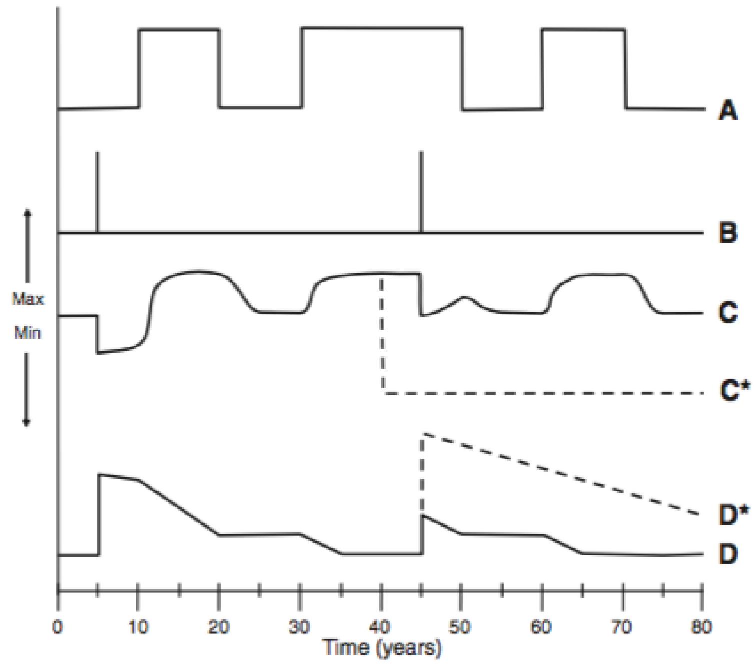

Figure 2. Biogeomorphic response model *of floodplain forest cover (C) and active channel width (D) of large Great Plains rivers in response to variable precipitation (A) and large floods (40-year return period in this case; B). Precipitation (wet versus dry period) and floods are independent variables and are independent of each other. Active channel width and floodplain forest cover are dependent variables and are dependent on each other through feedbacks; where increases in channel width from floods remove floodplain forests, and re-growth of floodplain forests, especially during wet periods, reduce channel width. C* and D* (dashed lines) represent a scenario in which all floodplain forests were cleared for agriculture in year 40. Model was based on the concept of Knox's (1972) biogeomorphic response model but modified with data and patterns from Julian et al. (2012).*

The active river channel begins to narrow following an erosion event, with the rate of narrowing dependent on the rate of encroachment by floodplain vegetation and the variability of sediment erosional/depositional events (Friedman et al. 1998). In the absence of another large destructive flood, the channel will narrow relatively rapidly due to reduced specific stream power (SSP), and then relatively slowly as it approaches its pre-flood width. The amount of channel widening is inversely related to riparian forest cover and riparian forest cover is likewise influenced by changes in channel width. If the riparian forest is removed, such as for agriculture (Figure 2C*), large floods will result in extraordinary channel widening due to the decreased resistance of non-forested banks (Knighton 1998). With less riparian forest for encroachment, channel narrowing will occur more slowly. All of these changes in channel width will have feedbacks on SSP, which in turn, will have feedbacks on riparian vegetation and channel width.

This study used the theoretical framework of the biogeomorphic response model espoused by Julian et al. (2012) to interpret results. While Julian et al. (2012) investigated many of the same variables examined in this study (floodplain land cover, channel geometry, soil composition, and SSP), they did not assess how these biogeomorphic interactions dictate habitat. This study aimed to explore how the interrelationships between hydrology, geomorphology, and ecology, with the imposed human-induced modifications (Figure 1) can be fitted to a biogeomorphic response model (Figure 2) to assess critical habitat. This expands the biogeomorphic response model used by Julian et al. (2012) to include ecological responses as well as hydrological and geomorphological responses to changes in river systems, and tests its usefulness in assessing critical riparian habitat.

Research Questions

The objective of this investigation was to use the Red River below Denison Dam from 1896 to 2014 as a case study to explore the interrelationships among flow, vegetation, land cover, channel geometry, sediment, and sandbar area in order to define the drivers and patterns of critical habitat for the endangered ILT. The guiding research question of this thesis was: How does sandbar habitat change over space and time in response to interdependent changes in flow, vegetation, land cover, sediment, and channel geometry? This ultimate question was resolved by answering the following series of research questions:

1) How has the flow regime of the Red River below Denison Dam changed over the period 1896 - 2014?
2) How has land cover in its floodplain changed over the same period?
3) How has the sediment budget changed over this period?
4) How has channel width, slope, and sandbar area changed along this reach over the same period?
5) How has ILT habitat changed over space and time in response to the above factors?

By answering each of these research questions with respect to a long period of data, channel processes and the interrelationships between streamflow, channel geometry, floodplain vegetation, and sandbar area was inferred. These processes and interrelationships were then used to gain an understanding of the broader impacts each of these factors has on ILT SNH, which in turn helps inform future management policies for critical habitat along large regulated river-floodplain systems.

III. BACKGROUND

Great Plains Rivers

The Great Plains of the United States encompasses the area from the Prairie Provinces of Canada to the Rio Grande, and from the Rocky Mountains to approximately the 96^{th} meridian, including the majority of ten U.S. states: Colorado, Kansas, Montana, North Dakota, Nebraska, New Mexico, Oklahoma, South Dakota, Texas, and Wyoming (Costigan and Daniels 2012; Drummond et al. 2012). The region is semi-arid and historically dominated by grassland biomes. Omernik and Griffith's (2014) Level I ecoregion definition describes the dominant vegetation pattern as shortgrass steppe in the west, mixed-tallgrass prairie in the central portion, tallgrass-woodland in the east, and forests in the floodplains of large rivers. The Level III ecoregions provide more detail on specific vegetation communities and their relationship with ILT nesting sites (Figure 3).

The rivers and floodplains of the Great Plains are some of the most dynamic in the world (Matthews et al. 2005). Most rivers in the region flow eastward and eventually drain into the Mississippi River. Channels tend to be wide and sand-bedded with high turbidity (Costigan and Daniels 2012). Planforms range from semi-braided to meandering.

Most of the Great Plains rivers have experienced considerable flow reductions from anthropogenic activities such as the construction of flood-control impoundments, unsustainable groundwater extraction practices, and irrigation (Graf 2001). It can be difficult to differentiate between climatic and anthropogenic sources of hydrologic alteration of Great Plains rivers due to the varying climate throughout the region (Costigan and Daniels 2012).

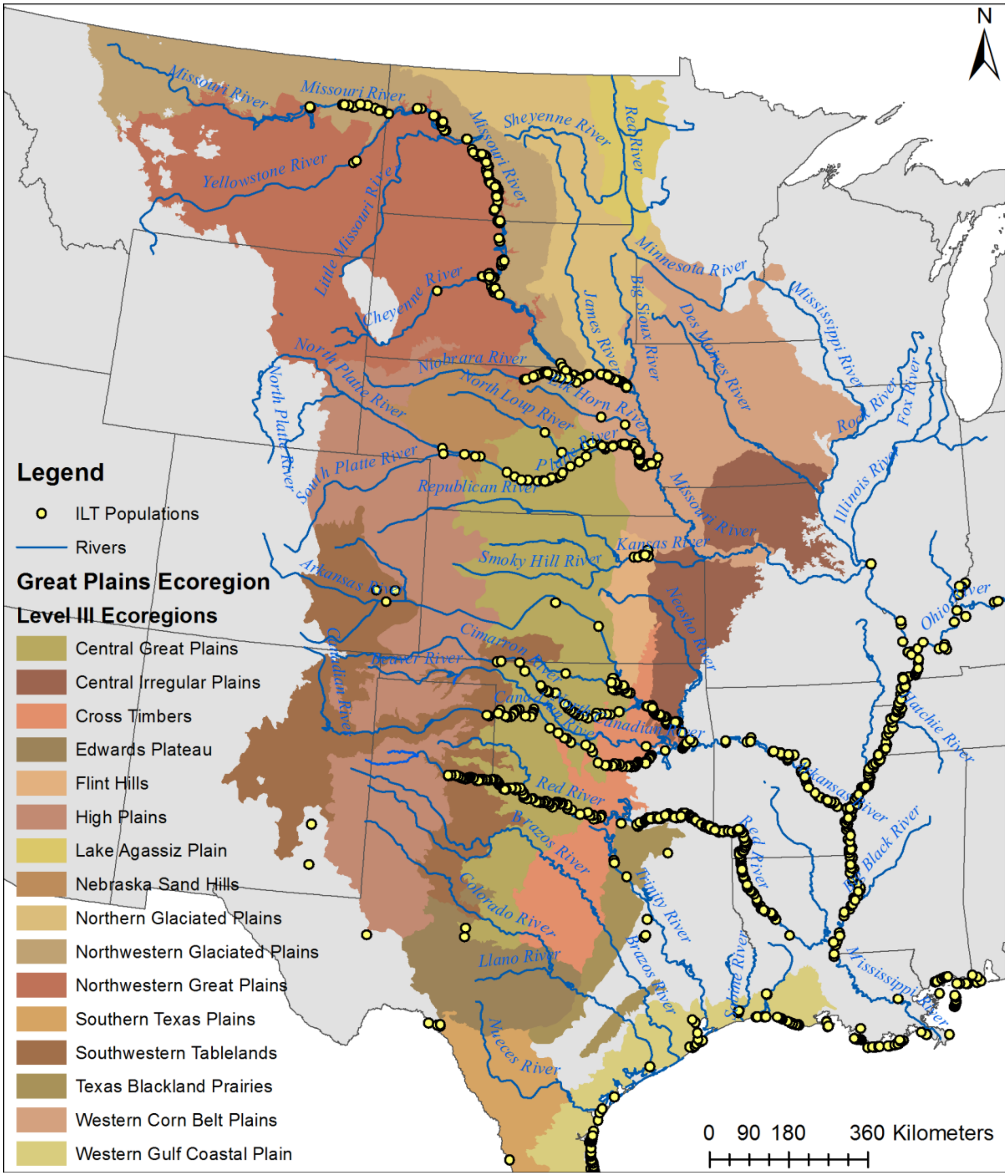

Figure 3. Level III ecoregions of the Great Plains. *Major rivers shown with ILT populations indicated by the yellow dots. Ecoregion data from USEPA (2005) and ILT population data from Lott et al. (2013).*

The Great Plains ecoregion sits in the semi-arid rain shadow of the Rocky Mountains, which produces characteristically flashy flow regimes, with large floods intermixed with periods of prolonged drought (Dodds et al., 2004; Costigan and Daniels 2012; Drummond et al. 2012). There is a west to east gradient of increasing precipitation (~25-125 cm) across the region (Drummond et al. 2012). River systems in the more southern portion of the Great Plains are also influenced by monsoons, hurricanes, dry line thunderstorms, and summer droughts.

Frequent intermittence of smaller streams, historic high flood frequencies with low predictability, periodic episodes of extreme drought that produce long periods of no flow, and high sediment loads and turbidity are aspects of the hydrologic regime of Great Plains rivers in which the local assemblage of aquatic fauna has adapted (Dodds et al. 2004; Costigan and Daniels 2012). However, this natural range of hydrologic extremes is being altered, not only by global climate change, but also by anthropogenic activities mentioned above and the widespread conversion of watershed land cover from grassland to agriculture (Drummond et al. 2012).

The response of riparian ecosystems to anthropogenic alterations in the Great Plains region is also complex (Friedman et al. 1998). For example, the construction of dams on the Missouri River has stopped the meandering of the river and formation of new point bars, and existing riparian cottonwood forests are being replaced by forests of later successional species (Johnson 1999). The Missouri River has been straightened and dredged for navigation, which also prevented the formation of sandbars (Tracey-Smith, Galat, and Jacobson 2012). On the Platte River, flow regulation, and the loss of natural flood disturbance, has promoted early successional processes and caused an increase in cottonwood forests and open channel areas are being replaced by cottonwood and willow woodlands (Johnson 1999). Downstream cottonwood forests have decreased along streams in Alberta, but have increased along streams in Nebraska and Colorado (Friedman et al. 1998). Most of the region's large rivers have narrowed due to floodplain vegetation encroachment in the active channel following flow reduction (Friedman et al. 1998; Julian et al. 2012), but there are examples that run contrary to this assertion. Friedman et al. (1998) points to studies on the Canadian River, Colorado River, Des Moines River, and Neches River that found no channel narrowing downstream of dams. This variety of dam effects highlights the importance of local processes that vary from river to river. Therefore, while generalizations can be made for Great Plains rivers, each river-floodplain system is dependent on its unique biological, hydrological, and geomorphic interactions (Julian et al. 2016).

Sandbar Habitat

Sandbars

A sandbar is a raised portion of a river bed that represents an accumulation of sediments within the channel, with substrates ranging in size from silt to boulders (Charlton 2008). Sandbars differ from islands in vegetation and permanence: sandbars have sparse plant cover, little or no woody vegetation, and are transient, while islands have woody riparian vegetation and tend to be more permanent features (Ward et al. 2002). Sandbar morphology is determined by the interaction among channel geomorphology, sediment transport, and river flow. Surface areas of sandbars fluctuate with cycles of erosion and deposition depending on flow magnitude and duration, tributary sediment supply, amount of sand stored in river channel, and local channel hydraulics (Tracey-Smith 2006). The fluctuation in water surface elevation changes the shape and location of the sandbar edge and defines areas that alternate between aquatic and terrestrial environments by this "moving littoral" (Junk, Bayley, and Sparks 1989). The dynamism of these aquatic/terrestrial environments on sandbars creates unique habitats for a variety of species including softshell turtles, shorebirds, and riverine fishes (Tracey-Smith 2006).

Sandbars can refer to point bars, mid-channel bars, or side bars. Point bars are deposited along the convex side of a migrating stream bend as the meandering stream strives towards equilibrium by compensating for channel widening (Saucier 1994). Point bar formation is a continual process, with a new increment of bar development from the stream's bed load deposited during each major high-stage event. The rate of bar formation differs greatly from reach to reach in a given river system, and even more so between different rivers.

There are two main types of mid-channel bars: longitudinal and transverse. Longitudinal bars are formed separate from the channel margins in areas of deposition of coarse material, usually in the center of a riffle (Hooke 1986). The longitudinal bar gradually extends over time, usually in the downstream direction. Like with point-bars, high flow events are important in longitudinal bar development. In later stages of development, a longitudinal bar may grow into a side bar as flow on one side of the bar increases and one channel becomes dominant. Eventually, the minor channel clogs with sediment and the former longitudinal bar becomes attached to the floodplain. While point bars are generally found in the convex side of most river bends, longitudinal bars tend to be associated with zones of mobility in the channel and noticeably absent from longer, stable sections (Hooke 1986). Longitudinal bars can also be more transient than point-bars, completing their whole cycle of development in a period from 5 to 15 years (Hooke 1986).

Transverse bars are lobe-shaped bars with relatively steep downstream faces. They tend to migrate downstream by the accumulation of sediment on the steep, lee face of the bar, as well as the sides, causing them to also expand laterally in the downstream direction (Smith 1971). Transverse bars form in a similar way to longitudinal bars, but tend to be found more commonly in braided streams (Smith 1971; Charlton 2008). However, they can also be found downstream of confluences, where flow separation occurs, and where there is an abrupt channel expansion (Charlton 2008).

Vegetation can play an important role in encouraging deposition on bars, but hydrogeomorphic processes (inundation, sediment erosion and deposition) provide disturbance mechanisms that prevent some mid-channel bars from stabilizing into a permanent wooded island (Tracey-Smith, Galat, and Jacobson 2012). Point bars, longitudinal bars, and transverse bars are utilized by ILT for SNH, so this study investigated all types of bars under the generic, umbrella term of 'sandbar.'

Sandbar Nesting Habitat Characteristics

SNH provides the physical and biological resources necessary to sustain ILT populations (Lott and Wiley 2012a). The term "emergent sandbar habitat" has also been widely used (i.e. Alexander, Schultze, and Zelt 2011), focusing on the land-cover type of bare sand above water levels. However, this definition can overestimate suitable ILT habitat because ILT only nest on portions of sandbars that remain above fluctuating water levels for the entire breeding season (Lott and Wiley 2012a; Lott et al. 2013). Lott and Wiley (2012a) identified five main criteria for ILT SNH, which Lott et al. (2013) summarize as follows: 1) sandbar elevation, 2) distance from large trees or shrubs greater than two meters high, 3) distance from channel margins, 4) absence or paucity of sandbar vegetation, and 5) the availability of small fishes within ten kilometers of areas that meet criteria 1-4.

Lott and Wiley (2012a) identified sandbar elevation as the primary factor of SNH availability. For successful ILT reproduction, sandbars must remain exposed for the entirety of the egg laying, incubation, and flightless chick-rearing periods of ILT life history, which takes place from May to August (Lott et al. 2013). Within this time period, ILTs need about 42 consecutive days that the nest is exposed above water levels for the most successful reproduction. Even though low elevation areas of sandbars may appear as bare sand, ILTs will avoid nesting in these areas because they are regularly inundated with high flows during the breeding season (Lott et al. 2013). ILTs rarely nest near trees or shrubs that are taller than two meters, as these features can provide cover for predators. Bluffs, bridges, power lines, and other tall structures, besides trees, that could provide perches for avian predators are also given this wide margin by ILTs. The distance given to these objects by ILTs varies slightly by river. Along the Missouri River, ILTs rarely nest within 150 meters of trees and other tall objects, but along the Platte River, the limit of SNH is only 76 meters (Lott and Wiley 2013). When surveying ILT nests along the Red River, Lott and Wiley (2012b) applied the criterion 76 meters from trees when determining whether part of a sandbar was suitable SNH. For consistency, this study applied the same criterion when determining habitat. In general, most ILT nesting colonies were located on sandbars in channels that were at least 300 meters wide and greater than 60 meters from channel margins, regardless of whether the banks had trees or not (Lott and Wiley 2012a; Lott and Wiley 2012b; Lott et al. 2013).

ILTs also avoid portions of sandbars that are covered in low vegetation, preferring areas of bare sand that are less than 30 percent covered by vegetation (Lott et al. 2013). Lott and Wiley (2012a) considered any portion of sandbars less than about 15 meters away from low sandbar vegetation as "unsuitable" habitat. This avoidance of sandbar vegetation means that during periods with few floods, vegetation succession can render otherwise good SNH as unsuitable. However, the data on either distance from low sandbar vegetation or percentage of vegetation cover is not considered reliable, especially since the percentage of vegetation cover varies extensively by time of year and field methodology (Casey Lott, VP for Conservation Information Synthesis at the American Bird Conservancy, 2 February 2015, personal communication via e-mail). Therefore, this study did not apply a distance criterion for vegetation on sandbars, but merely discounted any portion of a sandbar with vegetation as "unsuitable" habitat.

The availability of small fishes near nesting sites depends on the availability of shallow-water environments near sandbars. Stucker, Buhl, and Sherfy (2012) investigated shallow-water habitat characteristics that supported fish communities for the Missouri River, which has seen a decline in shallow-water habitats near sandbars. They found a strong negative relationship between water depth and the relative abundance of fish and inferred that channel incision, decreased sediment loads, and manipulated flows from dam operations reduce the tendency of the river to retain areas of shallow-water habitats.

However, Lott and Wiley (2012a) declared that food resources would unlikely be a limit on ILT population, at least on the Arkansas and Red Rivers, as they found a large variety of foraging microhabitats that were available in close proximity to ILT nesting sites on these rivers. Therefore, food availability criteria for SNH was not evaluated in this study.

Effects of Dams and Flow Regulation on Rivers

The effect of dams and flow regulation on rivers has been well documented. Dams designed for flood control or hydropower can alter sediment transport dynamics (Williams and Wolman 1984, Ligon, Dietrich, and Trush 1995; Wohl 2014), the natural flow regime (Poff et al. 1997; Graf 2001), channel and vegetation dynamics (Petts 1984; Gordon and Meentemeyer 2006), and increase fragmentation across the landscape (Ward and Sanford 1995; Ward 1997; Graf 2001; Wohl 2014). Dams usually cause channel degradation and narrowing immediately below the dam (Petts 1979; Williams and Wolman 1984) due to inadequate sediment loads that causes erosion as sediment becomes trapped behind the dam (Ligon, Dietrich, and Trush 1995; Graf 2006). Large dams can severely impact hydrology further downstream, especially in rivers that naturally have high annual variability, which is the case for Great Plains rivers (Graf 2006). Friedman et al. (1998) expounded on the effects of dams on Great Plains rivers, which include narrowing, decreased rate of migration, increased bank erosion, and channel deepening. According to Friedman et al. (1998), “the diversity of dam effects occurs because channel response is mediated by processes that vary in importance from site to site.” Therefore, while it is well-established that dams and flow regulation alter river channels, the exact responses vary from river-to-river. The Great Plains region has some of the greatest surface water impacts, making the region most likely to experience the greatest changes in river systems due to dams (Graf 1999). Consequently, the downstream effects of dams for the Great Plains regions continues to be researched and debated.

Dam Effects on Flow Regime

The natural flow regime of a river is connected to both the geomorphology and ecological integrity of a river (Poff, Bledsoe, and Cuhaciyan 2006) (Figure 1). Any change in the magnitude, frequency, duration, timing, or rate of change of a river's flow from its natural variation can affect water quality, energy sources, physical habitat, and biotic interactions in a river system with profound effects on the overall structure and function of these riverine ecological habitats (Poff et al. 1997; Poff, Bledsoe, and Cuhaciyan 2006). Dams can alter all of these aspects of flow regime, depending on the size of the dam and the size of the river. In general, dams on large rivers alter the natural flow regime by reducing or eliminating floods (Poff et al. 1997), increasing low flows, and altering the timing of peak and low flows (Juracek 2000; Graf 2006). While eliminating peak flows is good for the purposes of flood control, it can be detrimental to habitats and organisms that have adapted to a particular disturbance regime (Lytle and Poff 2004; Poff and Zimmermann 2010).

ILTs specifically benefit from a highly variable disturbance regime because they need high-flow events that can carry sediment to form and maintain sandbars as suitable SNH, but then they need summer low-flows during their actual nesting season. Unfortunately, reduced flood peaks, increased low flows, and altered timing of peak and low flows created by dams all affect ILT SNH.

Dam Effects on Sediment

Sediment in rivers is transported mostly as suspended load: clay, silt, and fine-medium grained sand held afloat in the water column by turbulence (Leopold, Wolman, and Miller 1964). Bedload consisting of coarse sand, gravel, cobbles, and boulders transported by rolling, sliding, or bouncing along the river bed generally makes up only a few percent of the total sediment load in lowland rivers. However, the arrangement of bedload sediments forms the "architecture" of sand- and gravel-bed channels (Kondolf 1997). A reduction in the supply of these channel-forming sediments may result in channel changes. Dams do not only affect sediment transport by physically trapping sediment behind structures, but also by reducing flood flows as most sediment transport occurs during floods (Kondolf 1997). Floods are responsible for most of the sediment transportation within a channel. Floods also control the building of new lands (lateral channel migration) by depositing large quantities of sediment (Sanford 2002). When dams reduce the frequency and magnitude of floods, bank erosion still occurs leading to degradation, and sometimes to widening of the river channel, with segments of aggradation further downstream.

The rate of sediment transport typically increases as a power function of flow (Kondolf 1997). Water released from dams possesses enough energy, or capacity, to move sediment, but has little or no sediment load to carry. This results in a "hungry water" effect where the excess energy is typically expended eroding the channel bed and banks downstream of the dam, resulting in channel incision and coarsening of the bed

(Kondolf 1997; Graf 2006). The hungry water flows do not always have the stream competency to entrain larger particles from the stream bed, which can create an armor layer that may continue to coarsen. This would limit the ultimate depth of incision, although the magnitude of incision depends also on reservoir operation, channel characteristics, bed-material size, and the sequence of flood events following dam closure (Kondolf 1997). With vegetation encroachment, this degradation can result in channel narrowing (Juracek 2000), however, bed armoring could cause the river to erode laterally instead of vertically, thus resulting in channel widening. The type, rate, duration, and downstream extent of channel degradation is controlled by numerous factors including discharge, sediment load, bank material composition, local bed-elevation control, channel geometry, climate, tributary in-flow, and vegetation.

Sediment and sediment-related processes help define the physical habitat template for riverine ecology (Wohl et al. 2015). This includes channel morphology, bed conditions and heterogeneity, disturbance regime, community structure, and water quality. Sediment conditions and various size distributions are important for riparian plants as well as many aquatic and riparian organisms (Wohl et al. 2015). Although river response to changes in sediment regime can occur at differing scales than the response to changes in the flow regime (Julian et al. 2016), the alteration of a river's sediment regime can be just as damaging to a river's ecological integrity as the alteration of its flow regime.

Dam Effects on Channel Geomorphology and Vegetation

The geomorphology of a river channel can have numerous responses to dams and flow regulation. Channel incision or aggradation, channel widening or narrowing, increased or decreased lateral migration channels, and streamed coarsening or fining are types of major geomorphic response to dams (Ligon, Dietrich, and Trush 1995; Friedman et al. 1998). Channel pattern can change, such as a braided or meandering river becoming single-threaded, or vice versa. Loss of riparian vegetation, riparian encroachment in active channels, and bank collapse can also occur in response to flow regulation (Ligon, Dietrich, and Trush1995). As Figure 1 shows, the geomorphology of the channel can affect habitat dynamics and structure, which in turn, affects riverine ecology.

In the Great Plains region, the most common planform changes resulting from dam construction are channel-narrowing and reduction in channel migration rates (Friedman et al. 1998). Vegetation may become established on the channel banks or bed if a dam reduces peak flows below that necessary to rework the entire channel bed. This new vegetation promotes deposition of cohesive fine sediment and increases resistance to erosion, thus stabilizing the channel at a narrower width. Reduction of peak flow and sediment load by dams can also impact the rates of bank erosion and bar deposition and lead to channel migration (Friedman et al. 1998). Channel migration may be exacerbated by channel incision resulting from sediment starvation in certain reaches of the river.

The initial channel pattern influences the relative importance of channel-narrowing or reduction in channel migration downstream from dams (Friedman et al. 1998). For example, braided streams tend to experience extensive channel-narrowing below dams. Their wide, aerially exposed bed provides large areas suitable for vegetation establishment, and large floods can typically destroy the non-cohesive banks common to braided stream systems (Friedman et al. 1998; Johnson 1999). This effect can be seen on the Platte River where reduced spring flows from flow regulation provided suitable conditions for seedling establishment across the braided channel. This led to the transformation of a wide, braided systems largely devoid of woody vegetation to a narrow, single thread channel with dense alluvial forest corridors (Ward and Sanford 1995; Johnson 1999). Indeed, channel widths on the Platte River have decreased overall from 1858 to 2006, and channel area decreased by an average of 46 percent from 1938 to 2006, although there were short-term increases from 1993-1999 (Horn, Joeckel, and Fielding 2012).

On the other hand, because the width-depth ratio for a meandering stream is small, the area made available for vegetation establishment during channel-narrowing is relative small (Friedman et al. 1998). Therefore, decreases in sediment load downstream from dams often causes erosion and channel widening in meandering channels. This was seen in the Missouri River, where the stabilization of the meandering channel created unsuitable environments for the establishment of new forest (Johnson 1999). Although the construction of dams reduced peak flow on the Missouri River, the total annual flow has not changed significantly, which has stopped the meandering of the river and the formation of new point bars. While braided streams like the Platte River tend to respond to flow regulation by channel narrowing and woodland expansion, meandering streams like the Missouri River respond by the reduction or cessation of channel migration, and sometimes by channel widening (Friedman et al. 1998; Johnson 1999).

Dam Effects on Sandbars

Dams can affect the distribution and morphology of sandbars along a river through its effects on both the sediment regime and flow regime. Large dams reduce flood magnitudes and frequencies as well as the amount of sediment available for deposition which can limit sandbar creation (Fischer, Paukert, and Daniels 2015). Reduced peak flows, especially the frequency of such flows, can also reduce the disturbance regime and lead to encroaching vegetation on sandbars. Sanford (2002) investigated dam impacts specifically on sandbars for the Missouri River, and found that sandbars tended to be larger, less clustered, and migrated more under a natural flow regime. The gradual disappearance of mobile sandbars on the Platte River has been attributed to the restricted sediment influx and discharge caused by numerous dams and diversion canals (Horn, Joeckel, and Fielding 2012).

Hydropower operations of a dam can also affect sandbars. When newly formed sandbars are repeatedly saturated for several hours each day then exposed to rapidly falling water levels, there can be intensified rates of undercutting and slab failure which serves to increase erosion (Knighton 1998). This process can lead to particularly steep banks on the high-energy thalweg margin of sandbars as well as reducing the size and persistence of sandbars (Lott and Wiley 2012a). Vegetation cannot be established on many sandbar shorelines since plants either have their substrate eroded from beneath them, their seeds re-suspended and transported prior to germination, or their young roots removed by flow forces. However, the effect of peak hydropower releases on plant establishment changes downstream from dams. The effects of hourly flow variation are attenuated with increasing distance such that many miles downstream from dams regular, short-term high releases for hydropower can turn into relatively consistent waterline elevations during the week of hydropower operations, followed by a short-term decrease in stage when hydropower releases are not operating on the weekend, with a return to consistent waterlines for the next week of hydropower operations (Lott and Wiley 2012a). This pattern favors the growth of vegetation that can tolerate periodic desiccation on shoreline sandbars. Herbaceous vegetation that can grow in these conditions serves to stabilize the sandbar and may prolong its persistence.

Dam Effects on Ecology and Habitat

The downstream alteration of water and sediment flux produced by dams also modifies biogeochemical cycles as well as the structure and dynamics of aquatic and riparian habitats (Poff and Hart 2002). Water released from dams is often a different temperature than the water downstream of the dam structure. This abrupt change in water temperature can influence organismal bioenergetics and vitality rates, and greatly modify the densities and kind of species present. This thermal alteration and biological disruption can persist for tens of kilometers downstream, depending on downstream tributary in-flows (Poff and Hart 2002).

Dam structures also create barriers to the movement of water, resources, and organisms between channel, aquifer, and floodplain, which limits connectivity or exchange (Ward and Sanford 1995; Poff and Hart 2002). High connectivity in river systems is maintained by a natural disturbance regime— floods. Natural disturbance regimes, or in this case, natural flood regimes, can provide many ecological benefits including providing fish and other organisms access to floodplain habitats used for feeding, spawning, and rearing, maintaining and rejuvenating plant habitats in riparian zones and the floodplain, importing woody debris and organic material into the channel, refreshing water quality conditions, and helping transfer nutrients (Fitzhugh and Vogel 2011). High flows just below flood stage can also move sediment through the channel, provide respite for organisms, and improve connectivity to upstream and downstream habitats. Dams can disrupt the frequency, intensity, and timing of these natural flood regimes, thereby impacting the connectivity and ultimately the ecological integrity of the river system (Ward and Sanford 1995).

The dam structure itself can limit upstream-downstream connectivity, while the reduction in the magnitude of peak flows can reduce lateral connectivity between the main channel and floodplain. Severed connections can cause reduced recruitment of riparian species and reduced access to floodplain habitats for fishes (Poff and Hart 2002). Extensive fragmentation of river systems can also result in ecosystem isolation and prevention of exchange among isolated populations.

The reduction in annual floods can also affect scour and sediment deposition, allowing riparian vegetation to encroach onto parts of the active channel (Williams and Wolman 1984; Gordon and Meentemeyer 2006). Changes in vegetation dynamics, as well as long-term storage and non-seasonal release of floodwaters, can severely impact food webs and aquatic productivity (Poff and Hart 2002), and can facilitate invasions by non-native species (Fitzhugh and Vogel 2011).

Wolman and Leopold (1957) found that floodplains of rivers flowing through diverse physiographic and climatic regions are typically inundated by channel overbank flows about once per year. Annual overspill creates various lentil, logic, and semi-logic habitats throughout the floodplain (Ward and Sanford 1995). Habitat diversity is created by spatio-temporal heterogeneity as well as by different stages of development of different water bodies. The reduction of flood peaks by dams reduces the frequency, extent, and duration of floodplain inundation. This can cause the replacement of productive pioneer species by less productive upland species. It also reduces the channel-forming flows which causes decreased channel migration, truncated sediment transport, disrupted frequency of flooding, altered successional pathways, and imposed equilibrium conditions on non-equilibrium communities (Ward and Sanford 1995). All these responses lead to a decrease in habitat heterogeneity, productivity, and biodiversity of the floodplain ecosystem.

In specific regards to ILT SNH, timing, magnitude, and duration of high flow events are critically important in creating and maintaining suitable SNH. Reduced flood peaks and increased low flows can allow vegetation succession on sandbars and render areas unsuitable for nesting. Altered timing of peak and low flows might either encourage vegetation succession before nesting season or wash out nests during the season. Although not an issue along the Red River, altered flow regimes can cause declines in shallow-water habitats near sandbars, affecting the availability of small fishes for ILT (Stucker, Buhl, and Sherfy 2012). Lastly, sandbars that are repeatedly saturated for several hours each day then exposed to rapidly failing water levels due to hydropower operations, become suitable SNH either by erosion of the sandbar itself, or simply through exclusion of the area by ILT.

Effects of Land Use Change on Rivers

Downstream changes in hydrology and geomorphology can also result from land use changes in the contributing watershed in addition to the impacts of dams and reservoirs. When the existing balance between land cover and climate is disrupted, a river system can experience significant changes in erosion, sediment transport, and channel morphology (Knox 1977). Human-induced land-use changes can affect fluvial systems in several ways, including the reduction or increase of water and sediment discharge, both of which can lead to various channel responses (Schumm 2005). Under cultivation and other agricultural activity, soil erosion rates can increase by an order of magnitude or more (Walling and Webb 1996), which can in turn impact the sediment load (Walling 1999; Sanford 2002; Foley et al. 2005). Streams in Wisconsin showed evidence of increased flooding, erosion, and sedimentation in response to post-1830 deforestation and cultivation of hillslopes (Knox 1972; 1977). Grassland watersheds can retain sediments and nutrients much more efficiently than cropland, so a watershed dominated by row-crop agriculture may experience substantial sedimentation and eutrophication of downstream reaches (Dodds et al. 2004). This effect is compounded by the fact that globally, there has been about a 12 percent increase in cropland area and about a 70 percent increase in irrigated cropland area (Foley et al. 2005). Up to approximately 40 percent of global croplands may also be experiencing some degree of soil erosion or overgrazing. Deforestation and overgrazing associated with increased agriculture can also increase sediment supply and widen channels (Wohl 2014). The growth of urban areas and the associated increase of impervious surfaces have similar effects (Trimble 1997; Wohl 2014). However, it can be difficult to determine the magnitude of land use change impacts due to entangling effects of climate change, feedback loops, and non-linear relationships (Knox 1977; Walling 1999; Julian et al. 2012). A long period of empirical data, though, can aid in inferring these interacting processes and patterns.

Land cover in the Great Plains region was once 81 percent grasslands, 13 percent hardwood deciduous forest, 3 percent sagebrush grasslands, and about 1 percent surface water (Johnsgard 1978). However, almost 95 percent of the grassland prairie of the Great Plains region has been converted into agricultural land or urbanized (Dodds et al. 2004). Today, the Great Plains region is a mosaic of rangeland, dryland farming, and intensive irrigated and industrial agriculture (Drummond et al. 2012). The contemporary dominant land cover types are grassland and agriculture, together accounting for about 89 percent of the total land cover of the Great Plains region. Along the Red River floodplain valley, what was once a mix of pine and hardwood forests (Omernik 1987; USEPA 2005), has now been converted to mostly pasture and cropland.

Sediment Supply Changes

Sediment yield is the total amount of sediment that exits a drainage basin over a given time period. Climate, drainage basin area, topography, soils, geology, and human activity can all affect sediment yield of a river (Charlton 2008). Land cover change from natural vegetation to cropland can increase soil erosion rates by an order or magnitude or more, which could lead to increased sediment transport by local streams (Walling and Webb 1996; Walling 1999). Damming, the building of artificial levees, and other river control works also contribute to changes in river sediment loads, besides land use or land cover change (Allison et al. 2012). Generally, damming and other river control works attribute to a declining suspended sediment load. Other factors affecting sediment supply include: tributaries that carry sediment to the main stem river, bank erosion, floodplain accretion from overbank flows, dredging, and land-use practices that promote erosion (Sanford 2002).

The sediment load is important in river systems for maintaining channel shape (Leopold 1997). An important balance exists between sediment supply and the ability of water to carry it. This balance has been described by Lane (1955) with the equation:

$$Q_S \times D_{50} \propto Q_w \times S \qquad (1)$$

where Q_s is sediment discharge, or sediment load, D_{50} is median sediment particle size, Q_w is stream discharge, and S is channel slope. If additional sediment is added to a stream without a change in the water discharge (the left side of Equation 1 becomes greater), the channel will aggrade with net deposition occurring along the reach (Lane 1955). This causes the channel slope to become steeper, increasing the transport capacity to balance the sediment supply (Lane 1955). On the other hand, if water discharge exceeds what is needed to transport the sediment load, the excess energy erodes the channel and the channel degrades (Lane 1955). Degradation can be caused by an increase in discharge and/or channel slope, or by a decrease in sediment supply and/or size.

Sediment is not only a vital component of river systems in terms of channel shape and stability, but also affects the physical habitat template of riparian ecosystems (Wohl et al. 2015). Many aquatic and riparian organisms depend on certain sizes and size distributions of bed materials for various life stages, and some aquatic organisms may have life history timing adapted to the typical timing of bed disturbances. Suspended sediment and turbidity can also influence food webs and water quality (Wohl et al. 2015).

Sediment conditions are important for riparian plants as well. Fine-sediment patches are commonly key colonization sites, and plant scour is strongly influenced by size-dependent scour of surrounding substrates.

Grain sizes can also influence moisture retention rates. When sediment conditions affect riparian plant communities, especially the distribution of these communities, this can in turn affect channel form. Vegetation on the banks and beds of river channels can increase erosion resistance and promote narrower channels than non-vegetated banks (Julian and Torres 2006).

The Red River has one of the highest suspended-sediment loads in the United States (Albertson and Patrick 1996). The high sediment discharge contributes to its complex, active meandering and results in rapid deposition of point bars. Copeland (2002) estimated the total sediment inflow at the U.S. Geological Survey (USGS) gage site at Arthur City, TX (which is within the study area of this study) to be about 14.32 billion tons per year, with an average annual deposition rate of about 4.954 million tons. Allison et al. (2012) estimated a water budget of 70 cubic kilometers per year entering the Mississippi River from the Red River, with a total suspended load from the Red estimated at about 36.8 million tons per year. Allison et al. (2012) also noted progressively declining sediment loads in the Lower Mississippi-Atchafalaya river system since the 1950s.

Channel Geometry Changes

The combining effects of flow regulation and land cover change can result in various changes in channel geometry (Julian et al. 2016). Channel adjustments, including width, depth, and gradient, can be achieved by channel degradation, channel aggradation, or changes in channel pattern and shape (Juracek 2000). In the Great Plains region, the most common planform changes are channel-narrowing and reduction in channel migration rate (Friedman et al. 1998). However, channel pattern and river type can cause differing planform channel changes. For example, braided streams like the Platte River have narrowed in response to dams, while meandering streams like the Missouri River have responded to flow regulation by a reduction in channel migration (Friedman et al. 1998; Johnson 1999). Along the Red River in McCurtain County, Oklahoma, migration rates did not change significantly after the completion of Denison Dam, but channel pattern changed with a major channel avulsion occurring around 1978 (Whitesell, Vitek, and Butler 1988). This channel avulsion straightened the river and decreased sinuosity and stream length in this section of the river. The stability of a channel has important implications for the protection of riparian resources, the protection of habitat for threatened and endangered species, and issues of bank stabilization related to loss of property, general aesthetics, and recreation (Juracek 2000).

The geometry of the channel is determined most directly by the quantity of water and by the quantity and quality of sediment moving through the river network (Wolman 1967). These variables, water and sediment, are in turn related to the soil, lithology, vegetation, and climate of the region. If these principal conditions are in equilibrium within a drainage basin, then it follows that the channel form and even channel gradients will be relatively stable with only small changes in influx of water and sediment (Wolman 1967). If, however, major disturbances enter the drainage basin, then one can expect resulting changes in channel form and behavior.

Channel Geometry and Effective Discharge

Bankfull flow is ascribed as having geomorphic significance as the “channel-forming flow” (Simon, Dickerson, and Heins 2004; Leopold 1997). The bankfull discharge is the maximum discharge that can be contained within the channel without overtopping the banks and (based on the annual maximum flow series) generally has a recurrence interval of about 1.5 years. Higher flows on average occur only once in 2 years, or once in 5 years or more (Leopold 1997). In stable streams, bankfull flow refers to hydraulic geometry relations in the channel and corresponds to a flow that is most effective at forming and maintain average channel dimensions (Dunne and Leopold 1978). Large amounts of sediments are carried by near-bankfull discharges, which help maintain channel form (Leopold 1997). In unstable streams, a bankfull level can be exceedingly difficult to identify and is often changing with time, so some authors use a consistent flow-frequency value instead of a form-based bankfull criteria (Simon, Dickerson, and Heins 2004). This “effective discharge” is the discharge or range of discharges that transports the largest proportion of the annual suspended-sediment load over the long-term (Wolman and Miller 1960), and can be linked to geomorphic processes, alluvial channel form, and sediment transport rates. In many cases, bankfull discharge appears to be the effective discharge controlling the development of the channel and floodplain, but in some cases effective discharge may be different than bankfull discharge (Wolman and Miller 1960). Often, the term “bankfull discharge” is used interchangeably with “effective discharge” (Simon, Dickerson, and Heins 2004) since in many rivers the bankfull discharge corresponds to the geomorphically effective discharge.

The concept of a bankfull discharge being the geomorphically effective discharge for all rivers with a universal return period is controversial. Not only is bankfull discharge difficult to define in the field, but other authors have observed bankfull discharges with recurrence intervals ranging from 1.01 to 32 years. Knighton (1998) also notes that bankfull discharge is not always the most effective flow since channel form is the product of a range of discharges rather than a single formative discharge. This range of discharges may include bankfull and might also include a temporal sequence of flow events (Knighton 1998). Costa and O'Conner (1995) highlight the importance of temporal aspects of flow events, arguing that flow duration in addition to magnitude can be a critical factor of geomorphic river response. Flow duration can explain why more frequent moderate flows can have greater geomorphic impact in some channels than floods with larger instantaneous values. Another option for effective discharge, besides bankfull discharge, is the mean annual flood. The mean annual flood (MAF; $Q_{2.33}$) is the average of the annual maximum series (or peak flow events for each year) and typically has a recurrence interval of 2.33 years. In other words, this flow will be equaled or exceeded by the highest flow of the year once every 2.33 years on average (Charlton 2008). This flow is large enough to shape the channel, but still infrequent enough to maintain active channel geometry (Julian et al. 2012). The MAF is used in this study as the dominant or effective discharge.

Channel Geometry and Specific Stream Power

Even flow duration in addition to flow magnitude is not the only factor in determining whether a discharge event is geomorphically effective. Also important is flow frequency, resistance of the land surface, the restorative and recuperative processes between effective events, and shear stress (Costa and O'Conner 1995). Shear stress specifically, as a force-resistance factor, can determine the width of a river (Nanson and Croke 1992). Shear stress reflects turbulence intensity and a measure of a stream's competence, or ability, to transport sediment. However, shear stress can be very difficult to calculate, so stream power is often used instead since it can be calculated from slope-discharge data and is closely related to shear stress. Gross stream power (Ω) is calculated by:

$$\Omega = \gamma Q S \tag{2}$$

where γ is the specific weight of water (9800 N/m^3), Q is the river discharge in m^3/s, and S is the water surface slope. Stream power is a useful measure of the total energy and total work done by the river at any point along its length. It can also be a useful predictor of boundary erosion and channel migration and sediment transport, which largely determines the geomorphology of the channel and floodplain (Nanson and Croke 1992). Gross stream power can be normalized by channel width producing specific stream power (SSP; ω) which is calculated by:

$$\omega = \Omega / W \tag{3}$$

where Ω is the gross stream power in W/m, and W is the channel width in meters. SSP is indicative of the power available to erode and construct individual landforms within the system. Therefore, it can also be a good indicator of channel change and is used as a channel change driver in this study, after the method of Julian et al. (2012). The MAF ($Q_{2.33}$) was used here as a threshold above which to compare SSP to channel geometry.

Channel Geometry and Vegetation

Vegetation on the banks and beds of rivers can also control channel form in various ways. Often, a dense network of roots can strengthen banks and increase erosion resistance by more than a factor of ten (Charlton 2008). However, the influence of vegetation depends on the character of vegetation that lines the bank and the river size (Anderson, Bledsoe, and Hession 2004). Grasses typically have shallower rooting depth than trees, but can have a denser network of roots that add greater cohesion for small streams, leading to narrower channels in grasslands than in forested areas. On larger rivers, grasses no longer add effective cohesion to the entire banks and forested rivers tend to be narrower than those whose banks are covered in grasses (Anderson, Bledsoe, and Hession 2004).

Vegetation, especially on stable portions of mid-channel bars, can initiate sediment deposition. If not scoured out by high flows, over time, this vegetation can encroach on point bars and mid-channel bars, narrowing the channel. Channel narrowing can thus be the result of a decrease in floodplain stripping and/or an increase in floodplain construction (Manners, Schmidt, and Scott 2014).

Effects of Tributaries

A tributary is generally the smaller of two intersecting channels, with the larger being the main stem. Where these two streams meet is a tributary junction, or confluence. The interaction of two independent sediment transport regimes at such a junction can produce dramatic and varying morphological effects in the main stem including gradient steepening, gradient lowering, upstream sediment deposition, changing substrate size, wider channel or floodplain, increased bank erosion, deeper pools, increased wood recruitment, more bars, greater lateral connectivity, and higher frequency and magnitude of disturbance (Benda et al. 2004). These effects may be transient or persistent, depending on the rate at which material is transported to the confluence and moved by receiving channels. Gradient-induced longitudinal variations in sediment transport rate near junctions can often be offset by other tendencies on the downstream side of the junction (Benda et al. 2004). For example, the main stem river may experience reductions in substrate size, increases in channel meandering, and increases in floodplain and terrace width upstream of the confluence, but downstream have coarser substrates, increases in channel width, pool depth, and the occurrence of bars.

Tributaries have generally been thought to buffer the effects of impoundment by re-supplying water and sediment to a regulated main stem channel. However, if the capacity and competence of the regulated main stem is reduced, the sediment load delivered by the tributaries may exacerbate the effects of impoundment (Svendsen et al. 2009).

Flow-Ecology Relationships for Sandbars

Many studies have attempted to define flow-ecology relationships between discharge and channel form, with a smaller number beginning to define these types of relationships between discharge and sandbar area specifically. Horn, Joeckel, and Fielding (2012) investigated the relationship between discharge and channel form on the central Platte River and noted that as channel width has decreased over time, mobile sandbars gradually disappeared. However, they were not able to show a clear relationship between annual discharge and channel width and area, but attributed channel shrinkage to stabilization of bars and channel banks to vegetation. This suggests again that other factors besides flow play an important role in maintaining channel morphology.

Alexander, Schultze, and Zelt (2011) investigated sandbar area, height, and location distributions along the Lower Platte River specifically for ILT SNH. The main goal for their project was to develop a “rapid-assessment” method for measuring and characterizing the spatial distribution and geometries of sandbars. However, they did note that median sandbar height tended to be higher during the spring than in the summer. This timing of exposed versus inundated sandbars is contrary to the timing needed for successful ILT reproduction. Although a direct flow-ecology relationship was not established here, this method of measuring sandbar area and height might prove useful for continued monitoring of SNH for tern populations and developing empirical relationships that can aid management strategies (Davies et al. 2013).

Lenhart, Naber, and Nieber (2013) established a sandbar area-discharge relationship curve for several rivers in Minnesota with riverine turtle SNH availability in mind. Sandbar exposure frequency and duration in the summer was found to decrease with increased magnitude and duration of summer flows in these Upper Midwest rivers.

It is also important to note the various species that utilize sandbars as habitat besides ILT, therefore successful conservation and management of river systems should not be solely aimed at one particular species. Sandbars comprise a large portion of habitat for many aquatic and terrestrial species, and studying habitat characteristics of certain biota can serve as indicators for overall river system health (Sanford 2002; Vaughan, Noble, and Ormerod 2007).

Tracey-Smith, Galat, and Jacobson (2012) developed sandbar-specific models of discharge-area relationships for a segment of the Lower Missouri River. These relationships were used to test how sandbar area responded to various flow conditions including a modeled natural flow regime, the current managed flow regime, and two different environmental flow conditions, all within the contemporary active channel. They found that reduced summer flows occurring under natural and environmental flows increased exposed SNH, but only current managed flows (not natural or environmental) provided more shallow-water foraging habitat. The results of reduced SNH variables in historical, pre-regulation flows compared to contemporary managed flows, suggests again that geomorphology might be equally as important as flow as a primary variable in highly regulated river systems (Tracey-Smith, Galat, and Jacobson 2012; Meitzen et al. 2013). Although these tests were performed with a range of selected biota in mind that use sandbars as habitat, ILT were not specifically investigated because they are not known to nest in the segment of the Missouri River studied here (Tracey-Smith, Galat, and Jacobson 2012). However, they did evaluate SNH for softshell turtles, which have similar nesting habitat characteristics as ILT, and thus, were able to infer how operational changes to flow regulation might affect ILT populations upstream. Under the existing channel morphology for this segment of the Missouri River, neither the natural or altered flow regimes produced much SNH during the nesting periods of ILT (Tracey-Smith, Galat, and Jacobson 2012). The development of empirical models, such as the ones produced by Tracey-Smith, Galat, and Jacobson (2012), can be a useful approach to help guide restoration activities and define success criteria for environmental flows (Poff and

Zimmerman 2010; Davies et al. 2013).

Tracey-Smith, Galat, and Jacobson (2012) also noted that, while sandbars under natural flow regimes are ephemeral or highly dynamic, on highly regulated and engineered rivers, sandbar locations and morphology can exist within the same river bends for many years, only changing in area in response to state fluctuations. Even when the longitudinal position changes, the migration of sandbars is not at a shorter time-scale sufficient to cause major differences in ILT nesting populations. Therefore, Tracey-Smith, Galat, and Jacobson (2012) suggests that a research focus should be to investigate why sandbars tend to occur in certain areas versus others, along with determining the relationship between areas of SNH to stage fluctuations.

The importance of sandbar height in creating a flow-ecology relationship for sandbars precludes this study from being able to create a sandbar area-discharge relationship curve, since sandbar height could not be investigated from aerial photography. Aerial photographs used were chosen in connection to the discharge on the date the photograph was taken in order to make fair comparisons. However, this only allows for a broad estimate of sandbar area since river stage can fluctuate daily. As Lott and Wiley (2012a) call for, a better understanding of the specific benchmark flows for SNH is needed to compare habitat to dam system operations. Despite this limitation, broad estimates of sandbar area and suitable SNH can aid in developing the understanding of how river management might affect ILT populations and how to best develop management strategies that will be effective in continuing to promote ILT recovery.

IV. STUDY AREA

The Red River

The Red River is a major tributary to the lower Mississippi River and is located along the Texas-Oklahoma border (Figure 4). The Red River rises in the Southern Rocky Mountains in northern New Mexico, flows through the Great Plains and Ouachita Province, turns south at the Great Bend near Fulton, Arkansas, then converges with the Atchafalaya and Mississippi rivers in the Coastal Plain in Louisiana. At approximately 2,224 kilometers long, the Red River drains an area of about 331,215 square kilometers. It is characterized by high sediment discharges that contribute to its active meandering and rapid deposition of point bars (Albertson and Patrick 1996). The Red River was chosen to investigate because it is habitat to a large population of ILT and has been little studied in this regard. In general, there is also a lack of knowledge of Great Plains rivers both geographically and historically (Graf 2001), even though these rivers continue to be highly utilized for water resources. Being on the Texas-Oklahoma border, the Red River is regulated under the Red River Compact and there is a long history of monitoring flows in this river, as well as an ample supply of imagery data available.

Figure 4. The Red River watershed in south-central United States*. The box shows where Figure 5A is located relative to the whole watershed. Red dots indicate USHCN climate stations, and black lines indicate major dams.*

The study area will be investigated at two different scales. The segment-scale (SS; Figure 5A) is a 170-kilometer segment located along the Red River directly below Denison Dam, centered on the confluence of the Red River with MBC, but also including confluences with the Blue River and the Kiamichi River. This SS will show the broad changes of the river in response to changes in hydrology, land cover, and sediment. The reach-scale (RS; Figure 5B) is a 50-kilometer reach focused specifically on the confluence of the Red River with MBC. This RS allows for the investigation of similar changes at a finer spatial and temporal resolution.

These areas were selected because Denison Dam is the largest impoundment on the Red River and thus exerts control over the downstream hydrology and geomorphology of the river channel where a large population of ILT breed and nest every summer. Also, MBC is one of the last undammed main tributaries to the Red River (Woods et al. 2005). This tributary acts as a sediment source for the downstream end of the study areas.

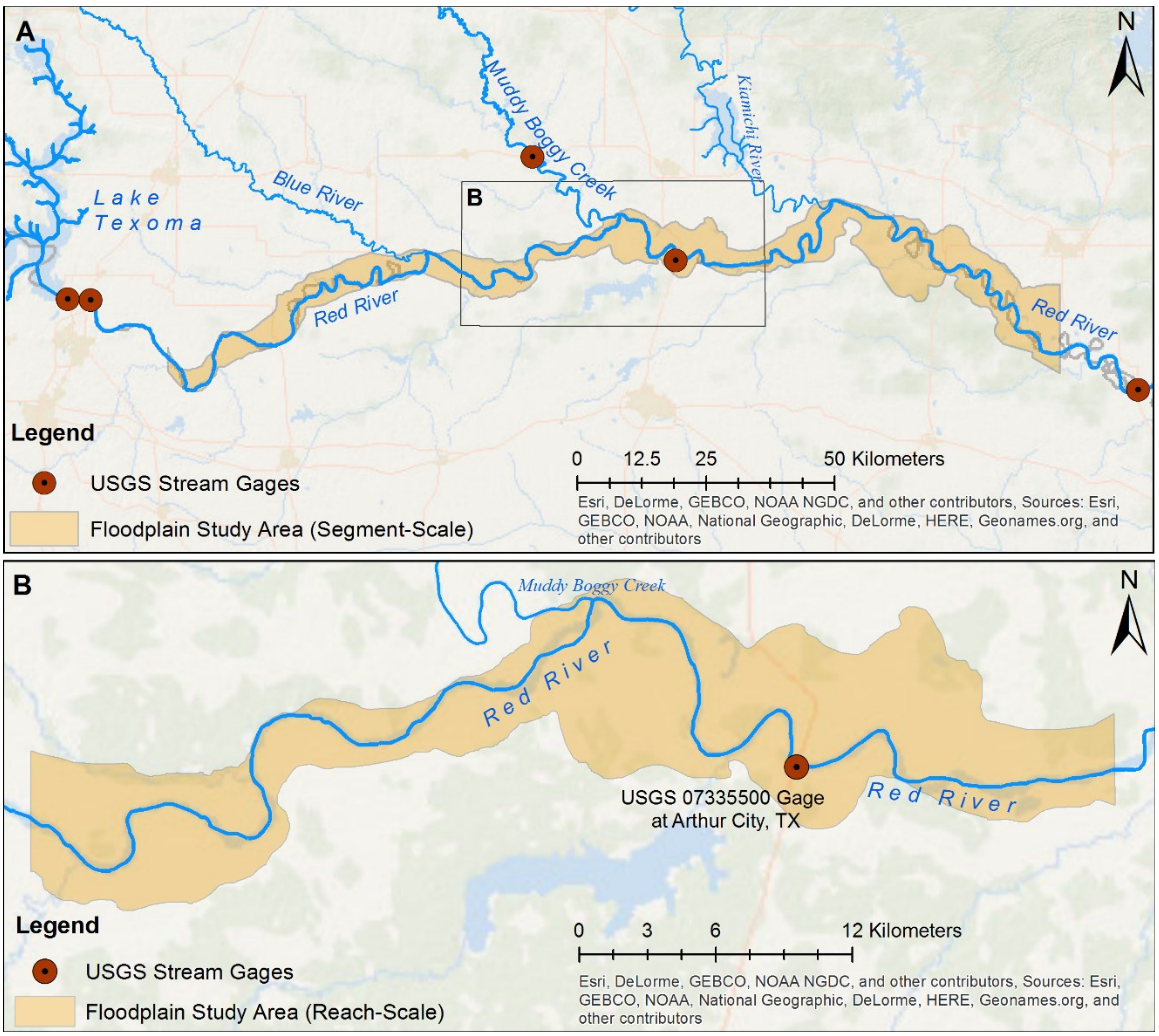

Figure 5. Floodplain study areas. *(A) The segment-scale, 170-km floodplain study area below Denison Dam and Lake Texoma. (B) The reach-scale, 50-km floodplain study area centered on the confluence of MBC and the Red River. Red dots indicated USGS stream gage sites.*

Regional Vegetation Patterns

Ecoregions of the Red River

The Red River flows through several Level III ecoregions as it makes its way across the Great Plains to the Mississippi River. "A thousand tiny rivulets" from the foothills of the Southern Rocky Mountains come together to form the headwaters of the Red River in the High Plains ecoregion, which is characterized by smooth to slightly irregular plains with a high percentage of cropland (Tyson 1977, 1; Griffith 2007). Natural vegetation in this region was once mostly grama-buffalo grass. The Red River next encounters the Southwestern Tablelands with canyons, mesas, badlands, and dissected river breaks. Much of this region is in sub-humid grassland and semiarid rangeland, and little has been converted to cropland. The natural vegetation here is also grama-buffalo grass, but with some mesquite-buffalo grass in the southeast, and juniper-scrub oak-midgrass savanna on escarpment bluffs (Griffith 2007).

As the Red River reaches the area where it starts to form the border between Oklahoma and Texas, it enters the Central Great Plains ecoregion. This ecoregion receives more precipitation and is slightly lower and more irregular than the High Plains regions to the west (Griffith 2007). The natural vegetation was once grassland with a mixed or transitional prairie: from the tallgrass in the east to shortgrass father west, but most now have been converted into cropland. Soils in this region are generally deep with shallow soils on ridges and breaks and scattered low trees and shrubs occur in the south.

Upstream from Denison Dam, the Red River flows through the Cross Timbers ecoregion. The Cross Timbers is a transitional area between the once prairie regions to the west and the forested low mountains of eastern Oklahoma and Texas. The ecoregion contains irregular plains with some low hills and tablelands and is a mosaic of forest, woodland, savanna, and prairie (Griffith 2007). The natural vegetation consists of some bluestem grassland with scattered blackjack oak and post oak trees, although most of the area has been cleared for rangeland and pastureland, with small areas of closed forest.

Downstream of Denison Dam, until the Red River encounters the Mississippi River, it flows through the South Central Plains ecoregion. This ecoregion consists mostly of irregular plains and represents the western edge of the southern coniferous forest belt (Griffith 2007; Omernik and Griffith 2014). The natural vegetation was once mix of pine and hardwood forests, but now loblolly and shortleaf pine plantations dominate, giving the region the nickname "piney woods." Soils are mostly acidic sands and sandy loams (Griffith 2007). Prairies once occurred on soils derived from limestone, marl, and calcareous shale, but today many of these upland prairies have been converted to pasturelands (Omernik and Griffith 2014). Mean annual rainfall varies from 114-140 centimeters and increases eastward in the region. About two thirds of the region is in forests and woodland, while only about one sixth is in cropland, primarily within the Red River floodplain (Griffith 2007).

Ecoregion of the Study Areas

The floodplain of the Red River in the study areas is classified as "Red River Bottomlands," near the channel, and "Pliestocene Fluvial Terraces" which are sub-ecoregions of the larger South Central Plains ecoregion (Omernik and Griffith 2014). The Red River Bottomlands include the highly meandering main channel of the Red River, oxbow lakes, meander scars, ridges, drainage ditches, levees, and backswamps. The ecoregion is veneered in Holocene alluvium associated with Red River deposition and is of variable texture and permeability.

Natural vegetation patterns consist of oak-hickory-pine forests on uplands and southern floodplain forest on bottomlands (Omernik and Griffith 2014). Bottomland hardwood forests include trees such as water oak (*Quercus nigra*), sweetgum (*Liquidambar styraciflua*), willow oak (*Q. phellos*), southern red oak (*Q. falcata*), eastern red cedar (*Juniperus virginianus*), black gum (*Nyssa sylvatica*), blackjack oak (*Q. marilandica*), overcup oak (*Q. lyrata*), river birth (*Betula nigra*), red maple (*Acer rubrum*), green ash (*Fraxinus pennsylvanica*), and American elm (*Ulmus americana*) (Griffith 2007). Some woodland still occurs in poorly drained and frequently flooded areas, but most of this natural woodland has been cleared for cropland and improved pasture.

The broad, nearly level bottomlands are now dominated by agriculture, with more cropland than other floodplains of the South Central Plains ecoregion (Griffith 2007; Omernik and Griffith 2014). The principle crops grown in this region include soybeans, sorghum, wheat, alfalfa, corn, and cotton.

Away from the channel, some of the floodplain is categorized as the Pliestocence Fluvial Terraces ecoregion. This ecoregion covers significant unconsolidated terrace deposits that are periodically wet. In Texas, land cover of this ecoregion is mostly pine-hardwood forest, with loblolly pine (*Pinus taeda*), shortleaf pine (*P. echinata*), post oak (*Quercus stellata*), Shumard oak (*Q. shumardii*), southern red oak (*Q. falcata*), water oak (*Q. nigra*), willow oak (*Q. phellos*), and sweetgum (*Liquidambar styraci ua*) (Griffith 2007). Westward, pine starts to be replaced with post oak (*Quercus stellata*), Shumard oak (*Q. shumardii*), and eastern red cedar (*Juniperus virginiana*) (Griffith 2007). Some common land use activities in this ecoregion include pine plantations, pasture, and livestock production.

V. DATA

Imagery Data

The data used for this investigation include imagery from historical surveys and aerial photographs for land cover mapping as well as measurements of channel and sandbar geometry. General Land Office (GLO) historical surveys from 1896-1899 gave the earliest date of "imagery" of the area (Table 1); however, only the Oklahoma side of the Red River was surveyed in detail. While GLO records have potential errors, because the Red River represents an important historical boundary that has often been contested, land cover and channel geometry depicted on the plats can be used with confidence. As Julian et al. (2012) notes, GLO plats have been successfully used in numerous studies to analyze land cover.

Aerial photographs of the study areas were acquired through either the USGS Earth Resources Observation and Science Center (EROS) via its online Earth Explorer portal or scanned manually from the archive at the Texas Natural Resources Information System (TNRIS). The EROS online portal also included products from NASA's Land Processes Distributed Active Archive Center (LP DAAC). These aerial photographs were compiled and georeferenced in ArcMap 10.4.1 using an average of 12-15 ground control points with reference to the 1996 National Agricultural Imagery Program (NAIP) images and Texas Department of Transportation (TxDOT) Roadways data set downloaded from the TNRIS website, as well as the Highways data set for Oklahoma, downloaded from the University of Oklahoma Center for Spatial Analysis (UOCSA) website.

Besides aerial imagery, 30-meter digital elevation models (DEMs) were also downloaded from the EROS online portal. Three 1 arc-second tiles from the National

Elevation Dataset (NED) provided elevation data for the study area and were used to delineate the modern floodplain and calculate slope (USGS NED n34w095, USGS NED n34w096, and USGS NED n34w097).

Hydrologic Data

Precipitation data of the region was obtained from the U.S. Historical Climate Network (USHCN) stations closest to the Red River, evenly spaced along the length of the river that acts as the boundary between Oklahoma and Texas (Figure 4). Daily data was used from Station 416794 in Paris, TX (33.6744 N, 95.5586 W), Station 342678 in Durant, OK (34.0003 N, 96.3686 W), Station 349395 in Waurika, OK (34.1747 N, 97.9964 W), and Station 417336 in Quanah, TX (34.2761 N, 99.7578 W). These stations were chosen based on their locations to the Red River and the span (1890s to 2014) and completeness of their records.

Streamflow data in the form of daily discharge (Q) and annual peak flows was acquired from the USGS Gage Station at Arthur City, TX (USGS 07335500, 33.875 N, 95.501 W). This gage station is located within the study areas, just below the confluence of the Red River and MBC (Figure 5B). The discharge record for this station spans from 1905 to 2014, with a gap between 1911 and 1936. Because this gage only had 14 years of data before Denison Dam was completed, additional discharge data (annual peak flow data) from the USGS Gage Station at Index, AR (USGS 07337000, 33.552 N, 97.808 W) was used to find the pre-dam MAF ($Q_{2.33}$).

Table 1. Inventory of Oklahoma General Land Office Surveys used.

Date Survey Commenced	Date Survey Completed	Date Survey Approved	Plat ID	Township	Range	County
2/22/1896	2/26/1896	11/12/1898	34975	6.0 S	13.0 E	Bryan, Choctaw
2/241896	2//27/1896	11/12/1898	34984	6.0 S	14.0 E	Choctaw
3/18/1896	3/21/1896	11/12/1898	34993	6.0 S	15.0 E	Choctaw
3/14/1896	3/18/1896	11/12/1898	35002	6.0 S	16.0 E	Choctaw
1/14/1897	1/21/1897	1/12/1899	35011	6.0 S	17.0 E	Choctaw
1/15/1897	1/22/1897	1/12/1899	35022	6.0 S	18.0 E	Choctaw
2/17/1897	2/22/1897	1/12/1899	35030	6.0 S	19.0 E	Choctaw
2/13/1896	2/20/1896	1/12/1899	35040	6.0 S	20.0 E	Choctaw
2/28/1896	3/3/1896	11/12/1898	34976	7.0 S	13.0 E	Bryan, Choctaw
2/28/1896	3/3/1895	11/12/1898	34985	7.0 S	14.0 E	Bryan, Choctaw
3/13/1896	3/17/1896	11/12/1898	34994	7.0 S	15.0 E	Choctaw
3/9/1897	3/13/1897	11/12/1898	35003	7.0 S	16.0 E	Choctaw
1/22/1897	1/29/1897	1/12/1899	35012	7.0 S	17.0 E	Choctaw
1/25/1897	2/2/1897	1/12/1899	35023	7.0 S	18.0 E	Choctaw
2/8/1897	2/15/1897	1/12/1899	35031	7.0 S	19.0 E	Choctaw
2/4/1897	2/11/1897	1/12/1899	35041	7.0 S	20.0 E	Choctaw
3/26/1897	4/2/1897	12/13/1898	35048	7.0 S	21.0 E	McCurtain
3/20/1898	3/25/1898	12/13/1898	35057	7.0 S	22.0 E	McCurtain
1/23/1896	1/26/1896	3/2/1899	34955	8.0 S	11.0 E	Bryan
1/23/1896	1/26/1896	3/2/1899	34967	8.0 S	12.0 E	Bryan
3/4/1896	3/7/1896	11/12/1898	34977	8.0 S	13.0 E	Bryan
3/11/1896	3/12/1896	11/12/1898	34996	8.0 S	15.0 E	Bryan, Choctaw
3/13/1896	3/13/1896	11/12/1898	35005	8.0 S	16.0 E	Choctaw
2/1/1897		1/12/1899	35015	8.0 S	17.0 E	Choctaw
1/28/1897	2/2/1897	1/12/1899	35024	8.0 S	18.0 E	Choctaw
2/4/1897		1/12/1899	35033	8.0 S	19.0 E	Choctaw
4/3/1896	4/5/1897	12/13/1898	35050	8.0 S	21.0 E	McCurtain
4/6/1897	4/12/1897	12/13/1898	35058	8.0 S	22.0 E	McCurtain
2/5/1898	2/16/1898	12/13/1898	35067	8.0 S	23.0 E	McCurtain
2/18/1898	2/24/1898	12/13/1898	35078	8.0 S	24.0 E	McCurtain
4/28/1898	5/6/1898	8/14/1899	34926	9.0 S	9.0 E	Bryan
5/7/1898	5/24/1898	8/14/1899	34943	9.0 S	10.0 E	Bryan
5/16/1898	5/20/1898	8/14/1899	34958	9.0 S	11.0 E	Bryan
2/7/1898	2/16/1898	3/7/1899	35079	9.0 S	24.0 E	McCurtain
4/29/1898	4/30/1898	8/14/1899	34931	10.0 S	9.0 E	Bryan
4/30/1898	4/30/1898	8/14/1899	34946	10.0 S	10.0 E	Bryan
2/17/1898	2/17/1898	3/7/1899	35081	10.0 S	24.0 E	McCurtain

This gage, although much further downstream from the study areas, was used because it was the next closest gage station with pre-dam daily discharges and annual peak discharges. Data from this gage was used to calculate the MAF, and was not used for any further analyses.

Sediment Data

Although sediment is a vital component of rivers and sandbars, comprehensive long-term data on sediment inputs, transport, or storage are rare (Wohl et al. 2015). The USGS gage at Arthur City, TX (USGS 07335500) had suspended-sediment concentration and suspended-sediment discharge data for various dates from 1938 to 1978, which can give general trends to how the sediment budget of the river is changing over time. Other sediment data was compiled from previous studies. Sedimentation yields from 1979 were also estimated in a report to the Texas Department of Water Resources (Greiner 1982). Simon, Dickerson, and Heins (2004) gathered data on suspended-sediment yields based on ecoregions, including the South Central Plains, but they used a 1.5-year recurrence interval for effective discharge. Copeland (2002) performed a numerical sedimentation model study for the Red River, which was probably the best source for this study. But otherwise, very little resources or literature were found with information on the sediment budget for the Red River. Despite these limitations, these studies can give at least a rough understanding of the sediment regime of the Red River.

Soils data was available from the Natural Resources Conservation Service's Soil Survey Geographic Database (SSURGO), which gives an idea of sediment composition.

Otherwise, the resources mentioned were used in this study just as a reference for understanding some of the changes in the sediment budget for the Red River over time.

VI. METHODS

<u>Hydrologic Analyses</u>

The precipitation daily data was compiled from the four stations to calculate an average daily value, the long-term mean, the 5-year mean, the 3-day mean, and the 3-day total. Following the methodology of Julian et al. (2012), the 3-day total was plotted against the discharge record to characterize the precipitation of the watershed and compare it to the flow regime of the river.

From the portion of the annual maximum series (peak flows) before Denison Dam was completed in 1944 (1905-1911, 1936-1944), the pre-dam MAF ($Q_{2.33}$) was calculated, which has a recurrence interval of 2.33 years. Because the Arthur City, TX gage station only had 14 years of pre-dam discharge data, the pre-dam peak flow data from the Index, AR gage station was also used in this calculation. The discharge values from Index, AR were scaled to account for the difference in drainage area size from Arthur City, TX to Index, AR. Even though the Index, AR gage station is well downstream of the study reach, it was the next closest gage station with data from before Denison Dam was completed. By including data from the Index, AR gage, there was a more robust dataset from which to calculate the MAF. The MAF is commonly used as a 'dominant' discharge– large enough to shape the channel, yet with a recurrence interval frequent enough to maintain the active channel geometry (Julian et al. 2012).

The entire daily discharge record from the Arthur City gage station was analyzed using the Indicators of Hydrologic Analysis (IHA) software, developed by The Nature Conservancy (TNC; 2009). IHA can be used to summarize long periods of daily hydrologic data into more manageable series of ecologically relevant hydrologic parameters (TNC 2009). It also can calculate characteristics of five components of flow that are important to river ecosystem health– extreme low flows, low flows, high-flow pulses, small floods and large floods. Specific magnitude or exceedance probability thresholds can be set to characterize these environmental flow components (EFCs), but the default settings were used here. The default definitions for EFCs are summarized as:

1. Extreme Low Flows represent hydrologic drought conditions, (10 percentile of flow).
2. Low Flows represent the dominant flow condition or base flow, (50 percentile of flow).
3. High-Flow Pulses represent quick flush flows greater than low flows, but do no overtop channel banks, (High-Flow Pulse begins when flow increases by more than 25 percent per day from Low Flow and exceeds the 75th percentile, and ends when flow decreases by less than 10 percent per day back down to the 50th percentile).
4. Small Floods represent flows that overtop the main channel but does not include more extreme, less frequent floods. Small Floods generally correspond to flood events with a 2-year recurrence interval.
5. Large Floods represent peak flow events that can re-arrange both the biological and physical structure of a river. Large Floods generally correspond to flood events with at least a 10-year recurrence interval.

IHA also can compare pre- versus post-impact data, such as the impact from a dam. However, at least 20 years of daily data is required on either side of the impact (Richter et al. 1996; TNC 2009). Because the discharge record from the Arthur City gage station does not meet this requirement (only 14 years of daily data before Denison Dam was completed), the IHA analysis was run as a single time period. The software automatically does linear interpolation over gaps in data, so the results show long-term trends over the data period. For this study, a single period, non-parametric analysis was run with the default EFC parameters.

Image Selection

'Static' sandbars do not exist due to seasonal and even hourly river stage variation on rivers with hydropower operations (Lott and Wiley 2012a). A sandbar with exposed dry sand measured at 18 square kilometers (km^2) at 340 cubic meters per second (m^3/s), may only measure 10 km^2 at 425 m^3/s, and may be completely inundated at 600 m^3/s, for instance. Therefore, sandbar areas must always be presented relative to specified flows. Because sandbar area, and therefore SNH area is critically dependent upon flow as it translates to river stage, direct comparison of habitat amounts (e.g., between two different time periods) should only occur at the same flow (Lott and Wiley 2012a). Unfortunately, the available aerial photography was not taken with river stage and sandbar areas in mind, and large scenes are often composed of imagery taken over a span of different dates. With this in mind, the dates of the available aerial photographs for the study area were matched to the discharge at that date and compared to the results of the EFC thresholds from the IHA analysis. Figures 6 and 7 show the coverage and matched discharges for all available imagery in the study area. For Great Plains rivers like the Red River, most of the year the average flow level lies somewhere between the Extreme Low Flow threshold (10 percent) and the Low Flow threshold (50 percent). The results of the

IHA analysis showed that these thresholds correspond to discharges of 29 m^3/s and 110 m^3/s, respectively. This range of discharges, along with the amount of coverage of the study areas, became the threshold selection criterion for selecting aerial photographs for mapping.

Segment-Scale Image Selection

Given that full coverage of the SS was rare until the later years, only four scenes (1890's, 1949, 1979, and 2010) were chosen to analyze at this scale. The 1890s scene, although spanning dates from 1896 to 1899 from the GLO surveys and only having coverage for the Oklahoma side of the river, was still chosen for analysis as it represents the beginnings of land cover change in the area due to European settlement. This scene was not able to be fully analyzed like the others (no streamflow measurements from this time), but the land cover change could be measured to give a baseline comparison for the other scenes. Likewise, a pre-settlement scene based on the natural potential vegetation (Duck and Fletcher 1945) patterns was added to give a comparison before European settlement changed the landscape. The shape of the river and sandbars were completely unknown at this time, but if pre-settlement is assumed as a time right before the land clearing seen in the 1890s scene, it can be estimated that the shape of the river channel and size of the sandbars were reasonably close to the shape and size of the channel and sandbars shown in the GLO surveys of the 1890s. Therefore, the channel and sandbars mapped from the 1890s scene were used in the pre-settlement scene as well. This provided a very rough estimate of what the river might have looked like during this time.

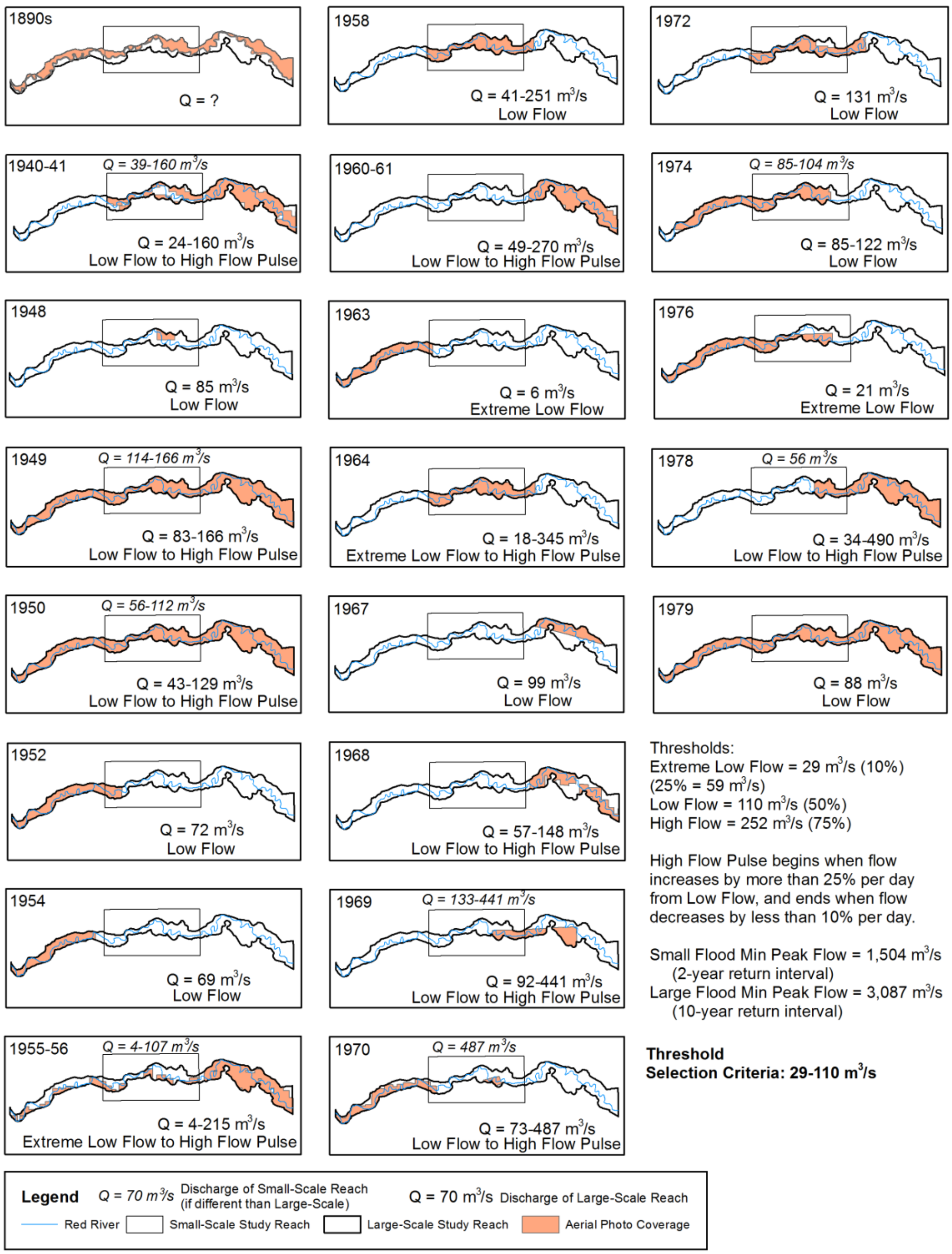

Figure 6. Aerial photography coverage of study areas from the 1890's to 1979. *Matched discharges for the segment-scale area are reported in the lower right-hand corner of each map. The small box outlines the region of the reach-scale, with matched discharges reported above.*

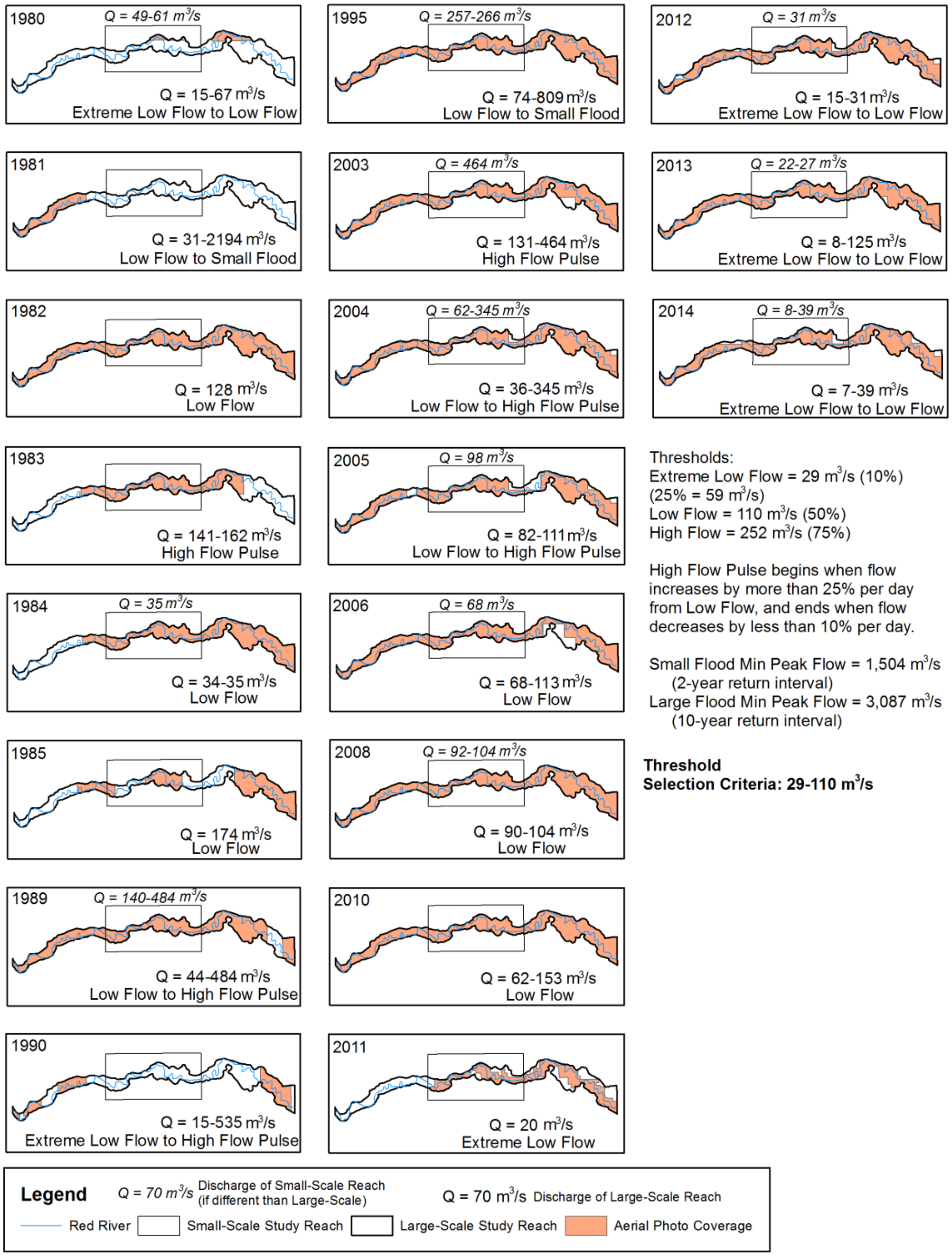

Figure 7. Aerial photography coverage of study areas from the 1980 to 2014. *Matched discharges for the segment-scale area are reported in the lower right-hand corner of each map. The small box outlines the region of the reach-scale, with matched discharges reported above.*

Even though the range of discharges for the 1949 scene extend slightly beyond the 110 m^3/s threshold, it was chosen for analysis because it represents the first available date of imagery with full coverage of the SS. Also, the discharges that were above 110 m^3/s were still classified as Low Flows by the IHA EFC parameters. Although the 1950 scene also had full coverage and reasonable discharges, because the 1949 scene was selected, and the goal was to see broad, large-scale impacts, it was not necessary to select consecutive scene years.

The next scene with full image coverage of the large-scale study area was 1979, which corresponded to discharges that fell with the threshold selection criterion range, and was therefore selected for analysis. Given that 30 years were between this scene and the 1949 scene, it seemed reasonable to select one more scene for the SS at about 30 years from 1979. The 2010 scene was selected for analysis as the final RS scene because it was close to the 30-year mark from 1979 and its range of discharges were only slightly above the 110 m^3/s threshold, but still categorized as Low Flows.

Reach-Scale Image Selection

More images were available for selection with full coverage of the RS (represented by the small box in Figures 6 and 7). It is noted that although the threshold selection criterion was defined as discharges between 29 and 110 m^3/s, if this limit was strictly adhered to there would be very little imagery to map and analyze for the RS. Therefore, some scenes were selected to map and analyze that had a few photographs taken at dates above or below this criterion. If a scene had a discharge slightly above the 110 m^3/s threshold, but was still classified as "Low Flow" from the IHA EFC parameters and it had adequate coverage, it was selected for analysis. If a scene had only a few aerial photographs with discharges categorized as a High Flow Pulse, but most of the scene coverage corresponded to Low Flow discharges, and a consecutive year was not already selected, the scene was selected for analysis. In the later years when Extreme Low Flows were more prevalent, if these discharges were restricted to only a small portion of the RS, and a consecutive year scene was not already selected, this scene was also selected for analysis. Lastly, some photographs matched to discharges that did not fall into the threshold selection criterion, but were non-river scenes. These scenes were selected since the threshold selection criterion was only important for river scenes. The average discharge across a scene year compared to the threshold selection criterion (Figure 8) shows the magnitude of uncertainty in preceding analyses that these scenes will give, especially regarding sandbar area. Even with five scenes slightly higher than the threshold selection criterion, the average discharge for these years still fell within the Low Flow EFC category. To show this slight uncertainty within the results, different symbols were used in graphs for measurements of sandbar, vegetated sandbar, and suitable SNH area when the average discharge of a scene year fell outside the threshold selection criterion.

The scene years selected for the SS were also selected for the RS since the coverages overlapped. The final scenes selected for the RS were 1890’s, 1949, 1964, 1972, 1979, 1982, 1984, 2004, 2006, 2008, 2010, 2012, and 2014. Table 2 gives a listing of the matched discharges for these scenes and a more specific explanation for the basis of selection.

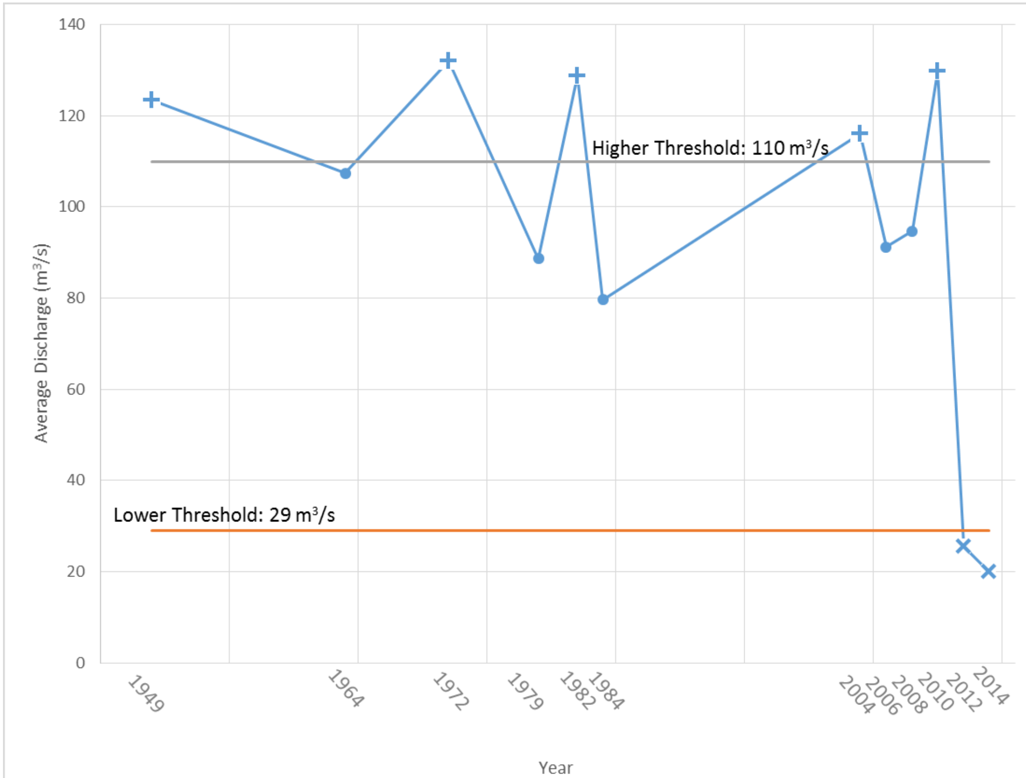

Figure 8. Comparison of average scene discharge to threshold selection criterion range. *Scene years 1949, 1972, 1982, 2004, and 2010 had average discharges across the scene that were slightly higher than the threshold selection criterion and in forthcoming graphs will be indicated by plus signs. Scene years 2012 and 2014 had average discharges that were slightly lower than the threshold selection criterion and in forthcoming graphs will be indicated by X's.*

Table 2. Scene selection for the segment-scale study area. Includes dates, matched discharges, and environmental flow components for selected aerial imagery with explanation for selection.

Scene Year	Date	Discharge (m^3/s)	Environmental Flow Component	Explanation
Pre-Settlement	Before 1821	Unknown	Unknown	Provides a baseline for the natural vegetation patterns of the area before European settlement.
1890's	Various	Unknown	Unknown	Provides a baseline for the beginnings of land cover change due to European settlement.
1949	2/7/1949	166.50	low flow	First available date with full coverage of the study area; high flow pulse is only small part of scene
	9/21/1949	145.27	low flow	
	10/16/1949	114.97	high flow pulse	
1964	10/31/1964	43.04	low flow	High flow pulse is only small part of scene, extreme low flows are close enough to threshold
	11/12/1964	18.52	extreme low flow	
	11/13/1964	22.68	extreme low flow	
	11/23/1964	345.47	high flow pulse	
1972	2/29/1972	131.96	low flow	Only slightly higher than threshold criteria and still categorized as Low Flow
1979	11/10/1979	88.63	low flow	Within threshold criteria
1982	3/7/1982	128.84	low flow	Only slightly higher than threshold criteria and still categorized as Low Flow
2004	8/31/2004	62.86	low flow	High flow pulse is only small part of scene
	9/30/2004	57.48	low flow	
	10/15/2004	345.47	high flow pulse	
2006	11/13/2006	68.53	low flow	Within threshold criteria
2008	7/2/2008	104.77	low flow	Within threshold criteria
	7/28/2008	92.03	low flow	
	8/2/2008	95.14	low flow	
	8/3/2008	90.61	low flow	
2010	8/2/2010	153.48	low flow	Only slightly higher than threshold criteria and still categorized as Low Flow
	8/10/2010	144.42	low flow	
	8/27/2010	62.01	low flow	
2012	7/5/2012	32.00	low flow	Within threshold criteria
2014	7/12/2014	8.27	extreme low flow	Extreme low flow is only small part of scene
	8/12/2014	39.64	low flow	

Land Cover Mapping

The modern floodplain of the study area was delineated using the 30-meter DEMs in combination with flood stage history and aerial photographs. The maximum floodplain elevation given by the elevation at the Arthur City, TX gage station plus the maximum flood stage at that station was 127 meters above mean sea level. This was used to help visually delineate the modern floodplain from the DEMs and aerial photographs.

For the Pre-Settlement scene, the land cover map was derived from the potential vegetation maps developed by Duck and Fletcher (1945). As mentioned before, the channel and sandbars mapped in this scene are taken from the 1890s scene as a rough estimate. The GLO surveys from the 1890s were georeferenced by the latitude and longitude of the survey boundaries for each plat, which corresponds to Oklahoma's township sections. All other aerial photographs were georeferenced in ArcMap 10.4.1 using an average of 12-15 ground control points with reference to the 1996 NAIP images and TxDOT Roadways data set downloaded from the TNRIS website, as well as the Highways data set for Oklahoma, downloaded from the UOCSA website. Several scenes had slight gaps in aerial coverage in areas that were non-river scenes, and in such cases, imagery was filled in from the next year available, as land cover far from the river does not change appreciably from year-to-year.

All imagery and maps were reviewed at a scale of 1:10,000 and digitized with a 60-meter minimum mapping unit. The active channel was delineated after the manner by Julian et al. (2012), which was done according to Osterkamp and Hedman (1977). This method defines the active channel as the area of channel being shaped by prevailing discharges and is marked by the lower limit of permanent vegetation, large trees in this case. Julian et al. (2012) used the Anderson et al. (1976) Level II classification system, with cropland and pasture segregated, that included the following land use groups: Forest (Deciduous Forest Land and Forested Wetlands), Grassland (Herbaceous Rangeland, Pasture, and Non-Forested Wetlands), Cropland, and Water/Sand. Different from Julian et al. (2012), this study separated water and sandbars into two distinct groups, and added a Developed Land use group as a major highway and small town lie within the study areas. In addition, areas of the sandbar that were vegetated were distinguished from bare sand, as this is important for ILT SNH. In some scenes, wet or slightly inundated sand could be identified, however, only exposed, dry sand was mapped as sandbars. Wet versus dry sand on older images were slightly harder to identify, but this study presents measurements as estimates and percentages, not absolute values, such that the broad impacts and trends can be seen. Grassland used as pasture and rangeland was sometimes difficult to distinguish from cropland laying fallow. Texture and the presences of fences was used to help determine grassland from cropland as pasture and rangelands tend to be fenced, and croplands can have either identifiable rows or a smoother texture on the image than grassland. Despite these difficulties, the extent of forested versus non-forest areas were more important to the study than grassland areas versus cropland areas.

Given the scale of this study using remote sensing, absolute or exact values would be impossible to measure. Estimates of the percentages of land cover, however, can give the order of magnitude of land cover change over time, allowing for broad patterns to be detected. The final land use groups mapped in this study were: Forest, Grassland, Cropland, Developed Land, Water, Sandbars, and Vegetated Sandbars. For the category of Sandbars, this includes the total sandbar area including both vegetated and non-vegetated areas of sandbars.

Suitable Habitat Calculations

When the land cover of each scene was mapped, areas of sandbars could be determined as “suitable” SNH based on the criteria from Lott and Wiley (2012a; 2012b). Sandbar elevation is not measurable from aerial photography, and Lott and Wiley (2012a) confirmed that food availability would not be a limiting factor to ILT SNH along this portion of the Red River, so this study was restricted to criteria measurable by remote sensing to delineate suitable SNH. Again, because vegetation cover varies extensively by time of year and data on the distance measurement from low sandbar vegetation is considered unreliable (Casey Lott, VP for Conservation Information Synthesis at the American Bird Conservancy, 2 February 2015, personal communication via e-mail), a distance criteria from low sandbar vegetation (e.g., grasses) was not used here.

The final criteria used in this study to determine suitable SNH are as follows:

1. Sandbar area must be at least 76 meters from large trees or shrubs.
2. Sandbar area must be at least 60 meters from the active channel margins.
3. Sandbar area must be free from vegetation.

A model was created in ArcMap 10.4.1 and run for each scene to automatically calculate suitable SNH based on the above criteria (Figure 9). The channel in some places lies adjacent to the edge of the floodplain study area, so additional forest was mapped outside the study area to account for the distance from trees criteria along these sections of the channel, but were not counted in land cover area measurements. Suitable SNH was calculated for both the SS and the RS, and again for both study areas divided into portions of the stream upstream and downstream of the confluence with MBC.

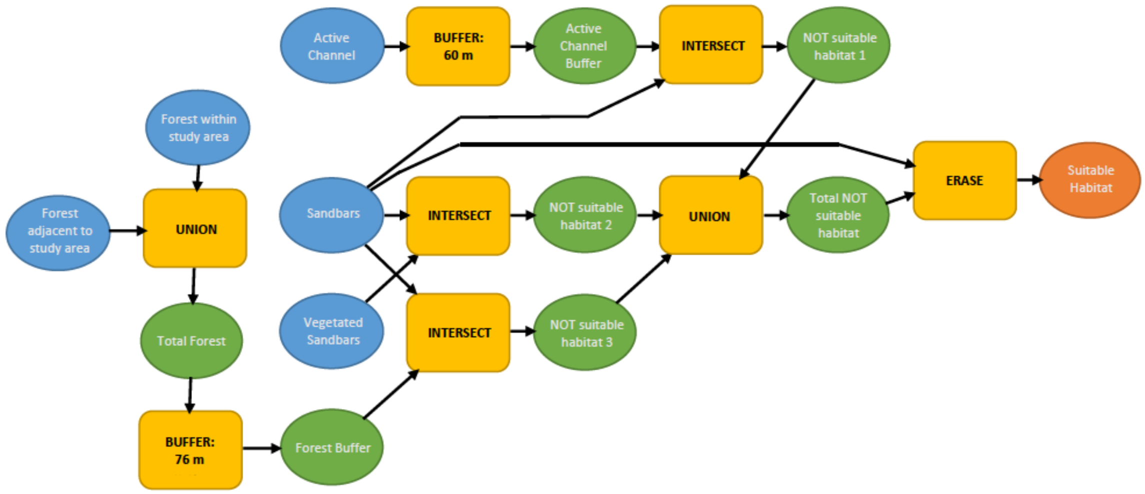

Figure 9. Suitable habitat calculation model. *Model work-flow built in ArcMap 10.4.1 to calculate suitable sandbar nesting habitat based on land cover and the suitable habitat criteria listed above.*

Channel Geometry Calculations

The 30-m DEMs were used to calculate the longitudinal profile along the SS. Elevations were extracted every 1 kilometer along the valley length. For each scene, the thalweg was delineated from the aerial photographs. In many cases, the deep water of the thalweg could be seen as darker water on the photograph. In cases where the thalweg was not identifiable as darker water, it was estimated based on the position of the channel and sandbars. The length of each thalweg was used in calculating sinuosity, surface water slope and mean active channel width. Sinuosity is calculated by the thalweg length divided valley length. Surface water slope (*S*) is given by change in elevation divided by the thalweg length. This was calculated by extracting elevations from the 30-m DEMS every 1 kilometer along the thalweg, and graphing these measurements to determine the slope from the linear regression equation. Mean active channel width (w_{ac}) is given by the active channel area divided by the thalweg length. The discharge record was used with slope and mean active channel width to calculate SSP (ω) in W/m^2 by the equation:

$$\omega = \gamma QS/w_{ac} \tag{4}$$

where γ is the specific weight of water (9800 N/m^3), Q is the river discharge in m^3/s, S is the surface water slope (change in elevation divided by stream length), and w_{ac} is the width of the active channel in meters. For each time period (first date of aerial imagery of one scene to the first date of aerial imagery of the next scene), event peak, magnitude, duration, and frequency of SSP were evaluated in the manner after Julian et al. (2012). The MAF ($Q_{2.33}$) was the threshold above which SSP was compared to channel geometry. Event peak (in W/m^2) is defined as the maximum SSP value (ω_{max}) of the period. Magnitude (in W/m^2) is defined as the sum of SSPs of the period when discharge is greater than the mean annual flood ($\Sigma\ \omega$ when $Q > Q_{2.33}$). Duration (in days) is defined as the time in which discharge is greater than the mean annual flood ($Q > Q_{2.33}$). Frequency (#) is the number of individual flood events with discharges greater than the MAF (# flood events $> Q_{2.33}$). Since the MAF represents the effective discharge, SSP values above this threshold indicate the types of flows that are changing the channel geometry. The channel geometry and SSP calculations were performed for both the SS and the RS. Because there is only one gage station within the study area that lies downstream of MBC, only the channel geometry measurements were repeated with the study areas split into portions of the stream upstream and downstream of the confluence with MBC.

Sediment and Soils

Soil composition, measured as weighted average silt-clay percentage (SC%) of the entire soil depth was mapped for the floodplain, derived from the SSURGO data. Suspended-sediment concentration (in mg/L) and suspended-sediment discharge (tons/day) from the Arthur City gage station were graphed with the corresponding instantaneous discharge (in m^3/s). Since sandbars are directly affected by the amount of suspended-sediment being transported (Sanford 2002), suspended-sediment data can give a rough idea of the change in sediment supply available to form sandbars over time. This information was compared to previous reports of sedimentation yields from Greiner (1982), Simon, Dickerson, and Heins (2004), and the numerical sedimentation model study for the Red River from Copeland (2002). Unfortunately, since sediment data is difficult to gather and therefore sparse, this study looked only for trends.

VII. RESULTS

Precipitation and Discharge

Precipitation was variable over the 118-year study period with droughts and large storms and a long-term mean of 90.0 cm (Figure 10A). This was slightly lower than the mean annual precipitation reported for the Red River Bottomland ecoregion, which was 106-122 cm (Griffith 2007). On average, precipitation cycled between wet and dry periods frequently– about every 5 years. From the beginning of the precipitation record, these wet and dry years differed in precipitation by 40-60 cm. After an extremely wet year in 1935, there was an overall slight downward trend in mean annual precipitation, which can be seen by the 5-year mean (green line in Figure 10A). During this time, while dry years had around the same annual precipitation, the wet years slowly decreased in annual precipitation. Then, from about 1956 to 1976, mean annual precipitation had about an even amount of wet and dry years, followed by an overall slow increase in mean annual precipitation from 1976 to an extremely wet year in 1994. After this peak precipitation year in 1994, the mean annual precipitation stayed close to the long-term mean with little variation between wet and dry years until about 2006. After 2006, the mean annual precipitation pattern began to look closer to the pattern seen from 1904 to about 1920, with a drought in 2007. When the 3-day total precipitation was graphed over the time period, a more consistent pattern was seen (top of Figure 10B). Peak precipitation events occurred about every 40-50 years and did not necessarily correspond to years with major floods (Figure 10B).

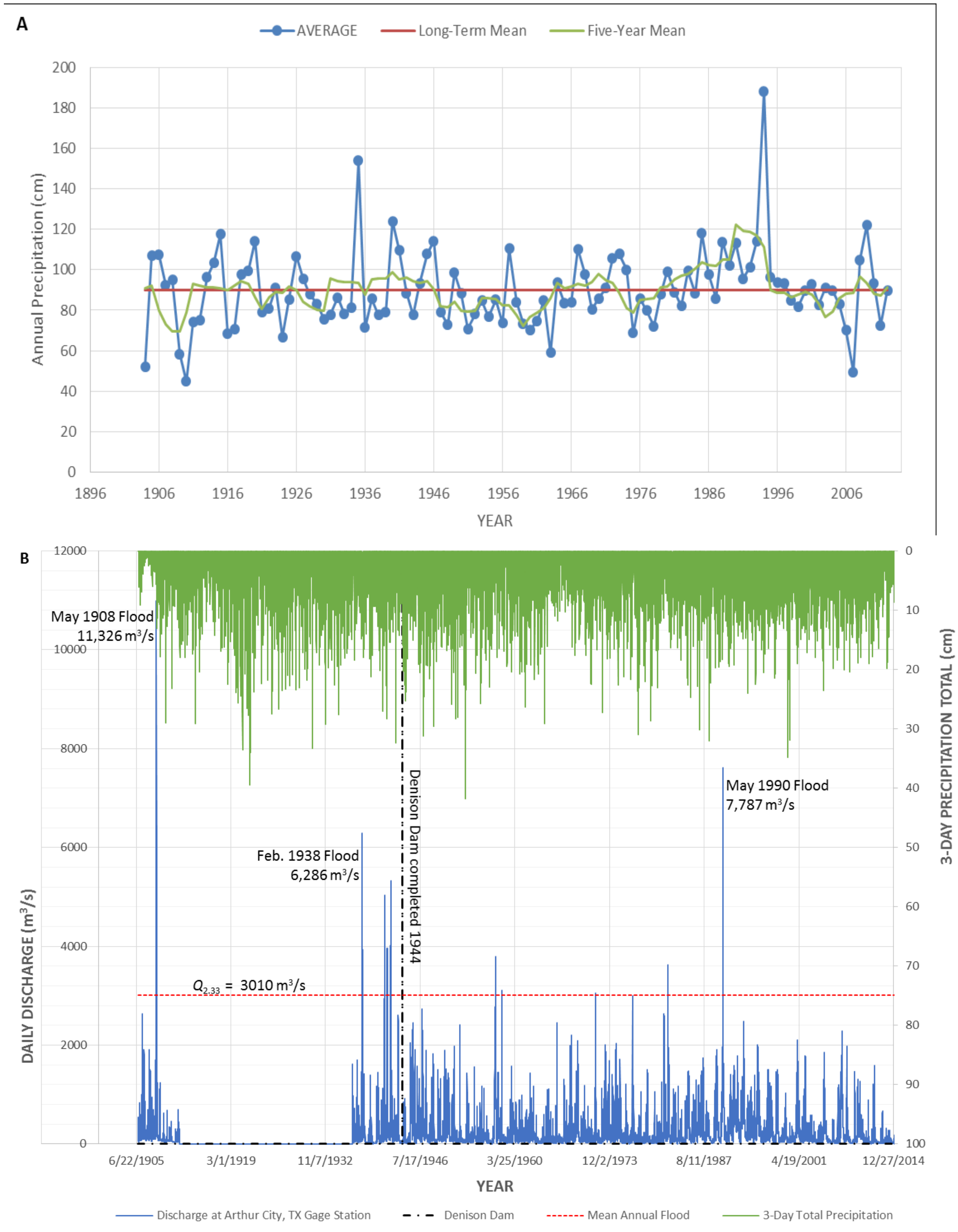

Figure 10. Precipitation and discharge time-series for the Red River below Denison Dam, 1896-2014. *(A) Annual mean precipitation. The red line is the long-term mean at 90.0 cm. The green line is the 5-year mean precipitation. (B) Daily discharge (blue) and three-day precipitation (green). Denison Dam was completed in 1944. The mean annual flood ($Q_{2.33}$) is 3010 m^3/s and represented by the dashed red line.*

Although the discharge record before Denison Dam was short, a discrepancy was seen between the pre-dam and post-dam discharges, with an overall decrease in post-dam discharges compared to pre-dam discharges (Figure 10B). The pre-dam MAF was calculated to be 3010 m^3/s. In the pre-dam period, discharges varied from low flows well below the MAF, to peak flood events well above the MAF. Notable floods included the May 1908 flood which peaked at 11,326 m^3/s, and the February 1938 flood which peaked at 6,286 m^3/s. In the post-dam period, very few flows exceeded the MAF. The largest flood from this period is the May 1990 flood, which peaked at 7,787 m^3/s. After 1990, no flows exceeded the MAF for the remainder of the study period.

Land Cover and Suitable Habitat

Segment-Scale Study Area

From the potential natural vegetation patterns (Duck and Fletcher 1945), this area of the Red River floodplain was mostly forested in pre-settlement times (see Figure 1 in Appendix A). Near the channel Bottomland Forest dominated, while further from the channel was Post-Oak forest. Occasional grasslands were interspersed among these forests. In the Eastern section of the floodplain, below the confluence with the Kiamichi River, Pine Hardwood forests and Oak-Hickory forests started to emerge. These vegetation patterns are consistent with the ecoregion characterization by Griffith (2007) and Omernik and Griffith (2014).

From pre-settlement to 2010, there was an overall trend of decreasing forest area with increasing cropland area (Table 3; Figure 11). Forest area increased slightly (6.6 percent) from 1979 to 2010, but overall decreased by about 53 percent from pre-settlement times to 2010. Cropland also decreased slightly (about 4 percent) from 1979 to 2010, and by 1949 onwards accounts for the majority of the floodplain land cover. Grassland accounted for more of the floodplain area in the 1890s than cropland, but by 1949 accounted for less area than cropland, even though the total percentage of floodplain it covered remained about the same. This indicates that between the 1890s and 1949, more forested lands were converted to croplands than grasslands. After 1949, grassland areas increased and decreased similarly to cropland area. Land cover maps for the SS scenes are found in Figures 1-16 in the Appendix A.

Looking at sandbar area, vegetated sandbar area, and suitable SNH, results show that suitable SNH tended to increase and decrease as total sandbar area increased or decreased (Table 3; Figure 12). From the 1890s to 1949, the largest increase in sandbar area was seen (increased by 3.5 percent), but suitable SNH only increased by 0.2 percent in the same time, although this was largely due to the fact that vegetation on sandbars was not mapped in the 1890s but was in the 1949 scene. If it is assumed that vegetation did occur on the sandbars in the pre-settlement and 1890s time periods, then the increase in suitable SNH in 1949 was likely greater than what was reported here.

Table 3. Timeline of changes in land cover, specific stream power, and channel geometry for the segment-scale study area.

$Q_{2.33} = 3010\ m^3/s$ Date (YYYY-MM-DD Floodplain Area	Valley Length = 173.8 km Land Cover % of Floodplain Study Area		Land Cover % of Sandbar Area	Specific Stream Power (ω) -Number of floods > $Q_{2.33}$ since prior date -Days that $Q > Q_{2.33}$ -Maximum ω (Q) -$\sum \omega$ when $Q > Q_{2.33}$	Channel Geometry -Active channel area -Mean width -Channel slope (m/m) -Sinuosity (km/km)
Pre-Settlement	79.7 % Forest	4.5 % Water	24.1 % Suitable Habitat	N/A	N/A
(567.8 km^2)	13.7 % Grassland	4.5 % Sandbars	N/A % Vegetated		
	0.0 % Cropland	N/A % Vegetated Sandbars			
	0.0 % Developed La	1.1 % Suitable Habitat			
1896-02-26	60.1 % Forest	8.3 % Water	50.6 % Suitable Habitat	12	93.33 km^2
(306.8 km^2)	21.7 % Grassland	4.8 % Sandbars	N/A % Vegetated	46 days	377 m
	4.8 % Cropland	N/A % Vegetated Sandbars		52.6 W/m^2 (10986 m^3/s)	0.00020
	0.1 % Developed La	2.4 % Suitable Habitat		969.3 W/m^2	1.43
1949-02-07	31.0 % Forest	6.8 % Water	31.6 % Suitable Habitat	3	133.84 km^2
(930.8 km^2)	18.8 % Grassland	8.4 % Sandbars	64.9 % Vegetated	8 days	535 m
	35.1 % Cropland	5.4 % Vegetated Sandbars		12.7 W/m^2 (3794 m^3/s)	0.00019
	0.1 % Developed La	2.7 % Suitable Habitat		91.8 W/m^2	1.44
1979-11-10	20.1 % Forest	5.9 % Water	31.1 % Suitable Habitat	2	95.39 km^2
(930.8 km^2)	28.1 % Grassland	5.4 % Sandbars	60.1 % Vegetated	11 days	396 m
	40.2 % Cropland	3.3 % Vegetated Sandbars		35.8 W/m^2 (7617 m^3/s)	0.00018
	0.3 % Developed La	1.7 % Suitable Habitat		287.1 W/m^2	1.39
2010-08-02	26.8 % Forest	6.3 % Water	24.9 % Suitable Habitat	0	84.82 km^2
(930.8 km^2)	26.5 % Grassland	4.2 % Sandbars	65.9 % Vegetated	0	350 m
	36.2 % Cropland	2.8 % Vegetated Sandbars		8.4 W/m^2 (1594 m^3/s)	0.00019
	0.3 % Developed La	1.0 % Suitable Habitat		0	1.4

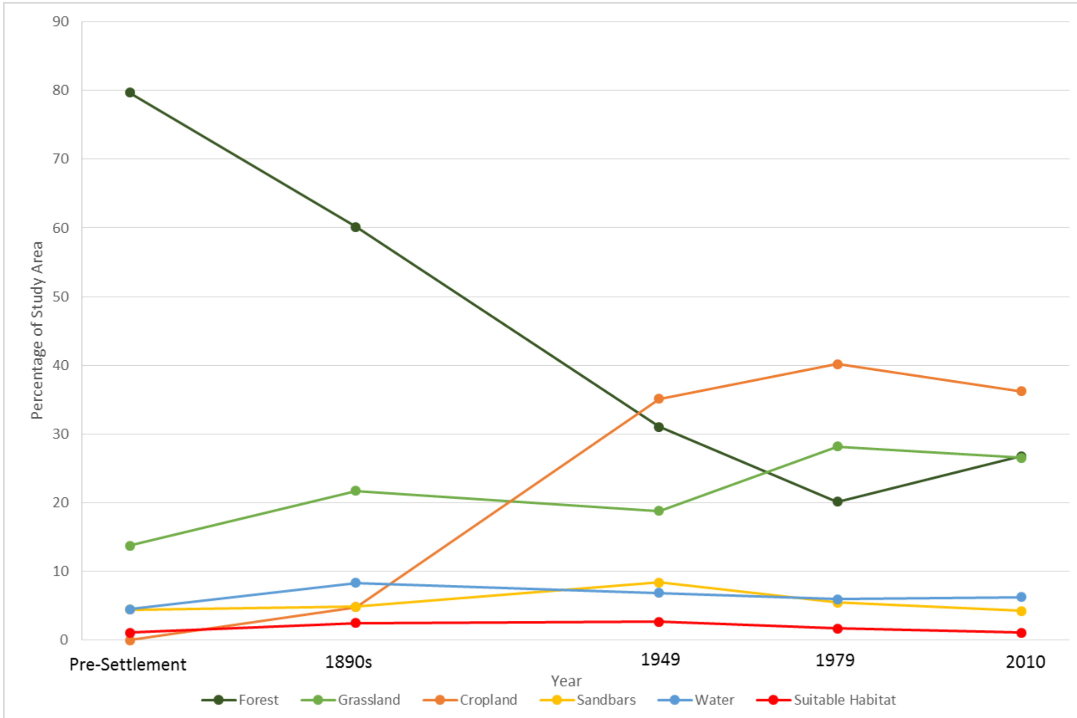

Figure 11. Land cover change over time for the segment-scale study area. *(Since Developed Land made up such a small percentage of the floodplain study area, it was not reported.)*

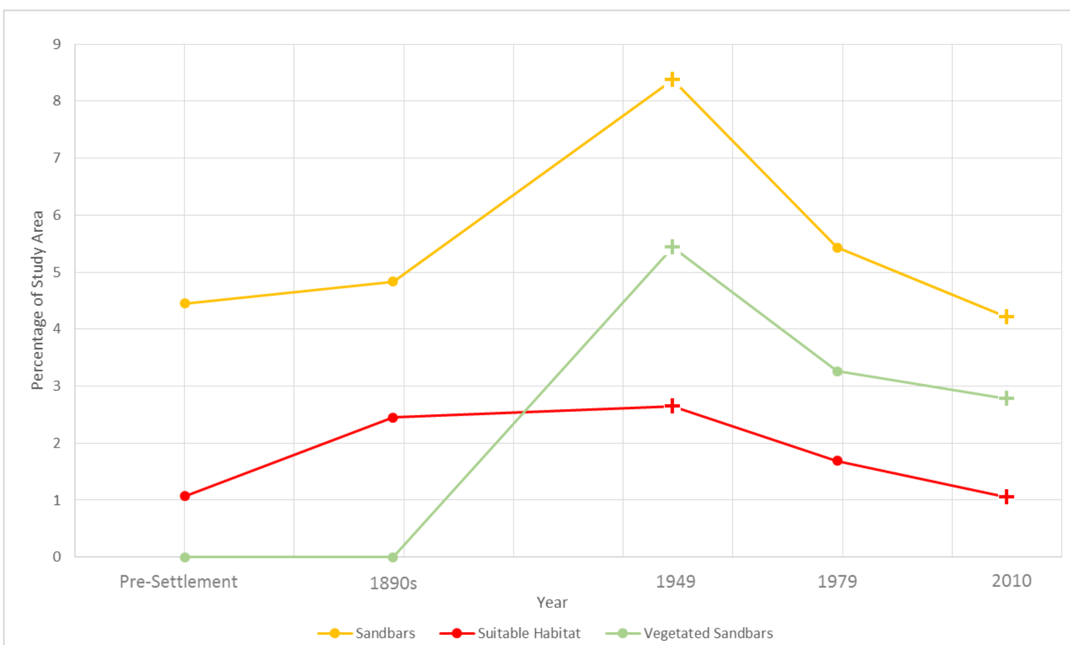

Figure 12. Change in sandbar, vegetated sandbar, and suitable habitat area over time for the segment-scale study area. *Data points marked by plus signs indicate scene years in which the average discharge across the scene was slightly higher than the threshold selection criterion.*

When vegetated sandbar areas and suitable SNH was reported as percentage of sandbar area, results showed a diverging pattern (Figure 13). Ignoring pre-settlement and 1890s time periods, when vegetation on sandbars was not reported, suitable SNH tended to decrease when vegetated areas of sandbars increased. From 1949 to 1979, however, vegetated sandbar area decreased by 4.9 percent, but suitable SNH stayed relatively the same at around 31 percent of total sandbar area. This decrease might be explained by the significant decrease in total sandbar area from 1949 to 1979 (about 3.0 percent). Even though the percentage of sandbars covered in vegetation was less in 1979, the overall sandbar area available for habitat use by ILTs was also less.

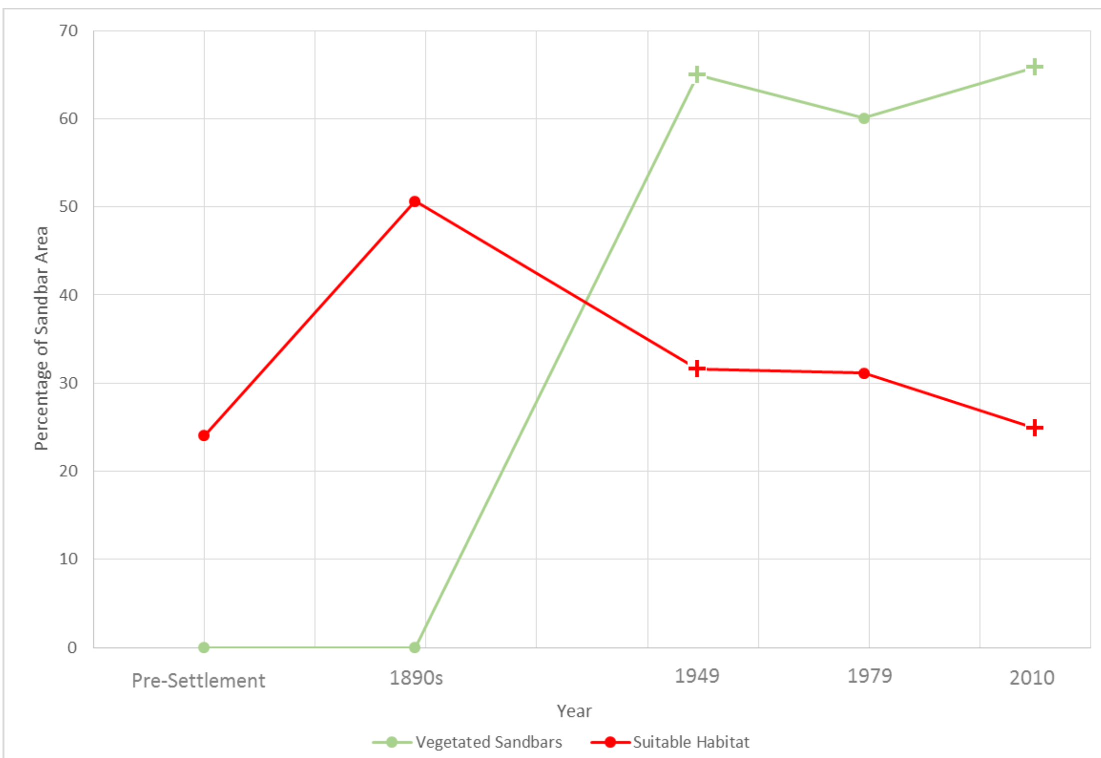

Figure 13. Change in vegetated sandbar area and suitable habitat over time as a percentage of total sandbar area for the segment-scale study area. *Data points marked by plus signs indicate scene years in which average discharge was slightly higher than the threshold selection criterion.*

Reach-Scale Study Area

The RS encompasses the middle ~ 50 km area of the SS, also centered on the confluence with MBC. A separate pre-settlement map was not made for the RS, but results were reported in the graphs and tables below. Again, both the pre-settlement and 1890s scenes were only analyzed for land cover and suitable habitat on the downstream section of MBC, where sandbars were mapped. The 1890s scene also was only analyzed for the Oklahoma side of the river, since the Texas side was not surveyed. In general, similar patterns of land cover change and suitable habitat can be seen in the RS as to the SS (Table 4; Figure 14). All land cover maps for the RS can be seen in Figures 17-23 in the Appendix B.

Overall, there was a decreasing trend for forest area and an increasing trend for grassland and cropland (Table 4; Figure 14). Forest area decreased from 70.7 percent of the study area in pre-settlement times to a low of 18.2 percent in 1979, although there was a slight increase (1.8 percent) in forest from 1949 to 1964. After 1979, forest area increased by 3.3 percent by 1982, and by an additional 0.5 percent by 1984. From 2004 to 2014, forest area stayed relatively consistent at around 24.3-25.4 percent of the total study area.

Grassland area increased in the 1890s from pre-settlement, as settlers started to cut down forest areas, especially near the river channel, for development into pastures and croplands. From the 1890s to 1949, grassland decreased only slightly (0.8 percent), even though forest decreased and cropland increased dramatically (by 35.6 percent). This seems to suggest that mostly forested lands were converted to croplands during this time and relatively little grassland was changed.

Table 4. Timeline of changes in land cover, specific stream power, and channel geometry for the reach-scale study area.

$Q_{2.33}$ = 3010 m^3/s -Date (YYYY-MM-DD) -Floodplain Area	Valley Length = 173.8 km Land Cover % of Floodplain Study Area		Land Cover % of Sandbar Area	Specific Stream Power (ω) -Number of floods > $Q_{2.33}$ since prior date -Days that Q > $Q_{2.33}$ -Maximum ω (Q) -∑ ω when Q > $Q_{2.33}$	Channel Geometry -Active channel area -Mean width -Channel slope (m/m) -Sinuosity (km/km)
Pre-Settlement (127.7 km^2)	70.7 % Forest 6.8 % Grassland 0.0 % Cropland 0.0 % Developed	16.2 % Water 6.3 % Sandbars N/A % Vegetated SBs 0.5 % Suitable SNH	N/A % Vegetated 7.4 % Suitable SNH	N/A	N/A
1896-02-26 (88.0 km^2)	66.6 % Forest 19.5 % Grassland 4.2 % Cropland 0.4 % Developed	5.5 % Water 3.7 % Sandbars N/A % Vegetated SBs 1.9 % Suitable SNH	N/A % Vegetated 49.8 % Suitable SNH	12 46 days 52.6 W/m^2 (10986 m^3/s) 969.3 W/m^2	26.11 km^2 356 m 0.00023 1.33
1949-02-07 (258.6 km^2)	26.8 % Forest 18.7 % Grassland 39.8 % Cropland 0.3 % Developed	6.8 % Water 7.6 % Sandbars 3.9 % Vegetated SBs 3.2 % Suitable SNH	50.9 % Vegetated 41.9 % Suitable SNH	2 7 days 13.8 W/m^2 (3794 m^3/s) 88.4 W/m^2	34.38 km^2 472 m 0.00020 1.33
1964-10-31 (258.6 km^2)	28.6 % Forest 26.3 % Grassland 33.9 % Cropland 0.4 % Developed	5.5 % Water 5.3 % Sandbars 2.9 % Vegetated SBs 1.8 % Suitable SNH	51.9 % Vegetated 34.1 % Suitable SNH	1 1 day 15.5 W/m^2 (3058 m^3/s) 15.5 W/m^2	24.67 km^2 337 m 0.00018 1.33
1972-02-29 (258.6 km^2)	21.7 % Forest 28.8 % Grassland 38.2 % Cropland 0.4 % Developed	6.3 % Water 4.6 % Sandbars 2.4 % Vegetated SBs 1.7 % Suitable SNH	51.9 % Vegetated 36.6 % Suitable SNH	0 0 15.6 W/m^2 (3001 m^3/s) 0	24.10 km^2 334 m 0.00017 1.31

Table 4 continued.

$Q_{2.33}$ = 3010 m^3/s -Date (YYYY-MM-DD) -Floodplain Area	Valley Length = 173.8 km Land Cover % of Floodplain Study Area		Land Cover % of Sandbar Area	Specific Stream Power (ω) -Number of floods > $Q_{2.33}$ since prior date -Days that $Q > Q_{2.33}$ -Maximum ω (Q) -$\sum \omega$ when $Q > Q_{2.33}$	Channel Geometry -Active channel area -Mean width -Channel slope (m/m) -Sinuosity (km/km)
1979-11-10	18.2 % Forest	6.2 % Water	40.7 % Vegetated	0	20.32 km^2
(258.6 km^2)	30.0 % Grassland	2.9 % Sandbars	37.0 % Suitable SNH	0	281 m
	42.3 % Cropland	1.2 % Vegetated SBs		16.2 W/m^2 (2639 m^3/s)	0.00018
	0.5 % Developed	1.1 % Suitable SNH		0	1.32
1982-03-07	21.5 % Forest	6.3 % Water	33.7 % Vegetated	1	21.59 km^2
(258.6 km^2)	24.7 % Grassland	3.8 % Sandbars	45.0 % Suitable SNH	1 day	300 m
	43.2 % Cropland	1.3 % Vegetated SBs		21.0 W/m^2 (3625 m^3/s)	0.00018
	0.4 % Developed	1.7 % Suitable SNH		21.0 W/m^2	1.31
1984-09-04	22.0 % Forest	5.3 % Water	24.1 % Vegetated	1	21.18 km^2
(258.6 km^2)	26.4 % Grassland	4.1 % Sandbars	50.2 % Suitable SNH	10 days	288 m
	41.8 % Cropland	1.0 % Vegetated SBs		44.9 W/m^2 (7617 m^3/s)	0.00019
	0.4 % Developed	2.0 % Suitable SNH		338.6 W/m^2	1.34
2004-08-31	24.9 % Forest	5.8 % Water	68.7 % Vegetated	0	26.13 km^2
(258.6 km^2)	26.6 % Grassland	5.0 % Sandbars	26.4 % Suitable SNH	0	346 m
	37.3 % Cropland	3.4 % Vegetated SBs		8.9 W/m^2 (1852 m^3/s)	0.00018
	0.4 % Developed	1.3 % Suitable SNH		0	1.38
2006-11-13	24.3 % Forest	4.4 % Water	61.7 % Vegetated	0	25.63 km^2
(258.6 km^2)	28.0 % Grassland	6.1 % Sandbars	31.0 % Suitable SNH	0	336 m
	36.8 % Cropland	3.7 % Vegetated SBs		11.1 W/m^2 (2288 m^3/s)	0.00018
	0.4 % Developed	1.9 % Suitable SNH		0	1.39

Table 4 continued.

$Q_{2.33}$ = 3010 m^3/s -Date (YYYY-MM-DD) -Floodplain Area	Valley Length = 173.8 km Land Cover % of Floodplain Study Area				Land Cover % of Sandbar Area		Specific Stream Power (ω) -Number of floods > $Q_{2.33}$ since prior date -Days that $Q > Q_{2.33}$ -Maximum ω (Q) -$\sum \omega$ when $Q > Q_{2.33}$	Channel Geometry -Active channel area -Mean width -Channel slope (m/m) -Sinuosity (km/km)
2008-07-02	24.9	% Forest	6.3	% Water	55.6	% Vegetated	0	25.48 km^2
(258.6 km^2)	27.7	% Grassland	5.3	% Sandbars	37.0	% Suitable SNH	0	339 m
	35.9	% Cropland	2.9	% Vegetated SBs			7.2 W/m^2 (1461 m^3/s)	0.00017
	0.8	% Developed	2.0	% Suitable SNH			0	1.37
2010-08-02	25.4	% Forest	6.7	% Water	68.7	% Vegetated	0	24.52 km^2
(258.6 km^2)	26.3	% Grassland	3.9	% Sandbars	23.8	% Suitable SNH	0	325 m
	37.2	% Cropland	2.7	% Vegetated SBs			8.1 W/m^2 (1594 m^3/s)	0.00018
	0.4	% Developed	0.9	% Suitable SNH			0	1.37
2012-07-05	24.4	% Forest	5.1	% Water	54.0	% Vegetated	0	24.68 km^2
(258.6 km^2)	27.0	% Grassland	5.4	% Sandbars	34.8	% Suitable SNH	0	324 m
	37.7	% Cropland	2.9	% Vegetated SBs			3.4 W/m^2 (673 m^3/s)	0.00016
	0.5	% Developed	1.9	% Suitable SNH			0	1.39
2014-07-12	23.7	% Forest	4.6	% Water	69.5	% Vegetated	0	24.48 km^2
(258.6 km^2)	29.0	% Grassland	5.6	% Sandbars	23.8	% Suitable SNH	0	323 m
	36.7	% Cropland	3.9	% Vegetated SBs			0.7 W/m^2 (128 m^3/s)	0.00019
	0.5	% Developed	1.3	% Suitable SNH			0	1.38

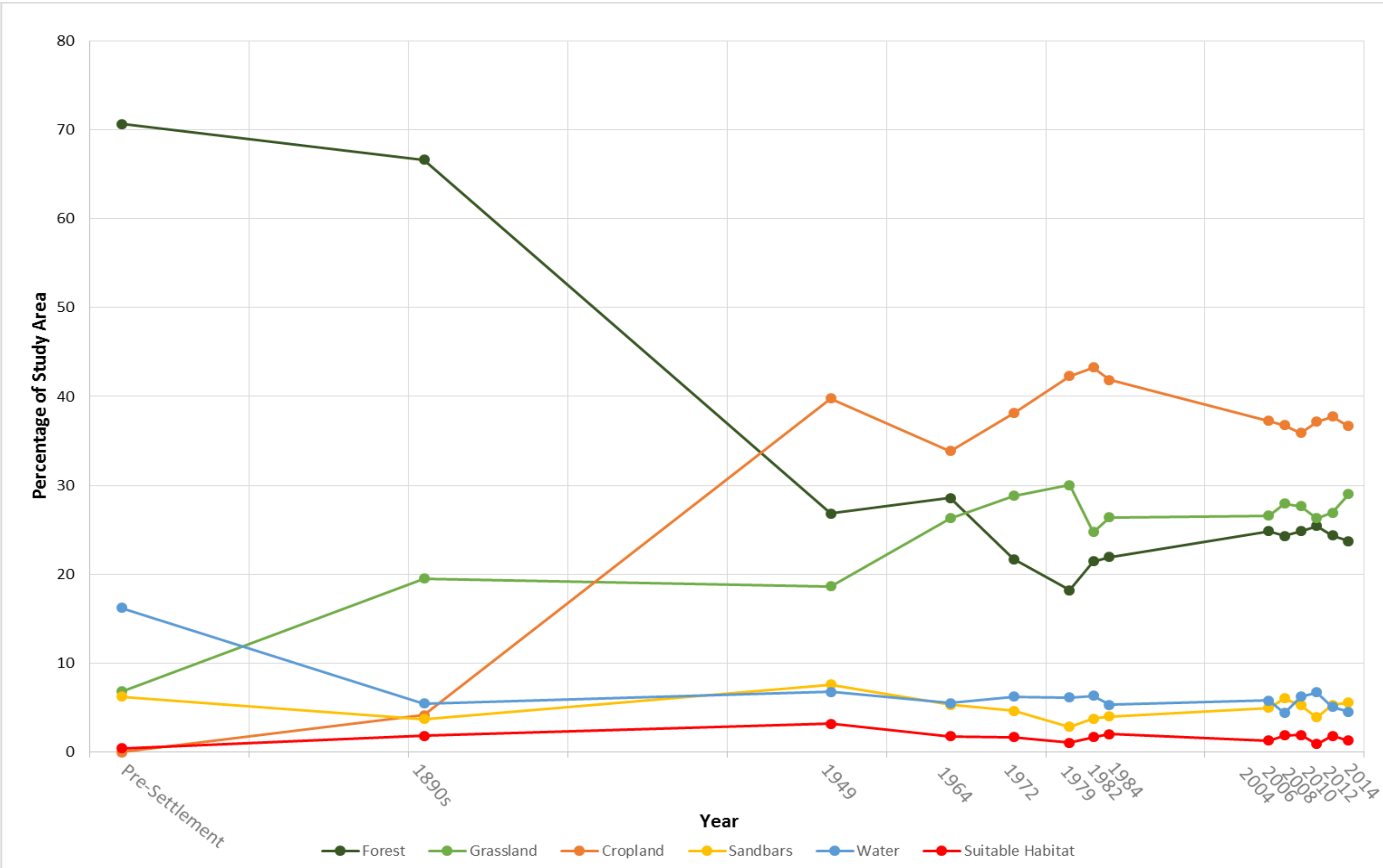

Figure 14*. *Land cover change over time for the reach-scale study area. *Because Developed Land accounted for such a small percentage of the floodplain study area, they were not reported.*

After 1949, grasslands continued to increase to 30.0 percent of the study area by 1979 (increase of 11.3 percent from 1949). Cropland area increased dramatically (35.6 percent) by 1949, but decreased by 5.9 percent by 1964. Grassland and forest areas increased from 1949 to 1964, suggesting that some cropland was converted back to grassland and forest during this time. Cropland continued to increases to a maximum of 43.2 percent in 1982 (a 9.3 percent increase from 1964).

Although grassland decreased from 1979 to 1982, cropland and forest area both increased, but as grassland and forest area increased again by 1984, cropland however, decreased by 1.4 percent. This suggests that grassland and forest areas were largely interchanging, and not related to changing cropland areas. Cropland decreased by 4.5 percent by 2004, and then remained relatively stable at around 35.9-37.7 percent of the total study area. Again, from 2004 to 2014, cropland area pattern did not follow the pattern of grassland or forest areas, and neither did it follow an opposite pattern. This suggests that grassland and forest areas were interchanging with each other, but cropland increases or decreases might be related to something else, perhaps the migration of the river channel.

Sandbar area, vegetated sandbar area, and suitable SNH followed an irregular trend over the 118-year timeline (Table 4; Figure 15). Suitable SNH was low in pre-settlement times, largely due to the presence of forested banks throughout the study area. Since the amount of vegetation on the sandbars at this time was unknown, suitable SNH in reality was even lower than reported here (0.5 percent of total study area).

Sandbars only accounted for 3.7 percent of the total study area in the 1890s, a decrease of 2.6 percent from the pre-settlement scene. However, this could be misleading because in the 1890s scene, only the sandbars on the Oklahoma side of the river were accounted for, while sandbars on both sides of the river were counted for the pre-settlement scene. In reality, total sandbar area was probably similar from pre-settlement times to 1890s, assuming there was little change in water and sediment input to the river over that time period.

After the 1890s, sandbar area increased by 3.9 percent to a maximum of 7.6 percent of the study area in 1949. Sandbar area then continued to decrease through 1979, by 4.7 percent. Then, sandbar area increased again through 2006, by 3.2 percent, followed by a sharp decrease (2.2 percent) in area over the next four years. From 2010 to 2014, sandbar area increased again by 1.7 percent to 5.6 percent of the study area by 2014.

For the most part, the total vegetated areas of these sandbars followed a similar pattern to the total sandbar area (Figure 15). Ignoring pre-settlement and 1890s times, when vegetation on sandbars was not mapped, vegetation on the sandbars decreased by 2.7 percent from 1949 to 1979, similarly to the decrease in total sandbar area over this time. Vegetation then increased slightly (0.1 percent) on sandbars by 1982, but this increase was not proportional to the increase in sandbar area. Sandbar area continued to increase by 1984, while vegetation on these sandbars decreased in 1984 by 0.3 percent. From 1984 to 2006, vegetation on sandbars increased in area by 2.7 percent, then decreased again by 1.0 percent by 2010. From 2010, vegetation on sandbars continued to increase by 1.2 percent to account for 3.9 percent of the total study area by 2014.

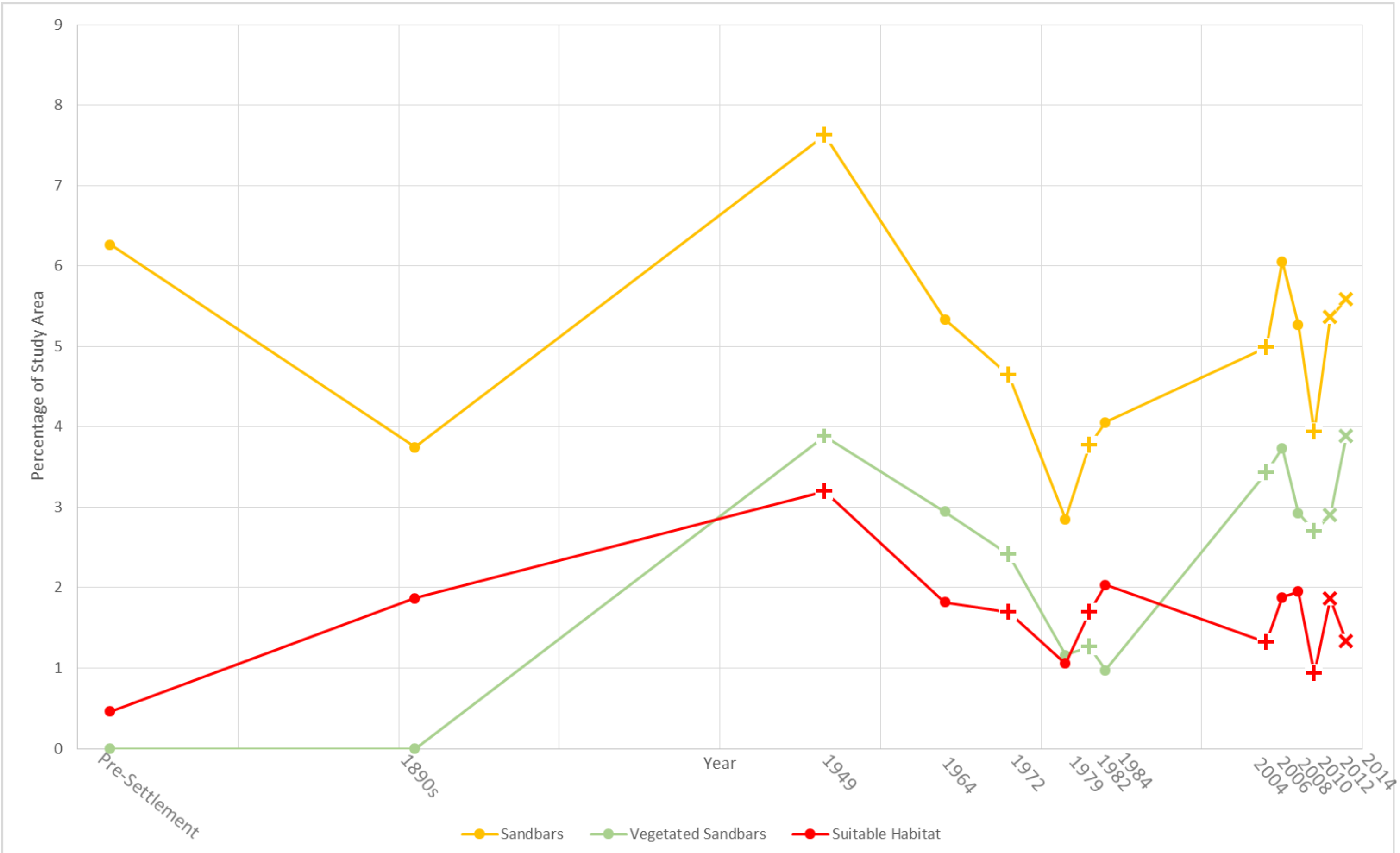

Figure 15. Changes in sandbar, vegetated sandbar, and suitable habitat area over time for the reach-scale study area. *Data points marked by plus signs indicate scene years in which average discharge was slightly higher than the threshold selection criterion, and data points marked by X's indicate scene years in which average discharge was slightly lower than the threshold selection criterion.*

Suitable SNH over this time period followed a pattern that largely mirrored the pattern seen by sandbar area, but did not correlate much to the pattern of vegetated sandbar area (Figure 15). With an increase in sandbar area from 1890s to 1949, suitable SNH also increased by 1.4 percent to a maximum of 3.2 percent of the total study area in 1949. When sandbar area decreased until 1979, suitable SNH also decreased (although at a slightly slower rate) by 2.1 percent. Then, suitable SNH increased again by 0.9 percent by 1984. Sandbar area continued to increase through 2006, but suitable SNH decreased from 1984 to 2004 by 0.7 percent. This decrease could perhaps be explained by the sharp increase in vegetated sandbar area from 1984 to 2006. Vegetated sandbar areas decreased again in 2008, but suitable SNH increased by another 0.7 percent from 2004 to 2008, which was opposite of the vegetation pattern. The increase in suitable SNH area from 2006 to 2008 also did not follow the sandbar area pattern, as total sandbar area decreased during this time. This suggests that a different criterion than vegetation or sandbar area for suitable SNH was the limiting factor in 2008. When sandbar area decreased in 2010, suitable SNH also decreased by 1.1 percent to only 0.9 percent of the total study area. Suitable SNH increased by 1.0 percent by 2012, as sandbar area increased, but when sandbar area continued to increase in 2014, suitable SNH decreased by 0.6 percent. Vegetated sandbar areas increased from 2012 to 2014, but again, since this pattern does not hold for most of the other dates, it suggests that other criteria were limiting suitable SNH during this time.

Even though there did not seem to be a correlation between suitable SNH and vegetated sandbars areas when looking at the percentage of total study area for those land cover categories, when viewed as percentages of total sandbar area, vegetation on the sandbars and suitable SNH seemed to be more closely correlated, at least after 1979 (Figure 16). Again ignoring pre-settlement and 1890s values, from 1949 to 1964, the percentage of sandbar area that was vegetated increased by 1.0 percent, although the percentage of sandbar area that was available for suitable SNH decreased by 7.8 percent. From 1964 to 1972, the amount of vegetation on the sandbars stayed the same, at 51.9 percent of sandbar area, but suitable SNH increased by 2.5 percent of sandbar area.

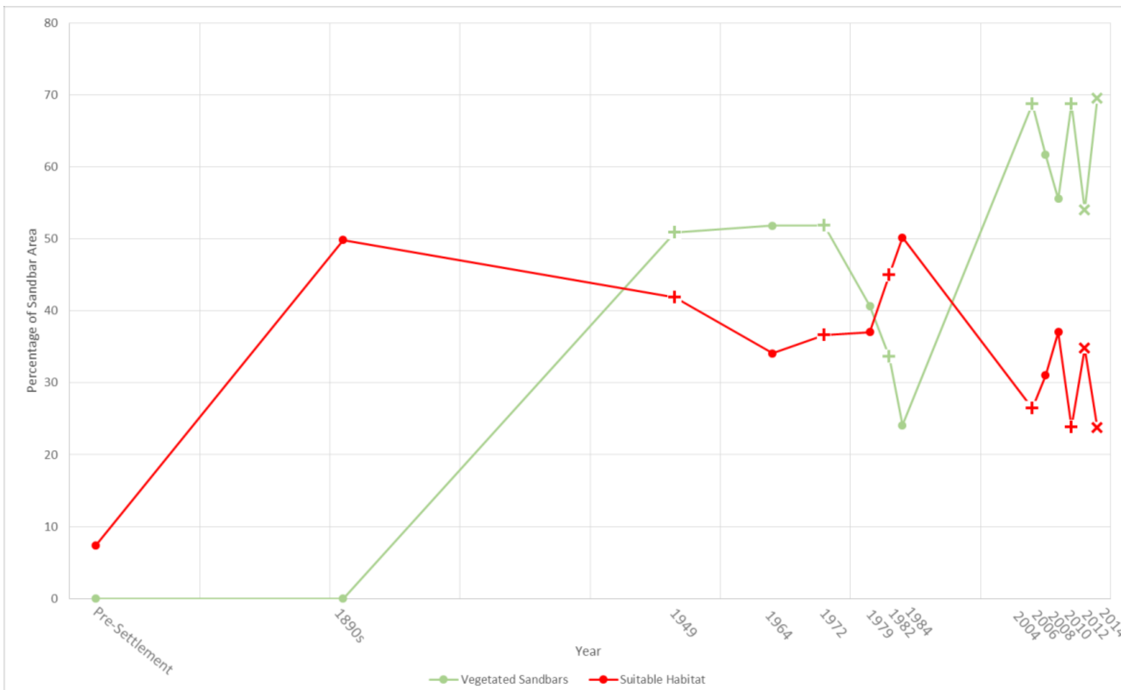

Figure 16. Change in vegetated sandbar area and suitable habitat over time as a percentage of total sandbar area for the reach-scale study area. *Data points marked by plus signs indicate scene years in which average discharge was slightly higher than the threshold selection criterion, and data points marked by X's indicate scene years in which average discharge was slightly lower than the threshold selection criterion.*

Suitable SNH continued to increase slightly by 0.4 percent by 1979, even though vegetated sandbar areas decreased by 11.2 percent of the total sandbar area. After 1979, a more expected pattern emerged where suitable SNH increased when vegetation decreased and decreased when vegetation increased. From 1979 to 1984, vegetation decreased by

16.6 percent of total sandbar area while suitable SNH increased by 13.2 percent of total sandbar area. Then vegetation increased by 44.6 percent by 2004, suitable SNH decreased by 23.8 percent of total sandbar area. By 2008, suitable SNH increased by 10.6 percent of sandbar area while vegetation decreased by 13.1 percent of sandbar area. From 2010 to 2014, suitable SNH first decreased in 2010 by 13.2 percent, then increased in 2012 by 11.0 percent, and finally decreased again by 11 percent by 2014. Vegetated sandbar areas followed the opposite pattern, increased in 2010 by 13.1 percent, then decreased in 2012 by 14.7 percent, and finally increased again in 2014 by 15.5 percent. From this data, vegetation on the sandbars seemed to be an important factor in the determining the amount of suitable SNH. However, since the change in percentage of sandbar area for vegetated areas and suitable SNH was not the same (vegetation changed by greater percentages than suitable SNH), this suggested that other criteria were influencing suitable SNH area.

Channel Geometry and Specific Stream Power

Segment-Scale Study Area

For SSP calculations, the discharge record was broken up into 4 periods each starting with the first date of imagery for that scene: 1896-1949, 1949-1979, 1979-2010, and 2010-2014. From the 1890s to 1949, there were 12 individual flood events that exceeded MAF (3010 m^3/s) (Table 3) lasting a total of 46 days and totaling 969.3 W/m^2 in SSP. The maximum SSP reached was 52.6 W/m^2 at a discharge of 10,986 m^3/s. This corresponds to the May 1908 flood, which was the largest flood on record for the Red River. In the 1890s, the active channel area was 93.33 km^2 and the mean channel width was 377 m. Slope was 0.00020 and sinuosity was 1.43. By the 1949 time period, the active channel area increased to 133.84 km^2, and the 12 flood events worked to widen the channel to a mean channel width of 535 m. Change in channel slope was negligible and the sinuosity increased slightly to 1.44.

From 1949 to 1979, which was after Denison Dam was built, there were only 3 individual flood events that exceeded the MAF, and these lasted a total of 8 days. The total SSP for these floods equaled 91.8 W/m^2, while the maximum SSP reached 12.7 W/m^2 at a maximum discharge of 3,794 m^3/s. This maximum discharge was only slightly higher than the MAF. With relatively little flood activity and power, by 1979, the active channel area decreased to 95.39 km^2 and the channel narrowed to a mean width of 396 m. Change in channel slope was negligible, but the sinuosity decreased to 1.39. This suggests that although the SSP was not high during this period, channel form became straighter.

From 1979 to 2010, there were only 2 individual flood events that exceeded the MAF, but these did last a total of 11 days. They totaled 287.1 W/m^2 in SSP, with a maximum SSP of 35.8 W/m^2 at a maximum discharge of 7,617 m^3/s, which corresponded to the May 1990 flood. This stream power did increase the sinuosity of the channel slightly to 1.4. However, despite the magnitude of these two flood events, the active channel area and mean channel width both decreased before 2010 to 84.82 km^2 and 350 m, respectively.

Reach-Scale Study Area

The RS showed similar changes in channel geometry over time as the SS. The active channel area and mean channel width in the 1890s was 26.11 km^2 and 356 m, respectively (Table 4). The channel slope was 0.00023 and the sinuosity was 1.33. Because there were no aerial imagery or other type of "imagery" again until 1949, the time period for analyzing SSP was the same here as for the SS, and hence the SSP values are the same as well. Again, this resulted in 12 individual flood events that exceeded the MAF of 3010 m3/s, which lasted 46 days and had a total SSP of 969.3 W/m^2. SSP peaked at 52.6 W/m^2 during a maximum discharge of 10,986 m3/s. These floods increased the active channel area and mean channel width to 34.38 km^2 and 472 m, respectively, by 1949. The sinuosity of the channel remained the same, while channel slope decreased slightly to 0.00020.

From 1949 to 1964, there were 2 individual flood events that lasted a total of 7 days and had a total SSP of 88.4 W/m^2. The maximum SSP reached 13.8 W/m^2 during a peak discharge of 3,794 m3/s. These floods did not appear to change the channel geometry by any significant amount. By 1964, the active channel area decreased by 9.71 km^2 and the mean channel width decreased by 135 m. However, sinuosity remained the same at 1.33 and channel slope slightly decreased again to 0.00018. Channel narrowing would suggest sediment deposition occurring during these floods, however, overall sandbar area decreased by 2.3 percent of the total study area from 1949 to 1964.

During the 1964 to 1972 time period, there was only one flood event that exceeded the MAF and it lasted only one day. The total and maximum SSP was 15.5 W/m^2 with a peak discharge of 3,058 m3/s, which was only slightly higher than the MAF value. Without large floods, the channel narrowed slightly to a mean width of 334 m by 1972 and active channel area decreased slightly by 0.57 km^2. Change in channel slope was negligible, although the sinuosity of the channel decreased by 0.02.

For the next two time periods (1972-1979 and 1979-1982), there were no flows that exceeded the MAF. The maximum SSP reached was 14.6 W/m^2 at a maximum discharge of 3,001 m^3/s in the 1972-1979 period, and in the 1979-1982 period, maximum SSP was 16.2 W/m^2 at a maximum discharge of 2,639 m^3/s. However, the channel area and width first decreased from 1972 to 1979, but then increased again by 1982. Active channel area decreased by 3.78 km^2 by 1979, then increased by 1.27 km^2 by 1982. From 1972 to 1979, mean channel width decreased by 53 m, then increased by 20 m in 1982. Sinuosity and channel slope remained relatively consistent over this time period, sinuosity being 1.32 in 1979 and 1.31 in 1982, and channel slope being 0.00018 in 1979 and 1982.

From 1982 to 1984, there was only one flood event that exceeded the MAF and it lasted only a day. The maximum (and total) SSP was 21.0 W/m^2 at a peak discharge of 3,625 m^3/s. The channel continued to narrow to 288 m by 1984, and active channel area decreased slightly by 0.41 km^2. Change in channel slope was again negligible, but the sinuosity increased to 1.34.

From 1984 to 2004, there was only one flood event that exceeded the MAF. This was the May 1990 flood that last 10 days and had a total SSP of 338.6 W/m^2 and a maximum SSP of 44.9 W/m^2 at the peak discharge of 7,617 m^3/s. Unfortunately, no imagery met the selection criteria again until 2004, so it was unknown how much this specific flood event widened the channel immediately. However, by 2004, the channel was still an average of 58 m wider in 2004 than it was in 1984. Active channel area increased by 4.95 km^2. Sinuosity increased to 1.38, suggesting that the work of the flood was mostly lateral.

From 2004 to 2014, there were no more flood events that exceeded the MAF. Maximum SSP ranged from 0.7 W/m^2 (in 2014) to 11.1 W/m^2 (in 2006) and peak discharges ranged from as low as 128 m^3/s (in 2014) to 2288 m^3/s (in 2006). The channel continued to slowly narrow by 23 m to a mean width of 323 m in 2014. Change in channel slope was again negligible. Sinuosity first increased to 1.39 by 2006, decreased to 1.37 over the next two time periods, and rose again to 1.39 by 2012, and fell slightly to 1.38 by 2014.

When the event peak, magnitude, duration, and frequency of SSP was compared to channel widening, reasonable relationships were found, given that only 5 of the time periods had flows that exceed the MAF (Figure 17). Increased event peak, magnitude, duration, and frequency were all roughly correlated to channel widening. Event peak of SSP was the most correlated to channel widening with an r^2 value of 0.75. However, a notable anomaly is seen from this relationship. From 1949 to 1964 the channel narrowed by 134 m but the maximum SSP was only 12.8 W/m^2 during that time. Yet, around the same maximum SSP (15.5 W/m^2) occurred from 1964 to 1972, yet the mean channel width only slightly decreased by 3m. This anomaly might be explained by the fact that from 1949 to 1964, the magnitude of SSP was significantly higher than the magnitude of SSP from 1964 to 1972 (difference of 72.9 W/m^2). The duration of flooding events was also higher from 1949 to 1964 than from 1964 to 1972. This suggests that although the event peak property of SSP was most closely correlated with channel widening, duration and magnitude of SSP might play an important role as well. In general, the channel widened when maximum SSP was greater than about 30 W/m^2 and narrowed when maximum SSP was less than this.

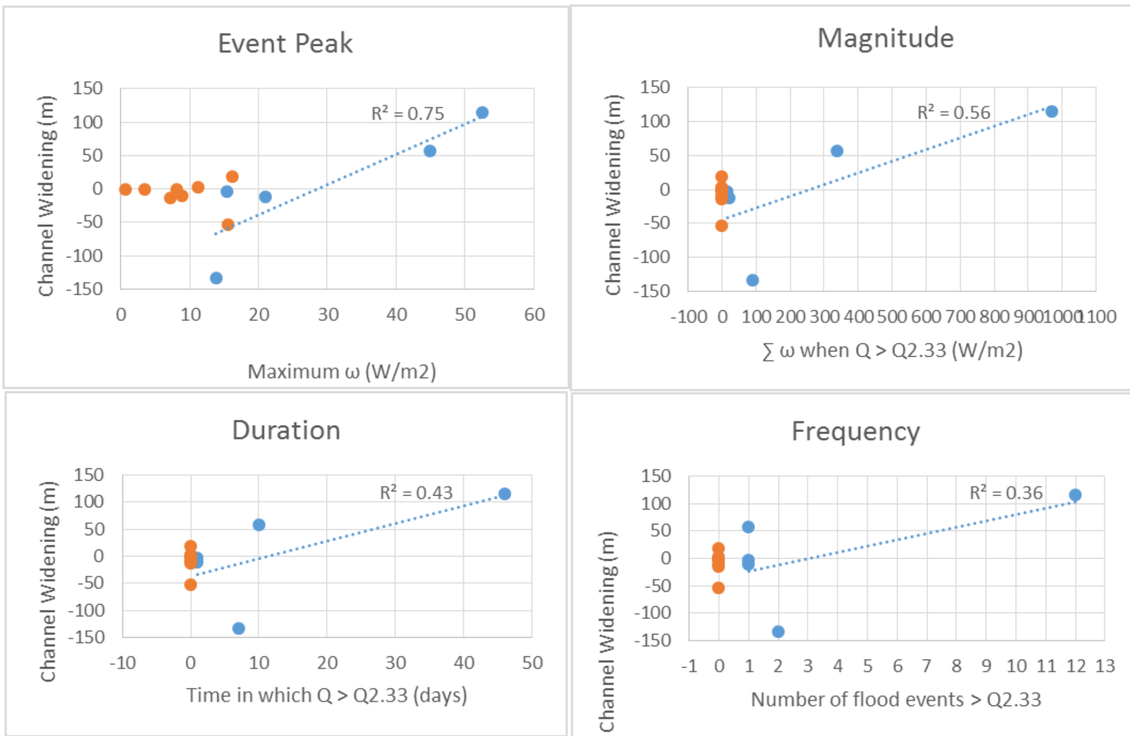

Figure 17. Relationships between channel widening and the specific stream power properties of event peak, magnitude, duration, and frequency. *In order to have an equal sample size for all four properties, only intervals with an active channel flood ($Q_{2.33}$) were used for regression analysis (blue dots). Intervals without a mean annual flood are denoted by orange dots. Negative values of channel widening represent channel narrowing.*

<u>Comparison of Upstream versus Downstream of Muddy Boggy Creek</u>

To analyze the effect that water and sediment input from MBC had on the Red River, the analyses outlined above were repeated, splitting the active channel area into upstream and downstream sections. For the upstream/downstream comparison, land cover of only the active channel area was analyzed since the channel could clearly be divided into upstream and downstream sections. It was less clear to determine where to make a division for upstream and downstream sections for the entire floodplain, and since forest, grassland, and cropland were spread fairly evenly over the length of the floodplain study area, they were not analyzed here. Also, SSP was not analyzed in this comparison since the discharge record comes from a gage station that was right below the confluence with MBC and was the only gage station within the floodplain study area. Channel geometry and the sandbar area, vegetated sandbar area, and suitable SNH could be compared upstream versus downstream of MBC.

Segment-Scale Study Area

In general, over the entire time period, upstream of MBC the Red River tended to be wider, have a larger active channel area, steeper slope, but was less sinuous than downstream of the confluence (Table 5). From 1896 to 1949, based on the 1890s scene, the active channel area upstream of MBC measured 50.24 km^2, while only measuring 42.93 km^2 downstream of MBC. The mean channel width was 380 m upstream of MBC, but slightly narrower downstream at 371 m. The channel slope was significantly steeper upstream versus downstream of MBC, being 0.00023 on the upstream side but only 0.00017 on the downstream side. The sinuosity was also higher on the upstream side than the downstream side, 1.55 and 1.30 respectively.

By 1949, sandbars can be measured on both side of the MBC confluence, and results showed that from this time forward, total sandbar area was greater upstream of MBC than downstream (Table 5). Total suitable habitat area and vegetated sandbar area was not as consistent. In 1949, there were 44.14 km^2 of sandbar area upstream of MBC. Vegetation on these sandbars covered a total area of 25.30 km^2, which only left 16.87

km^2 for suitable SNH. This accounted for 57.32 percent of total sandbar area covered in vegetation and 38.21 percent of total sandbar area available as suitable SNH.

Downstream of MBC, however, total sandbar area only accounted for 33.87 km^2, although the total vegetated sandbar area was slightly higher than upstream, at 25.36 km^2. Suitable SNH only made up 7.81 km^2 downstream of MBC, however. This accounted for 74.90 percent of total sandbar area being vegetated, and only 23.05 percent available for suitable SNH. The active channel area and mean channel width were both higher upstream of MBC than downstream. The active channel area was 68.95 km^2 upstream of MBC, and slightly less at 64.88 km^2 downstream of MBC. Mean channel width was 584 m upstream, but only 491 m downstream. The channel slope was also steeper upstream of MBC, at 0.00024 while being only 0.00014 downstream of MBC. However, the channel became more sinuous on the downstream side than in the 1890s. Upstream sinuosity was 1.39 but 1.49 downstream of MBC.

In the 1979 scene, the difference in sandbars upstream versus downstream of MBC was less. Total sandbar area upstream of MBC was 26.66 km^2 and downstream sandbar area was similar at 23.93 km^2. Vegetated sandbar area was also similar upstream versus downstream of MBC, at 16.95 km^2 and 13.44 km^2, respectively. Suitable SNH was slightly higher downstream, the total area upstream versus downstream was 7.39 km^2 and 8.36 km^2, respectively. This accounted for 63.57 percent of total sandbar area that was vegetated upstream of MBC, but only 56.16 percent vegetated downstream. Suitable SNH made up 27.73 percent of total sandbar area upstream of MBC, but was higher at 34.93 percent of total sandbar area downstream of MBC.

Table 5. Comparison of upstream versus downstream changes in sandbar area, vegetated sandbar area, suitable habitat, and channel geometry for the segment-scale study area.

Date	*Upstream of MBC* Land Cover Total Area (km^2)		% of Sandbar Area		Channel Geometry -Active channel area -Mean width -Channel slope (m/m) -Sinuosity (km/km)	*Downstream of MBC* Land Cover Total Area (km^2)		% of Sandbar Area		Channel Geometry -Active channel area -Mean width -Channel slope (m/m) -Sinuosity (km/km)
1896-02-26	(* No sandbars were mapped upstream of Muddy Boggy, so can't make upstream/downstream comparison)				50.24 km^2 380 m 0.00023 1.55	(* No sandbars were mapped upstream of Muddy Boggy, so can't make upstream/downstream comparison)				42.93 km^2 371 m 0.00017 1.30
1949-02-07	Sandbars Vegetated SBs Suitable SNH	44.14 25.30 16.87	57.32 38.21	% Vegetated % Suitable SNH	68.95 km^2 584 m 0.00024 1.39	Sandbars Vegetated SBs Suitable SNH	33.87 25.36 7.81	74.90 23.05	% Vegetated % Suitable SNH	64.88 km^2 491 m 0.00014 1.49
1979-11-10	Sandbars Vegetated SBs Suitable SNH	26.66 16.95 7.39	63.57 27.73	% Vegetated % Suitable SNH	47.20 km^2 401 m 0.00024 1.38	Sandbars Vegetated SBs Suitable SNH	23.93 13.44 8.36	56.16 34.93	% Vegetated % Suitable SNH	48.19 km^2 390 m 0.00013 1.39
2010-08-02	Sandbars Vegetated SBs Suitable SNH	16.53 12.70 2.93	76.80 17.71	% Vegetated % Suitable SNH	41.84 km^2 353 m 0.00022 1.39	Sandbars Vegetated SBs Suitable SNH	17.71 13.12 6.82	61.52 32.01	% Vegetated % Suitable SNH	42.96 km^2 346 m 0.00017 1.40

More suitable SNH occurring downstream of MBC in this scene was different from what was seen in the 1949 scene. However, the channel geometry upstream versus downstream mostly followed the same pattern seen in 1949, with the exception that the active channel area was actually slightly greater downstream of MBC. The active channel area upstream versus downstream of MBC was 47.20 km^2 and 48.19 km^2, respectively. Mean channel width was still greater upstream than downstream, at 401 m and 390 m, respectively. Channel slope continued to be steeper upstream versus downstream of MBC, at 0.00024 and 0.00013, respectively. The downstream section of river continued to be slightly more sinuous than the upstream section, at 1.39 downstream versus 1.38 upstream.

By 2010, the upstream/downstream pattern changes, with greater sandbar area, vegetated sandbar area, and suitable habitat area in the downstream section of the river, rather than in the upstream section. Total sandbar area accounted for 16.53 km^2 upstream of MBC, and 17.71 km^2 downstream of MBC. Total vegetated sandbar area was 12.70 km^2 upstream of MBC, and 13.12 km^2 downstream of MBC. Suitable SNH was 2.93 km^2 upstream of MBC, and higher downstream of MBC, at 6.82 km^2. This accounted for 75.80 percent of sandbar area to be vegetated and only 17.71 percent available for suitable SNH upstream of MBC, but downstream of MBC, 61.52 percent of sandbar area was vegetated and 32.01 percent was available for suitable SNH. The increase in sandbar area and suitable SNH downstream of MBC in this time could be the result of the fact that the downstream section of the river here was slightly wider and higher in total active channel area than the upstream section. Upstream of MBC, the active channel area and mean channel width were 41.84 km^2 and 353 m, respectively, but downstream of MBC, the active channel area and mean channel width were 42.96 km^2 and 346 m, respectively.

The channel slope was still steeper upstream ersus downstream, at 0.00022 and 0.00017, respectively. The river continued to be slightly more sinuous downstream of MBC, at 1.39 upstream and 1.40 downstream of MBC.

Reach-Scale Study Area

The RS showed similar patterns to the SS in terms of an upstream versus downstream comparison of the confluence with MBC (Table 6). Total sandbar area was greater upstream of MBC than downstream for all years (Figure 18). The total sandbar areas that were vegetated were also greater upstream than downstream of MBC for all years, and the same pattern held for the percentage of vegetated sandbar area except for in 1949 (Figure 19).

In 1949, even though the total vegetated sandbar area was higher upstream versus downstream, the percentage of total sandbar area that was vegetated was actually higher downstream of MBC. However, the total sandbar area upstream of MBC was significantly larger upstream than downstream of MBC (a difference of 12.02 km^2).

The percentage of sandbar area considered suitable for ILT SNH, however, varied upstream versus downstream of MBC (Figure 20). In 1949, mostly due to larger total sandbar areas upstream of MBC, suitable SNH was also a higher percentage of sandbar area upstream of MBC. However, by 1964, the percentage of suitable SNH was greater downstream of MBC than upstream. This trend continued until 1982, when the upstream section of the river again had the greater percentage of suitable SNH. In 1984, the percentage of suitable SNH continued to be higher upstream of MBC, but by 2004, it was less than the downstream portion of the river.

Table 6. Comparison of upstream versus downstream changes in sandbar area, vegetated sandbar area, suitable habitat, and channel geometry for the reach-scale study area.

Date	*Upstream of MBC* Land Cover Total Area (km²)		*Upstream of MBC* Land Cover % of Sandbar Area		Channel Geometry -Active channel area -Mean width -Channel slope (m/m) -Sinuosity (km/km)	*Downstream of MBC* Land Cover Total Area (km²)		*Downstream of MBC* Land Cover % of Sandbar Area		Channel Geometry -Active channel area -Mean width -Channel slope (m/m) -Sinuosity (km/km)
1896-02-26	(* No sandbars were mapped upstream of Muddy Boggy, so can't make upstream/downstream comparison)				16.25 km^2 388 m 0.00024 1.47	(* No sandbars were mapped upstream of Muddy Boggy, so can't make upstream/downstream comparison)				9.86 km^2 314 m 0.00021 1.19
1949-02-07	Sandbars Vegetated SBs Suitable SNH	15.86 7.62 7.06	48.03 44.49	% Vegetated % Suitable SNH	23.20 km^2 612 m 0.00023 1.33	Sandbars Vegetated SBs Suitable SNH	3.84 2.40 1.20	62.58 31.13	% Vegetated % Suitable SNH	11.19 km^2 319 m 0.00013 1.32
1964-10-31	Sandbars Vegetated SBs Suitable SNH	7.40 4.68 2.27	63.25 30.65	% Vegetated % Suitable SNH	14.23 km^2 370 m 0.00028 1.35	Sandbars Vegetated SBs Suitable SNH	6.35 2.93 2.40	46.21 37.79	% Vegetated % Suitable SNH	10.43 km^2 301 m 0.00001 1.31
1972-02-29	Sandbars Vegetated SBs Suitable SNH	7.70 4.37 2.80	56.67 36.38	% Vegetated % Suitable SNH	14.24 km^2 375 m 0.00025 1.33	Sandbars Vegetated SBs Suitable SNH	4.31 1.86 1.59	43.23 36.97	% Vegetated % Suitable SNH	9.86 km^2 289 m 0.00001 1.29

Table 6 continued.

Date	*Upstream of MBC* Land Cover: Total Area (km^2)		% of Sandbar Area		Channel Geometry -Active channel area -Mean width -Channel slope (m/m) -Sinuosity (km/km)	*Downstream of MBC* Land Cover: Total Area (km^2)		% of Sandbar Area		Channel Geometry -Active channel area -Mean width -Channel slope (m/m) -Sinuosity (km/km)
1979-11-10	Sandbars	5.25	46.50	% Vegetated	12.17 km^2	Sandbars	2.13	26.24	% Vegetated	8.15 km^2
	Vegetated SBs	2.44	36.74	% Suitable SNH	318 m	Vegetated SBs	0.56	37.72	% Suitable SNH	239 m
	Suitable SNH	1.93			0.00022	Suitable SNH	0.80			0.00004
					1.34					1.29
1982-03-07	Sandbars	6.67	36.94	% Vegetated	12.69 km^2	Sandbars	3.07	26.52	% Vegetated	8.90 km^2
	Vegetated SBs	2.47	45.80	% Suitable SNH	335 m	Vegetated SBs	0.81	43.14	% Suitable SNH	261 m
	Suitable SNH	3.06			0.00026	Suitable SNH	1.32			0.00002
					1.33					1.29
1984-09-04	Sandbars	6.63	26.51	% Vegetated	12.38 km^2	Sandbars	3.82	20.07	% Vegetated	8.80 km^2
	Vegetated SBs	1.76	53.38	% Suitable SNH	319 m	Vegetated SBs	0.77	45.08	% Suitable SNH	254 m
	Suitable SNH	3.54			0.00026	Suitable SNH	1.72			0.00005
					1.363982					1.31
2004-08-31	Sandbars	6.88	75.90	% Vegetated	14.56 km^2	Sandbars	6.01	60.50	% Vegetated	11.57 km^2
	Vegetated SBs	5.22	21.01	% Suitable SNH	366 m	Vegetated SBs	3.64	32.64	% Suitable SNH	323 m
	Suitable SNH	1.45			0.00024	Suitable SNH	1.96			0.00004
					1.40					1.35

Table 6 continued.

Date	*Upstream of MBC* Land Cover: Total Area (km^2)		% of Sandbar Area		Channel Geometry -Active channel area -Mean width -Channel slope (m/m) -Sinuosity (km/km)	*Downstream of MBC* Land Cover: Total Area (km^2)		% of Sandbar Area		Channel Geometry -Active channel area -Mean width -Channel slope (m/m) -Sinuosity (km/km)
2006-11-13	Sandbars	8.97	64.20	% Vegetated	14.51 km^2	Sandbars	6.69	58.30	% Vegetated	11.12 km^2
	Vegetated SBs	5.76	29.75	% Suitable SNH	359 m	Vegetated SBs	3.90	32.79	% Suitable SNH	310 m
	Suitable SNH	2.67			0.00021	Suitable SNH	2.19			0.00012
					1.42					1.36
2008-07-02	Sandbars	8.07	64.77	% Vegetated	14.40 km^2	Sandbars	5.56	41.97	% Vegetated	11.09 km^2
	Vegetated SBs	5.23	32.50	% Suitable SNH	365 m	Vegetated SBs	2.33	43.63	% Suitable SNH	311 m
	Suitable SNH	2.62			0.00020	Suitable SNH	2.42			0.00009
					1.39					1.35
2010-08-02	Sandbars	5.51	78.44	% Vegetated	13.90 km^2	Sandbars	4.66	57.28	% Vegetated	10.62 km^2
	Vegetated SBs	4.32	16.04	% Suitable SNH	348 m	Vegetated SBs	2.67	33.05	% Suitable SNH	299 m
	Suitable SNH	0.88			0.00023	Suitable SNH	1.54			0.00001
					1.40					1.34
2012-07-05	Sandbars	7.85	61.55	% Vegetated	13.95 km^2	Sandbars	6.01	44.12	% Vegetated	10.74 km^2
	Vegetated SBs	4.83	30.98	% Suitable SNH	348 m	Vegetated SBs	2.65	39.74	% Suitable SNH	297 m
	Suitable SNH	2.43			0.00022	Suitable SNH	2.39			0.00005
					1.41					1.36
2014-07-12	Sandbars	8.28	74.91	% Vegetated	13.75 km^2	Sandbars	6.16	62.30	% Vegetated	10.73 km^2
	Vegetated SBs	6.20	19.38	% Suitable SNH	346 m	Vegetated SBs	3.84	29.68	% Suitable SNH	299 m
	Suitable SNH	1.60			0.00021	Suitable SNH	1.83			0.00003
					1.40					1.36

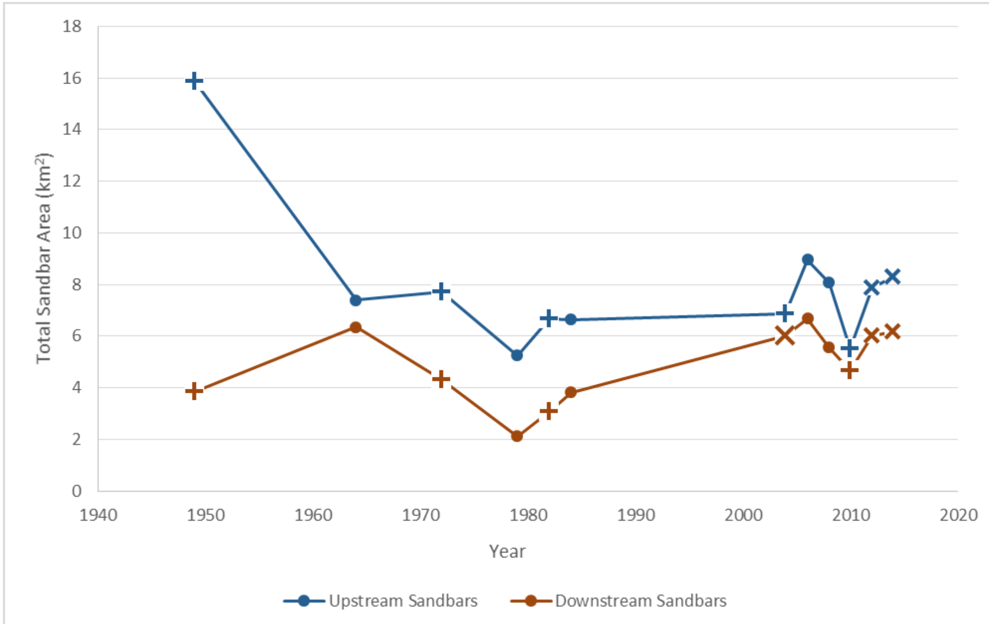

Figure 18. Comparison of total sandbar area upstream versus downstream of Muddy Boggy Creek. *Data points marked by plus signs indicate scene years in which average discharge was slightly higher than the threshold selection criterion, and data points marked by X's indicate scene years in which average discharge was slightly lower than the threshold selection criterion.*

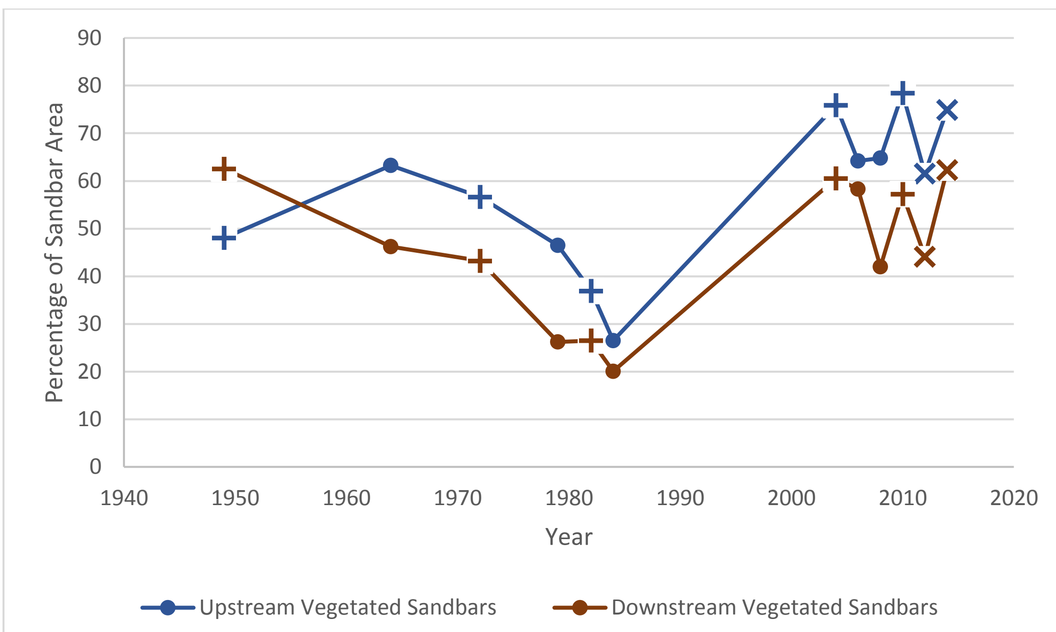

Figure 19. Comparison of the percentage of sandbar areas vegetated upstream versus downstream of Muddy Boggy Creek. *Data points marked by plus signs indicate scene years in which average discharge was slightly higher than the threshold selection criterion, and data points marked by X's indicate scene years in which average discharge was slightly lower than the threshold selection criterion.*

From 2004 to 2014, the percentage of suitable SNH continued to be greater downstream of MBC, and from 2008 to 2014, the amount of suitable SNH both upstream and downstream of MBC mirrored each other in falling and rising.

The mean active channel width was greater upstream than downstream of MBC for all years (Figure 20). The largest difference was seen in 1949, where the upstream section of the river was on average 293 m wider than the downstream section of the river. From 1964 to 1984, the difference in mean channel width stayed relatively consistent from between 65-86 m in difference.

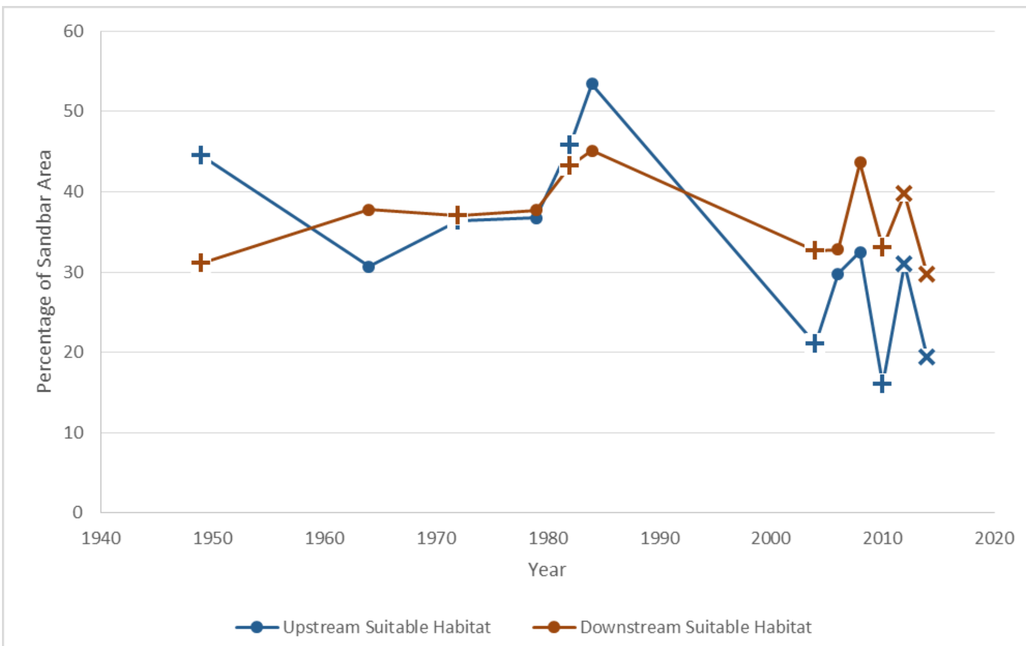

Figure 20. Comparison of the percentage of sandbar area considered suitable sandbar nesting habitat upstream versus downstream of Muddy Boggy Creek. *Data points marked by plus signs indicate scene years in which average discharge was slightly higher than the threshold selection criterion, and data points marked by X's indicate scene years in which average discharge was slightly lower than the threshold selection criterion.*

From 2004 to 2014, the downstream channel width continued to mirror the pattern seen in the upstream channel width, with a relatively consistent difference in width of about 50 m.

The active channel area was also consistently higher upstream than downstream of MBC (Figure 21). Similarly to mean channel width, the largest difference occurred in 1949, when the upstream channel area was 12.01 km^2 greater than the downstream channel area (Table 6). After 1949, the upstream channel area stayed relatively consistently larger than the downstream channel area by an average of about 3.5 km^2.

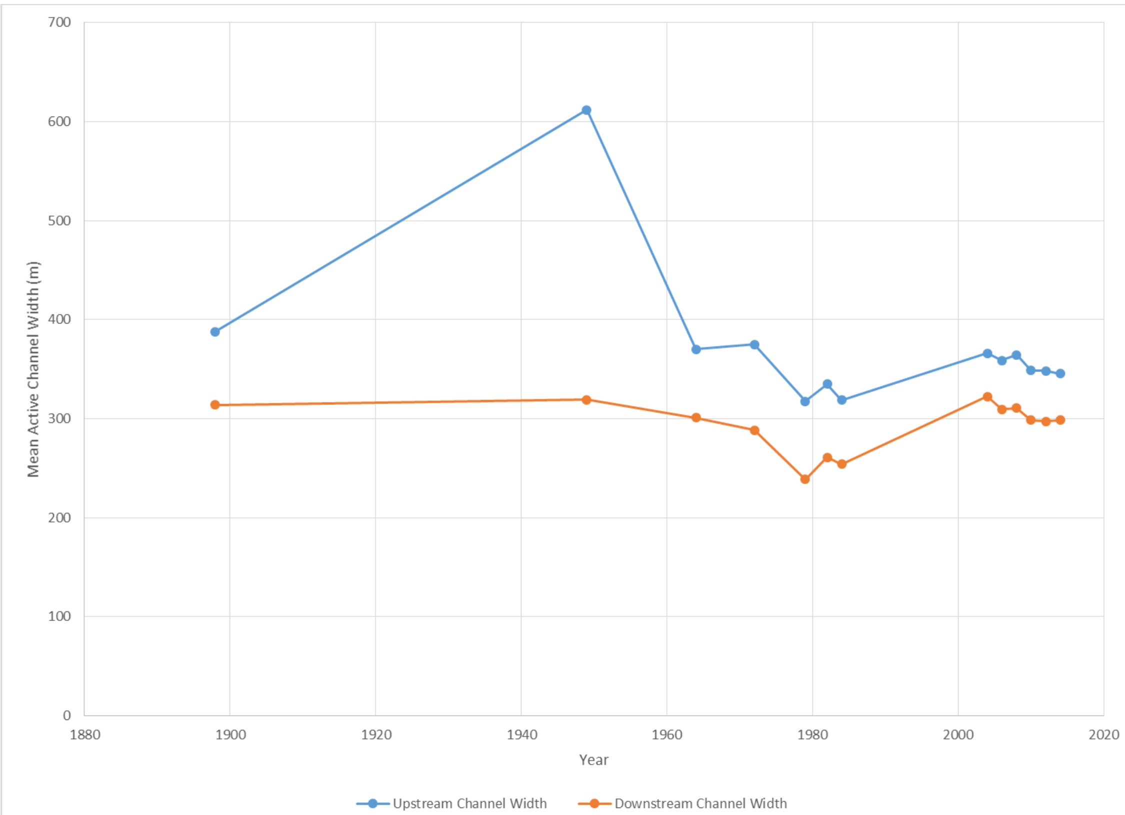

Figure 21. Comparison of mean active channel width upstream versus downstream of Muddy Boggy Creek.

Upstream of MBC, the channel slope varied between 0.00020 and 0.00028, but mostly stated consistent around an average of 0.00023 (Table 6). The downstream section of the river decreased in slope significantly between the 1890s and 1964, changing from 0.00021 in the 1890s to only 0.00001 by 1964. Channel slope in the downstream section increased to 0.00012 in 2006, but then stayed flat over the years at an average of 0.00005.

On average, though, the upstream channel slope was about 0.00018 greater than the downstream channel slope.

The sinuosity of the river also consistently remained higher for the upstream section (Figure 22). The largest difference in sinuosity was in the 1890s, when the upstream section had a sinuosity index that was 0.29 higher than the downstream section. In 1949, the sinuosities of both sections converged, with the smallest difference of only 0.01. After 1949, the sinuosity index for the upstream section alternated between being 0.04 and 0.06 higher than the downstream section. The downstream section mostly mirrored the upstream section pattern, first by both slightly decreasing from 1949 to 1984, then with both slowly rising, or becoming more sinuous, from 1984 to 2014.

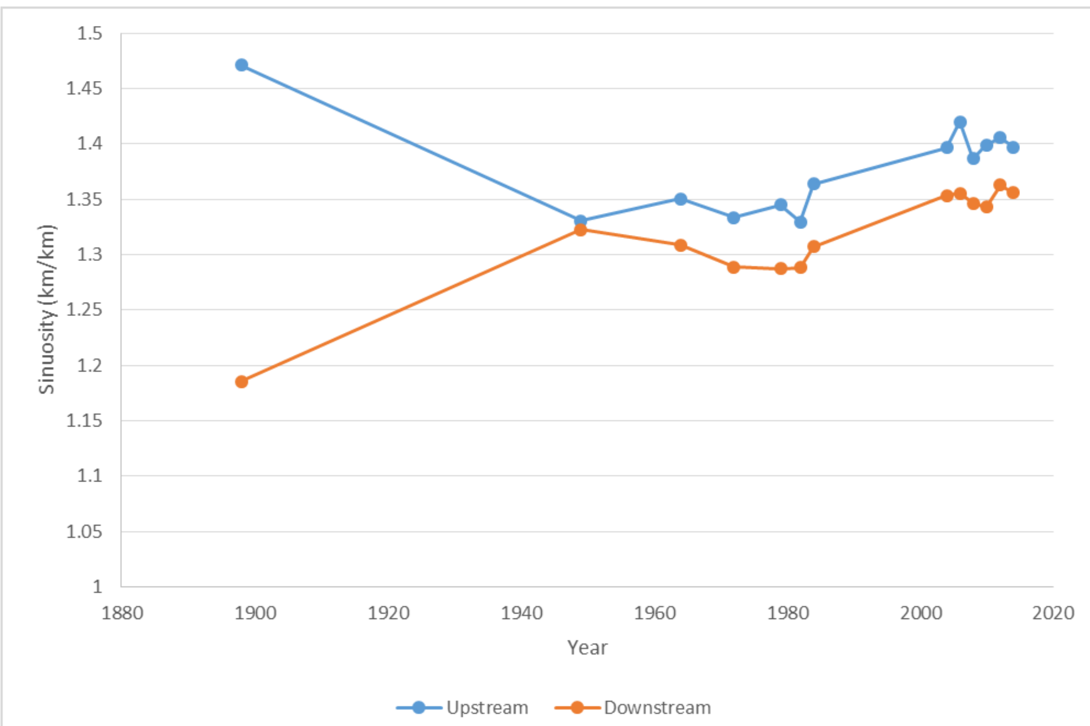

Figure 22. Comparison of channel sinuosity upstream versus downstream of Muddy Boggy Creek.

Sediment and Soils

The sediment supply for the Red River is originally derived from Permian red beds of Texas, Oklahoma, and New Mexico (Albertson and Patrick 1996). Below Denison Dam, the valley is filled with alluvium grading downward from red clay at the surface through red silt, brown and gray sand, to gravel encountered at 60-95 feet (Copeland 2002). From the SSURGO data, soil composition varied widely across the floodplain, with silt-clay percentage (SC%) ranging from 6-91 percent (Figure 23). The sandiest areas (~6 SC%) occurred near the channel margins. Further from the channel, the soil becomes more clayey. High percentages of clay (~91 SC%) tend to occur in areas that coincide with croplands.

Simon, Dickerson, and Heins (2004) reported suspended-sediment transport rates at the 1.5-year recurrence interval ($Q_{1.5}$) for each Level III ecoregion for the United States. For the South Central Plains ecoregion, which includes this section of the Red River below Denison Dam, the median suspended-sediment concentration at $Q_{1.5}$ varied from 46 to 140 mg/L. The median suspended-sediment yield at $Q_{1.5}$ varied from 0.81 to 6.5 tons/day/km^2 (Simon, Dickerson, and Heins 2004). Higher concentrations of suspended-sediment were found in different ecoregions along the Red River upstream of Denison Dam, but overall the reported values for the South Central Plains ecoregion falls in the middle range for all reported values across the United States. Although the Red River as a whole is reported to have one of the highest suspended-sediment loads in the United States (Albertson and Patrick 1996), the section of the Red River that flows through the South Central Plains (below Denison Dam) perhaps has less amounts of suspended-sediment loads from work by Simon, Dickerson, and Heins (2004).

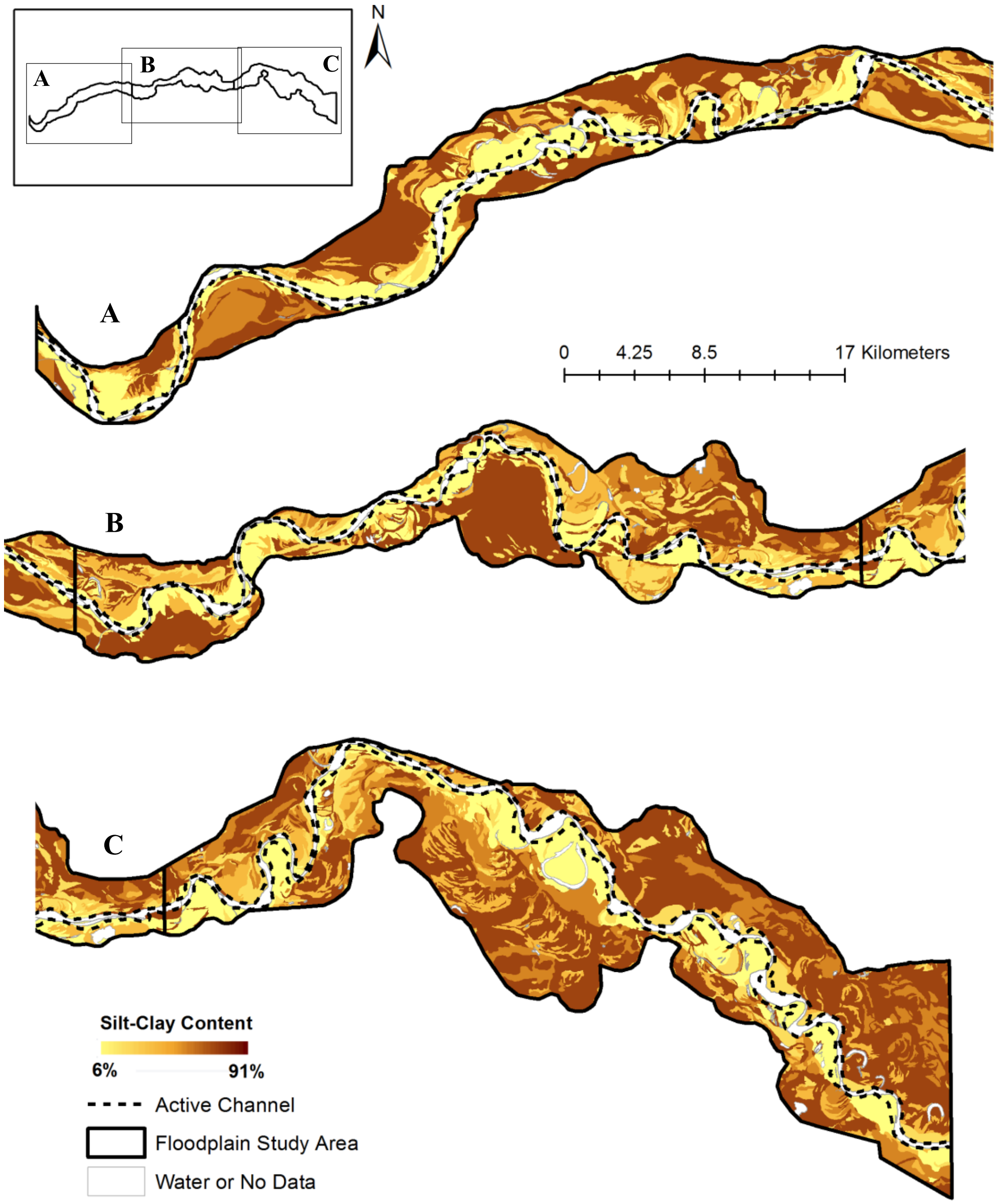

Figure 23. Soil composition for the study areas. *The reach-scale is also seen in part (B) of the map. Soil map was derived from SSURGO data collected in 2003. The active channel for 2003 is shown for reference. White areas are either water or areas with no data.*

Given that the work by Simon, Dickerson, and Heins (2004) was performed across the South Central Plains as a whole ecoregion and not specifically the Red River, and that it used an effective discharge of $Q_{1.5}$ rather than the $Q_{2.33}$ used in this study, it is difficult to make specific inferences for this study section. It is possible that the Red River had slightly higher suspended-sediment loads than the rest of the South Central Plains ecoregion.

In a report to the Texas Department of Water Resources, Greiner (1982) compiled estimates of the amounts of gross sheet and rill erosion and gully and streambank erosion occurring on an average annual basis above 300 yield points across the state of Texas from 1979 data. There were various yield points along the Red River, and incremental sediment yields varied from 469.50 tons/km^2 to 4892.68 ton/km^2 along the lower Red River (Table 7) (Greiner 1982). Accumulative sediment yield along the lower Red River was 135.91 tons/km^2 (Greiner 1982). Sediment yields from Red River tributaries were also reported, however, these only include tributaries on the Texas side of the Red River. Incremental and accumulative sediment yields for the Texas tributaries were 1,482.63 tons/km^2 and 19.77 tons/km^2, respectively (Greiner 1982).

Copeland (2002) performed a numerical sedimentation model study for the Red River below Denison Dam, which gave the best source for sediment data for this study. Copeland (2002) used watershed erosion, channel bank erosion, and channel degradation as sediment sources, but ignored sediment delivered by tributaries since reservoirs capture most of the sediment load generated off of watersheds. Denison Dam effectively captures the entire sediment load from the 102,874 km^2 watershed above it, and downstream of the dam, runoff is heavily controlled by reservoirs on most of the major tributaries (Copeland 2002). However, there is still about 12,000 km^2 of uncontrolled watershed above the gage at Arthur City, TX but below Denison Dam, which includes the watershed of the last two undammed major tributaries: the Blue River and MBC.

Table 7. Incremental and accumulative sediment yield estimates for yield points along the Red River. Compiled from Greiner (1982) and units converted from tons/acre to tons/km^2. Red River tributaries only includes Texas tributaries.

				Incremental	Accumulative
	Land Area (km^2)	Controlled Drainage Area (km^2)	Non-Contributing Area (km^2)	Sediment Yield (tons/km^2)	Sediment Yield (tons/km^2)
Prairie Dog Town Fork Red River	3824	435	4	3162.95	51.89
Upper Salt Fork Red River	1896	1184	495	469.50	22.24
Salt Fork Red River	1366	141	47	1408.50	34.59
North Fork Red River	2051	75	27	1284.95	44.48
Lake Texoma	922	14	0	1111.97	17.30
Lower Red River	1821	59	0	4892.68	135.91
Red River Tributaries	935	105	0	1482.63	19.77

Copeland (2002) reports that immediately below Denison Dam, sediment concentrations were very small, but increased in the downstream direction before the Arthur City, TX gage station. MBC drains an area of about 6,291 km^2, and after the Arthur City, TX gage station, sediment concentrations decreased again because the remaining tributaries are all dammed. The calculated total sediment inflow at the Arthur City, TX gage was estimated to be 14.32 million tons/year, with the sand inflow estimated to be 6.10 million tons/year (Copeland 2002). Copeland (2002) estimated that 1.40 million tons of this total came from bank erosion and about 1.03 million tons came from degradation. If 14.32 million tons/year is converted to tons/year/km^2 for the total contributing drainage area for the Arthur City, TX gage station (about 94,578.77 km^2), then this estimate becomes 151.41 tons/year/km^2, which was slightly higher than the accumulative sediment yield for the lower Red River reported by Greiner (1982), which was 135.9 tons/km^2. Adding the sediment input from the Texas tributaries to this value gives an estimate of 155.68 tons/km^2 (Greiner 1982) (Table 7), which was much closer to the value reported by Copeland (2002). However, Copeland (2002) ignored sediment delivery by any tributary. The actual value of sediment load including inputs from the Blue River and MBC, then, are probably higher than the 155.68 tons/km^2 reported by Greiner (1982) and the 151.41 tons/year/km^2 reported by Copeland (2002). This estimate reported in tons/day/km^2 becomes 0.41 tons/day/km^2 which falls below the range reported by Simon, Dickerson, and Heins (2004), which was 0.81-6.5 tons/day/km^2 for the South Central Plains ecoregion.

Actual sediment data from the Arthur City, TX gage station was sparse, although suspended-sediment concentration and suspended-sediment discharge was reported from 1938 to 1978 (Figures 24-25). The average suspended-sediment concentration was about 760 mg/L, which was much higher than the range reported by Simon, Dickerson, and Heins (2004) (46-140 mg/L). The average suspended-sediment discharge, when taking drainage area into account, was about 0.69 tons/day/km^2, which was slightly higher than the 0.41 tons/day/km^2 estimated by Copeland (2002), and still smaller than the range (0.81-6.5 tons/day/km^2) estimated by Simon, Dickerson, and Heins (2004). Given that Copeland (2002) did not take tributary inputs into account, the 0.69 tons/day/km^2 seems reasonable compared to Copeland's (2002) estimate.

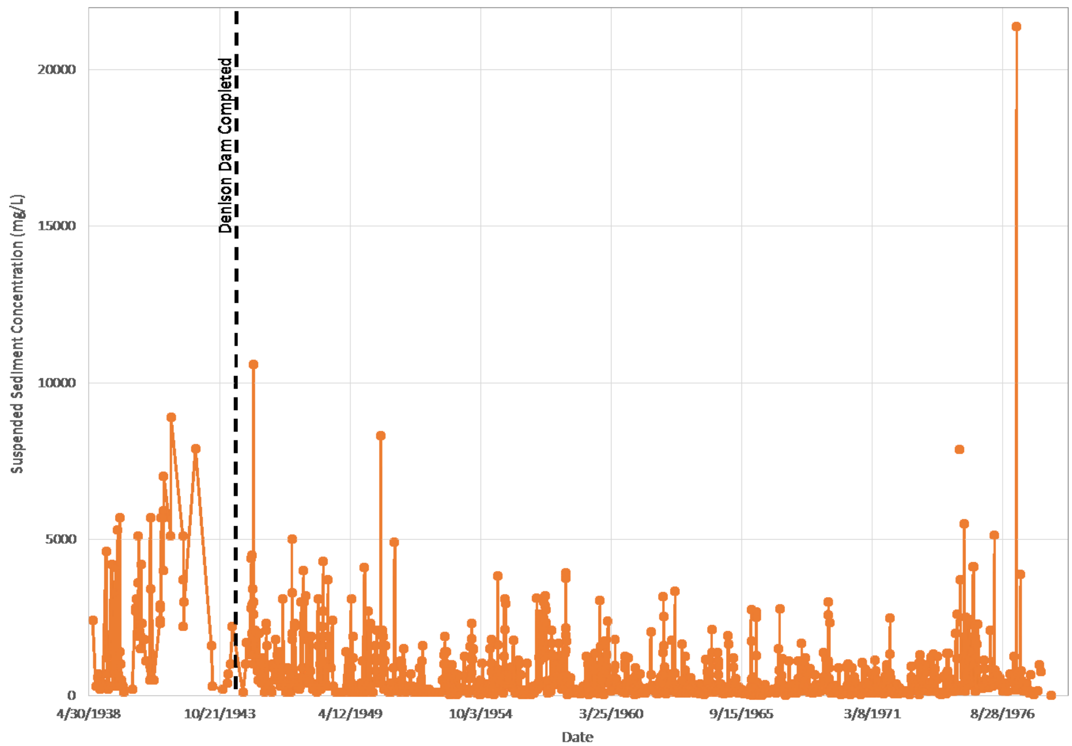

Figure 24. Change in suspended-sediment concentration over time at Arthur City, TX.

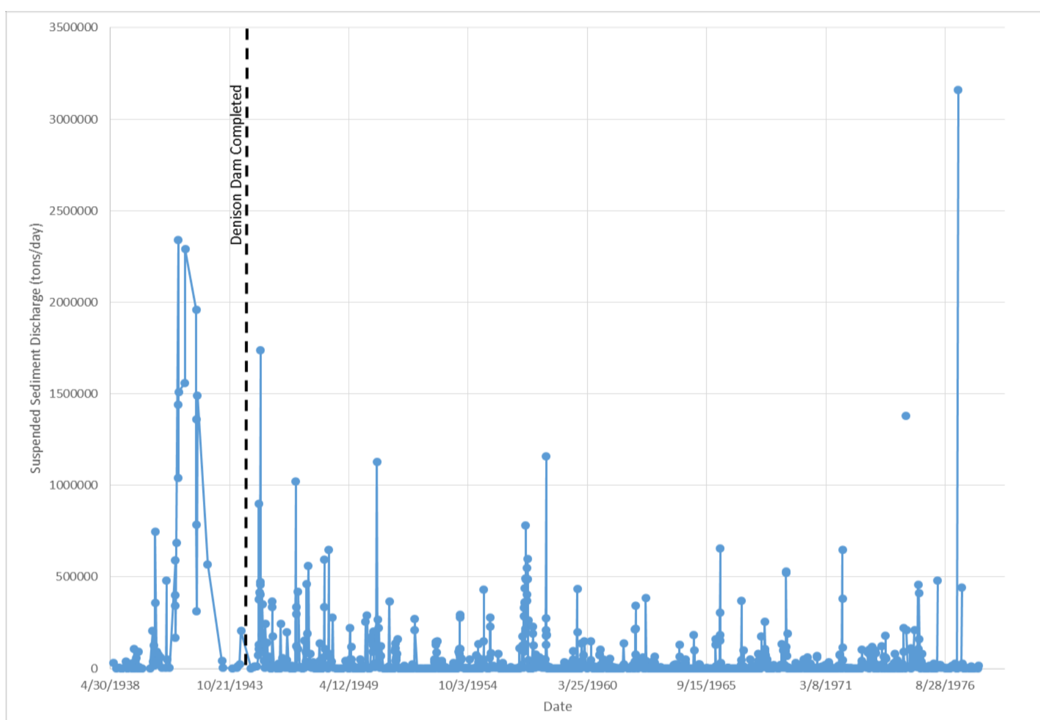

Figure 25. Change in suspended-sediment discharge over time at Arthur City, TX.

Other than a few anomalies, (especially an unusually high suspended-sediment concentration and discharge in 1977) for the most part, suspended-sediment yields were higher before Denison Dam was completed (Figure 25). The average suspended-sediment discharge reported here, was about 251.10 tons/year/km^2, which was about 100 tons/year/km^2 difference from Copeland's (2002) estimate.

VIII. DISCUSSION

Uncertainty in Sandbar, Vegetated Sandbar, and Suitable Habitat Area Measurements

Because several scene years had average discharges across the scene that were higher or lower than the threshold selection criterion, there was a small level of uncertainty in the measurements of sandbar area, vegetated sandbar area, and suitable SNH area. In years where the imagery was taken during high discharges, correlating to high river stage, the reported area measurements of sandbars, vegetated sandbars, and suitable SNH were most likely lower than what the measurements would be had the discharge of the scene been within the threshold selection criterion. Conversely, in years where the imagery was taken during low discharges, correlating to low river stage, the reported area measurements of sandbars, vegetated sandbars, and suitable SNH were likely slightly inflated to what they would have been if the imagery had been taken during a time where discharge was within the threshold selection criterion. However, the average discharges per scene graphed against the total sandbar area per scene does not reveal a strong correlation (Figure 26).

Scene 2012 which was marked by low average discharge did have total sandbar area slightly higher than the scene years which fell within the threshold selection criterion (scene years 1964, 1979, 1984, 2006, and 2008). However, 2014 showed total sandbar area that was less than the total sandbar area for years 2006 and 2008, even though the average discharge across the 2014 was low. Similarly, for the scenes in which average discharge was higher than the threshold selection criterion, some years reported higher total sandbar area than those scenes within the threshold selection criterion, (for example, 1949 and 1972) while others reported total sandbar areas that were comparable to those scenes within the threshold selection criterion (for example, 1982, 2004, and 2010). Scenes 1984 and 1979 reported lower total sandbar area than all other scenes, even though the average discharge for these scenes fell within the threshold selection criterion.

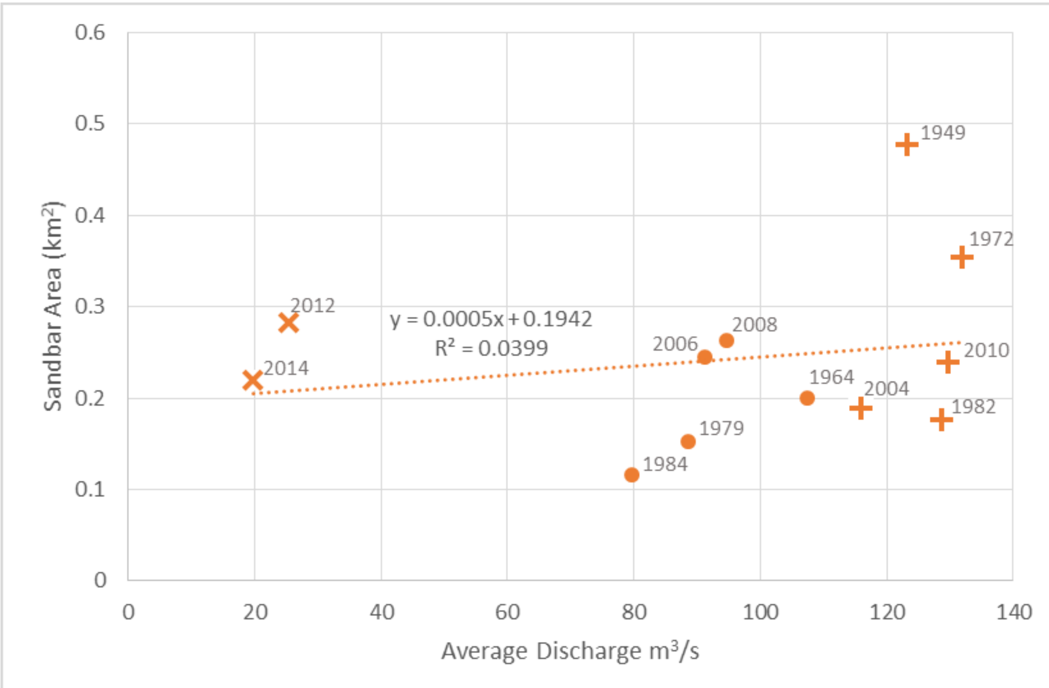

Figure 26. Comparison of total sandbar area to average discharge per scene. *Data points labeled by scene year. Those marked by plus signs indicate years in which average discharge was slightly higher than the threshold selection criterion (20-110 m^3/s) and those marked by X/s indicate years in which average discharge was slightly lower than the threshold selection criterion.*

Part of the reason for the lack of pattern seen in Figure 26 was that in some scene years, only a small portion of entire scene corresponded to a discharge that was outside the threshold selection criterion. Only a portion of the sandbars mapped in these scenes were mapped at higher or lower river stages. Graphing the average discharge versus the total sandbar area then, is a bit misleading. Selecting specific sandbars to graph against the discharge of that part of the scene, and not the average discharge across the whole scene would be a more accurate way to compare discharge to sandbar area. However, the average discharge and total sandbar area was graphed here for the sake of simplicity.

The uncertainty in the measurements of sandbar area, and in turn, vegetated sandbar area and suitable SNH area, was considered reasonable since the trends over time were clearly seen within the results. Figure 26 shows the complexity of establishing a discharge-area curve for sandbars. Although shown here in a simplified form to give understanding to slight uncertainty within the results, this study did not aim to generate an accurate discharge-area curve for sandbars as it would have required more precise field measurements that were beyond the scope of this study.

Influence of Stream Power and Land Cover on Channel Geometry

The width of a river is determined by force-resistance relationships (Julian et al. 2012), so both SSP and floodplain land cover, especially near the banks, can affect channel geometry. In a study of the Cimarron River, a Great Plains river similar to the Red River, Schumm and Lichty (1963) concluded that riparian vegetation played a major role in affecting channel width, with forested banks being much more resistant to widening. Therefore, one would expect that, during a period of high stream power applied to riparian cropland areas, channel width would be greater.

Segment-Scale Study Area

Across the SS, these relationships were difficult to discern. When forested areas decreased from the 1890s to 1949, largely due to clearing of the forests for croplands and rangelands, channel width increased considerably (Figures 27-28). The pre-dam floods, with considerable SSP (in both event peak and magnitude), in addition to less resistant banks with the removal of riparian forests, allowed for the channel to significantly widen. From 1949 to 1979, although forested lands continued to decrease and croplands increased, there were only 3 flood events with relatively low SSP (both event peak and magnitude). The channel narrowed by 1979, mostly as vegetation encroached on many of the large sandbars from the 1949 active channel and those areas become floodplain. Seen from the visual evidence of the land cover maps (Figures 5-8 in Appendix A), most of the forest clearing for croplands between 1949 and 1979 occurred away from the channel, while mostly grass and shrubs encroached on the 1949 sandbars and claimed it as floodplain.

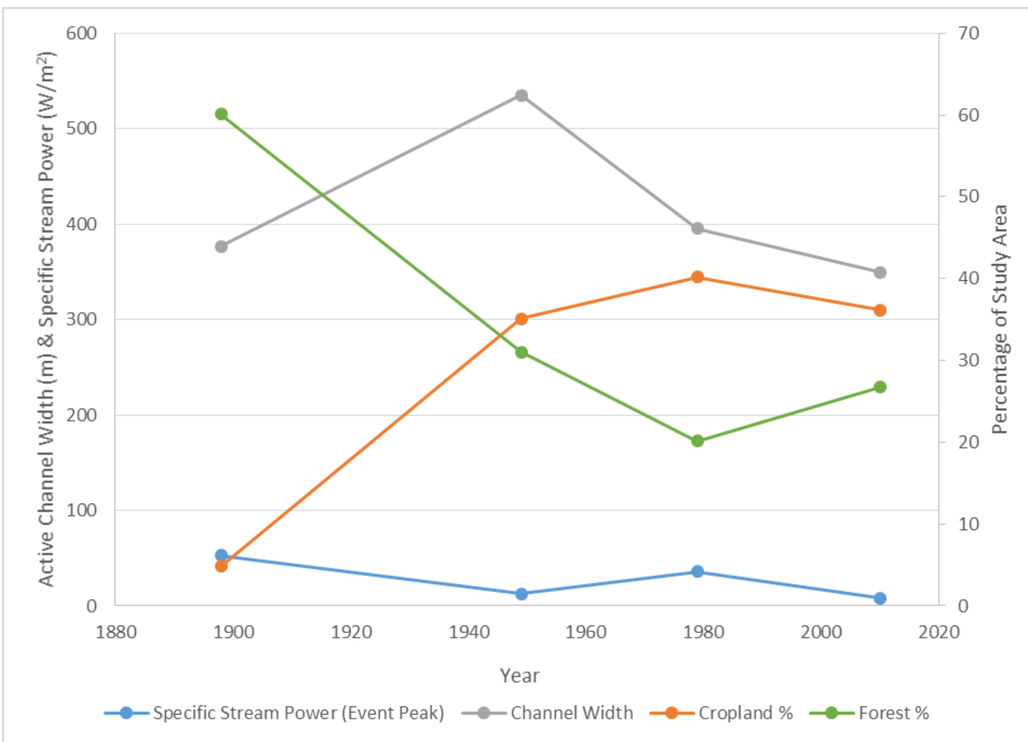

Figure 27. Comparison of specific stream power (event peak) and active channel width to land cover for the segment-scale study area. *Note that SSP values come from the range of discharges between the dates of scenes. For example, the event peak data point marked at 1949 represents the event peak during the time period from 1949 to 1979.*

In localized areas, especially downstream of the Kiamichi River, channel migration eroded into banks adjacent to croplands, and vegetation encroachment onto sandbars was more prevalent, resulting in channel narrowing. This vegetation encroachment was aided by the lack of large floods to scour out the sandbars.

From 1979 to 2010, cropland decreased slightly, while forested areas increased. Mean channel width continued to decline, even though the period had a relatively high flood event in May 1990. With one other short flood event in 1982, the SSP totaled a magnitude of 287.1 W/m^2, considerably larger than the SSP magnitude during the period from 1949 to 1979. Again, downstream of the confluence with the Kiamichi River, the channel migrated through some areas of cropland, but some loss of cropland occurred away from the channel, being abandoned to forest or grasslands. Most of the forest increase occurred in areas where grass and shrubs had encroached on the sandbars from the previous period. As vegetation on these newly acquired floodplain areas matured, channel banks were strengthened by tree roots, which were more resistant to the floods during this time. Further vegetation encroachment (both grass and trees) onto the sandbars from 1979, even after the 1990 flood, continued to narrow the channel, especially in the absence of high flows after 1990.

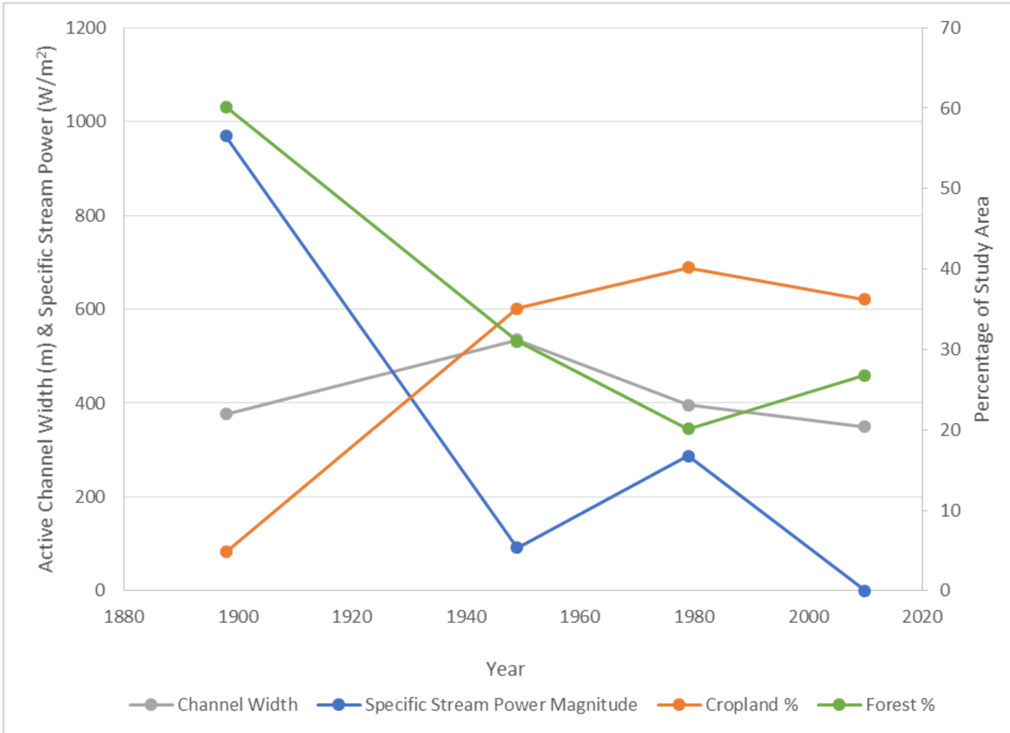

Figure 28. Comparison of specific stream power (magnitude) and active channel width to land cover for the segment-scale study area. *Note that SSP values come from the range of discharges between the dates of scenes. For example, the magnitude data point marked at 1949 represents the magnitude of SSP during the time period from 1949 to 1979.*

Reach-Scale Study Area

Similar patterns were seen in the RS as in the SS. The first period for the RS was the same as for the SS (1890s-1949), so the same pattern of channel widening influenced by high SSP and loss of forested lands to croplands was seen here as well (Figures 29-30). From 1949 to 1964, cropland decreased, while forest and grassland increased. There were a few places, mostly upstream of MBC where the channel migrated across croplands, but some of the loss of cropland during this time could also be due to the fact that fallow-lying cropland is very difficult to distinguish from grassland in aerial photography, especially in older imagery. The 1949 imagery had the poorest resolution of all imagery used, so cropland area might be slightly overestimated at that time. However, many of the areas that were cropland in 1949 but abandoned in 1964, remained abandoned in 1972, where croplands increased into new areas that were previously forested or grassland. It remains unclear as to whether the loss in cropland from 1949 to 1964 was slightly overestimated due to inconsistencies in land cover mapping, or if something else was driving farmers to abandon croplands only to increase croplands later in different locations.

Nevertheless, from 1949 to 1964, most of the forest expansion occurred along the channel margins, with forest areas expanding onto areas that were previously sandbars. This occurred on both sides of MBC, although the areas taken over by vegetation were slightly larger upstream of MBC than downstream. One large sandbar remained un-encroached upon by vegetation even though a large area of forest is adjacent to it. This sandbar was located in the first large bend in the river within the RS, and was just downstream of both the Blue River and Bois D’arc Creek. Although Bois D’arc Creek is relatively small compared to the Blue River, perhaps the combined flow was enough to keep vegetation from establishing permanently on this sandbar. In general, the significant decrease in SSP and high flow events from the previous period led to vegetation encroachment which resulted in channel narrowing during this time.

From 1964 to 1972, discharges and SSP were similar to the previous time period, remaining low. Cropland areas expanded, mostly into previously forested areas and grassland areas. Even though forested areas declined, mean channel width stayed about the same, with only 3 m difference from the previous time period.

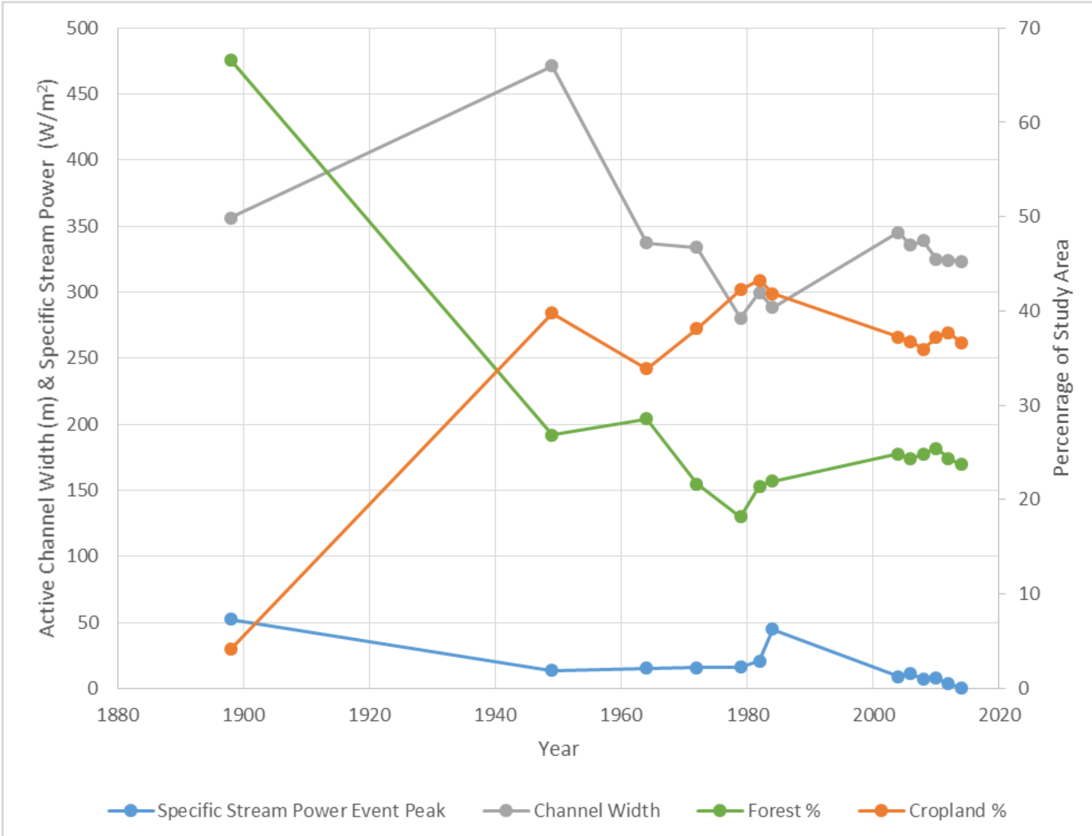

Figure 29. Comparison of specific stream power (event peak) and active channel width to land cover for the reach-scale study area*. Note that SSP values come from the range of discharges between the dates of scenes. For example, the event peak data point marked at 1984 represents the event peak during the time period from 1984 to 2004.*

Most of the forested banks from 1964 remained forested by 1972, and only minimal vegetation encroachment occurred on the sandbars. With low flows that had little erosive power and a consistency in forested banks, the channel geometry remained mostly consistent from 1964 to 1972.

From 1972 to 1979, there were no flood events that exceeded the MAF. Croplands continued to increase, while forested area decreased, and mean channel width continued to decrease. The channel did not migrate much during this time, so most of the channel narrowing occurred from vegetation encroachment (both grass and trees) on the sandbars.

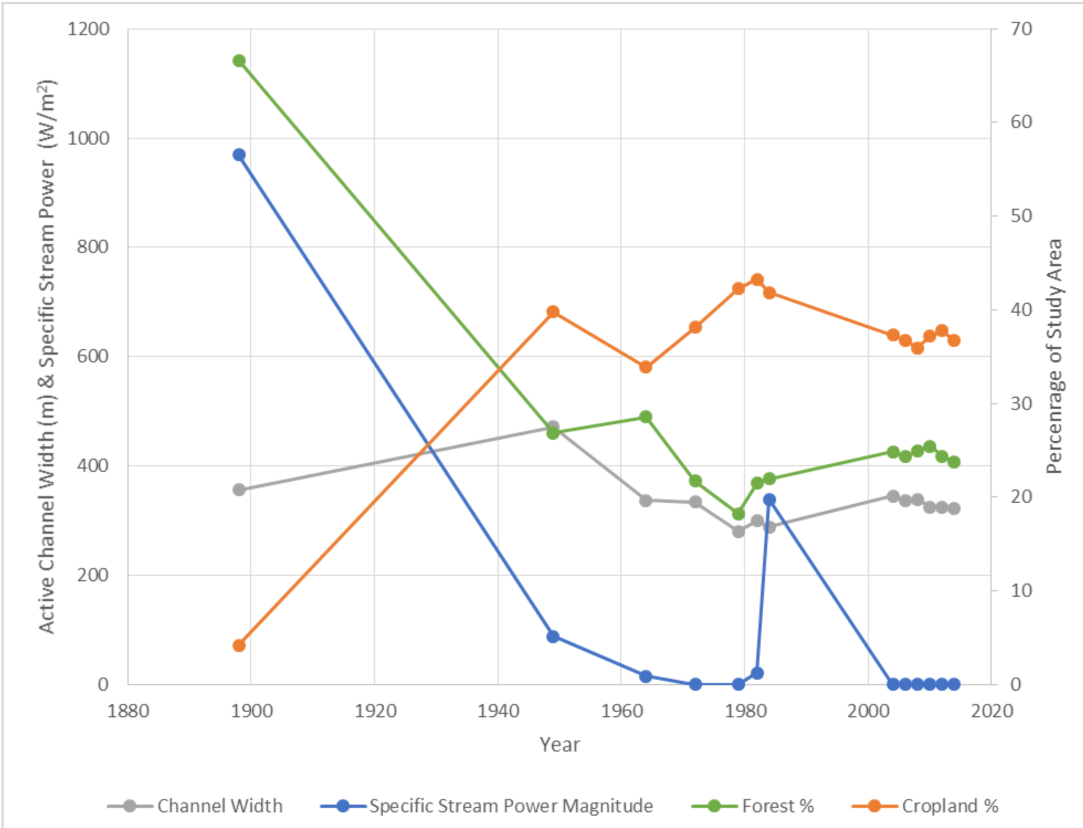

Figure 30. Comparison of specific stream power (magnitude) and active channel width to land cover for the reach-scale study area. *Note that SSP values come from the range of discharges between the dates of scenes. For example, the SSP data point marked at 1984 represents the event peak during the time period from 1984 to 2004.*

From 1979 to 1982, there were again no flood events that exceeded MAF, however the channel widened slightly even though both forest and cropland increased during this time. Most the forest increase occurred away from the channel, and channel widening occurred in areas of the channel that were adjacent to either cropland or grassland, mostly upstream of MBC. Yet, these areas were not newly expanded croplands, but areas where cropland had been adjacent to the channel for some time. This loss of cropland and grassland was enough to cause the mean channel width to increase, but other areas of cropland expansion (mainly into grassland areas) caused an overall increase in the total area of cropland for the floodplain. There were about 3 locations where the channel narrowed but slightly more locations with localized channel widening that averaged out to an overall mean widening of the channel. The locations of channel widening occurred just downstream of MBC and, on the upstream side of MBC, closer to the confluence with the Blue River which lies just outside the study area. Tributary input to the flow of the river appeared to be enough to push back encroaching grass on the sandbar and have the active channel widen and reclaim part of the sandbar. With a cursory look at peak streamflow data for both the Blue River (USGS 07332500, Blue, OK) and MBC (USGS 07334000, Farris, OK) with data scaled to the drainage area of MBC at Unger, OK (USGS 07335300, Unger, OK), both rivers had a peak flow event in 1981. The Blue River peaked at 1846 m^3/s on October 14, 1981, and MBC peaked at about 2246 m^3/s on October 16, 1981. Both of these flows rank in the top 5 peak stream flows for the data record at each gage station. Although flows from the main channel of the Red River during this time were low, high tributary flows allowed for slight channel widening. Apart from these locations, the channel shape and position largely remained stable between 1979 and 1982.

From 1982 to 1984, there was one flood event, lasting only a day, which exceeded the MAF. Forest area increased slightly, while cropland areas decreased slightly, but overall channel width decreased by 12 m. There was slight channel migration immediately upstream and downstream of MBC, but channel narrowing was seen where vegetation again encroached onto sandbars. This occurred on both side of MBC, but notably along the large sandbar directly below the confluence with Bois D'arc Creek. Grass and trees took over a significant portion of this large sandbar, significantly narrowing the channel at this location. Trees and grasses also took over small areas of the elongated sandbars seen downstream of MBC.

From 1984 to 2004, the May 1990 flood had a SSP of 338.6 W/m^2 in magnitude. This event undoubtedly contributed to the channel widening seen in this time period. The channel migrated eastward (in the downstream direction) significantly during this time. Past the Arthur City, TX gage station, the channel not only widened, but also became more sinuous with the active channel eroding away large areas of cropland. For the most part, the areas where the channel moved or widened occurred where either grasslands or cropland were adjacent to the banks. In the section of the river below MBC but upstream of the Arthur City, TX gage station, the banks of the channel remained highly forested, so despite peak flows also being contributed to the river by MBC during the May 1990 flood event, the channel mostly resisted erosion and did not change geometry by any significant amount. This attests to the Schumm and Lichty's (1963) assertion that riparian vegetation is important in dictating channel width.

From 2004 and onward, there were no flood events that exceeded the MAF. Maximum SSP stayed especially low, and the mean channel width slowly declined. Forest and cropland had minor variations year-to-year, but mostly remained at around the same percentages of the study area as they were in 2004. Overall channel narrowing occurred as grass and trees encroached on sandbars, especially on the in the sinuous section of the river below the Arthur City, TX gage station that were newly created after the 1990 flood.

The feedbacks between floodplain land cover change, channel widening/narrowing, and changes in SSP seen here on the Red River are similar to historical variability and feedbacks on the Canadian River as shown in Julian's (2012) work. Riparian vegetation played a major role in dictating channel width for the Canadian River as it did for the Red River, with forested banks being much more resistant to widening. From 1898 to 1964, (pre-dam period on the Canadian River) when previously forested floodplain was converted to either cropland or pasture, the channel was most vulnerable to channel widening and meander cutoffs (Julian 2012). However, in the post-dam period, (1964-2008) cropland expansion corresponded to channel narrowing, due to a positive feedback where the elimination of overbank floods led to decreased SSP, which allowed inactive channel margins to be encroached upon by floodplain vegetation, which promoted sediment deposition and thus more cultivation (Julian 2012). Likewise, from the 1890s to 1949 on the Red River, intensive increase in agricultural activity corresponds to an increase in channel width. Yet, later in the post-dam period, cropland expansion corresponded to decreased channel width (1964-1984). Similar processes and feedbacks described on the Canadian River were also occurring on the Red River.

Another similarity was seen in the role major floods had in shaping both rivers. The precipitation event that caused the May 1990 flood that occurred along the Red River also caused major flooding along the Canadian River at the same time. With increased SSP, both the Canadian and Red river channels significantly widened, especially in non-forested agricultural areas.

Influence of Stream Power and Channel Geometry on Sandbars and Habitat

The SSP of flows, channel geometry, and land cover also affects the distribution of sandbars. The conversion of land to agriculture can increase run-off rates, increasing sediment delivery to channels, which can result in either aggradation or degradation of the river channel (Knighton 1998). Conversely, sediment delivery to channels is decreased by the net trapping effect that many dams have on sediment. Indeed, in the Red River watershed, cumulative normal storage by impoundment increased by 127 percent from 1949 to 1979 (Figure 31). This in turn, can influence the number and size of sandbars (Fischer, Paukert, and Daniels 2015). At the same time, as encroaching vegetation increases the boundary resistance of banks, greater stream power is required for erosion (Knighton 1998). If not enough sufficient stream power is attained, then floodplain sediment cannot be reworked into the channel. Some bars occur downstream from a migrating bend when flows encounter easily eroded material (Saucier 1994), but this would be more difficult with bank material strengthened by tree roots.

Increased stream flow can potentially carry more sediment and promote sandbar growth in low-gradient reaches, but it often reduces sandbar deposition in higher gradient streams (Lenhart, Naber, and Nieber 2013). Dams both trap sediment used for sandbar creation and capture high flows that can reduce the disturbance of encroaching vegetation. Since ILTs are sensitive to both vegetation on sandbars, riparian vegetation, and channel width, the combination of these factors that affect sandbars in general, have an even greater impact to SNH.

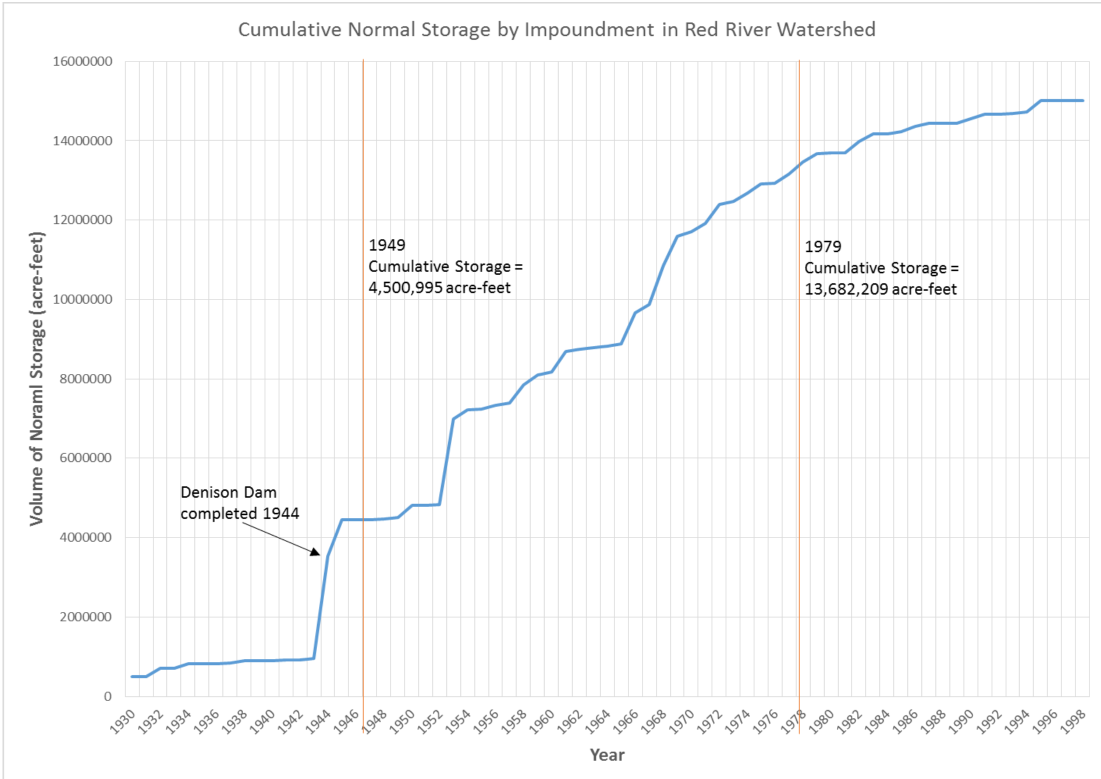

Figure 31. Cumulative normal storage by impoundment in the Red River watershed.

Although this study was not able to fully assess the change in the sediment regime of the Red River over time, the suspended-sediment discharge and concentration data from the Arthur City, TX gage station did show a gradual decrease in suspended-sediment transported in the river after the completion of Denison Dam (Figures 24 and 25). This evidence, along with the increase in cumulative normal storage by impoundment in the Red River watershed, (Figure 31) suggests that sediment delivery to the channel has generally been decreasing over time, which would affect the development of sandbars. However, to better understand the sediment regime of the Red River, additional studies including field surveys with in-stream sediment sampling would be required.

Segment-Scale Study Area

From the 1890s to 1949, the high flow events throughout the period had sufficient stream power to both widen the channel and create new sandbars (Figures 32-33). In the 1890s map, sandbars along the Red River are mostly long and narrow. By 1949, the channel became slightly more sinuous (Figure 34), mostly downstream of the Kiamichi River, and wider. As the channel widens, the stream attempted to reach equilibrium again by compensating for this change by deposition of sediment in the convex side of a meander bend (Saucier 1994). Even mid-channel bars, on which ILTs also nest on, tend to be associated with locations where channel changes have been greatest (Hook 1986). Mid-channel bars and zones of sedimentation are also commonly found downstream of sharp corners in straight limbs or in low-curvature downstream parts of developing bends (Hooke 1986), so the sinuosity of the channel can definitely play a role in the distribution of sandbars. As the channel widened in 1949, sandbars became larger and wider as well. Increased width of the channel, in addition to more sandbar area, in combination with a decrease in riparian vegetation, combined to create vast areas of sandbars that were suitable for ILT SNH. Although a large percentage of sandbars in 1949 were vegetated, the total sandbar area was greater than any other scene in the 118-year timeline. Likely this vegetation was newly acquired after the completion of Denison Dam. Before 1949, there were 12 individual flood events that last a total of 46 days and resulted in a cumulative SSP of 969.3 W/m^2. These flood events would have scoured out vegetation on the sandbars and deposited large amounts of new sand as well. The large channel width and decreased riparian forests allowed this date to have the highest suitable SNH area of any other scene analyzed as well.

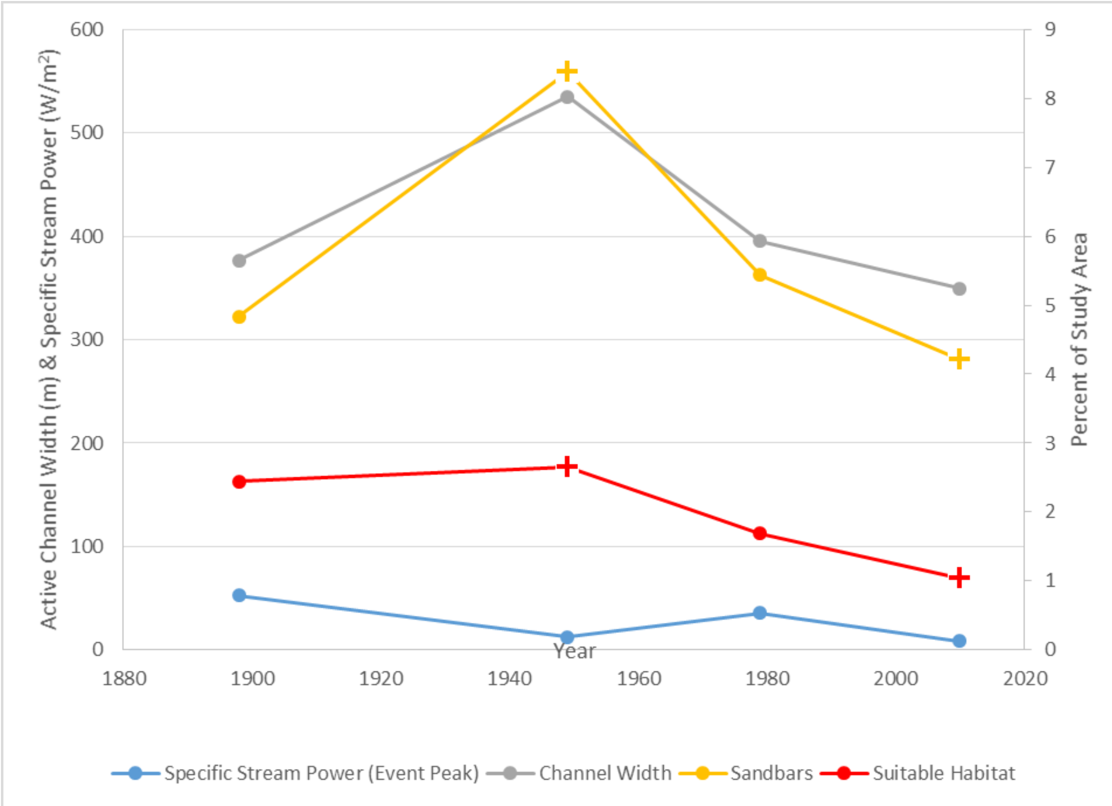

Figure 32. Comparison of specific stream power (event peak) and active channel width to sandbar and suitable habitat area for the segment-scale study area. *Note that SSP values come from the range of discharges between the dates of scenes. For example, the SSP data point marked at 1949 represents the event peak during the time period from 1949 to 1979. Data points marked by plus signs indicate scene years in which average discharge was slightly higher than the threshold selection criterion.*

From 1949 to 1979, a decrease in sandbar area and suitable SNH area was seen, largely due to channel narrowing and permanent vegetation encroachment on sandbars. As mentioned before, the flows during this period had relatively low stream power. Sinuosity also decreased, as vegetation encroachment onto sandbar areas caused certain sections of the channel to straighten (Figure 34). Surprisingly, although the total sandbar area decrease from 1949 to 1979 was relatively high, suitable SNH did not decrease by as much. Also, the percentage of sandbar area that was vegetated decreased from 1949 to

1979, and the percentage of sandbar area that was considered suitable SNH only decreased by 0.5 percent.

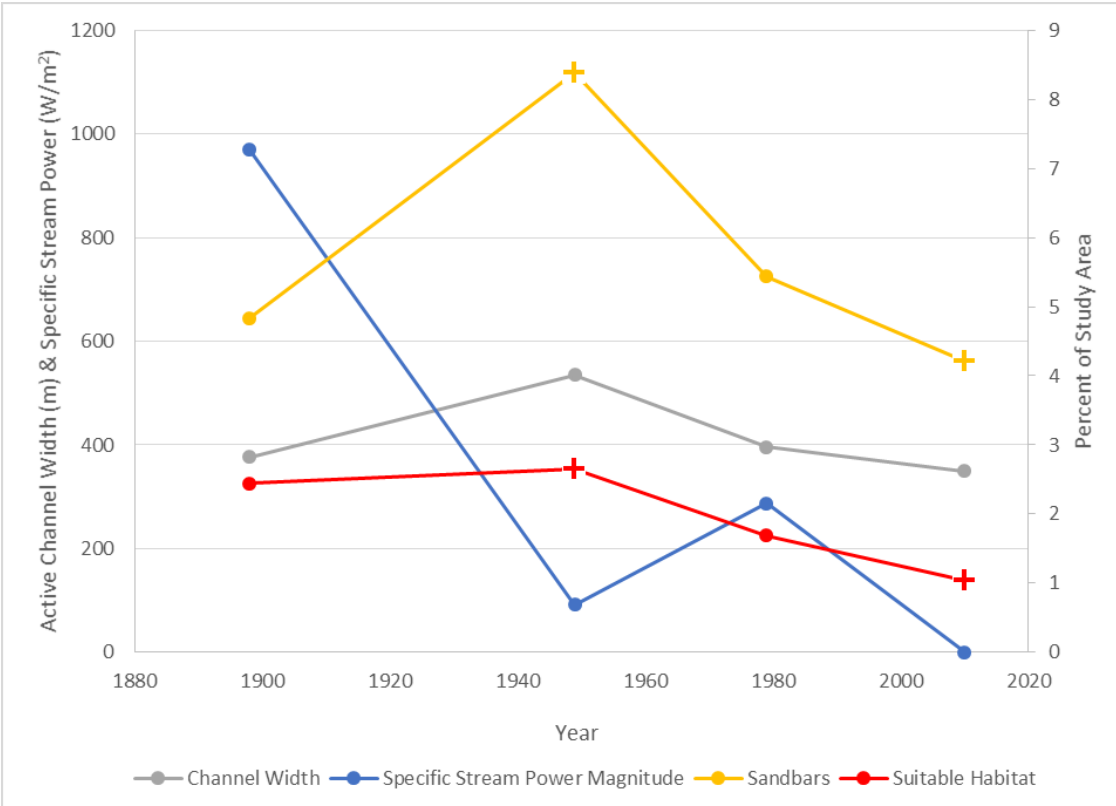

Figure 33. Comparison of specific stream power (magnitude) and active channel width to sandbar and suitable habitat area for the segment-scale study area. *Note that SSP values come from the range of discharges between the dates of scenes. For example, the SSP data point marked at 1949 represents the event peak during the time period from 1949 to 1979. Data points marked by plus signs indicate scene years in which average discharge was slightly higher than the threshold selection criterion.*

Considering that the total sandbar area decreased and the channel narrowed, it is unusual that the suitable SNH would make up such a large percentage of what sandbar area was available. There might be two contributing factors to this: (1) forest area continued to decrease from 1949 to 1979, and generally in areas away from the channel, but localized forest clearing near the channel might have created small increases in suitable SNH areas despite the overall decrease in channel width and sandbar area, and

(2) there were noticeably more mid-channel bars in 1979 than in 1949, which tended to be less vegetated than point-bars, and further from the channel margins, allowing for suitable SNH.

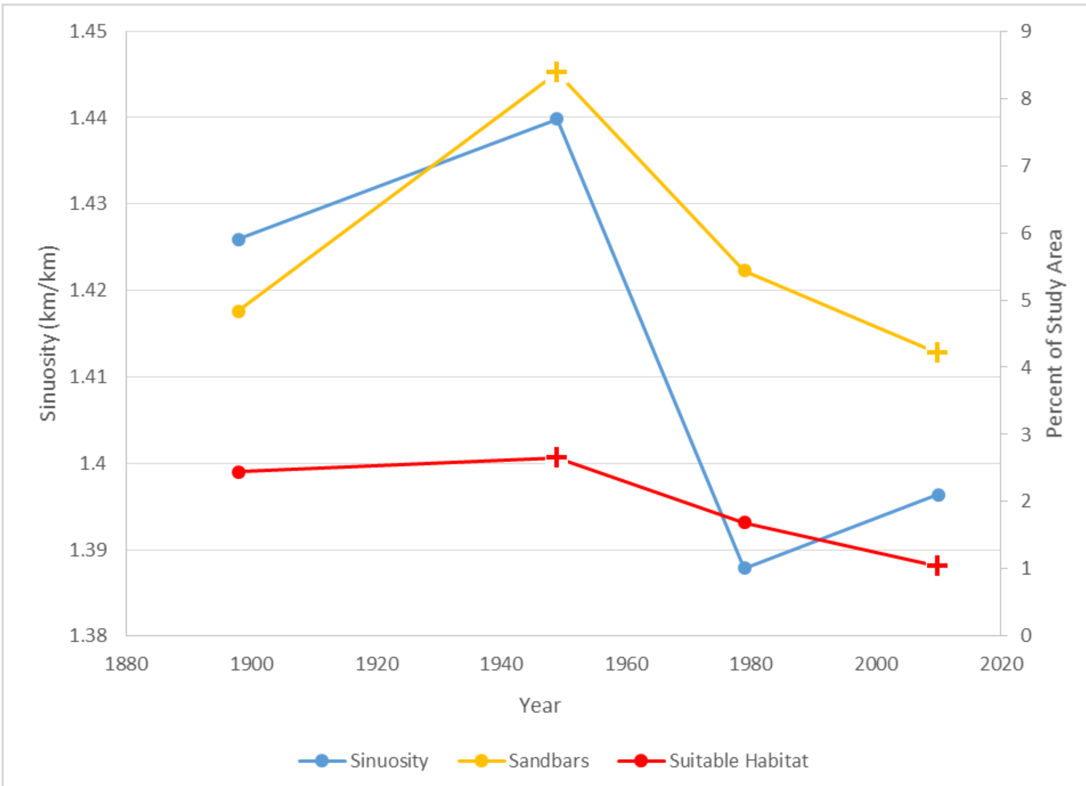

Figure 34. Comparison of channel sinuosity to sandbar and suitable habitat area over time for the segment-scale study area. *Data points marked by plus signs indicate scene years in which average discharge was slightly higher than the threshold selection criterion.*

From 1979 to 2010, although there was the May 1990 flood event to shape the channel and increase sinuosity, sandbar area and suitable SNH area continued to decrease, although this decrease was less than the decrease in sandbar area from 1949 to 1979. Sandbar area seemed to be limited by the decrease in channel width, and suitable SNH decreased because of channel narrowing but also largely due to increased vegetation on the sandbars. In all likelihood, the May 1990 flood increased sandbar size and extent significantly, but with no imagery from around this time, these changes cannot be analyzed. In the absence of any high flows after the May 1990 flood, rapid encroachment of vegetation onto the sandbars not only narrowed the channel and contributed to sandbar loss, but also severely limited suitable SNH extent.

Reach-Scale Study Area

When focused on the RS, a slightly different picture emerged than from the SS, although the same processes were at work. From 1890s to 1949, the increased stream power and decreased forest land cover promoted channel widening that also led to an increase in sandbar area and suitable SNH area, as explained above. From 1949 to 1964, large areas of sandbars were converted to floodplain through the permanent encroachment by vegetation, with a lack of flows with sufficient stream power to maintain these sandbars (Figures 35-36). The channel narrowed, and sandbar area was lost. Suitable SNH was also lost, from a combination of loss of total sandbar area, channel narrowing, and an increase in some location of riparian forests, especially in areas where vegetation encroached on previous sandbars. Although the channel as a whole became slightly more sinuous, this was not enough to counteract the loss of sandbar area occurring from channel narrowing.

From 1964 to 1972, although stream power remained low, sinuosity decreased (Figure 37), and forested areas decreased; the channel width decreased minimally. Sandbar area and suitable SNH area decreased as a whole, but the percentage of suitable SNH to sandbar area increased slightly, even while the percentage of vegetated sandbar remained the same.

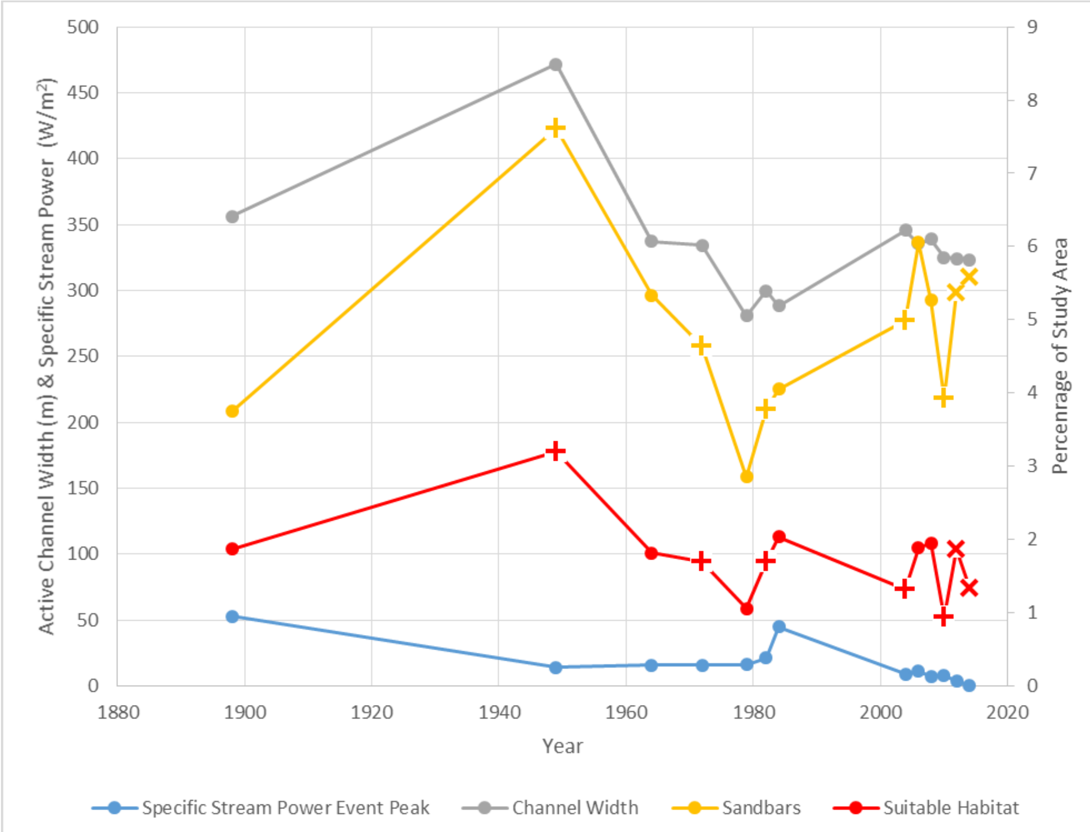

Figure 35. Comparison of specific stream power (event peak) and active channel width to sandbar and suitable habitat area for the reach-scale study area. *Note that SSP values come from the range of discharges between the dates of scenes. For example, the SSP data point marked at 1984 represents the event peak during the time period from 1984 to 2004. Data points marked by plus signs indicate scene years in which average discharge was slightly higher than the threshold selection criterion, and data points marked by X's indicate scene years in which average discharge was slightly lower than the threshold selection criterion.*

Forested areas along the banks did not decline during this time, so the increased percentage of suitable SNH cannot be attributed to forest removal at the channel margins. However, there was a greater presence of small mid-channel bars in 1972 that were sufficient distance from both trees and channel margins to be considered suitable SNH (Figure 18 in Appendix B). Since these mid-channel bars were small, they did not contribute to an overall increase in sandbar area, but because they were non-vegetated, they allowed suitable SNH to make up a larger percentage of sandbar area than in 1964.

Mid-channel bars, although more transient than point bars, appear to be equally important SNH for ILT. Many of the smaller mid-channel bars likely would not be utilized by ILT for SNH, as they are more likely to be ephemeral or low enough in elevation to be inundated by medium to high flows. However, larger mid-channel bars, or those high in elevation, could be prime SNH, as they tend to be void of vegetation and are located far from both the channel margins and any riparian trees.

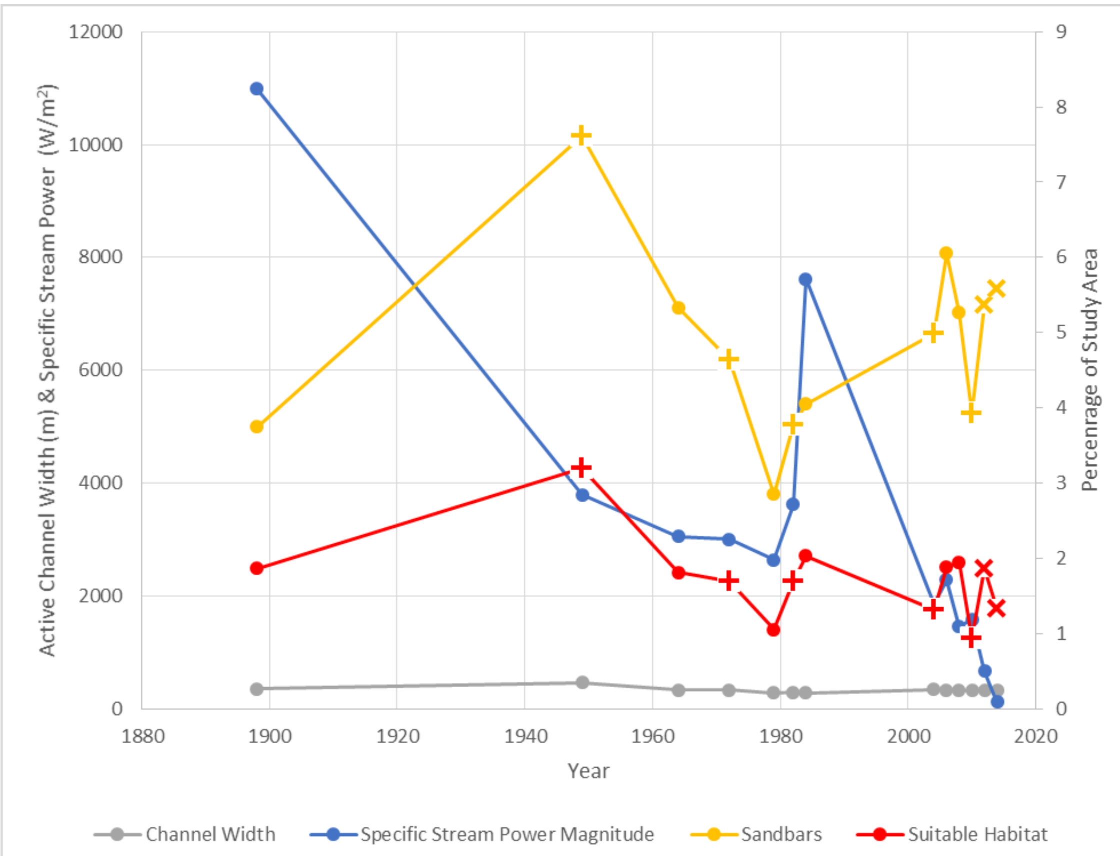

Figure 36. Comparison of specific stream power (magnitude) and active channel width to sandbar and suitable habitat area for the reach-scale study area*. Note that SSP values come from the range of discharges between the dates of scenes. For example, the SSP data point marked at 1984 represents the event peak during the time period from 1984 to 2004. Data points marked by plus signs indicate scene years in which average discharge was slightly higher than the threshold selection criterion, and data points marked by X's indicate scene years in which average discharge was slightly lower than the threshold selection criterion.*

Indeed, in a survey of ILT nesting sites along the Red River in 2008, Lott and Wiley (2012b) found several ILT nesting sites located on mid-channel bars. Also, ILTs are known to nest on some mid-channel bars, and there is yet to be a quantified minimum sandbar size criterion for SNH. With no way of determining the sandbar elevation and no planform size limitation, these small mid-channel bars could not be ruled out in this study as areas of potentially suitable SNH.

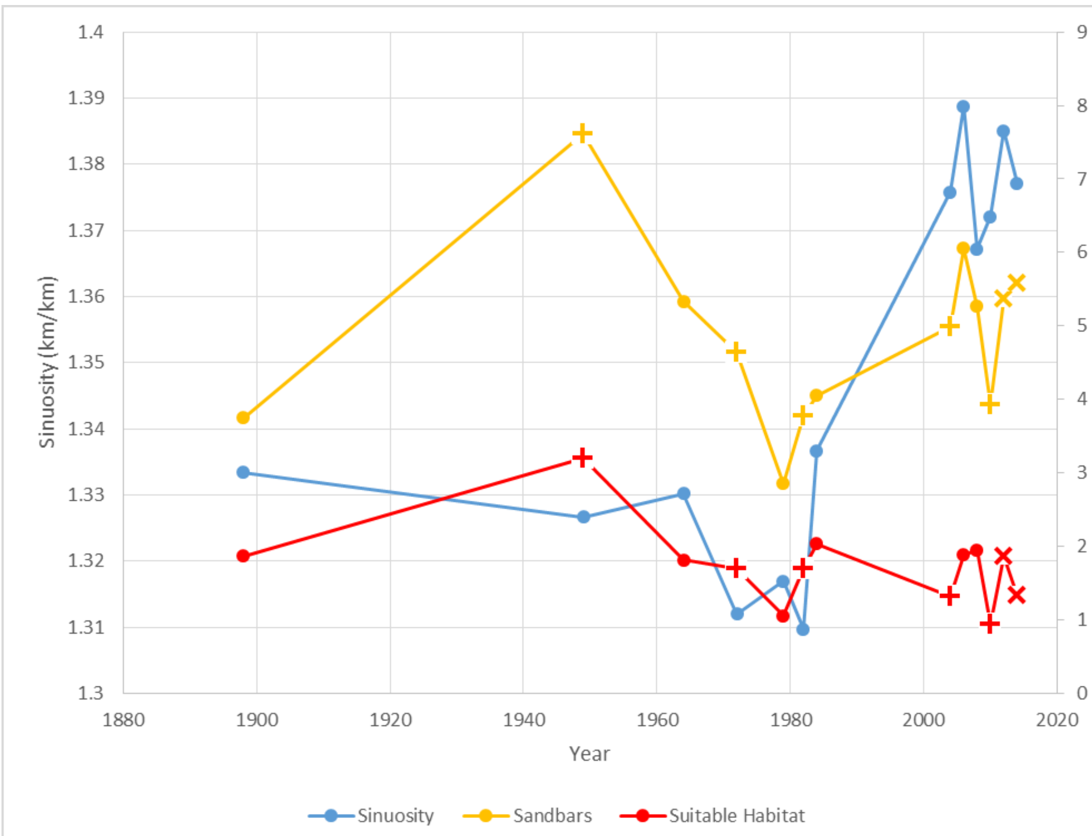

Figure 37. Comparison of channel sinuosity to sandbar area and suitable habitat area for the reach-scale study area. *Data points marked by plus signs indicate scene years in which average discharge was slightly higher than the threshold selection criterion, and data points marked by X's indicate scene years in which average discharge was slightly lower than the threshold selection criterion.*

From 1972 to 1979, continued low stream power and vegetation encroachment on sandbars resulted in continued channel narrowing, coinciding with continued declines in both sandbar area and suitable SNH area. From 1979 to 1982, there were again, no flood events along the main stem of the Red River that exceeded the MAF. However, there were areas of new sandbar deposition, especially upstream of MBC, which increased both sandbar area and suitable SNH at this time. As mentioned before, although there was no flood event on the main stem, in 1981 both the Blue River and MBC experienced peak flow events. Unfortunately, the Arthur City, TX gage station does not have suspended-sediment data during this time nor does the most downstream gage stations on either the Blue River, or on MBC. However, the Farris, OK gage station on the MBC (USGS 07335300), although upstream on MBC, does have one suspended-sediment measurement on October 18, 1981, just after the date of the peak flow. It gave a suspended-sediment concentration of 480 mg/L and a suspended-sediment discharge of 38,000 tons/day, which ranked as the 9th highest suspended-sediment discharge recording from 1938 to 1981 for that gage station. However, a cursory glance at the measurements with higher suspended-sediment discharges than this shows higher suspended-sediment discharges in dates ranging from 1946 to 1974, but sandbar area continued to decrease from 1949 to 1979. From the Unger, OK gage station, although sediment data stops at 1980, the highest suspended-sediment discharges occurred on similar dates between 1945 and 1977. It seems that sediment input from the tributaries was not a major factor in the creation of new sandbars seen in 1982, but perhaps the discharge input from the 1981 floods on the tributaries did rework floodplain sediment into new sandbars.

From 1982 to 1984, channel width decreased, but sandbar area and suitable SNH area increased. Although the one flood event did not have sufficient stream power to widen the channel, existing sandbar expanded into the channel, and vegetated areas of sandbars were reduced. It appears that this flood event had sufficient stream power to scour out encroaching vegetation and deposit more sediment on existing sandbars. The slight increase in sandbar area combined with a large reduction in vegetated sandbar area, created a relatively moderate increase in suitable SNH area by 1984.

From 1984 to 2004, both channel width and sinuosity of the channel increased, mostly due to the May 1990 flood. Total sandbar area increased, but suitable SNH decreased. New sandbars were mostly created downstream of MBC and the Arthur City, TX gage station, where the channel became much more sinuous. Suitable SNH remained limited by vegetation encroachment on these newly created sandbars. Low flows after 1990 most likely promoted this vegetation encroachment. Although the vegetation was still on active portions of the sandbars in the channel, this prevented these sandbar areas from being used by ILTs for SNH.

From 2004 to 2014, channel width varied slightly and slowly decreased, but sandbar area and suitable SNH varied much more. Sinuosity of the channel varied slightly around 1.38 and the channel geometry remained relatively constant during this time. Sandbar area was seen to increase in 2006, then sharply decrease by 2010, then increase again by 2014. Suitable SNH increased through 2008, decreased in 2010, increased again in 2012, followed by a decrease in 2014. These sandbar area changes have less to do with overall channel geometry changes, and more to do with in-channel evolution. Bar formation, especially mid-channel bar development, can occur within the channel while the bankline pattern may remain unchanged (Schumm 2005). In 2006, many dissected sandbars grew and merged together into larger areas. More, larger mid-channel bars also occur especially upstream of MBC (Figure 38). These changes occurred with little channel geometry changes, but resulted in increased sandbar area. The same thing happened from 2012 to 2014. Times of decreased sandbar area occur with less mid-channel bars. From 2004 to 2006, suitable SNH increases with the expansion of sandbar area increased. Vegetated sandbar area increased slightly, but not at the same scale as sandbar area in part due to mid-channel bars which tend to lack vegetation and therefore are more likely to be suitable for SNH. From 2006 to 2008, even though sandbar area decreased, suitable SNH area increased, largely due to a decrease in vegetated sandbar areas. From 2006 to 2008, SSP was higher than in any other time from 2004 to 2014. Although still low, and although sandbar area decreased, it may have been enough to at least scour out some vegetation which allowed for more suitable SNH area. From 2010 to 2012, suitable SNH largely increased with an increase in total sandbar area. Lastly, even though sandbar area continued to increase slightly into 2014, again, from the presence of mid-channel bars, suitable SNH decreased as most of the large point bars became almost completely covered by vegetation.

It is interesting to note that when channel width remains relatively stable, sandbar area can still widely vary. This indicates that localized, in-channel processes play an important role in sandbar area size and distribution, and in turn, affect suitable SNH distribution as well. Indeed, mid-channel bars tend to occur in zones of high channel mobility and rapid erosion, and also tend to coincide with reaches of relatively high gradient and stream power. Steep slopes induce greater stream power for a given discharge which results in greater bank erosion and then a lag deposit of coarse sediment, generally in the middle of a riffle (Knighton 1998).

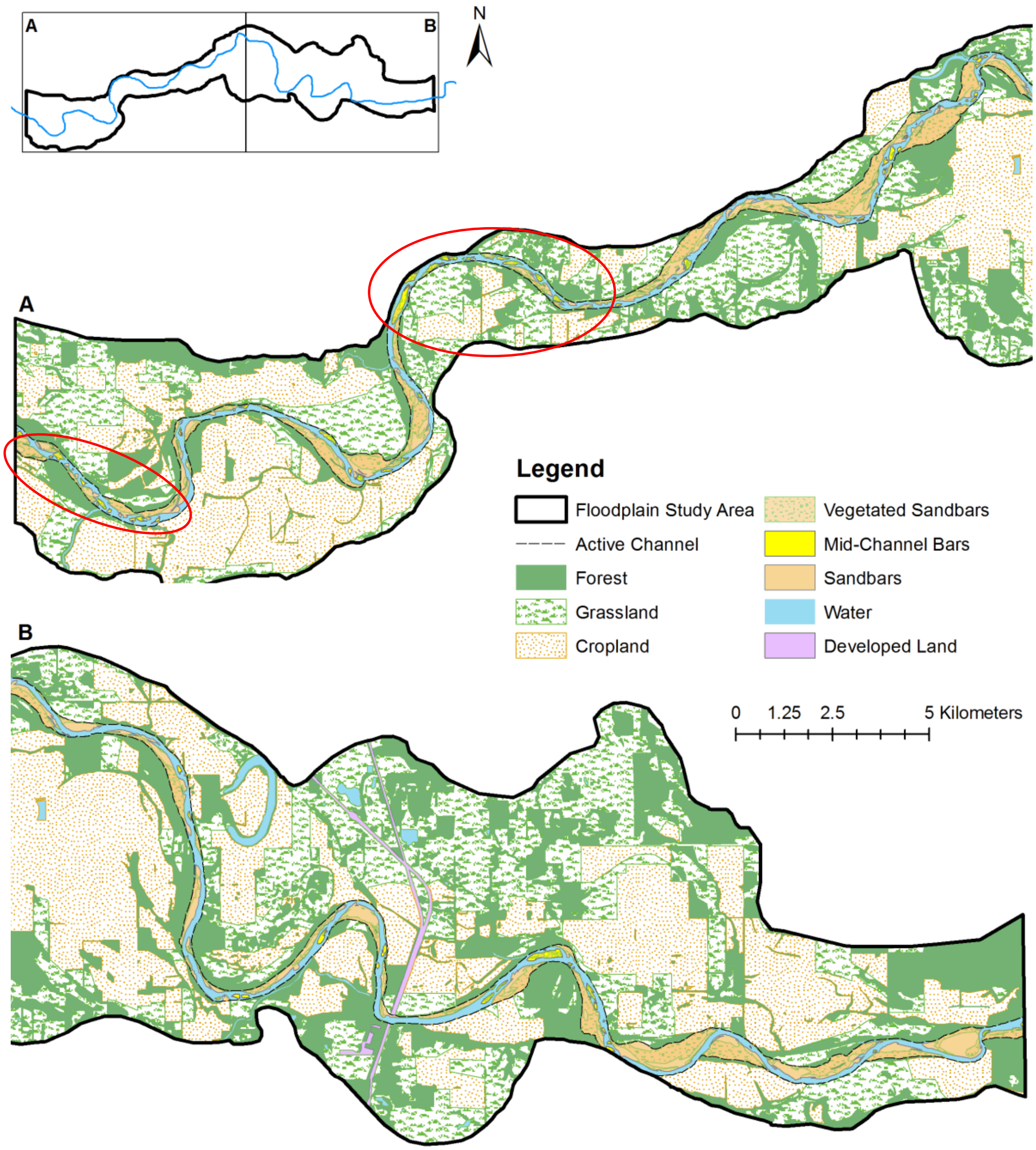

Figure 38. Comparison of mid-channel bars upstream (A) and downstream (B) of Muddy Boggy Creek in 2006. *The red circles indicate sections of the river with numerous mid-channel bars.*

Mid-channel bars also tend to be associated more with braided or anastomosing streams than meandering streams. Around 1833, before the giant log-jam known as the Great Raft was cleared, the Red River was actually in an anastomosing regime (Albertson and Patrick 1996). This most likely meant that mid-channel bars were more prevalent. With the clearing of the Great Raft, the planform of the Red River began to change (Albertson and Patrick 1996). Later changes in both flow and sediment regimes have continued to cause the Red River to evolve from a more braided or anastomosing stream to a meandering stream. As this evolution occurs, the Red River might be experiencing continued loss of mid-channel bars, similarly to the Platte River (Johnson 1999; Horn, Joeckel, and Fielding 2012). As mid-channel bars can be preferable SNH for ILT, as described before, the loss of such bars could be contributing to the loss in suitable SNH over time.

Further study would be required to completely understand the in-channel processes that affect sandbars, and thus suitable SNH, especially when channel pattern is not changing. This might include field sampling to estimate bank erosion rates, field surveys to more accurately measure channel bed slope for these sections of the river, as well as measuring the pattern and spacing of mid-channel bars.

Comparison of Upstream versus Downstream of Muddy Boggy Creek

Centering both the SS and RS on the confluence with MBC allowed for a natural experiment to investigate tributary effects on sandbars and suitable SNH. It was hypothesized that the unregulated flow from MBC would contribute enough discharge and sediment to create more sandbars and thus, more suitable SNH downstream from the confluence. However, for both the SS and RS, sandbar area was exclusively higher upstream from MBC than downstream, although the loss of sandbar area over time was greater upstream from MBC than downstream.

Although the Blue River is also unregulated, it is considerably smaller in size, both in terms of drainage area and discharge. Therefore, it was thought that it would not play as a significant role as MBC, in terms of tributary effects to the main channel. Most mid-channel bars occurred upstream of MBC and helped to increase sandbar area on that side of the confluence. However, loss of both sandbar area and suitable SNH over time was greater upstream of MBC than downstream, which suggests that MBC did contribute enough discharge and sediment to mitigate sandbar and suitable SNH loss downstream. These results indicated that factors dictating upstream versus downstream sandbar distribution may be more complex than simple tributary input of water and sediment.

From the SS, upstream versus downstream comparison of sinuosity showed a different picture than the same comparison in the RS. Within the SS, aside from the 1890s scene, downstream of MBC was more sinuous than upstream. However, in the RS, the opposite was true: sinuosity remained greater for all years in the upstream section. For the SS, the most sinuous section of the entire study area occurred downstream of the confluence with the Kiamichi River, but this section is excluded from the RS.

For channel slope, upstream of MBC remained steeper than downstream for all years for both the SS and RS. Although the channel slope was steeper upstream than downstream of MBC, over time the change in channel slope for the upstream section of the river was negligible. Within the RS, from the 1890s to 1964, channel slope decreased significantly for the downstream section of the river; but after 1964, change in channel slope remained negligible.

For the SS, the valley slope was slightly steeper upstream of MBC than downstream (Figure 39). Increased valley and channel slope can increase stream power, which increase both the stream's erosive ability and its ability to transport sediment. While the change in channel slope over time was negligible, the steeper valley slope upstream of MBC, with increased stream power and little sediment input upstream of MBC, meant that the excess energy tended to erode the banks and widen the channel. Work by river discharge was done more in the lateral direction: that is, reworking floodplain sediments and either creating or destroying floodplain. Downstream of MBC, the sediment supplied by the Blue River, MBC, and the Kiamichi River, along with re-worked sediment from the floodplain, was deposited as stream power decreased with a decrease in valley slope. Although channel width was generally greater upstream of MBC than downstream, sandbar area was greater downstream of MBC than upstream, largely due to the change in sediment supply from the major tributaries and change in channel and valley slope across the SS.

Suitable SNH, on the other hand, did not follow a specific trend upstream versus downstream of MBC for the SS. However the loss of suitable SNH over time was greater upstream than downstream of MBC. In 1949, suitable SNH was greater upstream of MBC than downstream, yet the opposite occurred in 1979 and 2010. This was mostly because suitable SNH is also dependent on sandbar vegetation and riparian plant composition in addition to sandbar area. After 1949, many of the sandbars downstream of MBC, especially those downstream of the Kiamichi River, were also adjacent to forested banks, which limited suitable SNH. After 1949, vegetated areas of sandbars consistently took up more percentage of sandbar area upstream of MBC than downstream. Perhaps high flows from the major tributaries helped to scour out vegetation from sandbars downstream of these confluences. From 1949 to 2010, suitable SNH decreased by 4.47 km^2 upstream of MBC, while only decreasing by 1.53 km^2 downstream of MBC, even though the loss in vegetated sandbar area over time was relatively the same on both sides of MBC. The loss of total sandbar area upstream of MBC was also greater than downstream of MBC (loss of 27.61 km^2 upstream and 16.16 km^2 downstream from 1949 to 2010). This suggests that even though total sandbar area and suitable SNH has been decreasing overall, perhaps sediment and discharge input from tributaries were substantial enough to mitigate some loss of habitat on the downstream side of these tributaries.

For the RS, however, a slightly different picture was seen when comparing upstream versus downstream of MBC. Within the RS, greater channel width on the upstream section influenced greater sandbar area and suitable SNH area (Figure 40). However, the mean channel width changed drastically more over time in the upstream section than in the downstream section. Upstream of MBC, channel width decreased by about 11 percent from the 1890s to 2014, while downstream of MBC, channel width decreased by only about 5 percent in the same time period.

The total active channel area remained higher for all years in the upstream section than downstream of MBC, but experienced about 15 percent loss in area from the 1890s to 2014 in the upstream section while the downstream section gained about 9 percent more active channel area.

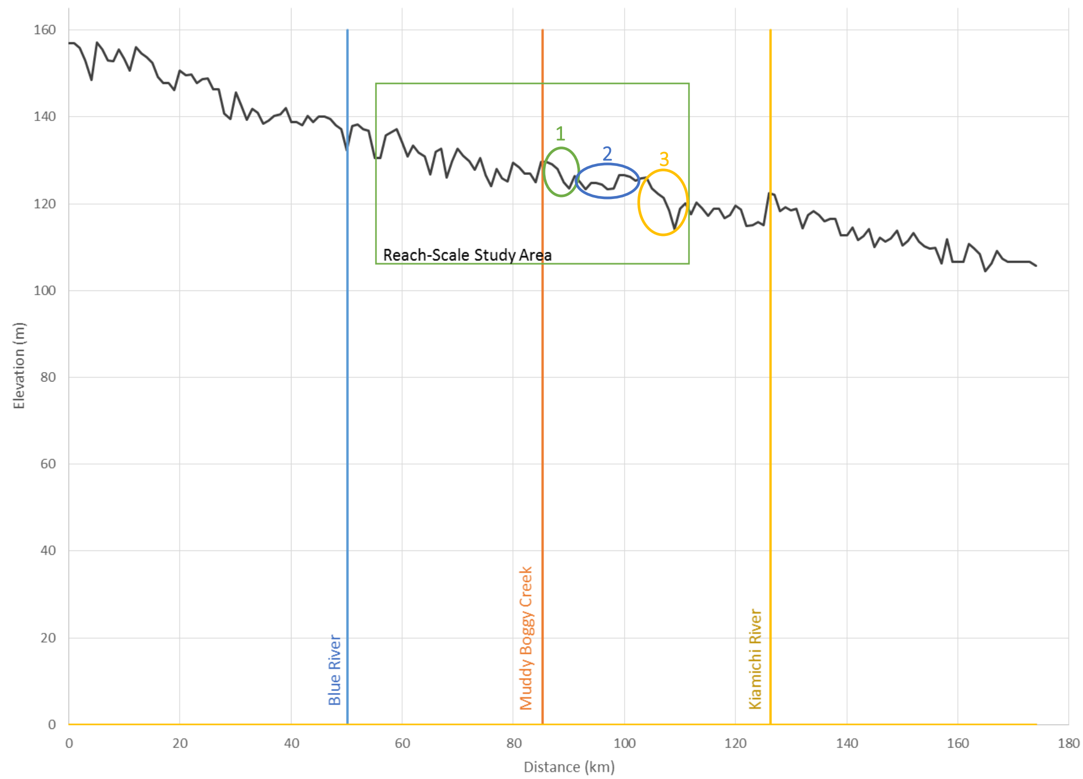

Figure 39. Longitudinal profile of the segment-scale study area. *The green box shows the extent of the reach-scale study area. Blue, orange, and yellow lines indicate location of tributary junctions with the Red River by the Blue River, Muddy Boggy Creek, and Kiamichi River, respectively. The green, blue, and yellow circles (1, 2, and 3) correspond to river locations shown in Figure 39A.*

The downstream section of the river appeared to be more stable over time than the upstream section (Figure 40), with channel width, sandbar area, and suitable SNH fluctuating around consistent values over time. The upstream section, though, was not as stable and experienced loss in channel width, sandbar area, and suitable SNH over time.

Total sandbar area was higher in all years upstream of MBC than downstream. However, the upstream section experienced greater sandbar loss over time than the downstream section.

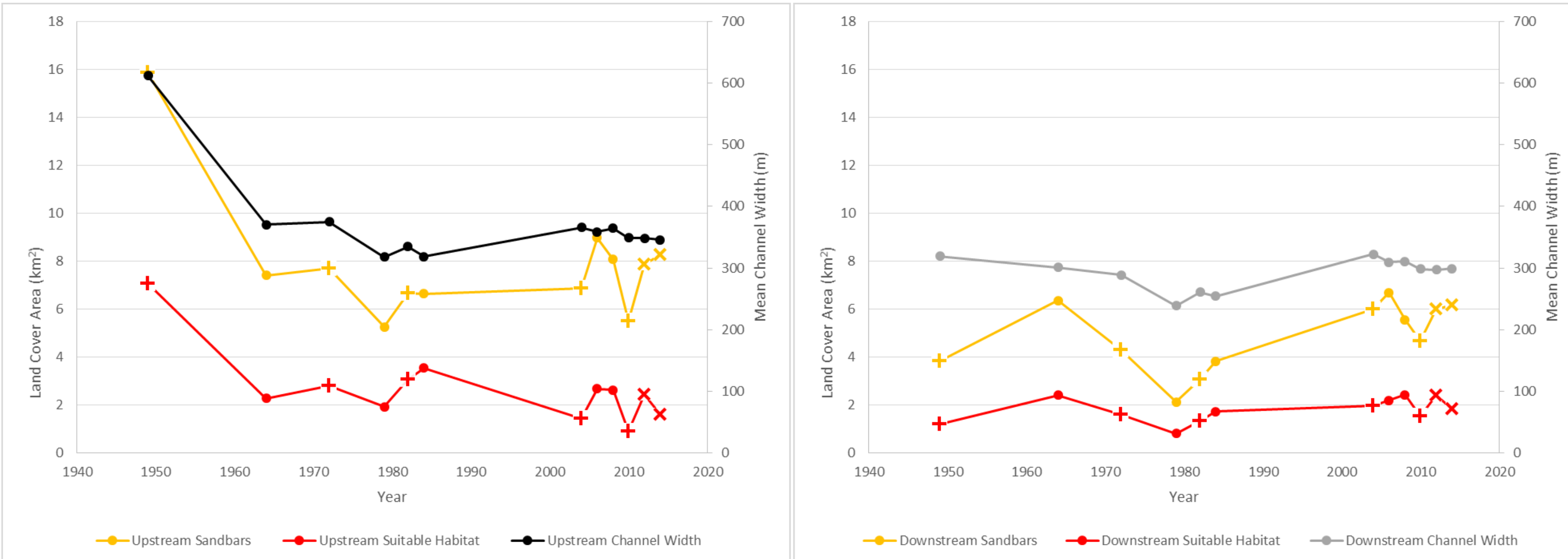

Figure 40. Upstream versus downstream comparison of channel width to sandbar area and suitable habitat area for the reach-scale study area. *(A) Comparison of upstream channel width to sandbar area and suitable SNH. (B) Comparison of downstream channel width to sandbar area and suitable SNH. Data points indicated by plus signs indicate scene years in which average discharge was slightly higher than the threshold selection criterion, and data points marked by X's indicate scene years in which average discharge was slightly lower than the threshold selection criterion.*

From 1949 to 2014, total sandbar area in the upstream section decreased by about 48 percent, while in the downstream section, total sandbar area actually increased by almost 60 percent. The percentage of sandbar area that was vegetated was also higher upstream than downstream for all years except 1949.

The total vegetated sandbar area decreased over time by about 18 percent for the upstream section of the river, but increased by about 60 percent for the downstream section of the river. For suitable SNH, the percentage of sandbar area that was considered suitable SNH was higher upstream than downstream for 1949, 1982, and 1984. In the remaining years, the percentage of sandbar area that was considered suitable SNH was higher downstream than upstream. The total loss of suitable SNH area over time for the upstream section was about 77 percent. However, the downstream section gained about 53 percent more suitable SNH area over time. While sandbar area and suitable SNH were decreasing overall from 1949 to 2014, the losses were greater on the upstream section of the river than downstream of MBC. This suggests that perhaps sediment and discharge input from MBC was mitigating some of the loss of sandbar area and suitable SNH area over time. Large floods and abundant sediment are needed to create/maintain sandbars. With the entrapment of sediment by Denison Dam after 1944, sediment from the MBC becomes critical for sandbar development. The continued decrease of sandbar area and suitable SNH on both sides of MBC suggests that other factors were contributing to the total loss of sandbar area and suitable SNH on both sections of the river. Yet, the discrepancy of loss of sandbar and suitable SNH area over time seemed to suggest that if MBC were to be impounded, that greater losses of sandbar and suitable SNH area downstream of MBC could be expected in the future.

One factor that contributed to this upstream/downstream pattern of suitable SNH was vegetation and valley and channel slope. Immediately downstream of MBC, the channel took a wide, gentle bend south and throughout the years, remained heavily forested along the banks. The forested banks, without scouring floods, kept the channel stable here, as evidenced by very little change in channel width or location over time. This narrowed channel in this area also corresponded to a localized steepening of valley and channel slope that occurs just after the confluence with MBC (Circle 1 in Figures 39 and 41). Increased discharge from input of MBC, along with increased valley slope, increased the stream power here, which carried sediment further downstream before depositing it. The channel was deeper and narrower, suggesting that the increase in SSP was incising the river channel here, with net erosion occurring rather than deposition (Figure 42). These conditions do not favor sandbar development, and thus a lack of both sandbars and suitable SNH was seen here.

After the initial bend south, the channel bent north again and had a quick series of large meander bends. The Arthur City, TX gage station lies within this second southerly bend. The bends allowed for more sandbar area as point bars in the convex side of the bends, but the overall channel shape still remained mostly stable throughout time. Valley slope and channel slope both flattened out in this section of the river, allowing sinuosity to increase (Circle 2 in Figures 39 and 41). The increase in sinuosity of the channel suggested that sediment deposition began as stream power starts to decrease.

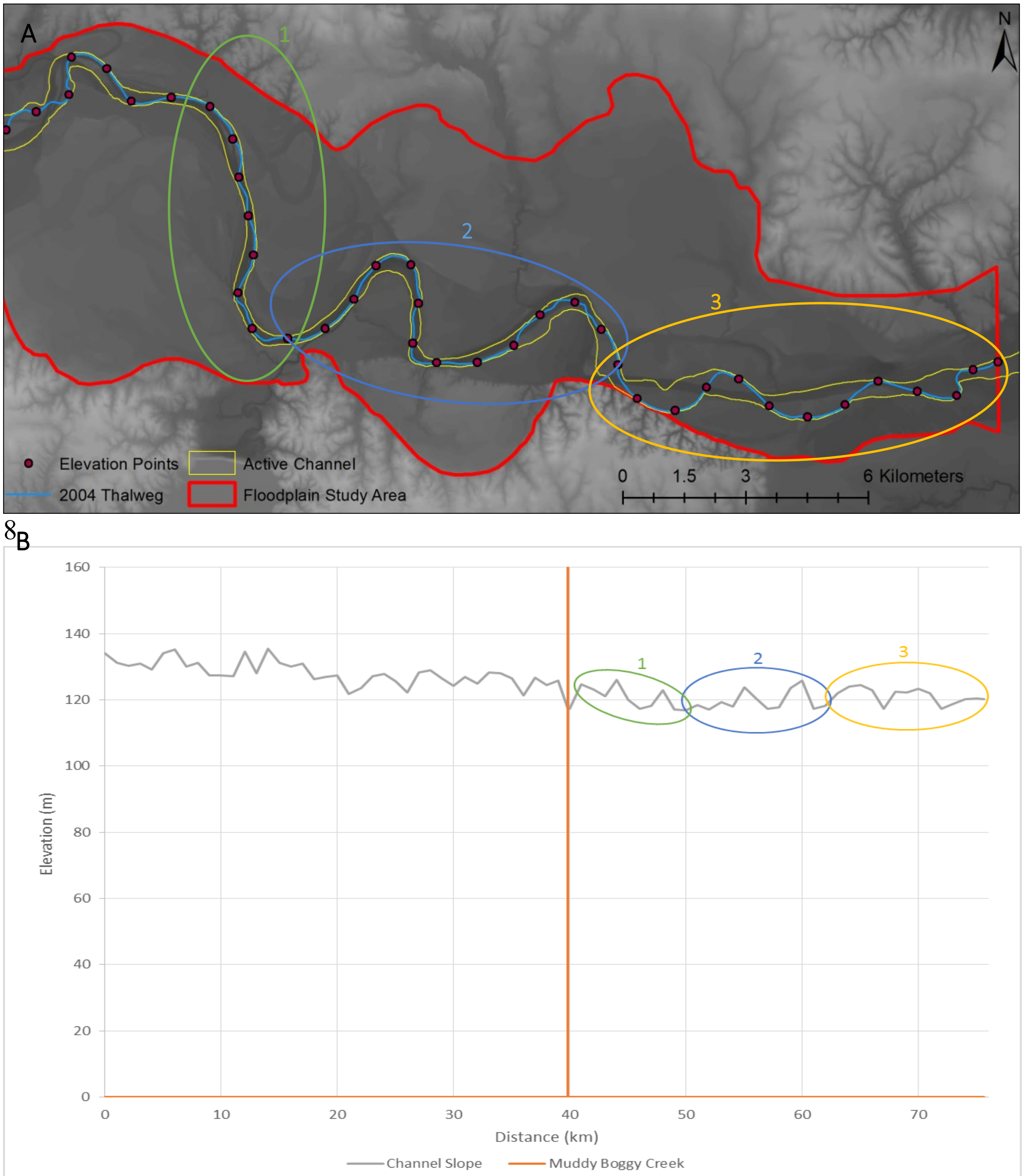

Figure 41. Change in channel slope downstream of Muddy Boggy Creek. *(B) Shows the channel elevation for the 2004 thalweg and (A) shows the DEM and the locations of circles 1, 2, and 3 from (B). These circles also correspond to the circles in Figure 36.*

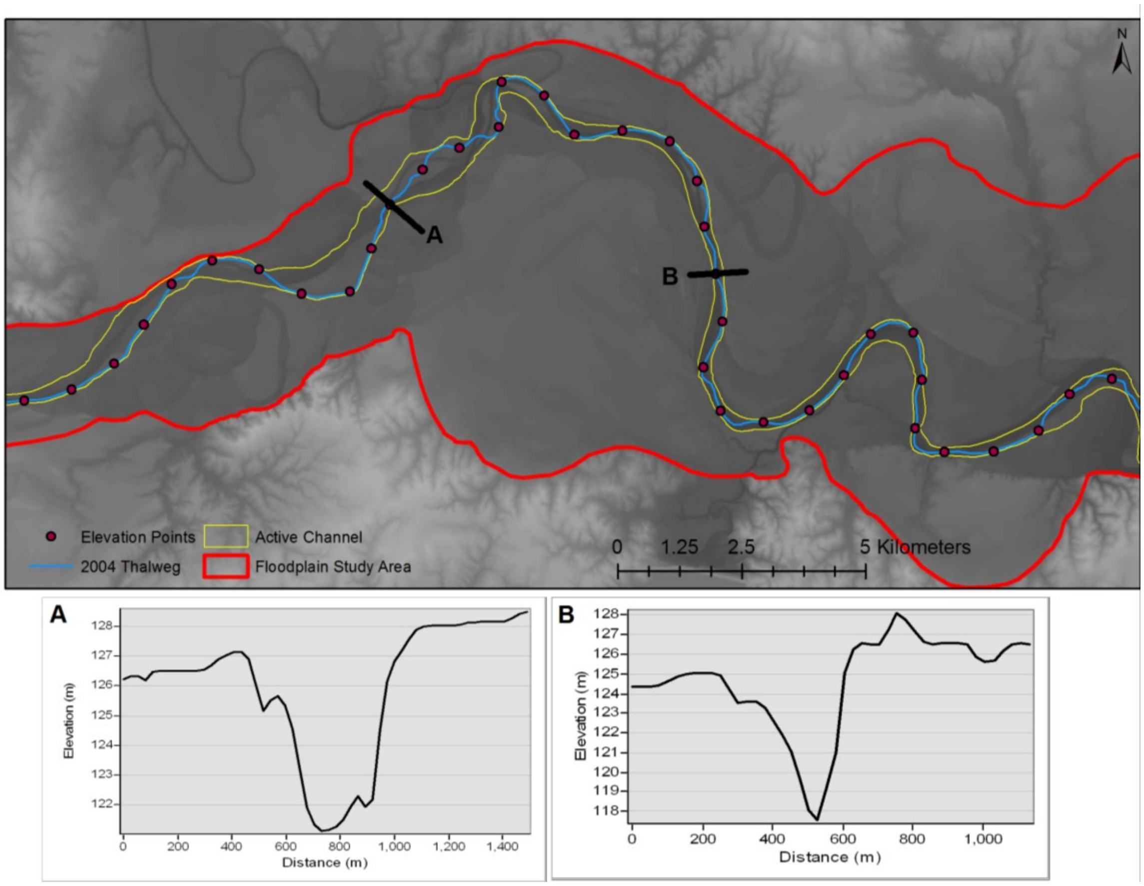

Figure 42. Cross-section transects upstream and downstream of Muddy Boggy Creek. *Transects (black lines) show channel cross-section geometry upstream and downstream of MBC. The downstream cross-section (B) shows the channel to be deeper and slightly narrower than the upstream cross-section (A).*

Major channel changes did not occur until further downstream, where the last large southerly bend in the river was seen to slowly migrate downstream over time. This section of the river remaining within the study area starts out straight and after the 1990 flood, began to be more sinuous with very subtle meanders developing, helping to create more sandbar area.

This straight section also corresponded to a dramatic decrease in valley slope, (Circle 3 in Figure 39) even though channel slope did not show a corresponding decrease (Circle 3 in Figure 41). The steep valley slope explains the straight shape of the channel seen from the 1890s to 1984. After the 1990 flood, this straight section developed subtle meanders, and channel slope was seen to first decrease in gradient slightly by 2004, then dramatic steepened by 2006. Unfortunately, with no imagery from around that time, how the 1990 flood immediately changed the river in this area is unknown. Presumably, the high stream power from this flood eroded the banks of this section of the river, widening the channel. As the high flows subsided, the wider channel decreased SSP, which caused the stream to start to aggrade and deposit large amounts of sediment in this section. By 2004, this section of the Red River is more sinuous, less steep, with large sandbars, all created after the May 1990 flood.

Sandbar and suitable SNH area continued to increase in 2006, even though the channel slope steepened. Channel slope decreased dramatically again by 2010, and remained low through 2014. This dramatic decrease corresponded to a decrease in sandbar and suitable SNH from 2006 to 2010, which seems counterintuitive, as one would expect an increase in sandbar deposition associated with a decrease in channel slope. The decrease in sandbar and suitable SNH from 2006 to 2010 can be explained by encroaching vegetation on the sandbars. With no flows that exceeded the MAF during that time, vegetation encroached upon the sandbars, converting some areas back into floodplain. Even though channel slope decreased, any net deposition of sediment was not enough to counteract the loss of sandbar area from encroaching vegetation. The change in channel slope may also have not been enough to decrease SSP to the threshold of sediment deposition either.

Upstream of MBC, but immediately downstream of the Blue River confluence, the Red River was straight and steep, with many mid-channel bars. As the Red River entered the western boundary of the RS, it began to meander with large bends in the river that were seen to migrate downstream over time, and valley and channel slope flatten out. Where these bends turn south, the channel widened considerably, narrowing again as the channel turns north, but widening again when the channel turned south again. This pattern, again was controlled in part by vegetation. The north side of the river remained forested along the banks, preventing channel migration in that direction. South of the river, areas that were cleared for cropland or rangeland, allowed for channel widening and migration. The narrowness of the floodplain valley here could also have a geologic control, however, the geology of the area was not investigated in this study. Further study into the geology of the Red River watershed could help explain patterns of valley shape and slope, which in turn would aid in more detailed understanding of the change in channel pattern over time.

With only the one gage station within the study area, downstream of MBC, there was no way to compare stream power upstream versus downstream of MBC. However, the changes in valley slope seen in the longitudinal profile of the river (Figure 39) can give clues as to how stream power might be changing along the course of the river, as steeper gradients relate to increased stream power. Usually confluence effects cause a lower gradient and wider channel upstream, which in turn cause a reduction in the transport of sediment (Benda et al. 2004). If stream power and channel gradient were lower upstream of MBC, it could account for the increased deposition of sand along the wider channel. This was seen in both the SS and RS. Although, further downstream of a tributary the channel width can increase, and sediment deposition is expected. Immediately downstream of the junction, “mixing effects” of sudden input of water can steepen the channel gradient (Benda et al. 2004). The steep channel gradient immediately downstream of a tributary can increase stream power, resulting in a section of river that is degrading and either eroding or transporting sediment, rather than depositing it. Increased channel gradient, narrowed channel width, and little sediment deposition was seen immediately downstream of all three major tributaries. Further downstream, sections of the river widen, become more sinuous, and have increased sediment deposition, as expected when the channel gradient flattens further from the tributary junction (Figure 43).

Overall, the increased sediment supply, along with decreased channel slope, created more sandbar deposition downstream of a tributary junction, as seen by the results of the SS. However, this picture was not seen in the RS. The boundaries of the RS happened to fall in such a way that the upstream portion captured part of the river where, downstream of the Blue River confluence, the channel began to widen, became less steep, and sediment was deposited. The channel steepening and lack of sediment deposition immediately downstream of the confluence with the Blue River was not captured within the RS. On the downstream section of the RS, though, the boundaries did capture the immediate channel steepening and narrowing that occurred just after the MBC confluence. The RS boundary ended before the channel had a chance to widen, decrease in slope, and deposit sediment. Therefore, the results from the upstream versus downstream comparison for the SS in terms of sandbar area and suitable SNH, were a bit misleading. MBC does contribute significant amounts of water and sediment to create suitable SNH, but those sandbar areas are seen further downstream than captured by the boundaries of the RS (Figure 44).

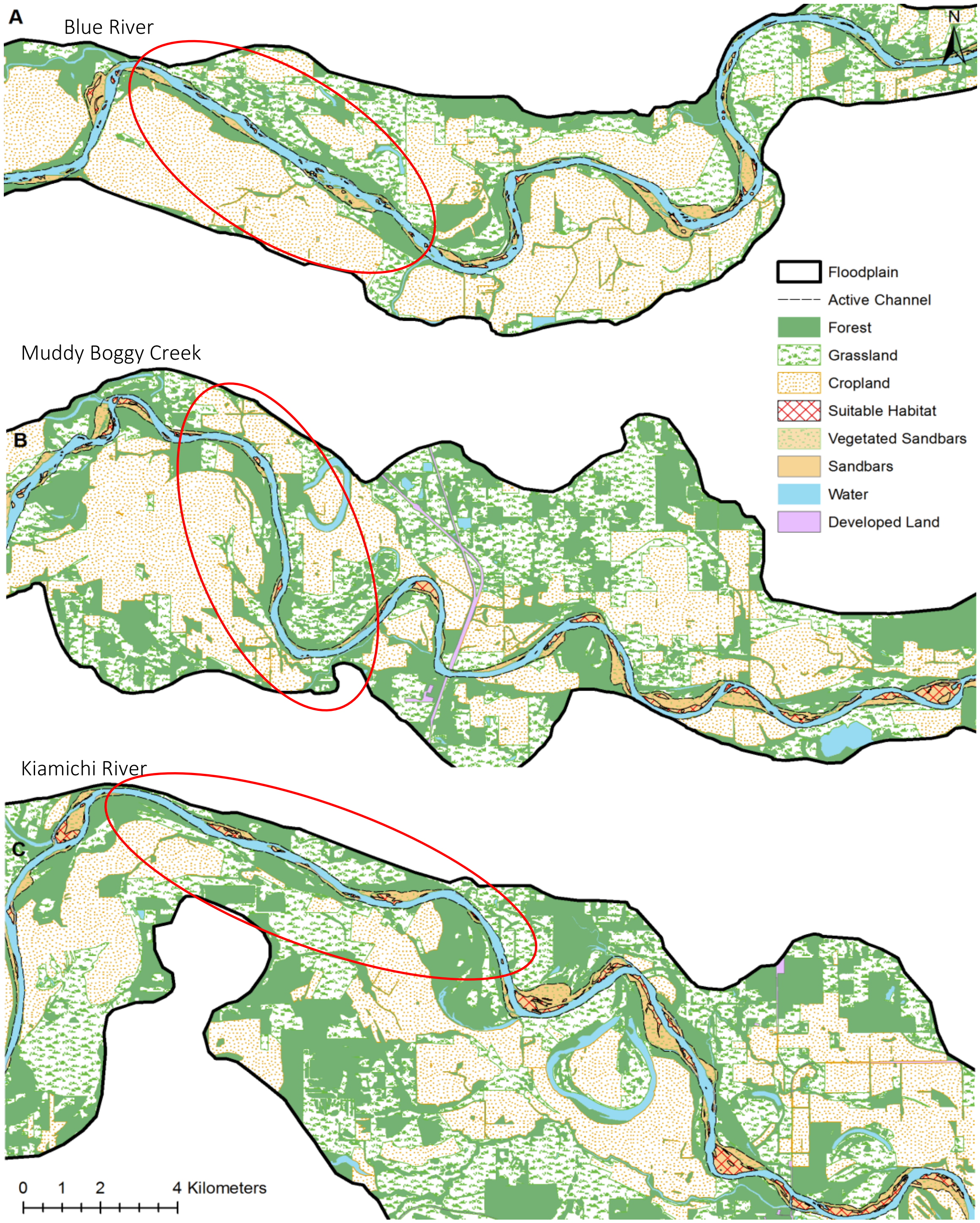

Figure 43. Zones of steep channel slope and narrow channel width with little sediment deposition downstream of major tributaries. *Red circles highlight these zones of increased channel gradient, narrow channel width, with little sandbar deposition for all three major tributaries: (A) Blue River, (B) Muddy Boggy Creek, and (C) Kiamichi River. Downstream of red circles, channel width is seen to increase, channel slope decreases, and increased sediment deposition results in more sandbars.*

It is also likely that downstream effects from the Blue River were mixing in complex ways with upstream effects from MBC. The degree of a tributary's influence is controlled by the relative contributing drainage area (Benda et al. 2004) which would lead to the conclusion that the confluence effects of MBC should be greater, or more important, than those of the Blue River given the greater drainage area of MBC than the Blue River. However, large tributary junctions that are closely spaced along the main stem may have confluence effects that overlap (Benda et al. 2004). This might explain what occurred here between the Blue River and MBC, and perhaps even the Kiamichi River as well. Immediately upstream of the MBC was also the portion of the river downstream of the Blue River where the channel gradient lessened and sediment deposition occurred (Figure 45). If the Blue River connected to the Red River further away from the MBC confluence, perhaps more traditional upstream versus downstream changes would be seen around the MBC. Further study into these overlapping tributary effects would be required to more adequately understand the sandbar dynamics around these confluences.

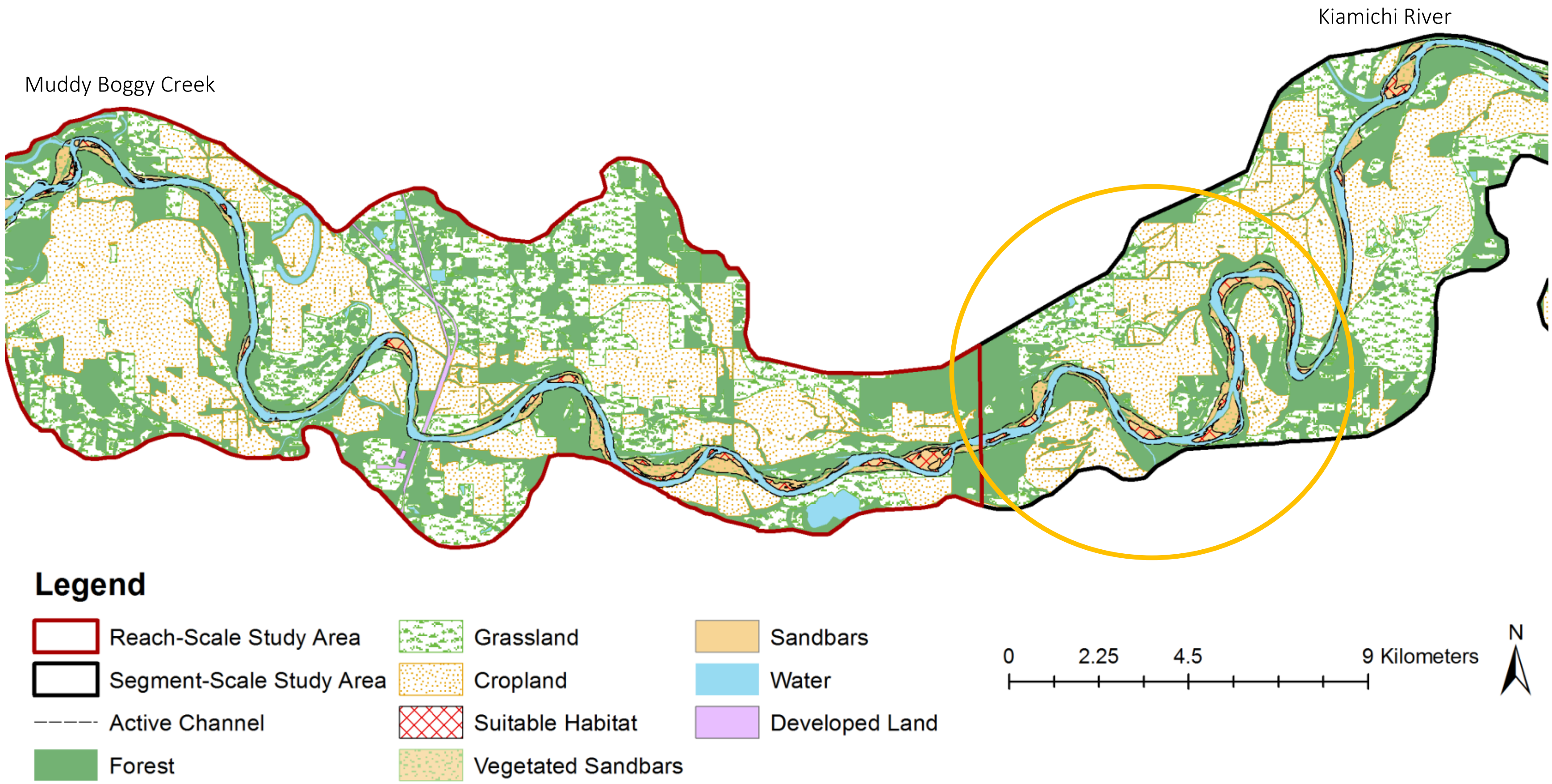

Figure 44. Area of the Red River downstream of Muddy Boggy Creek that was not included in the reach-scale study area. *Yellow circle highlights this area, where sinuosity, channel width, sandbar and suitable SNH area are all seen to increase. This area was captured by the segment-scale study area, but not the reach-scale study area.*

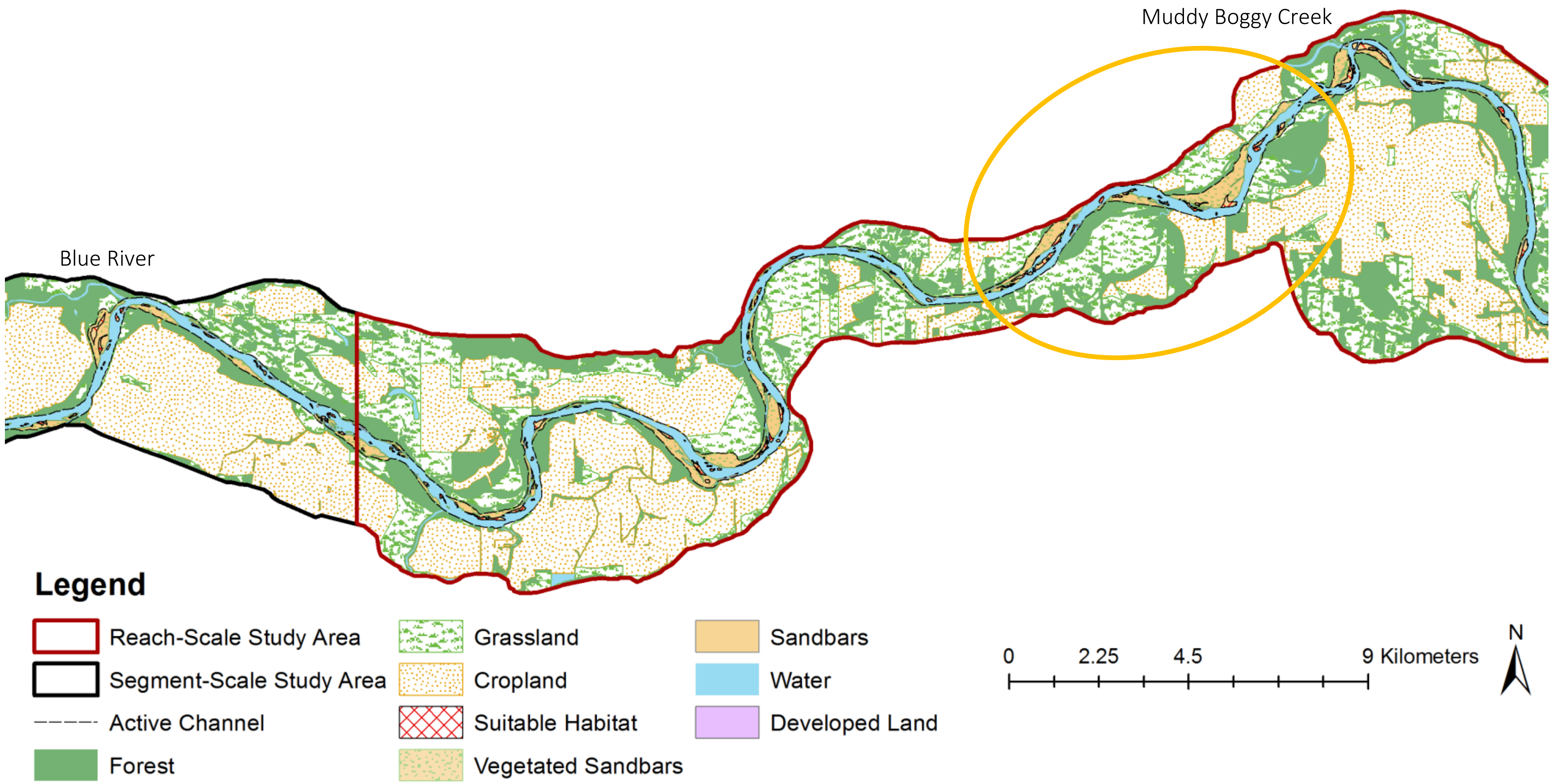

Figure 45. Area of the Red River upstream from Muddy Boggy Creek with decreased channel slope, increased channel width, and sediment deposition. *Yellow circle highlights this area which is immediately upstream of MBC, but downstream of the Blue River.*

Comparison of Suitable Habitat to Known Populations

Lott and Wiley (2013) compiled surveyed ILT nests from 2002-2011. During this time, 128 nesting sites at different locations were recorded within the SS. The breakdown of these known ILT nesting sites by year is shown in Table 8. For the 2006 breeding season, all 5 nesting sites fall within the calculated suitable SNH from this study: 3 sites located upstream of MBC and 2 sites located downstream of MBC.

Table 8. Number of Interior Least Tern nesting sites by year within study areas. Data from Lott and Wiley (2013).

Year	# of Nesting Sites within Segment-Scale Study Area	# of Nesting Sites within Reach-Scale Study Area
2003	18	5
2005	25	4
2006	18	5
2008	38	13
2009	18	6
2010	5	2
2011	6	1

For the 2008 breeding season, all 13 nesting sites also fall within the calculated suitable SNH: 9 sites located upstream of MBC and 4 sites located downstream of MBC. For the 2010 breeding season, however, only 1 nesting site falls within the calculated suitable SNH, it is located within the RS upstream of MBC. However, 4 of the 5 nesting sites within the SS are located mid-channel very close to a mapped mid-channel sandbar with suitable habitat. Depending on when in the season these sites were surveyed compared to the dates of the imagery used here, some of the mid-channel bars might have been larger in size when the nests were surveyed compared to when the imagery was taken. Therefore, it is reasonable to assume that 4 total nesting sites in 2010 corresponded to the calculated suitable SNH. The remaining 1 nesting site was located along a channel bank, within 20 meters of the channel margin. This is highly unusual, given that normally, ILTs will not nest within 60 meters of the channel margin, so our suitable SNH model did not capture this site. Overall, the surveyed nesting site data shows that our suitable SNH model did a fairly accurate job in determining where ILTs are likely to nest.

It is interesting to note that the suitable SNH model calculated far more suitable sandbar sites than ILTs used. Field methodology for counting ILT nests and populations could account for some of the underestimation. Yet, Lott and Wiley (2012b) also found that previous surveys vastly underestimated the extent of SNH for ILT when they surveyed suitable sites along the Red River in 2008 and suggested that further research was needed to explain why ILT are not utilizing as much suitable SNH as was available. Lott and Wiley (2012b) determined suitable SNH by the 5 criteria defined by them listed previously. Because Lott and Wiley (2012b) were able to conduct a field survey, they were able to include the criterion that sandbars not be inundated at a daily maximum flow typical of normal hydropower production during low-runoff conditions, which was not able to be a criteria in this study. From Denison Dam to Index, AR, Lott and Wiley (2012b) identified a total of 117 sandbar sites covering a total of 4.7 km^2 of suitable SNH area. For the RS in 2008, which is a much smaller area than what Lott and Wiley (2012b) surveyed, this study calculated a total of 5.04 km^2 of suitable SNH. While the suitable SNH model in this study does a reasonable job of matching locations of known ILT nesting sites, it overestimates the amount of suitable SNH. This overestimation is largely due to the fact that sandbar elevation could not be considered. Lott and Wiley (2012b) note that survey crews encountered vast areas of sandbars at low elevations that would not typically be exposed during the breeding season, and did not measure these areas when measuring total sandbar area.

Indeed, Lott and Wiley (2012b) noted that between Denison Dam and the confluence with MBC, all sandbar perimeters displayed evidence of stage fluctuations due to hydropower peaking surges. The difference between the maximum elevation of suitable SNH and the peak hydropower flow elevation increased downstream, as these hydropower peaking surges attenuated in the downstream direction. This could account for Lott and Wiley (2012b) finding that total sandbar area (above the high water line) and total suitable SNH area increased downstream of MBC. This could also account for the overestimation of both total sandbar area and total suitable SNH from this study. Even though sandbar areas that were clearly underwater in the imagery were not measured, aerial imagery represents a static picture, a snapshot in time. Daily hydropower stage fluctuations cannot be seen in these images, and since sandbar elevation is also not known from these data, this study most likely mapped large areas of sandbars that Lott and Wiley considered too low in elevation to measure— areas that were likely to be inundated from hydropower surges.

Even though more suitable SNH was found downstream of MBC, the flooding risk for these areas was also higher, due to inputs from unregulated tributaries (Lott and Wiley 2012b). The 50th percentile of flows (around 311 m3/s) from 1945-2008 from Denison Dam corresponded to only 0.01 m higher water level than the peak hydropower water level (Lott and Wiley 2012b). However, at the Arthur City, TX gage station, which is located below two unregulated major tributaries to the Red River, the 50th percentile flows (about 603 m^3/s) equated to a water stage that was 2.34 m higher than the peak hydropower water level (Lott and Wiley 2012b). So while sandbars downstream of these tributaries tend to be higher in elevation and SNH has less risk from flooding of peak hydropower flows than upstream, they have a greater risk from major flood events and high flows that are contributed to the Red River from major tributaries. Again, more detailed study in relating flows, especially peak hydropower flows, to sandbar elevation would be required to continue to refine suitable SNH models for the Red River.

IX. CONCLUSIONS

Sandbar area and suitable SNH was affected by changes in ecology (floodplain vegetation), hydrology (stream power and discharge), and geomorphology (valley morphology, channel width, slope, and sinuosity). Human modifications in the form of land use change, impoundment, and flow regulation) imposed upon this web of interacting variables also affected sandbar area and suitable SNH over time. Sandbar area and suitable SNH can be added to the biogeomorphic response model (Figure 46) since results showed that sandbar area and suitable SNH are affected by changes in land cover and channel width.

Although precipitation in the Red River watershed was slightly more varied than the 5-year alternating wet-dry cycle typical of the Great Plains (Matthews et al. 2005), there were still periods of decreased precipitation (roughly 1936 to 1964, and 1996 to 2014) and increased precipitation (roughly 1964 to 1996; Figure 46A) that corresponded to increases and decreases in floodplain vegetation (Figure 46B). As floodplain forest cover increases in times of increased precipitation (Schumm and Lichty 1963), their roots strengthen bank resistance to erosion (Charlton 2008) and active channel width narrows (Figure 46D). When active channel width narrows, stream power tends to increase, and sediment deposition does not occur, resulting in less sandbar area (Figure 46E). Vegetation growth on sandbars is also somewhat dependent on precipitation patterns, and the percentage of sandbar area vegetated tends to expand during wetter periods and contract during drier periods (Figure 46F). The percentage of sandbar area considered suitable SNH (Figure 46G), which is dependent upon sandbar area and vegetation growth on sandbars, then expands when vegetation growth is low and sandbar area is high, and contracts when vegetation growth is high and sandbar area is low.

Periodic large floods (Figure 46B), though, are common phenomena in Great Plains rivers (Matthews et al. 2005). These large floods are independent of decadal precipitation patterns (Schumm and Lichty 1963), and are particularly destructive to mostly non-cohesive boundary materials, such as the sandy soil found along the Red River margins (Figure 23). Large flood events have enough stream power to widen the active channel (Figure 46D), and remove large areas of both floodplain forest cover (Figure 46C) and vegetation on sandbars (Figure 46F). Following the erosion event, as high flows subside, the widened channel decreases the stream power of the channel and encourages sediment deposition, increasing sandbar area (Figure 46E). Removed vegetation on sandbars and freshly deposited sediment enhance suitable SNH area (Figure 46G). In the absence of another large flood, the active channel will slowly narrow, depending upon the variability of sediment erosional/depositional events and the rate of encroachment by floodplain vegetation (Friedman et al. 1998). As active channel narrows and vegetation growth in both the floodplain and on sandbars increases, sandbar area and suitable SNH slowly decreases as well.

This alternating pattern of channel widening followed by channel narrowing, in addition to sandbar and suitable SNH expansion followed by contraction, would likely have continued for hundreds of years as it had probably done before. Human-induced modifications, however, disrupted this feedback loop. First, floodplain forest clearing for agriculture (Figure 46C*) removed root systems that added cohesion to bank materials. When the next large flood event came, the banks of the Red River were easily eroded and the channel over-widened (Figure 46D*). This is seen in the 1949 scene (Figures 26-27; Figures 5-9 in Appendix A and bottom of 17 in Appendix B).

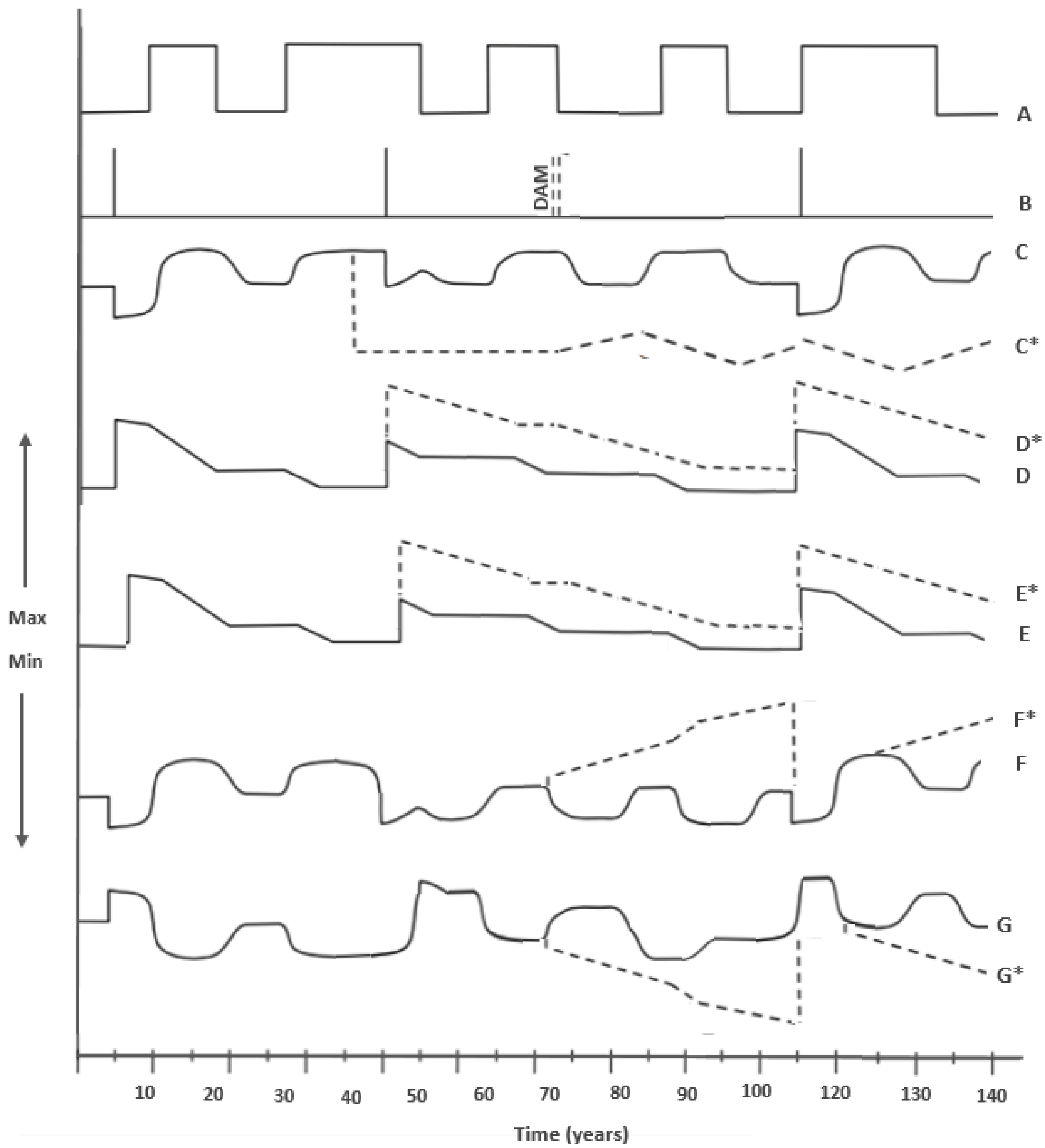

Figure 46. Extended biogeomorphic response model *of floodplain forest cover (C), active channel width (D), sandbar area (E), percentage of sandbar area covered in vegetation (F), and percentage of sandbar area considered suitable SNH (G) in response to variable precipitation (A) and large floods (40-year return interval in this case; B). Precipitation (wet versus dry periods) and floods are independent variables and are independent of each other. Active channel width and floodplain forest cover are dependent variables and are dependent on each other through feedbacks; where*

increases in channel width from floods remove floodplain forests, and re-growth of floodplain forests, especially during wet periods, reduce channel width. Similarly, sandbar area is dependent on active channel width; where increases in channel width allow decreased stream power to deposit sediment, slightly lagging behind the channel widening. Vegetation on sandbars is dependent upon precipitation and large floods; where increase in precipitation during low water stage encourages vegetation growth on sandbars, and large floods remove vegetation from sandbars. Active channel width is also dependent on vegetation encroachment onto sandbars through feedbacks; as vegetation encroaches on sandbars, active channel width continues to narrow. Lastly, suitable SNH is dependent on sandbar area, floodplain forest cover, and vegetated sandbar area. As sandbar area decreases, so does suitable SNH, though at a different rates. As vegetation on sandbar area grows, and active channel narrows, suitable SNH decreases. When floodplain forest cover is high, suitable SNH will be low, and when floodplain forest cover is cleared by floods or for agriculture, suitable SNH area increase. C (dashed line) represents a scenario in which most floodplain forest cover were cleared for agriculture. The double-dashed lines along line B represents river impoundment, restricting high flows. Both the clearing of floodplain forest cover and lack of floods results in feedbacks where active channel width (D*) first increases due to floodplain forest clearing, but then continues to decrease due to lack of flooding events. E* is the sandbar area response to this scenario, where initial channel widening increases sandbar deposition, but continued lack of flood allows for vegetation to encroach on sandbars (F*) thereby narrowing the channel and decreasing sandbar area. As vegetation increases, suitable SNH continues to decrease (G*). Rare, major flood events after dam completion can restart the cycle. Model was based on the concept of Knox's (1972) biogeomorphic response model but was modified and expanded upon with data and patterns, first from Julian et al. (2012) and then from results of this study.*

Again, following the erosion event, as high flows subsided, the decreased stream power of the channel begins to deposit sediment forming large sandbars (Figure 46E*). Vegetation growth on the sandbars previously is removed from the flood event and suitable SNH increases dramatically. Again, in the absence of another large flood, vegetation growth on sandbars increases, the active channel begins to narrow, and sandbar and suitable SNH area decrease.

The second human-induced modification came in the form of Denison Dam (double-dashed line on Figure 46B). As seen by the discharge record for the Red River (Figure 10), Denison Dam reduces the frequency and magnitude of large flood events.

Lack of high flows encourages continued vegetation growth on sandbars (Figure 46F*). With no major floods to scour out this vegetation or deposit fresh sediment, vegetation encroached on the sandbars, growing into riparian forest cover, and eventually narrowing the channel. As forest cover grew back, localized clearing for agriculture took place sometimes (Figure 46C*). As the channel continued to narrow, and vegetation growth on sandbars converted areas of active channel into floodplain, sandbar area continued to decrease (Figure 46E*). The lack of high flows reduced the river's capacity to move and deposit sediment, which limited sandbar area. As sandbar area decreased, and vegetation growth on sandbars greatly increased, suitable SNH dramatically decreased (Figure 46G*). Although clearing of floodplain forest cover allowed some localized increases in suitable SNH, this was not enough to counteract the decrease in suitable SNH due to decreased sandbar area, channel width, and increased vegetation growth on sandbars. Dams prevent many high flows through a channel, but they do not prevent rare, major flood events. A flood event after the completion of a dam restarts the cycle explained above.

The pattern described above by the extended biogeomorphic model was seen to occur on the Red River from pre-settlement times to 2014. The May 1990 flood was one exception to this pattern, being the largest flood occurring after Denison Dam was completed in 1944. Active channel width, sandbar area and suitable SNH was seen to be mostly decreasing from 1949 to 1984, but the May 1990 flood was large enough to "reset" this pattern. Increased stream power widened the channel, removed both riparian forests and vegetation on sandbars, and deposited sediment to form new sandbars or increase areas of existing sandbars, which in turn increased suitable SNH for ILT.

However, because of the lack of high flow events following the 1990 flood, these river characteristics quickly fall back into the pattern seen before the flood─ active channel width narrows again, sandbar area decreases, vegetation growth increases on sandbars, and suitable SNH decreases.

The processes and patterns captured by the extended biogeomorphic model help to give an understanding of the importance of high flow events and channel geometry to the creation and maintenance of sandbars for suitable SNH. However, it does not encompass the entire picture of suitable SNH dynamics because sandbar elevation was not able to be considered here. Suitable SNH is especially limited by the elevation of the sandbar above hydropower surges in water level, which fluctuate daily. The inability to account for sandbar elevation by the remote sensing approach used here caused an overestimate of suitable SNH area in this study. Understanding how sandbar elevation (rather than simply planform area) interacts with the other factors affecting suitable SNH will be key in developing a more accurate assessment of this critical ILT habitat.

Another complicating factor that was not captured by the extended biogeomorphic model was the effect that tributaries play. Within the study areas, there were significant differences in channel width, sinuosity, slope, sandbar area, and suitable SNH between upstream and downstream of MBC, especially within the RS. The upstream section of the river tended to be wider, more sinuous, steeper, and have larger sandbar areas and suitable SNH for the RS. Lott and Wiley (2012b), however, determined that there were more sandbars and most suitable SNH downstream of MBC. Although this pattern was seen within the SS, it was not captured in the RS largely because the RS boundaries captured the downstream effects of the Blue River mixing with the upstream effects of

MBC. The RS also did not capture enough river downstream of MBC to see the increase in sandbar and suitable SNH that was seen within the SS and within Lott and Wiley's (2012b) survey. The discrepancy in sandbar and suitable SNH area estimates between this study and Lott and Wiley (2012) can also be explained by the fact this study was not able to evaluate sandbar elevation, and therefore overestimated the amount of suitable SNH. At the same time, this study did show that the loss of sandbar and suitable SNH area over time was greater upstream of MBC.   This hints to the important role that sediment and discharge input from MBC plays into sandbar and suitable SNH dynamics downstream of the confluence, and is more aligned to the results of Lott and Wiley (2012).

Regardless, more refined estimations of suitable SNH is needed, as well as a better understanding of the overlapping confluence effects to determine where along the Red River sandbar occur and why they occur there. At the same time, the suitable SNH model developed here was shown to be accurate in determining similar locations of suitable SNH to ILT nests in reality, even if the extent of estimated SNH was greater. The extended biogeomorphic response model shows that ecological variables can be incorporated into such a model since they are interrelated with hydrologic and geomorphologic variables. Although the extended biogeomorphic response model needs refining before it can fully assess suitable SNH for ILT, this study does show that such a tool could be useful in assessing the multitude of factors that dictate critical riparian habitat over time. Understanding of the patterns and processes that led to current habitat conditions can aid in future work determining how to best manage such a dynamic system for the benefit of the unique species that utilize such rivers for habitat. This will be especially important in the future, as Oklahoma considers building new reservoirs on both the Blue River and MBC to meet forecasted increased water demand in the area (OWRB 2012). Given that the loss of sandbar and suitable SNH area was seen to be greater upstream from an unregulated tributary, it would be reasonable to assume that impoundment on these tributaries would exacerbate future losses of both sandbar and suitable SNH downstream. This increase in loss would occur along the area of the river below MBC where Lott and Wiley (2012) found amble suitable SNH, and could prove to be detrimental to ILT populations in the future. Again, a more detailed understanding of the patterns and processes that affect habitat conditions on this section of the Red River will help to inform management decisions related to water demands and new reservoir locations, as well as guiding potential environmental flow releases from existing reservoirs.

APPENDIX SECTION

APPENDIX A: LAND COVER MAPS FOR SEGMENT-SCALE STUDY AREA

Pre-Settlement

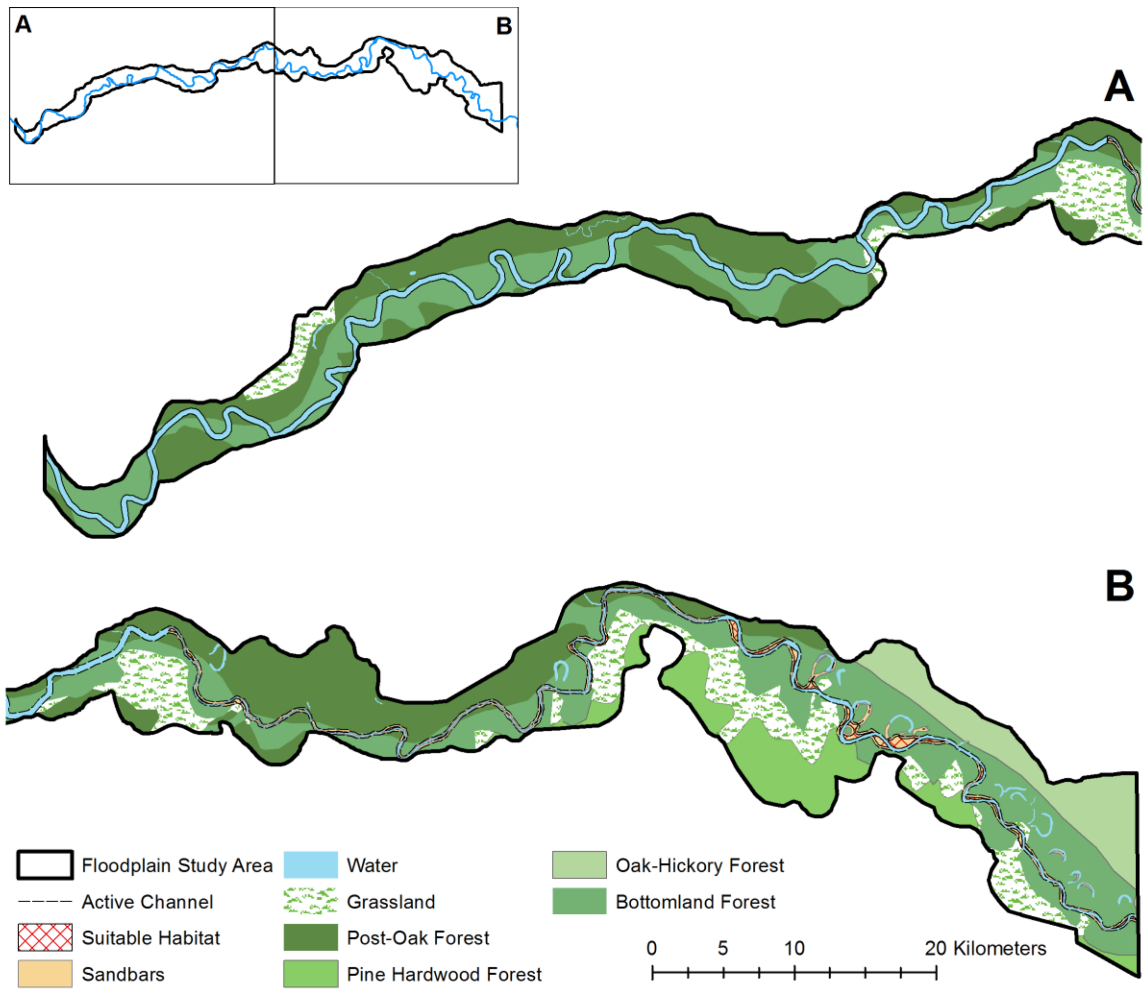

Figure 1. Pre-settlement land cover of the segment-scale. *Vegetation patterns represent the potential natural vegetation. The channel and sandbars are taken from the 1890's data. The entire segment-scale study area is shown here, but only the right-hand side (B) of the study area was analyzed for land cover area measurements and suitable habitat since the left-hand side (A) had no sandbars that were mapped.*

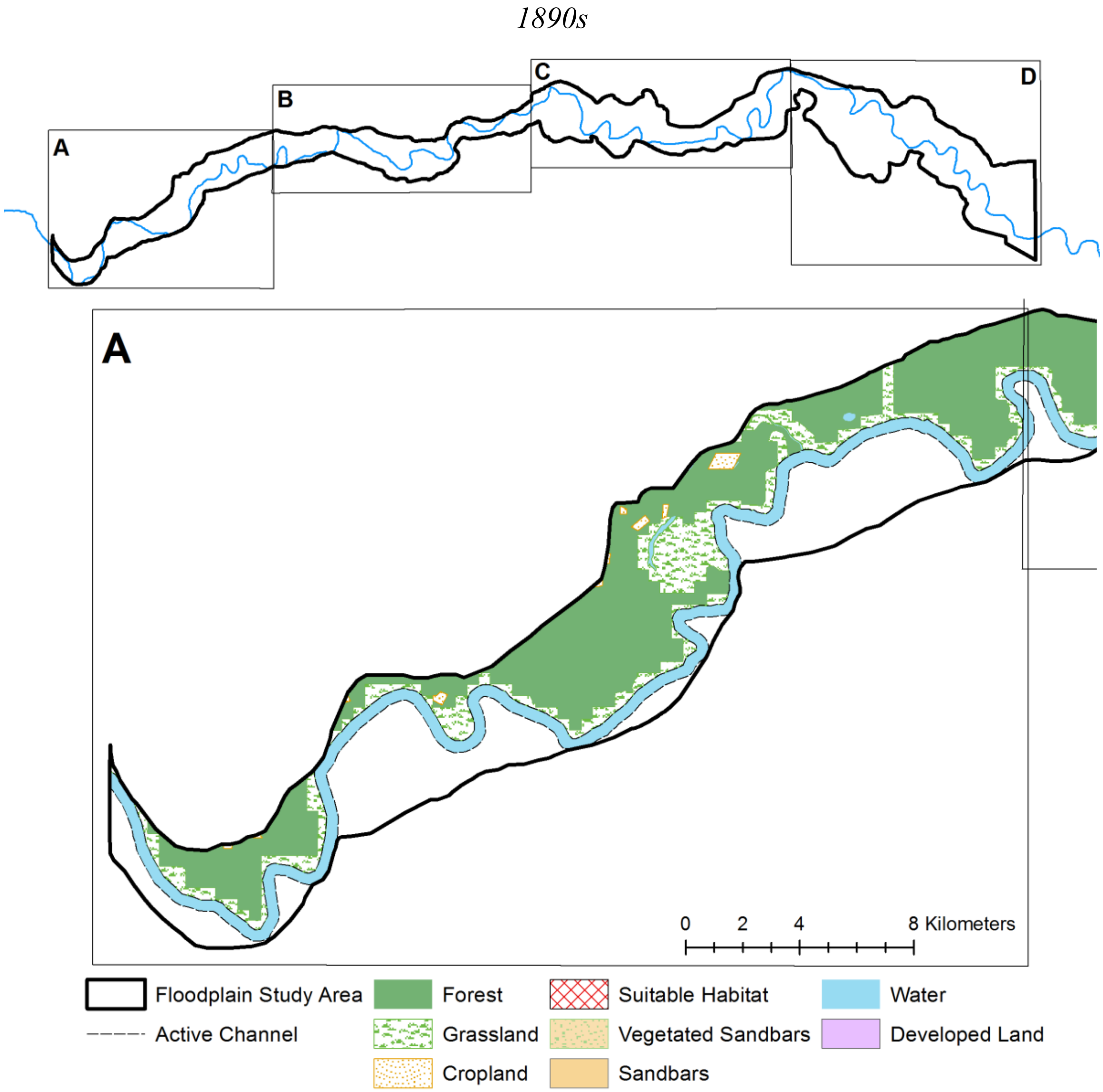

Figure 2. Section A of the segment-scale land cover map for the 1890s. *This section is shown here for reference, but was not analyzed for land cover or suitable habitat.*

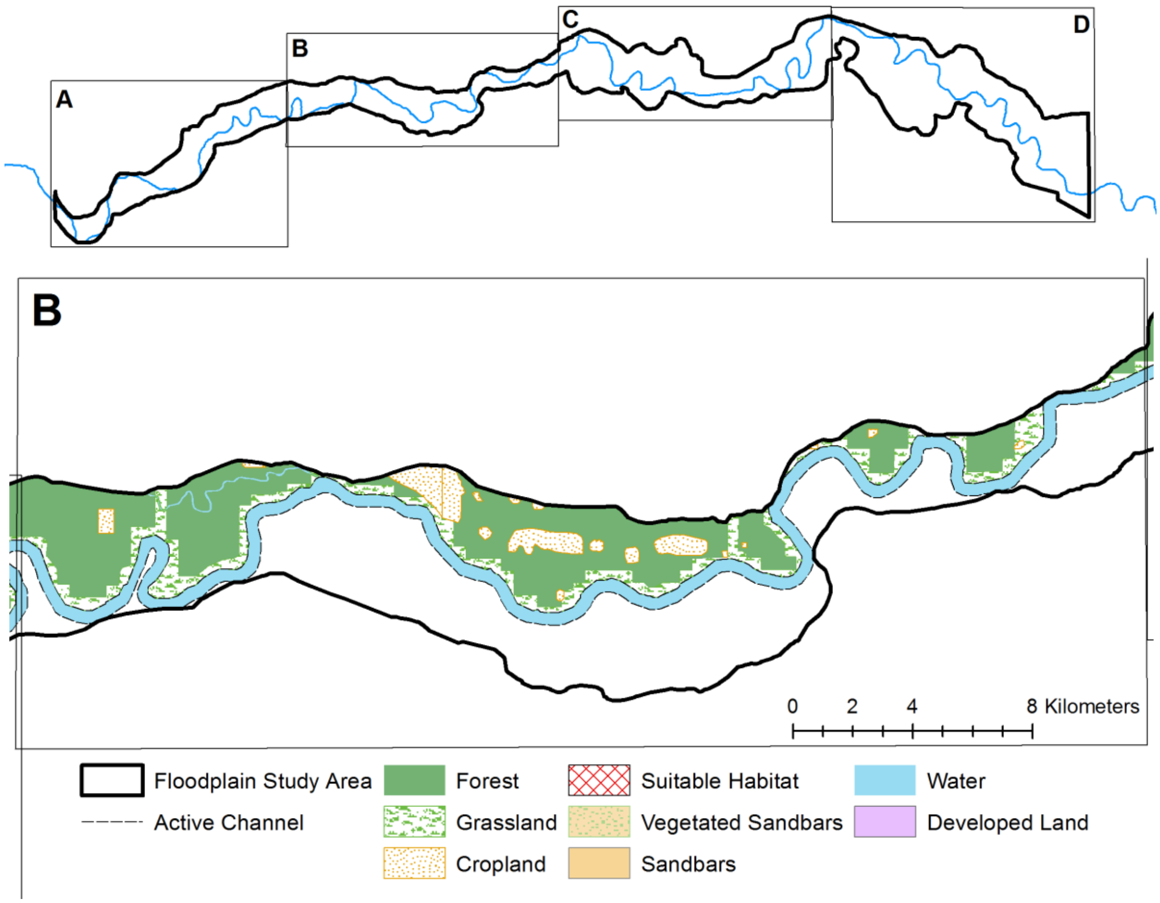

Figure 3. Section B of the segment-scale land cover map for the 1890s. *This section is shown here for reference, but was not analyzed for land cover or suitable habitat.*

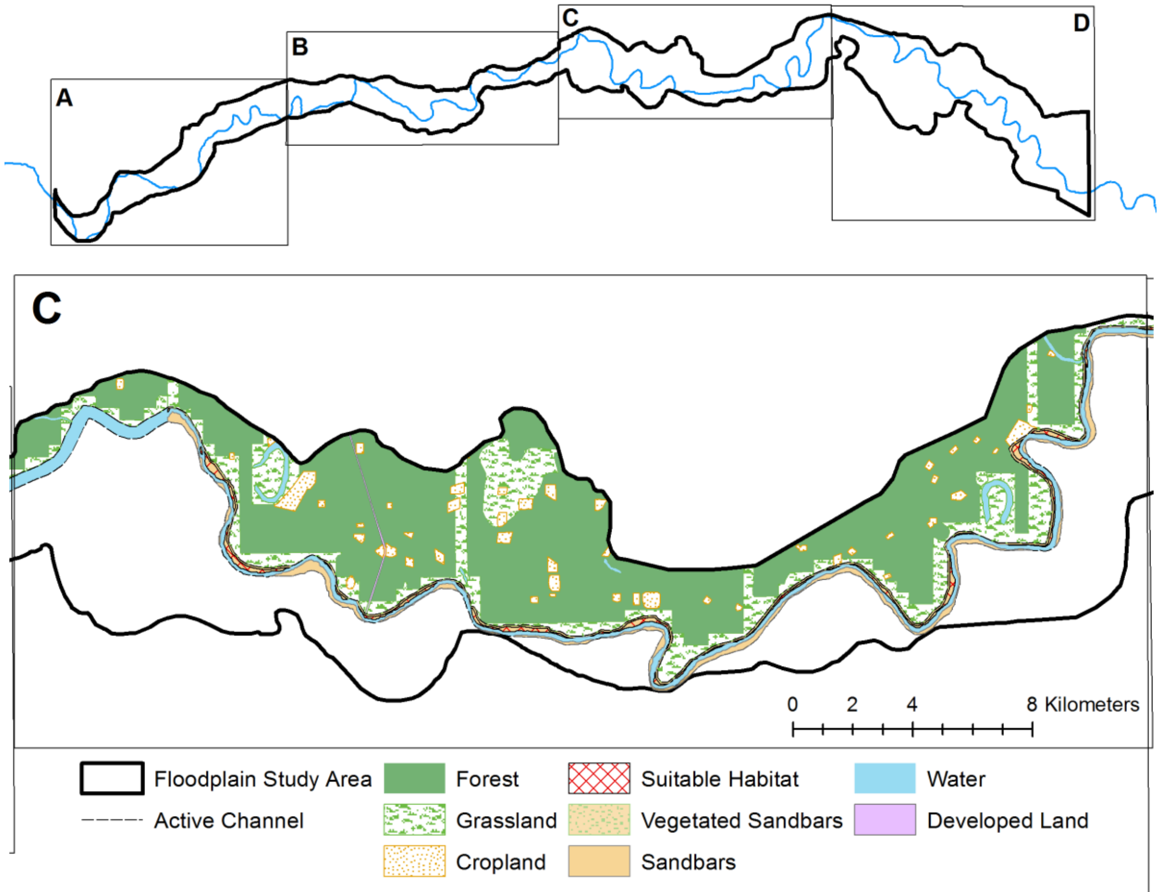

Figure 3. Section C of the segment-scale land cover map for the 1890s*, just below the confluence with Muddy Boggy Creek. Sandbars on the Texas side of the river were not analyzed.*

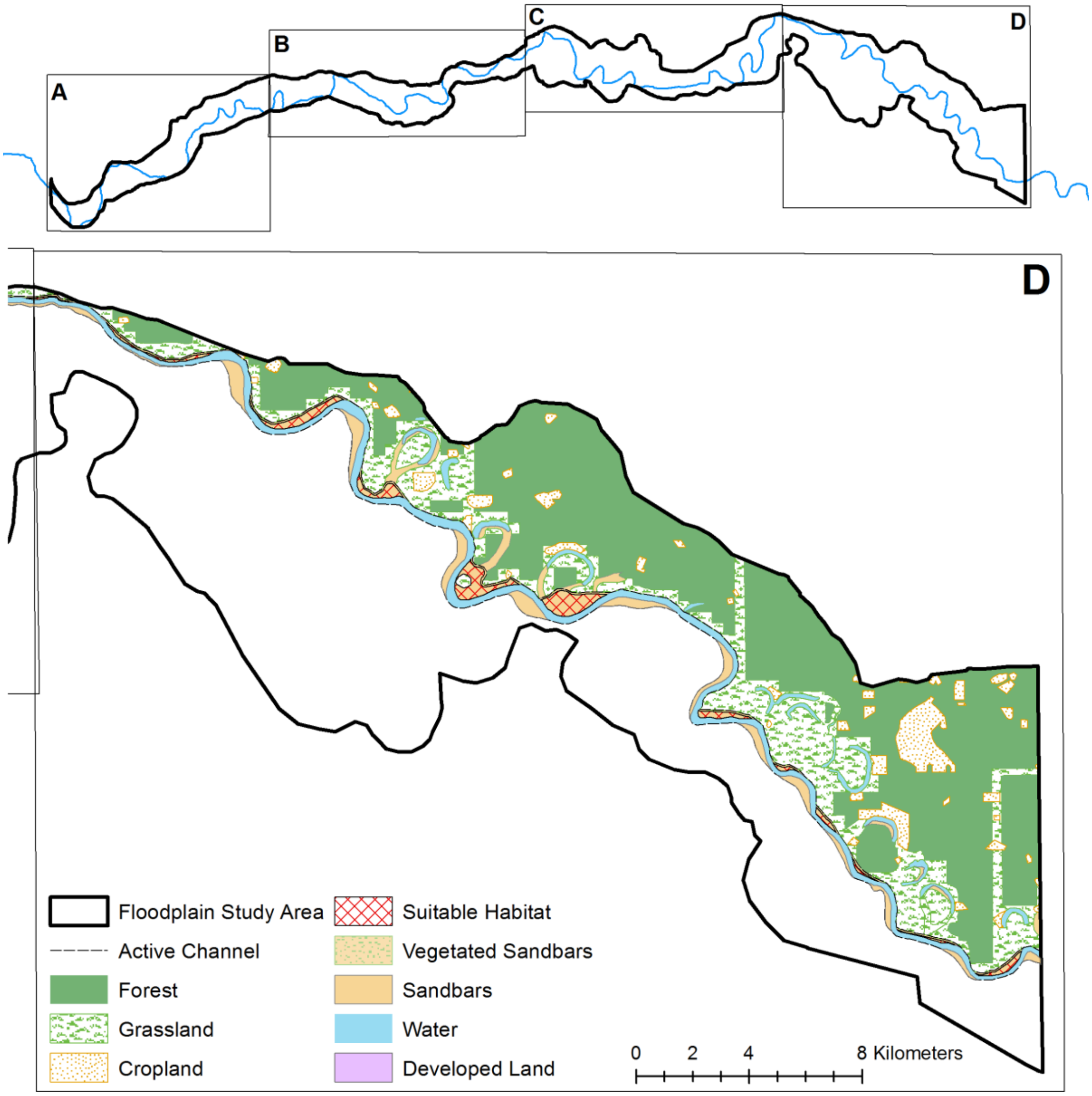

Figure 4. Section D of the segment-scale land cover map for the 1890s. *Sandbars on the Texas side of the river were not analyzed.*

1949

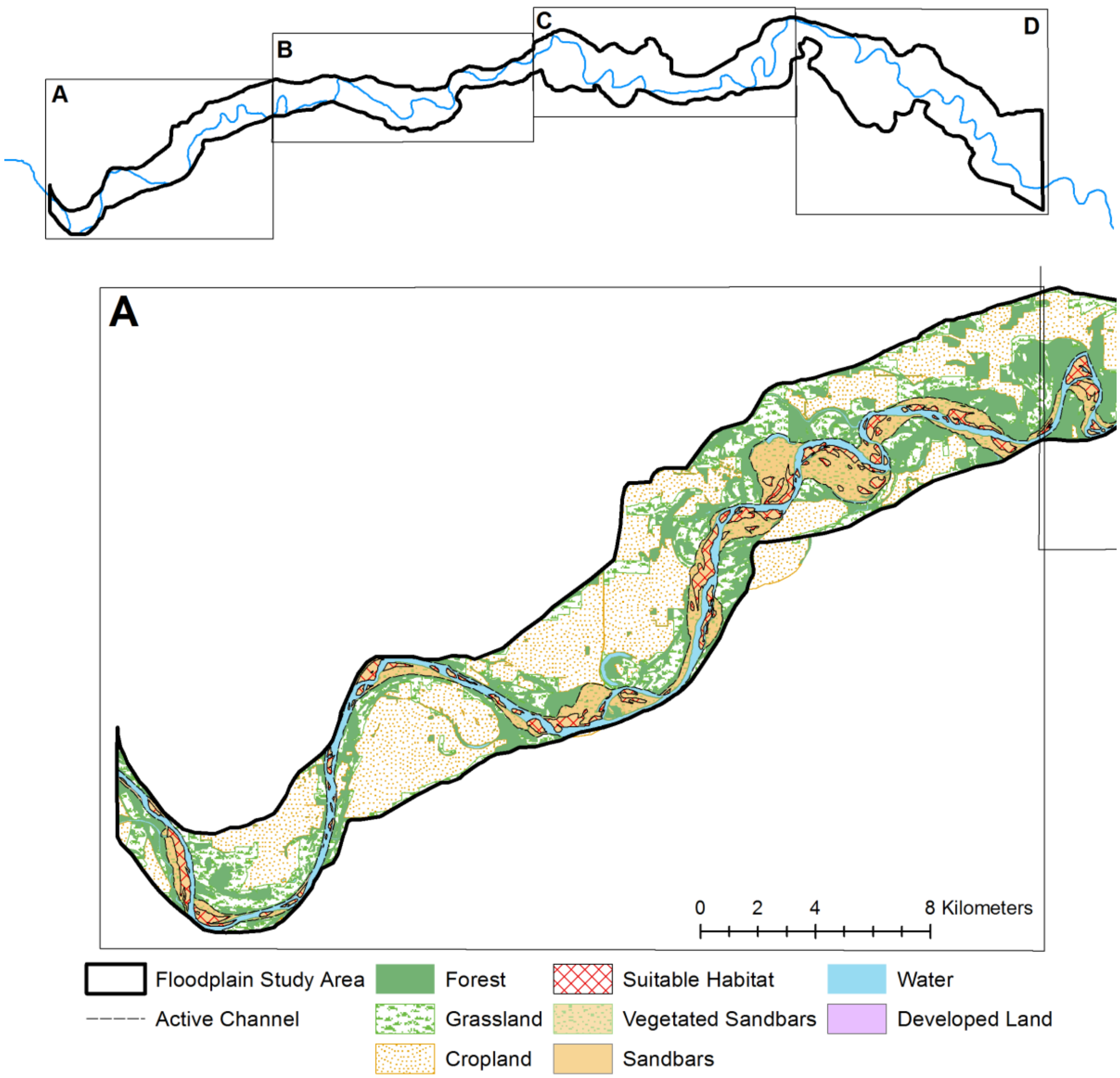

Figure 5. Section A of the segment-scale land cover map for 1949.

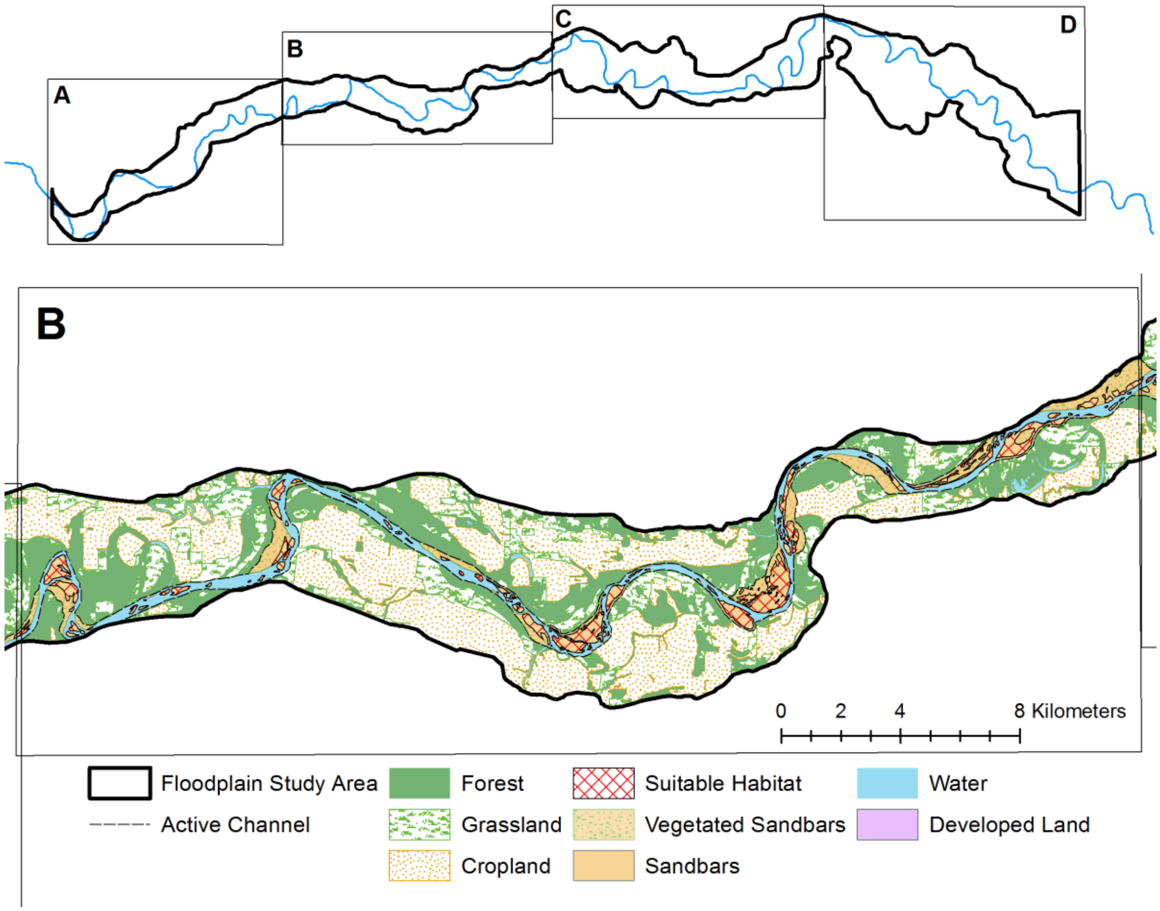

Figure 6. Section B of the segment-scale land cover map for 1949.

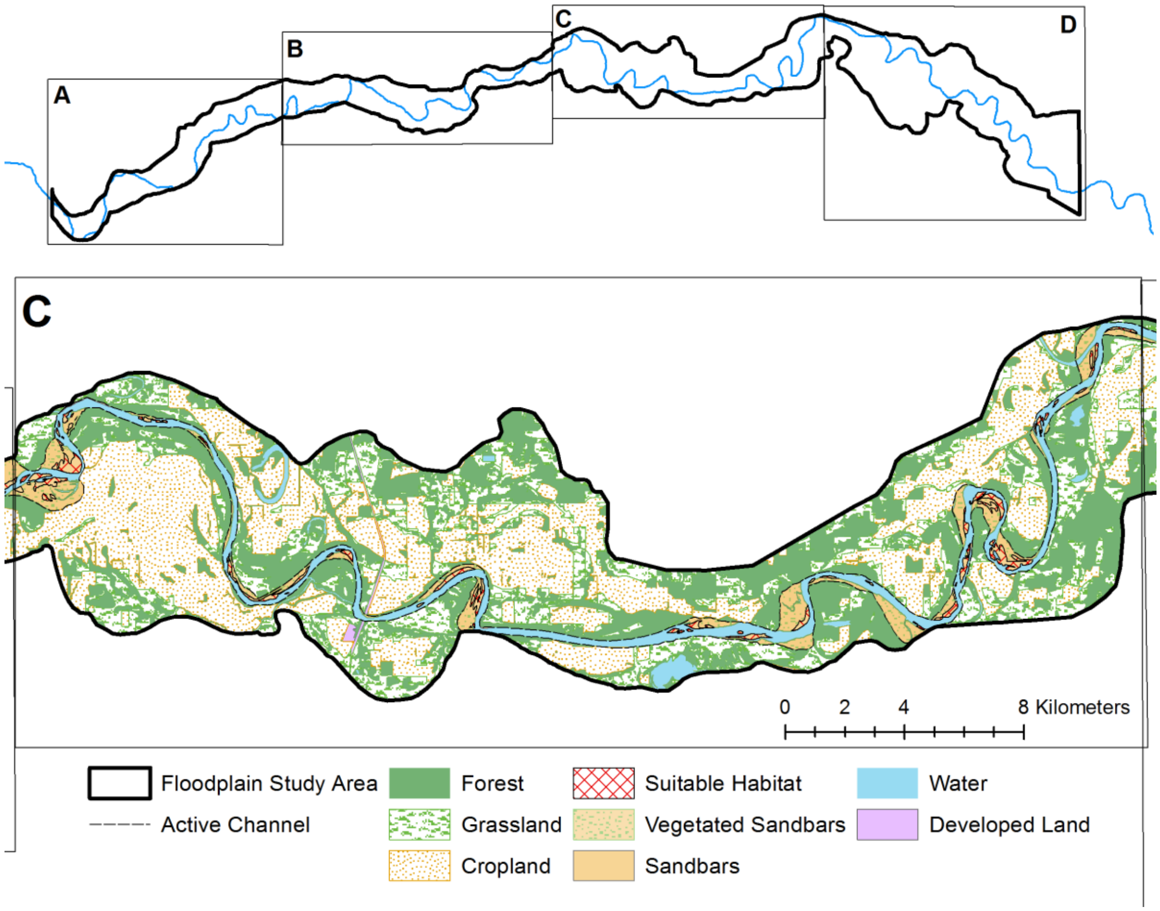

Figure 7. Section C of the segment-scale land cover map for 1949.

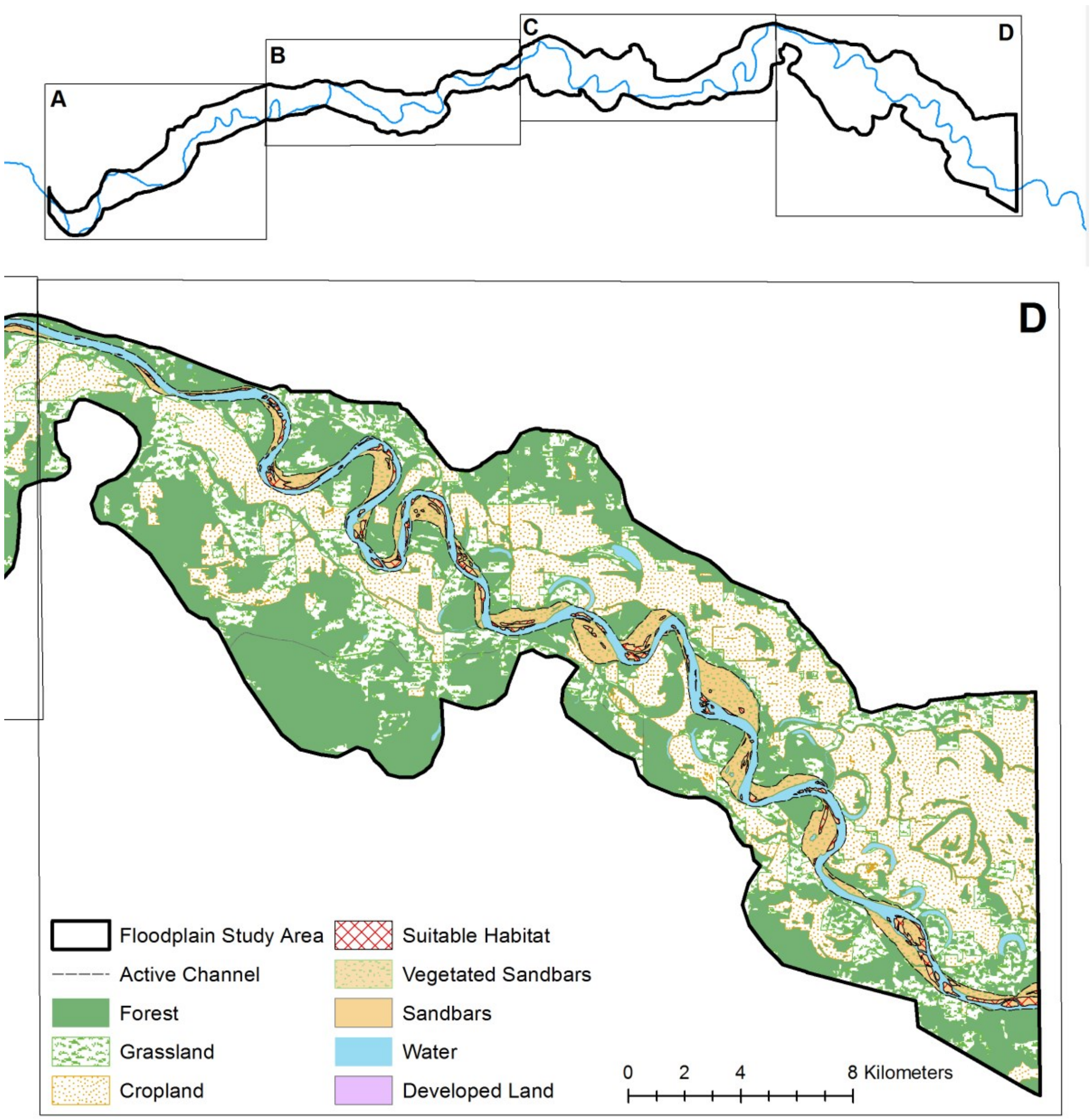

Figure 8. Section D of the segment-scale land cover map for 1949.

1979

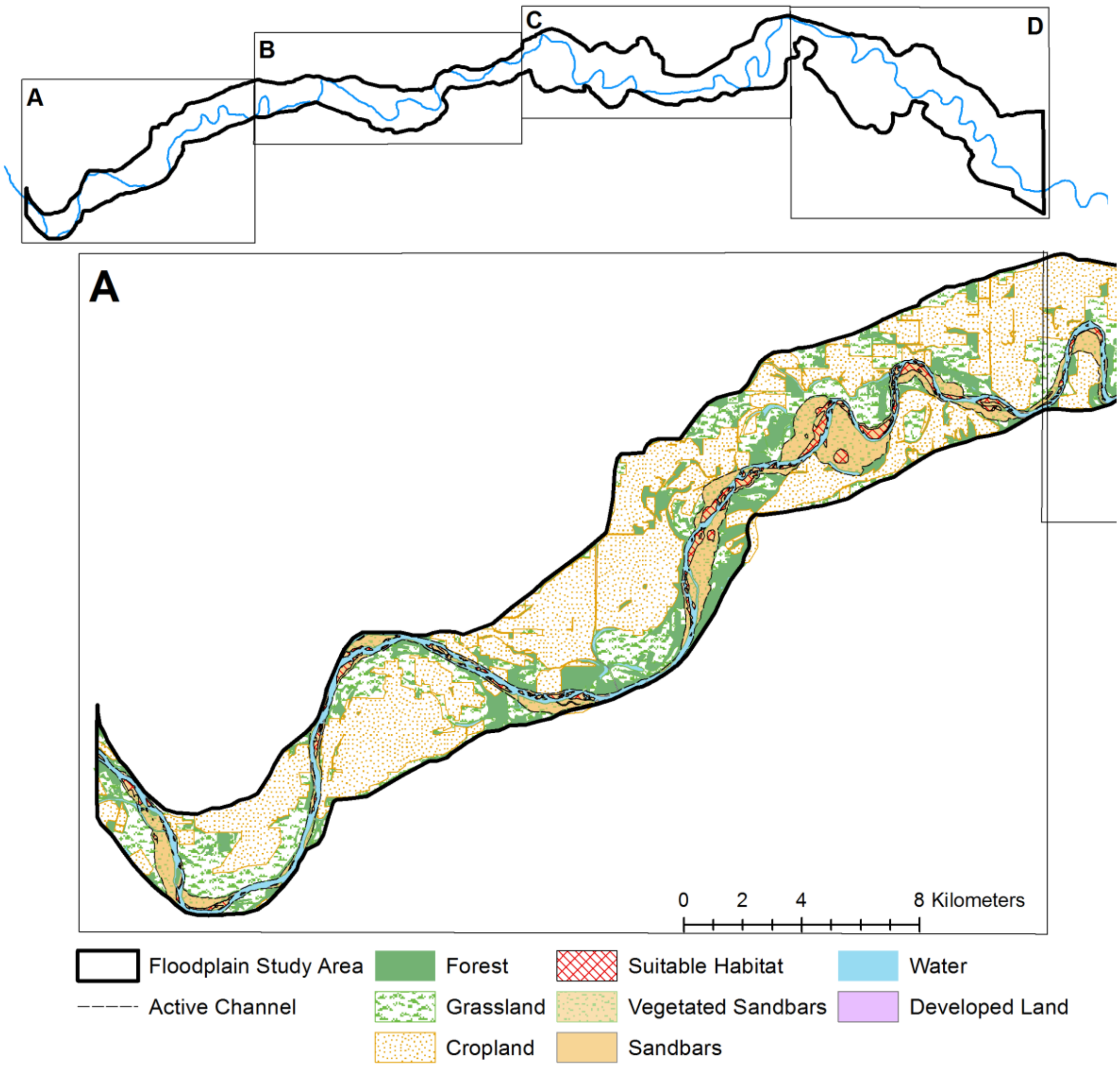

Figure 9. Section A of the segment-scale land cover map for 1979.

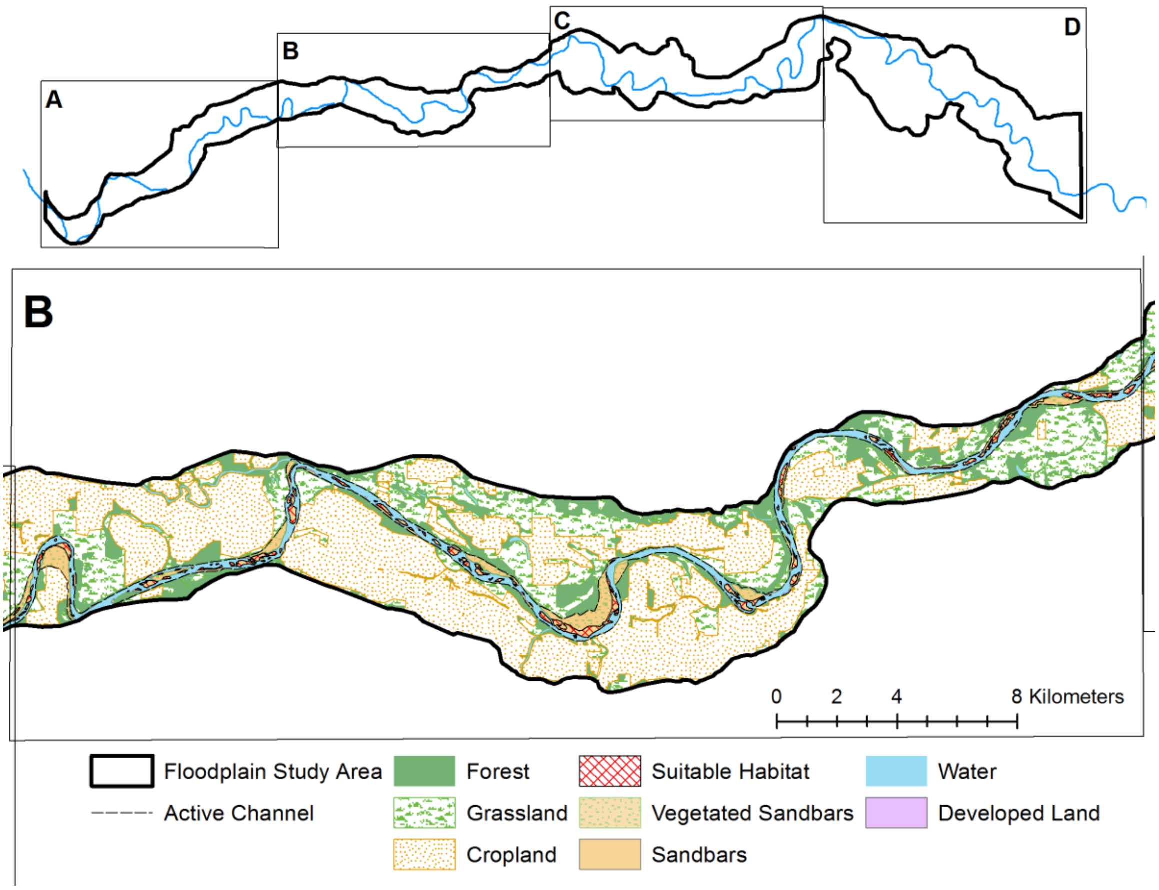

Figure 10. Section B of the segment-scale land cover map for 1979.

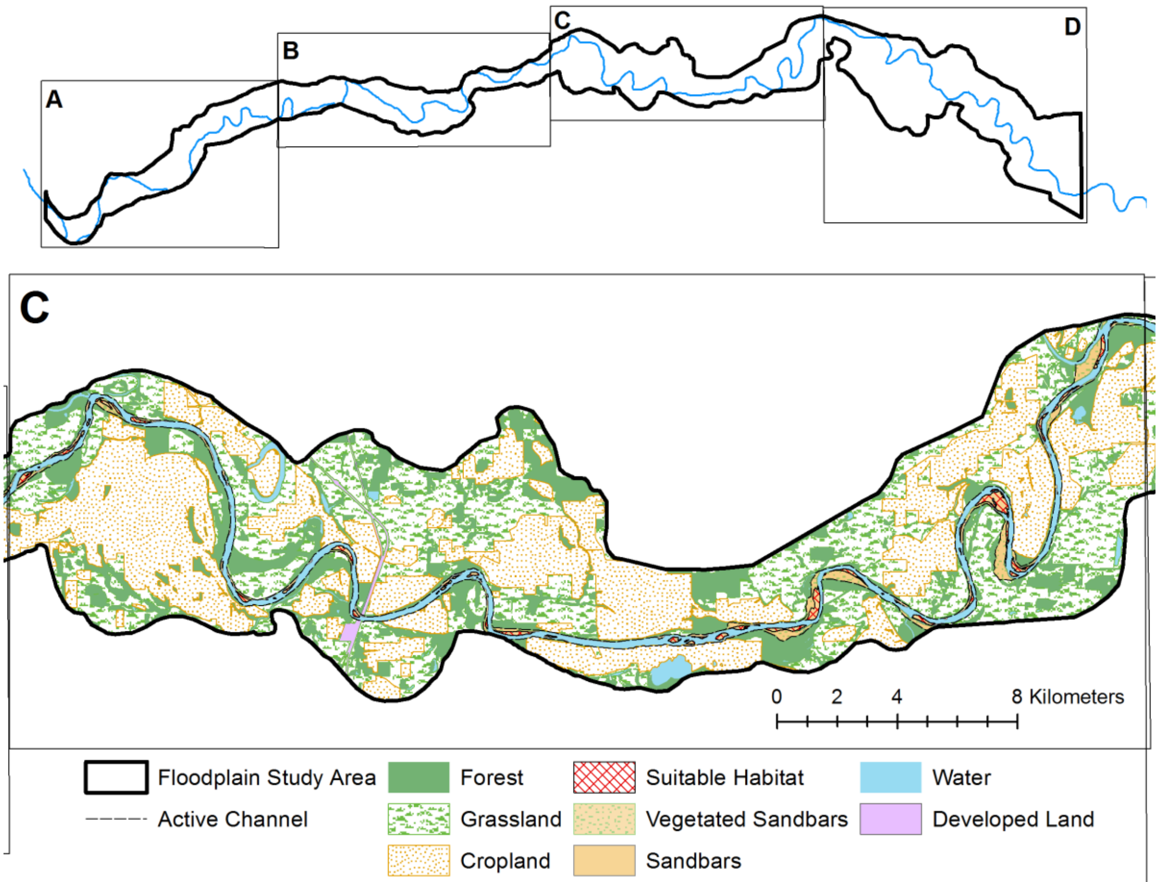

Figure 11. Section C of the segment-scale land cover for 1979.

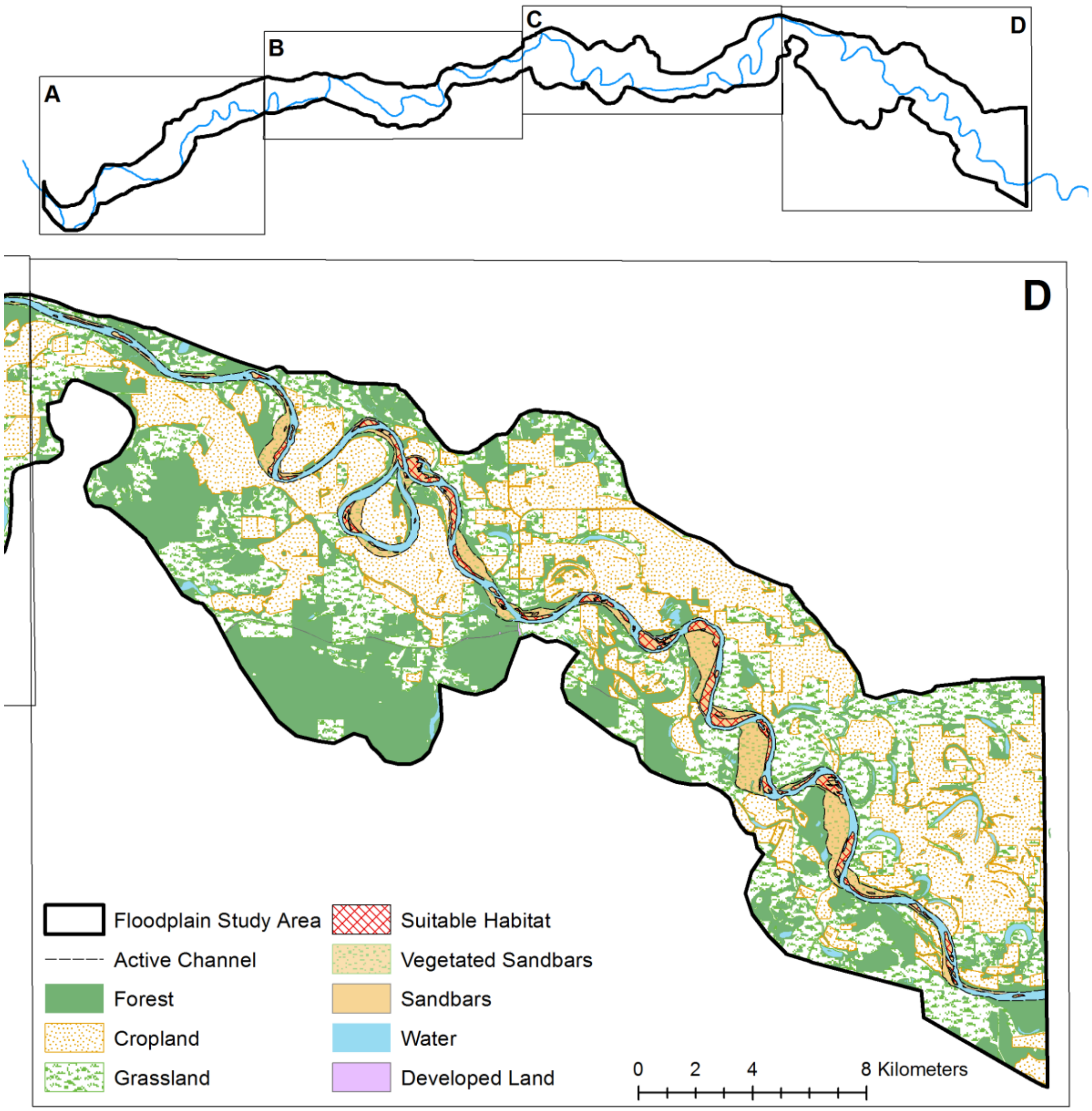

Figure 12. Section D of the segment-scale land cover map for 1979.

2010

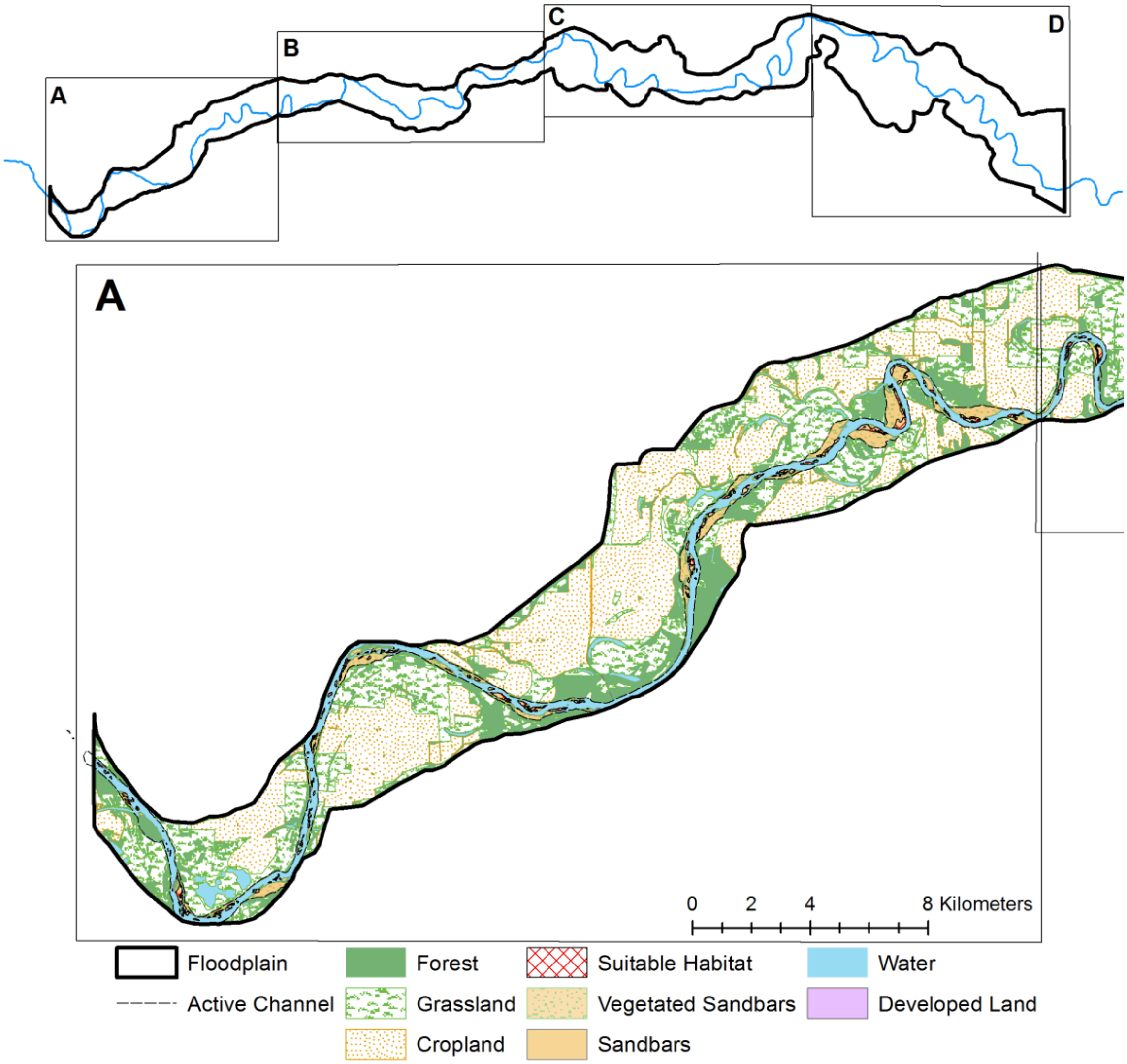

Figure 13. Section A of the segment-scale land cover map for 2010.

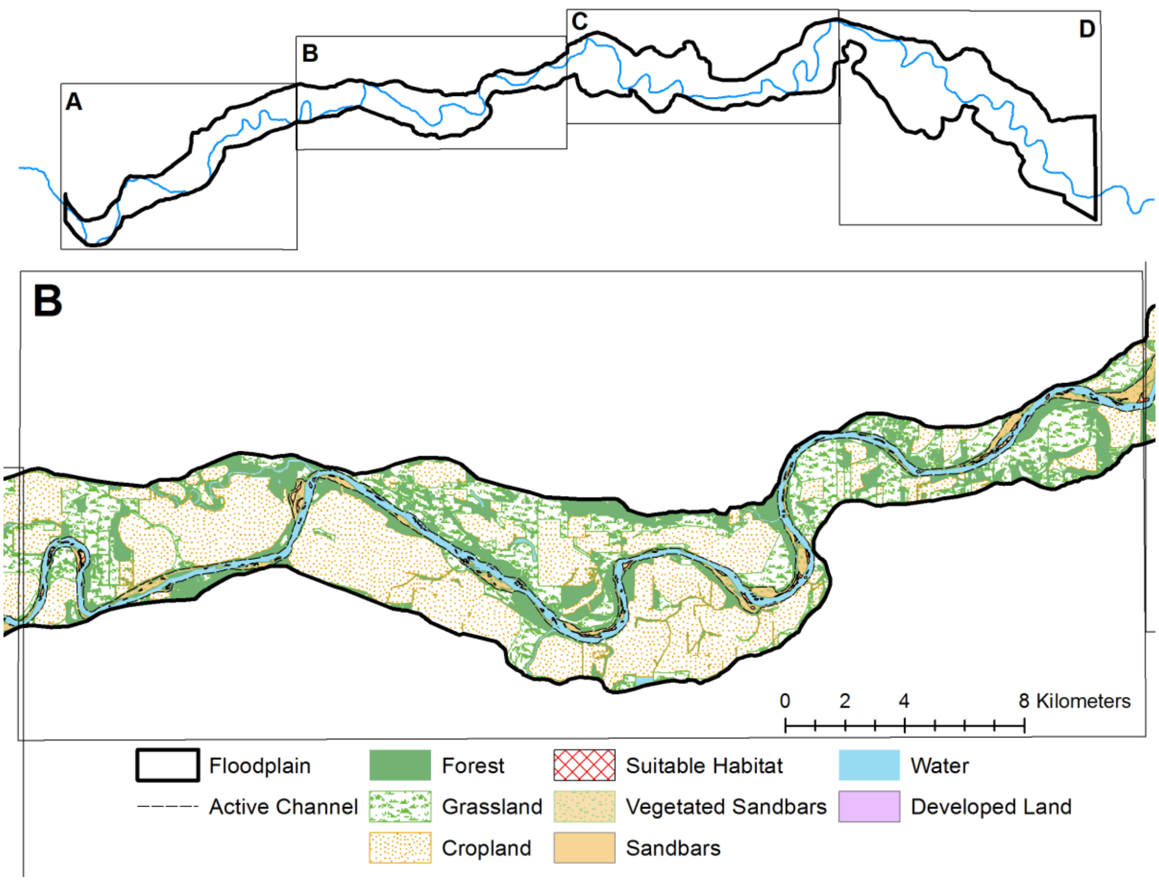

Figure 14. Section B of the segment-scale land cover map for 2010.

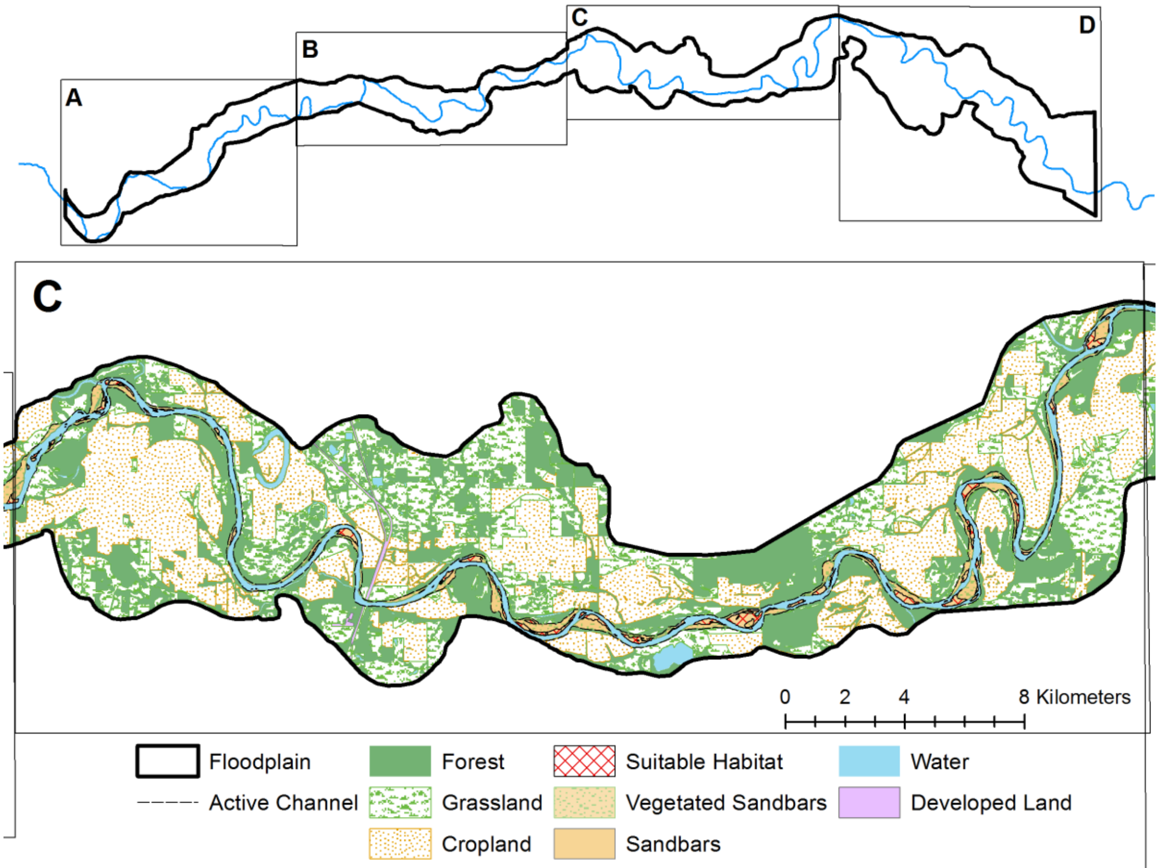

Figure 15. Section C of the segment-scale land cover map for 2010.

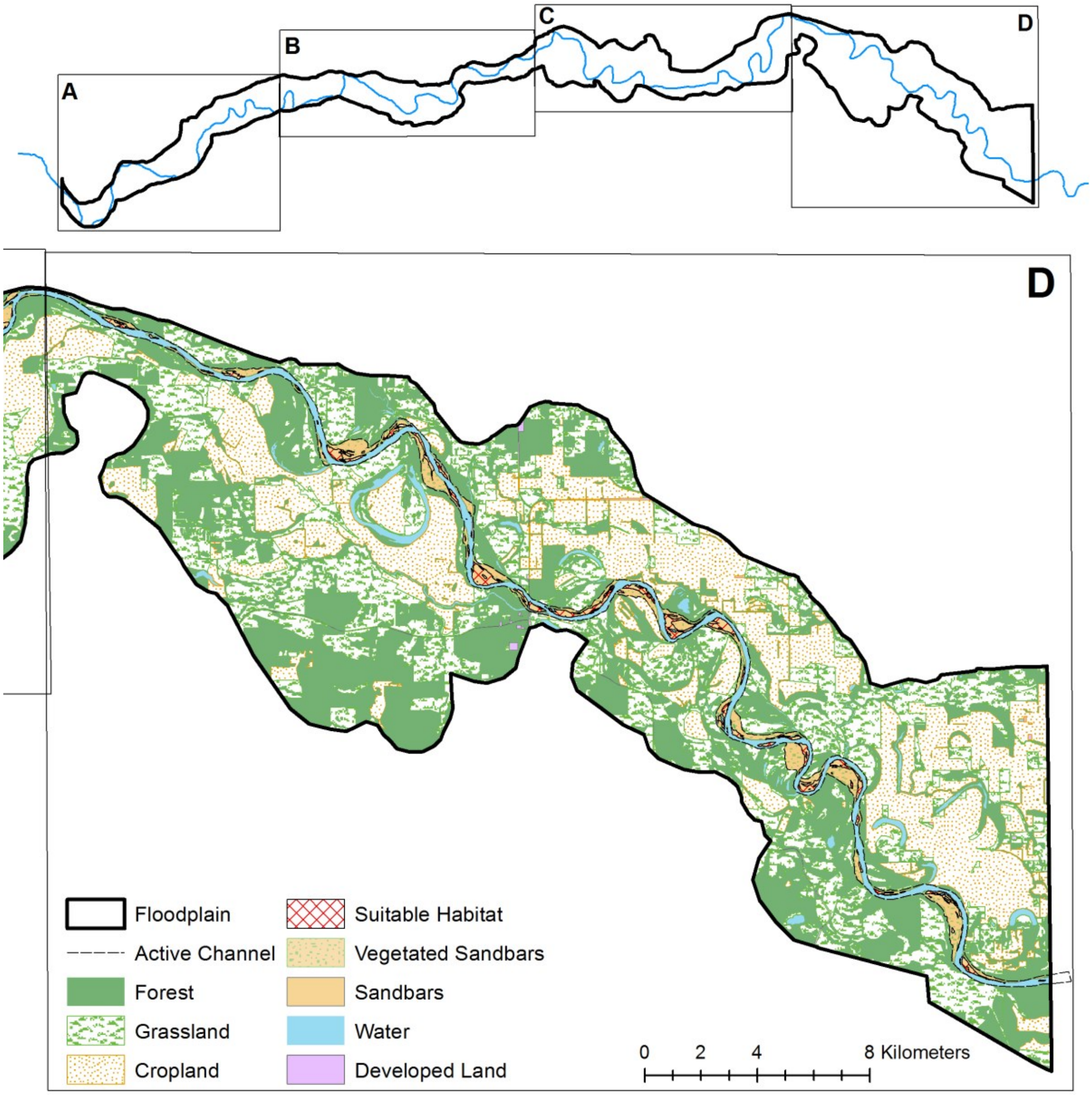

Figure 16. Section D of the segment-scale land cover map for 2010.

APPENDIX B: LAND COVER MAPS FOR REACH-SCALE STUDY AREA

1890s – 1949

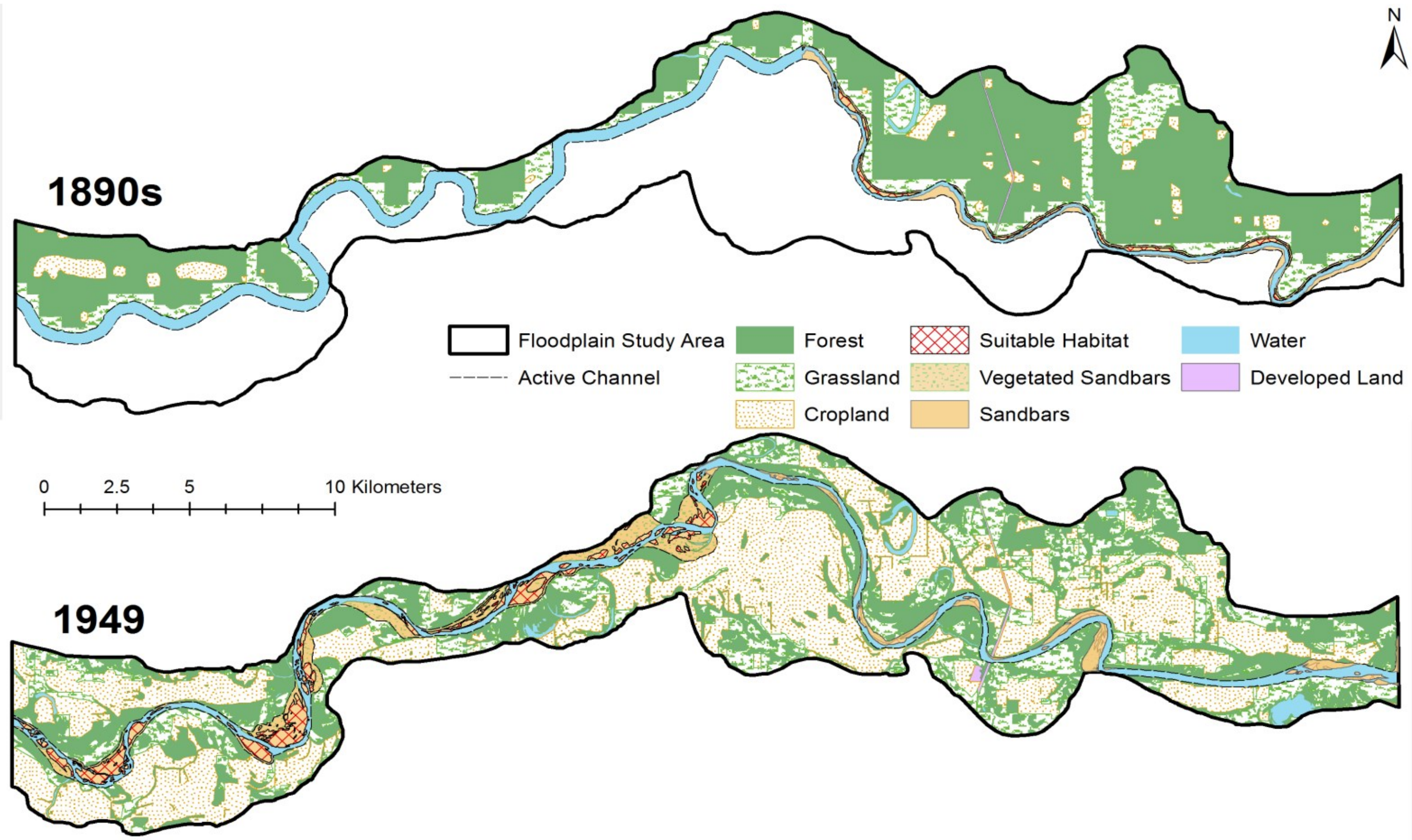

Figure 17. Land cover maps for the reach-scale for the 1890s and 1949.

1964 - 1972

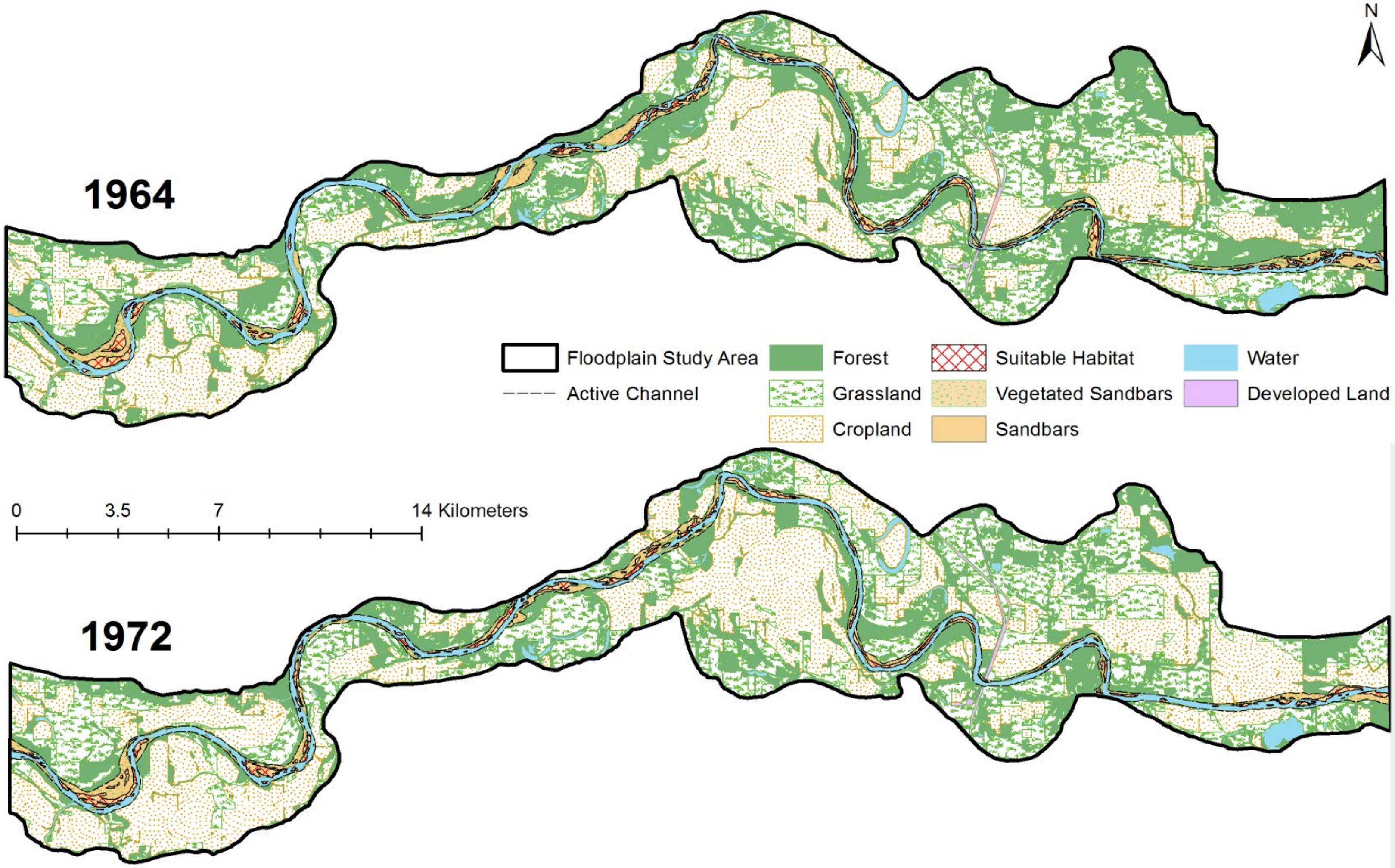

Figure 18. Land cover maps for the reach-scale for 1964 and 1972.

1979 - 1982

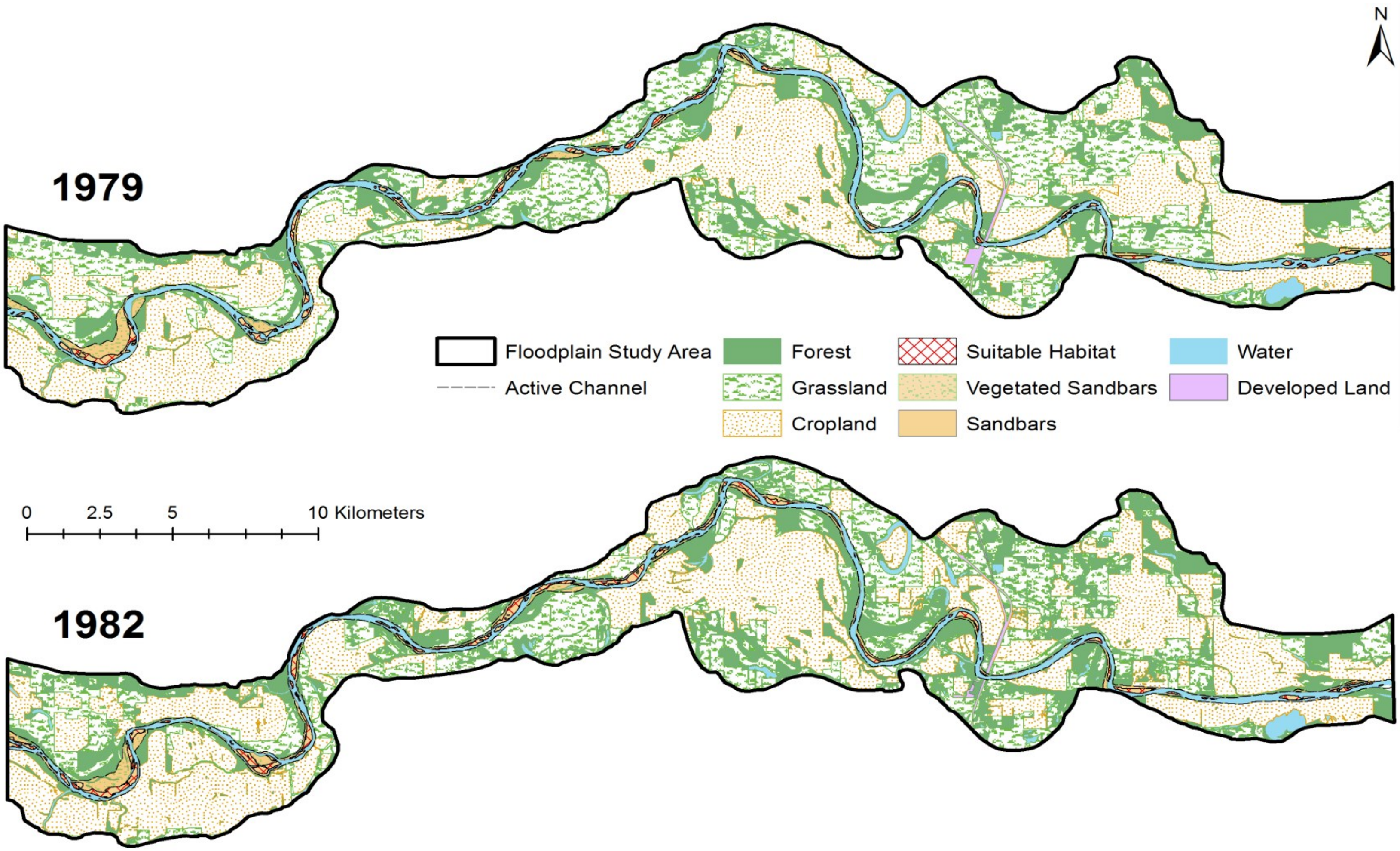

Figure 19. Land cover maps for the reach-scale for 1979 and 1982.

1984 - 2004

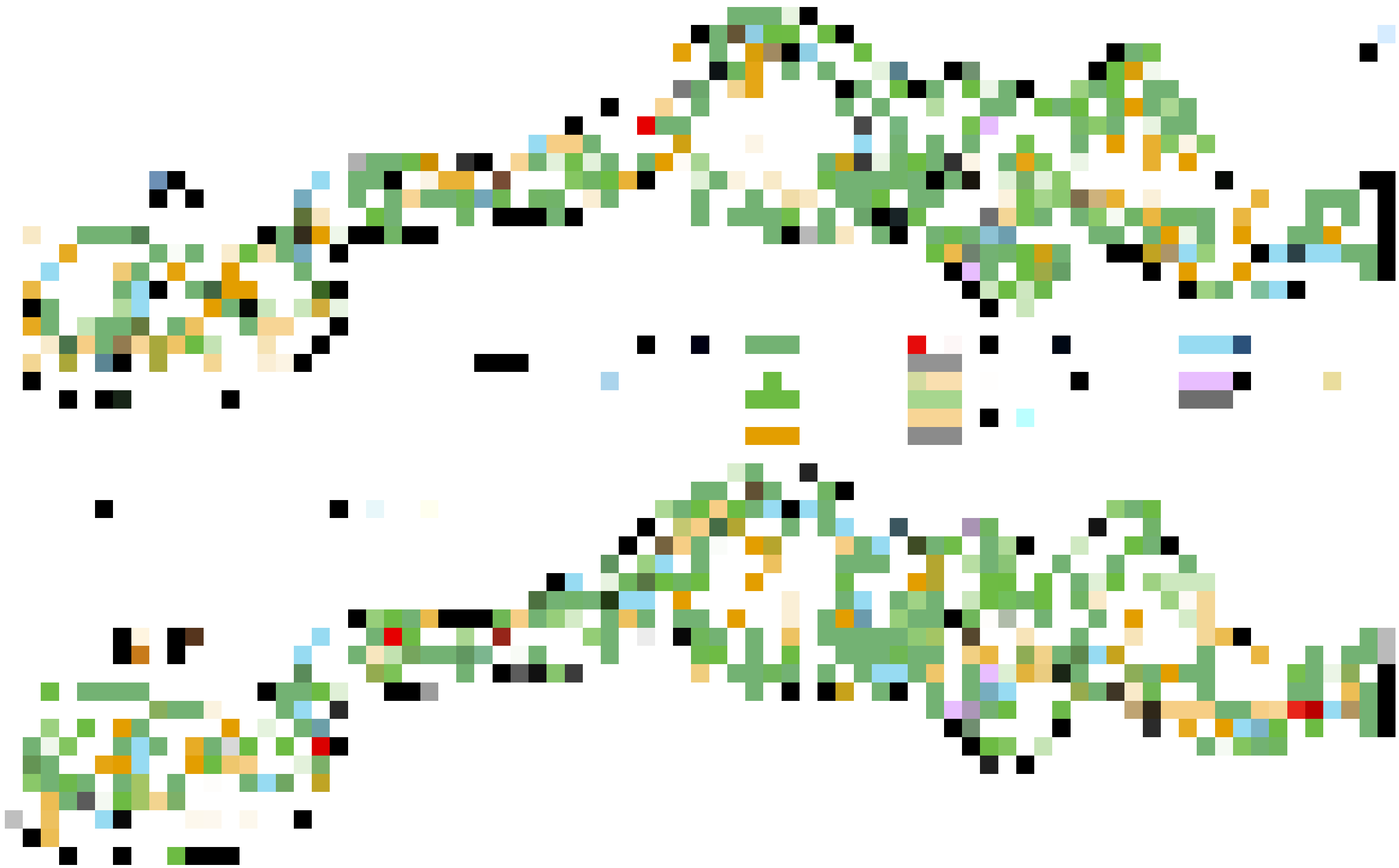

Figure 20. Land cover maps for the reach-scale for 1984 and 2004.

2006 - 2008

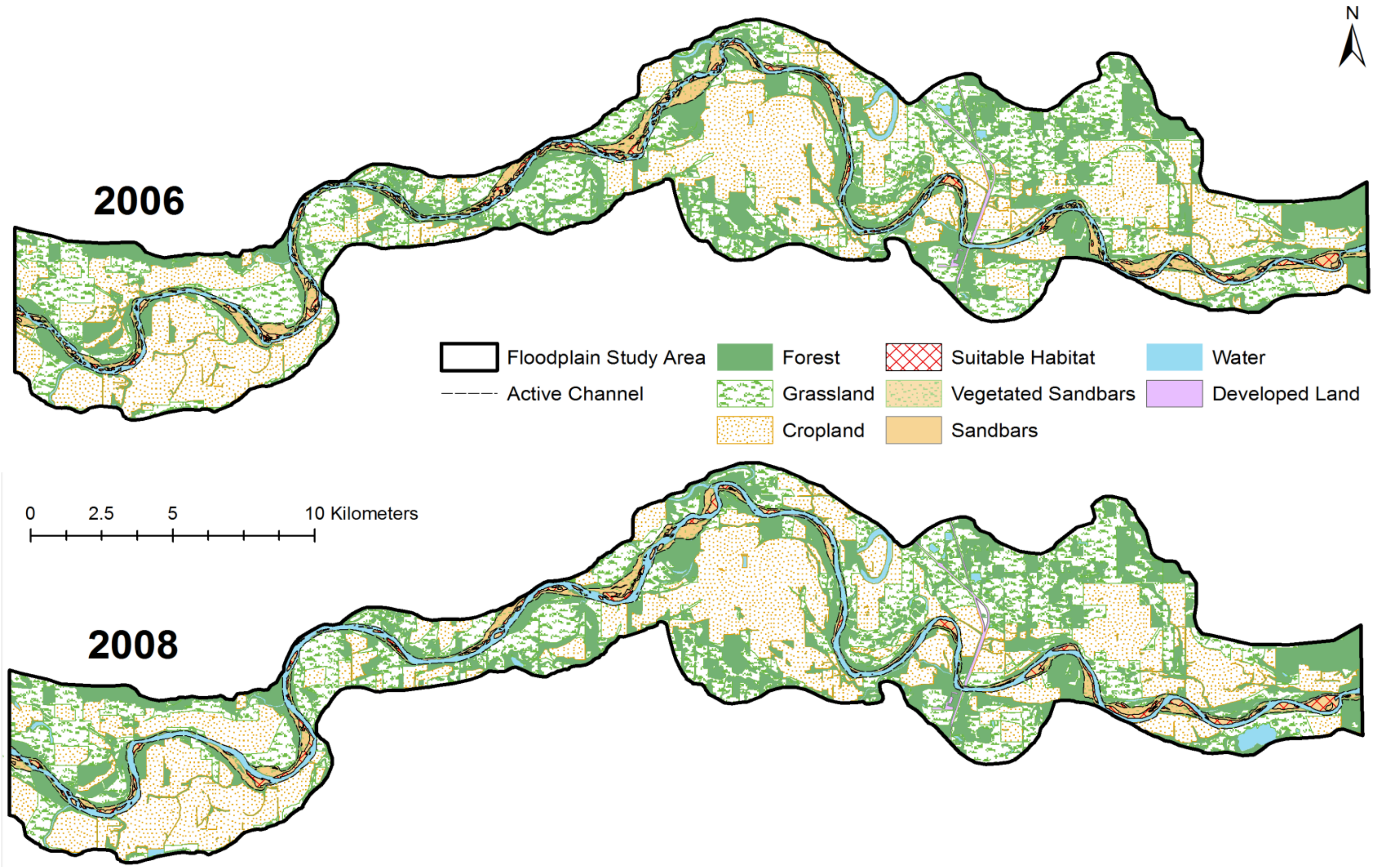

Figure 20. Land cover maps for the reach-scale for 2006 and 2008.

2010 - 2012

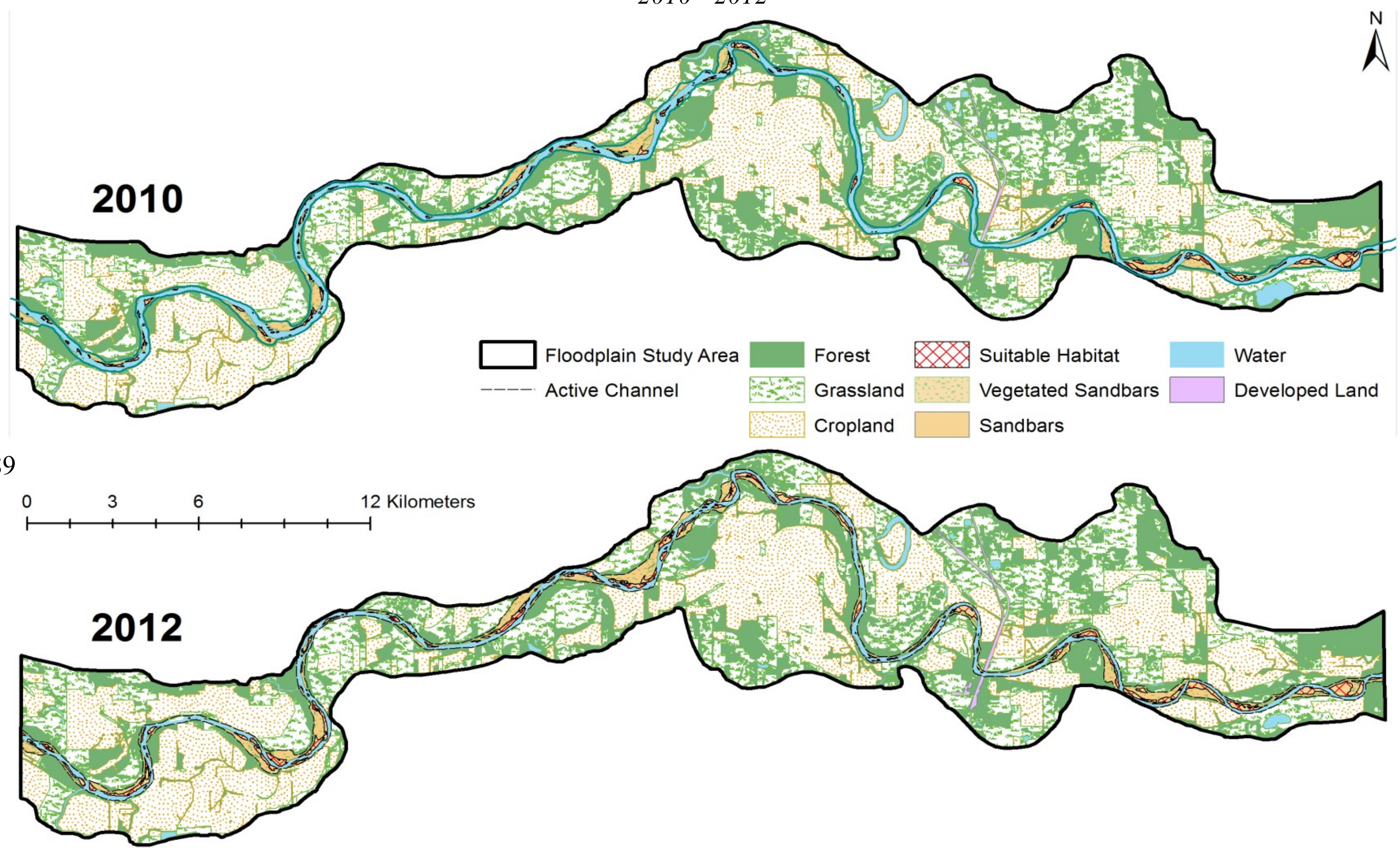

Figure 21. Land cover maps for the reach-scale for 2010 and 2012.

2014

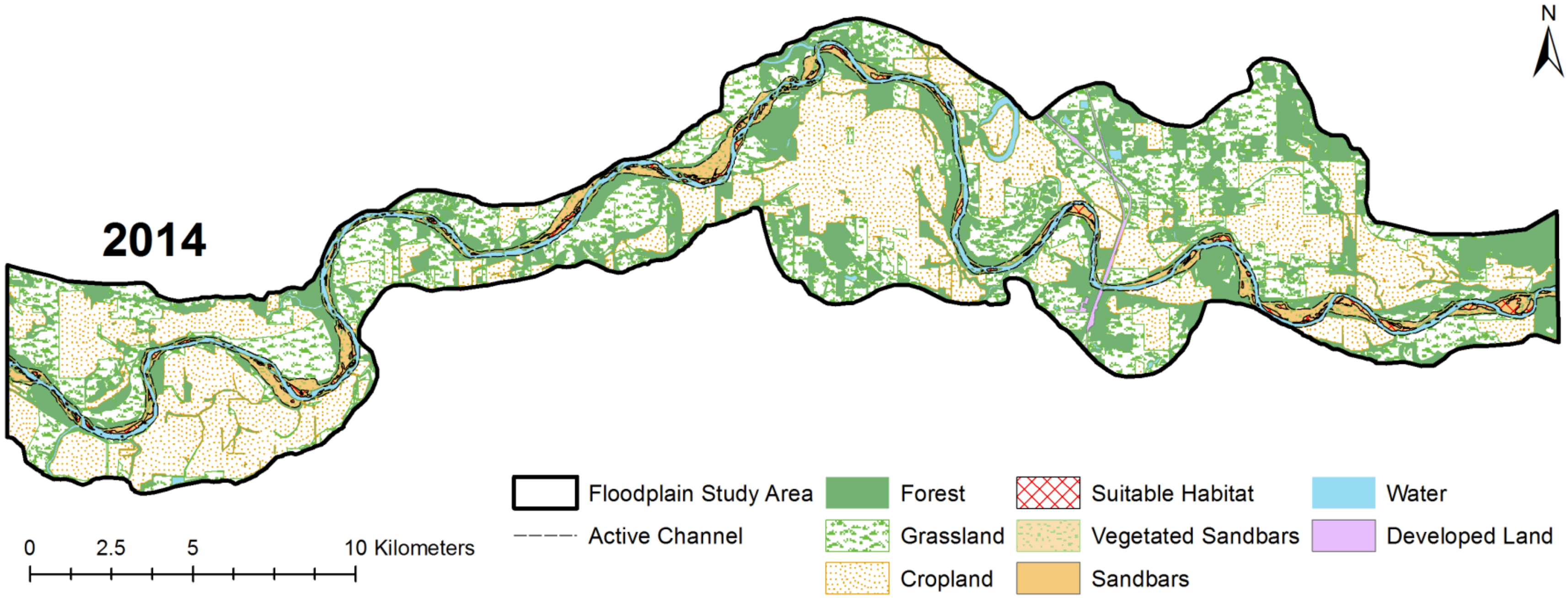

Figure 22. Land cover maps for the reach-scale for 2014.

LITERATURE CITED

Albertson, P. E., and D. M. Patrick. 1996. Lower Mississippi River tributaries: contributions to the collective science concerning the "Father of Waters." *Engineering Geology,* 45: 383-413.

Alexander, J. S., D. M. Schultze, and R. B. Zelt. 2013. *Emergent sandbar dynamics in the Lower Platte River in Easter Nebraska- methods and results of pilot study, 2011*. U.S. Geological Survey Scientific Investigations Report 2013-5031, 42 p.

Allan, J. D. 2004. Landscapes and riverscapes: The influence of land use on stream ecosystems. *Annual Review of Ecology, Evolution, and Systematics,* 35(1): 257-284.

Allison, M. E., C. R. Demas, B. A. Ebersole, B. A. Kleiss, C. D. Little, E. A. Meselhe, N. J. Powell, T. C. Pratt, and B. M. Vosburg. 2012. A water and sediment budget for the lower Mississippi-Atchafalaya River in flood years 2008-2010: Implications for sediment discharge to the oceans and coastal restoration in Louisiana. *Journal of Hydrology,* 432-433: 86-97.

Anderson, J. R., E. E. Hardy, J. T. Roach, and R. E. Witmer. 1976. *A land use and land cover classification system for use with remote sensor data,* Geological Survey Professional Paper 964. U.S. Government Printing Office: Washington, D.C.

Anderson, R. J., B. R. Bledsoe, and W. C. Hession. 2004. Width of streams and rivers in response to vegetation, bank material, and other factors. *Journal of the American Water Resources Association,* 40(5): 1159-1172.

Bayley, P. B. 1995. Understanding large rivers: Floodplain ecosystems. *Bioscience,* 45(3): 153-158.

Benda, L., N. L. Poff, D. Miller, T. Dunne, G. Reeves, G. Press, and M. Pollock. 2004. The network dynamics hypothesis: How channel networks structure riverine habitats. *Bioscience,* 54(5): 413-427.

Campbell, Linda. 2003. Endangered and Threatened Animals of Texas: Their Life History and Management. Texas Parks and Wildlife Division: Austin, Texas.

Charlton, R. 2008. *Fundamentals of Fluvial Geomorphology.* New York, NY: Routledge.

Copeland, R. R. 2002. *Red River below Denison Dam, Texas, Oklahoma, Arkansas, and Louisiana: A numerical sedimentation model study*. ERDC/CHL TR-02-5. U.S. Army Engineer District: Tulsa, OK.

Costa, J. E., and J. E. O'Connor. 1995. Geomorphically effective floods. In *Natural and Anthropogenic Influences in Fluvial Geomorphology,* Costa, J. E., A. J. Miller, K. W. Potter, and P. R. Wilcock, 45-56. Washington, D.C.: American Geophysical Union.

Costigan, K. H., and M. D. Daniels. 2012. Damming the prairie: Human alteration of Great Plains river regimes. *Journal of Hydrology*, 444-445: 90-99.

Davies, P. M., R. J. Naiman, D. M. Warfe, N. E. Pettit, A. H. Arthington, and S. E. Bunn. 2013. Flow-ecology relationships: Closing the loop on effective environmental flows. *Marine and Freshwater Research,* 65: 133-141.

Dodds, W. K., K. Gido, M. R. Whiles, K. M. Fritz, and W. J. Matthews. 2004. Life on the edge: The ecology of Great Plains prairie streams. *Bioscience,* 54(3): 205-216.

Drummond, M. A., R. F. Auch, K. A. Karstensen, K. L. Sayler, J. L. Taylor, and T. R. Loveland. 2012. Land change variability and human-environment dynamics in the United States Great Plains. *Land Use Policy,* 29(3): 710-723.

Duck, L. G., and J. B. Fletcher. 1945. *A survey of the game and furbearing animals of Oklahoma;* Chapter 2, The Game Types of Oklahoma. Oklahoma Game and Fish Commission, Division of Wildlife Restoration and Research: Oklahoma City.

Dunne, T., and L. B. Leopold. 1978. *Water in Environmental Planning.* New York, NY: W. H. Freeman and Company.

ESRI. 2016. ArcGIS Desktop Software: Release 10.4. Redlands, CA: Environmental Systems Research Institute.

Fischer, J., C. Paukert, and M. Daniels. 2015. Influence of riparian and watershed alterations on sandbars in a Great Plains river. *River Research and Applications,* 31: 1140-1150.

Fitzhugh, T. W., and R. M. Vogel. 2011. The impact of dams on flood flows in the United States. *River Research and Applications,* 27(10): 1192-1215.

Friedman, J. M., M. L. Osterkamp, M. L. Scott, and G. T. Auble. 1998. Downstream effects of dams on channel geometry and bottomland vegetation: Regional patterns in the Great Plains. *Wetlands,* 18(4): 619-633.

Foley, J. A., R. Defries, G. P. Asner, C. Barford. G. Bonan, S. R. Carpenter, F. S. Chapin, M. T. Coe, G. C. Daily, H. K. Gibbs, J. H. Helowski, T. Holloway, E. A. Howard, C. J. Kucharik, C. Monfreda, J. A. Patz, I. C. Prentice, N. Ramankutty, and P. K. Snyder. 2005. Global consequences of land use. *Science,* 309(5734): 570-574.

Graf, W. L. 1999. Dam nation: A geographic census of American dams and their large-scale hydrologic impacts. *Water Resources Research,* 34(4): 1305-1311.

———. 2001. Damage control: Restoring the physical integrity of America's rivers. *Annals of the Association of American Geographers,* 91(1): 1-27.

———. 2006. Downstream hydrologic and geomorphic effects of large dams on American rivers. *Geomorphology,* 79: 336-360.

Greiner Jr., J. H. 1982. *Erosion and Sedimentation by Water in Texas: Average Annual Rates Estimated in 1979.* Report 268 to Texas Department of Water Resources.

Griffith, G., S. Bryce, J. Omernik, and A. Rogers. 2007. *Ecoregions of Texas,* Project Report AS-199 to Texas Commission on Environmental Quality. Austin, TX: USEPA.

Gordon, E., and R. K. Meentemeyer. 2006. Effects of dam operation and land use on stream channel morphology and riparian vegetation. *Geomorphology,* 82(3-4): 412-429.

Hooke, J. M. 1986. The significance of mid-channel bars in an active meandering river. *Sedimentology,* 33: 839-850.

Horn, J. D., R. M. Joeckel, and C. R. Fielding. 2012. Progressive abandonment and planform changes of the central Platte River in Nebraska, central USA, over historical timeframes. *Geomorphology*, 139-140: 372-383.

Johnsgard, P. A. 1978. The ornithogeography of the Great Plains states. *The Prairie Naturalist,* 10(4): 97-112.

Johnson, W. C. 1999. Response of riparian vegetation to streamflow regulation and land use in the Great Plains. *Great Plains Research: A Journal of Natural and Social Sciences,* 9: 356-369.

Julian, J. P., and R. Torres. 2006. Hydraulic erosion of cohesive riverbanks. *Geomorphology*, 76: 193-206.

Julian, J. P., R. E. Thomas, S. Moursi, B. W. Hoagland, and A. Tarhule. 2012. Historical variability and feedbacks among land cover, stream power, and channel geometry along the lower Canadian River floodplain in Oklahoma. *Earth Surface Processes and Landforms,* 37: 449-468.

Julian, J. P., M. W. Doyle, C. J. P. Podolak, R. B. Manners, K. M. Meitzen, S. Ensign, and N. Wilgruber. 2016. Shaping the physical template: Biological, hydrological, and geomorphic connections in stream channels. In *Streams in a Changing Environment*, ed. J. B. Jones and E. H. Stanley, 85-133. London: Academic Press.

Junk, W. J., P. B. Bayley, and R. E. Sparks. 1989. The flood pulse concept in river-floodplain systems. In *Proceedings of the International Large River Symposium,* ed. D. P. Dodge, Canadian Special Publication. Fisheries and Aquatic Science 106: 110-127.

Juracek, K. E. 2000. Channel stability downstream from a dam assessed using aerial photographs and stream-gage information. *Journal of the American Water Resources Association*, 36(3): 633-645.

Knighton, D. 1998. Fluvial forms and processes: a new perspective. John Wiley and Sons Ltd, New York, NY. 383 pp.

Knox, J. C. 1972. Valley alluvation in southwestern Wisconsin. *Annals of the American Geographer,* 62(3): 401-410.

———. 1977. Human impacts on Wisconsin stream channels. *Annals of the American Geographer,* 67(3): 323-342.

Kondolf, G. M. 1997. PROFILE: Hungry water: Effects of dams and gravel mining on river channels. *Environmental Managament,* 21(4): 533-551.

Lane, E. W. 1955. The importance of fluvial morphology in hydraulic engineering. *Proceedings (American Society of Civil Engineers),* 81(745): 1-17.

Lenhart, C., J. Naber, and J. Nieber. 2013. Impacts of hydrologic change on sandbar nesting availability for riverine turtles in Eastern Minnesota, USA. *Water*, 5(3): 1243-1261.

Leopold, L. B., M. G. Wolman, and J. P. Miller. 1964. *Fluvial Processes in Geomorphology.* New York, NY: Dover Publications.

Leopold, L. B. 1997. *Water, Rivers, and Creeks.* Sausalito, CA: University Science Books.

Ligon, F. K., W. E. Dietrich, and W. J. Trush. 1995. Downstream ecological effects of dams: a geomorphic perspective. *Bioscience,* 45: 183-192.

Lott, C. A., and R. L. Wiley. 2012a. *Effects of dam operations on Least Tern nesting habitat and reproductive success below Keystone Dam on the Arkansas River*. ERDC/EL CR-12-4. U.S. Army Engineer District: Vicksburg, MS.

———. 2012b. *Final report to the USACE-Tulsa District: Sandbar nesting habitat for Interior Least Terns* (*Sternula antillarum*) *on the Red River below Denison Dam*, 2008: US Army Corps of Engineers.

Lott, C. A., R. L. Wiley, R. A. Fischer, P. D. Hartfield, and J. M. Scott. 2013. Interior Least Tern (*Sternula antillarum)* breeding distribution and ecology: implications for population-level studies and the evaluation of alternative management strategies on large, regulated rivers. *Ecology and Evolution 3*: 3613-3627.

Lytle, D. A., and N. L. Poff. 2004. Adaptation to natural flow regimes. *Trends in Ecology and Evolution,* 19(2): 94-100.

Manners, R. B., J. C. Schmidt, and M. L. Scott. 2014. Mechanisms of vegetation-induced channel narrowing of an unregulated canyon river: Results from a natural field-scale experiment. *Geomorphology,* 211: 100-115.

Matthews, W. J., C. C. Vaughn, K. B. Gido, E. Marsh-Matthews. 2005. Southern Plains rivers. In *Rivers of North America*, Benke, A.C., Cushing, C.E. (eds). Academic Press: Burlington; 283-325.

Meitzen, K. M., M. W. Doyle, M. C. Thomas, and C. E. Burns. 2013. Geomorphology within the interdisciplinary science of environmental flows. *Geomorphology,* 200: 143-154.

Naiman, R. J., and H. Décamps. 1997. The ecology of interfaces: Riparian zones. *Annual Review of Ecology and Systematics,* 28: 621-658.

Nanson, G. C., and J. C. Croke. 1992. A genetic classification of floodplains. *Geomorphology,* 4(6):459-486.

The Nature Conservancy (TNC). 2009. Indicators of Hydrologic Alteration Version 7.1 User's Manual.

———. 2009. Indicators of Hydrologic Alteration (IHA) Software: Release 7.1. Arlington, VA: The Nature Conservancy.

Oklahoma Water Resources Board (OWRB). 2012. *Blue-Boggy Watershed Planning Region Report.* Oklahoma Comprehensive Water Plan. Oklahoma City: Oklahoma Water Resources Board.

Omernik, J.M. 1987. Ecoregions of the conterminous United States (map supplement). *Annals of the Association of American Geographers,* 77:118-125.

Omernik, J. M., and G. E. Griffith. 2014. Ecoregions of the conterminous United States: Evolution of a hierarchical spatial framework. *Environmental Management,* 54(6): 1249-1266.

Osterkamp, W. R. and E. R. Hedman. 1977. Variation of width and discharge for natural high-gradient stream channels. *Water Resources Research,* 13(2): 256-258.

Petts, G. E. 1979. Complex response of river channel morphology subsequent to reservoir construction. *Progress in Physical Geography,* 3(3): 329-362.

———. 1984. *Impounded Rivers — Perspectives for Ecological Management.* New York, NY: John Wiley & Sons.

Poff, N. L., J. D. Allan, M. B. Bain, J. R. Karr, K. L. Prestegaard, B. D. Richter, R. E. Sparks, and J. C. Stromberg. 1997. The natural flow regime: a paradigm for river conservation and restoration. *Bioscience*, 52: 769-784.

Poff, N. L., and D. D. Hart. 2002. How dams vary and why it matters for the emerging science of dam removal. *Bioscience,* 52(8): 659-668.

Poff, N. L., B. P. Bledsoe, and C. O. Cuhaciyan. 2006. Hydrologic variation with land use across the contiguous United States: Geomorphic and ecological consequences for stream ecosystems. *Geomorphology,* 79: 265-285.

Poff, N. L., and J. K. H. Zimmerman. 2010. Ecological responses to altered flow regimes: a literature review to inform the science and management of environmental flows. *Freshwater Biology,* 55: 194-205.

Richter, B. D., J. V. Baumgartner, J. Powell, and D. P. Braun. 1996. A method for assessing hydrologic alteration within ecosystems. *Conservation Biology,* 10(4): 1163-1174.

Sanford, J. P. 2002. Dam regulation effects on sand bar migration on the Missouri River: Southeaster South Dakota. *MS Thesis*, Department of Geology, Montana State University.

Saucier, R. T. 1994. Landforms and geomorphic processes. In *Geomorphology and Quaternary Geologic History of the Lower Mississippi Valley,* ed. R. T. Saucier, 87-129. Vicksburg, MS: U.S. Army Engineer Waterways Experiment Station.

Schumm, S. A., and R. W. Lichty. 1963. *Channel widening and flood-plain construction along Cimarron River in southwestern Kansas: Erosion and sedimentation in a semiarid environment*, Geological Survey Professional Paper 352-D. Washington, D.C.: U.S. Geological Survey.

Schumm, S.A. 2005. *River Variability and Complexity*. Cambridge, New York. 220 pp.

Simon, A., W. Dickerson, and A. Heins. 2004. Suspended-sediment transport rates at the 1.5-year recurrence interval for ecoregions of the United States: transport conditions at the bankfull and effective discharge? *Geomorphology,* 58(1-4): 243-262.

Smith, N. D. 1971. Transverse bars and braiding in the Lower Platte River, Nebraska. *Geological Society of America Bulletin* 82(12): 3407-3420.

Stucker, J. H., D. A. Buhl, and M. H. Sherfy. 2012. Emergent sandbar construction for Least Terns on the Missouri River: Effects on forage fishes in shallow-water habitats. *River Research and Applications,* 28(8): 1254-1265.

Svendsen, K. M., K. H. Nislow, M. J. M. Kaste, C. E. Renshaw, and F. J. Magilligan. 2009. Flow and sediment regimes at tributary junctions on a regulated river: impact on sediment residence time and benthic macroinvertebrate communities. *Hydrological Processes,* 23(2): 284-296.

Tracey-Smith, E. K. 2006. Relation of Missouri River flows to sandbar morphology with implication for selected biota. *MS Thesis*, University of Missouri, Columbia.

Tracey-Smith, E. K., D. L. Galat, and R. B. Jacobson. 2012. Flow dynamics on the aquatic-terrestrial transition zone (ATTZ) of Lower Mississippi River sandbars with implications for selected biota. *River Research and Applications,* 28: 793-813.

Trimble, S. W. 1997. Contribution of stream channel erosion to sediment yield from an urbanizing watershed. *Science*, 278: 1442-1444.

Tyson, C. N. 1977. *The Red River in Southwestern History.* Norman, OK: University of Oklahoma Press.

U.S. Environmental Protection Agency. 2005. *Level III Ecoregions of the continental United States* (revision of Omernik, 1987): Corvallis, Oregon, USEPA-National Health and Environmental Effects Research Laboratory, Western Ecology Division, Map M-1, various scales.

U.S. Fish and Wildlife Service (USFWS). 2013. *Biological Opinion to the U.S. Army Corps of Engineers (USACE) on the Channel Improvement Program for the Mississippi River and Tributaries Project for the Lower Mississippi River*. Southeast Region, Mississippi Field Office, Jackson, Mississippi.

Vaughan, I. P., D. G. Noble and S. J. Ormerod. 2007. Combining surveys of river habitats and river birds to appraise riverine hydromorphology. *Freshwater Biology*, 52: 2270-2284.

Walling, D. E., and B. W. Webb. 1996. Erosion and sediment yield: a global overview. *IAHS Publications-Series of Proceeding and Reports-Intern Assoc Hydrological Sciences,* 246:3-20.

Walling, D. E. 1999. Linking land use, erosion, and sediment yields in river basins. *Hydrobiologia,* 410: 223-240.

Ward, J. V., and J. A. Sanford. 1995. Ecological connectivity in alluvial river ecosystems and its disruption by flow regulation. *Regulated Rivers Research and Management*, 11: 105-119.

Ward, J. V. 1997. Riverine landscapes: Biodiversity patterns, disturbance regimes, and aquatic conservation. *Biological Conservation,* 83(3): 269-278.

Ward, J. V., K. Tockner, D. B. Arscott, and C. Claret. 2002. Riverine landscape diversity. *Freshwater Biology,* 47: 517-539.

Whitesell, B. L., J. D. Vitek, and D. R. Butler. 1988. Changes in the planform of the Red River, McCurtain County, Oklahoma, 1938-84. *Oklahoma Geological Survey* 48 (5): 196-210.

Williams, G. P., and M. G. Wolman. 1984. *Downstream effects of dams on alluvial rivers*. U.S. Geological Survey Professional Paper 1286; 83.

Wohl, E. 2014. *Rivers in the Landscape: Science and Management*. Oxford, U.K.: Wiley and Sons, Ltd.

Wohl, E., B. P. Bledsoe, R. B. Jacobson, N. L. Poff, S. L. Rathburn, D. M. Walters, and A. C. Wilcox. 2015. The natural sediment regime in rivers: Broadening the foundation for ecosystem management. *Bioscience,* 65 (4): 358-371.

Wolman, M. G., and L. B. Leopold. 1957. *River floodplains: Some observations on their formation.* U.S. Geological Survey Professional Paper 282C: 87-107.

Wolman, M. G., and J. P. Miller. 1960. Magnitude and frequency of forces in geomorphic processes. *The Journal of Geology,* 68 (1): 54-74.

Wolman, M. G. 1967. A cycle of sedimentation and erosion in urban river channels. *Geografiska Annaler Series A, Physical Geography,* 49 (2/4): 385-395.

Woods, A. J., J. M. Omernik, D. R. Butler, J. G. Ford, J. E. Henley, B. W. Hoagland, D. S. Arndt, and B. C. Moran. 2005. Ecoregions of Oklahoma. (2-sided color poster map, descriptive text, summary tables, and photographs). U.S. Geological Survey, Reston, VA. Scale 1:1,250,000.